

LA-12885

LA-12885
C.3

C.3

CIC-14 REPORT COLLECTION
REPRODUCTION
COPY

*Lawrence Livermore Pulsed Sphere Benchmark
Analysis of MCNP™ ENDF/B-VI*



Los Alamos
NATIONAL LABORATORY

*Los Alamos National Laboratory is operated by the University of California
for the United States Department of Energy under contract W-7405-ENG-36.*

*Edited by Patricia W. Mendius, Group CIC-1
Prepared by M. Ann Nagy, Group X-6*

An Affirmative Action/Equal Opportunity Employer

This report was prepared as an account of work sponsored by an agency of the United States Government. Neither The Regents of the University of California, the United States Government nor any agency thereof, nor any of their employees, makes any warranty, express or implied, or assumes any legal liability or responsibility for the accuracy, completeness, or usefulness of any information, apparatus, product, or process disclosed, or represents that its use would not infringe privately owned rights. Reference herein to any specific commercial product, process, or service by trade name, trademark, manufacturer, or otherwise, does not necessarily constitute or imply its endorsement, recommendation, or favoring by The Regents of the University of California, the United States Government, or any agency thereof. The views and opinions of authors expressed herein do not necessarily state or reflect those of The Regents of the University of California, the United States Government, or any agency thereof.

LA-12885

UC-700
Issued: December 1994

*Lawrence Livermore Pulsed Sphere Benchmark
Analysis of MCNP™ ENDF/B-VI*

*John D. Court
Ronald C. Brockhoff
John S. Hendricks*



Los Alamos
NATIONAL LABORATORY
Los Alamos, New Mexico 87545

**LAWRENCE LIVERMORE PULSED SPHERE BENCHMARK
ANALYSIS OF MCNP™ ENDF/B-VI**

by

John D. Court, Ronald C. Brockhoff, and John S. Hendricks

ABSTRACT

Twenty-eight Lawrence Livermore pulsed sphere experiments were modeled using MCNP for the purpose of benchmarking the new MCNP ENDF/B-VI data library. The twenty-eight pulsed sphere experiments contain thirty-four of the 124 isotopic or elemental evaluations contained in the new ENDF/B-VI set. The ENDF/B-VI results are compared to experimental neutron time-of-flight data, the results obtained from using ENDF/B-V, and against an additional data set, the MCNP Recommended Library, which includes Los Alamos group T-2 evaluations. The results show that ENDF/B-VI results give better or comparable results in comparison to experiment to ENDF/B-V in many cases, and do not deviate grossly in the other cases.

MCNP is a trademark of the Regents of the University of California, Los Alamos National Laboratory.

I. Introduction

In the late 60's, Lawrence Livermore National Laboratory undertook a series of pulsed sphere experiments.^{1,2,3,4} The objective of the program was to measure, with relatively good resolution, the neutron spectra from spherical targets bombarded with 14 MeV neutrons. These spectra were then used to benchmark neutron transport codes and neutron cross sections.⁵

The original program consisted of 54 different experiments on 38 different spheres. Of the 38 different spheres, 16 different material compositions were used, with the balance made up of spheres of differing radii. Table I shows an outline of the target materials.⁴ The sphere sizes are given in nominal mean free paths for 14 MeV neutrons. Each sphere was fabricated with an opening to accommodate a low mass target assembly containing a thin tritiated titanium target disk, which utilized the T(d,n)⁴He reaction when bombarded with a 400 keV D⁺ ion beam. The result was a nearly isotropic source of 14 MeV neutrons. Figure 1 contains a schematic drawing of the experimental setup.⁵

Of the 38, 28 were chosen to be modeled in the MCNP benchmark validation of ENDF/B-VI. As seen in Table I, the omitted experiments were intermediate radii spheres.

II. MCNP ENDF/B-VI

Although the ENDF/B-VI data set⁶ has been available for some time, the capability to utilize it for Monte Carlo continuous energy computations has only recently been available. The NJOY⁷ processed data set was subjected to several benchmarking analyses and released for general use in October 1994 as the ENDF60 library.^{8,9}

The version of MCNP used, MCNP4A,¹⁰ incorporates the ability to use the new ENDF/B-VI physics. In particular, the ⁹Be ENDF/B-VI cross sections utilize the new ENDF/B-VI File 6-Law 7 coupled energy-angle distribution formulation. The deuterium cross sections utilize the new ENDF/B-VI File 6-Law 6 phase space formalism. And many of the nuclear data used to model the Livermore pulsed spheres, particularly iron, use the new Kalbach-87 formalism (File 6-Law 1-Lang 2) which also has coupled energy-angle scattering.

III. MCNP Calculations

Of the 124 cross sections in the MCNP ENDF/B-VI library, 34 are used in the Livermore pulsed sphere benchmark. These were compared to the ENDF/B-V library and the MCNP Recommended Library, which is the ENDF/B-V library with some Los Alamos group T-2 evaluations included. Table II lists the cross-section files used in the calculations. Although only three T-2 evaluations from the MCNP Recommended Library are used, they affect fifteen of the twenty-eight experiments, because iron is included in many of the spheres. The T-2 libraries are referred to as T-2 Recommended or MCNP Recommended because they are presently the MCNP Recommended Cross-Section Evaluations, and they were evaluated by the Los Alamos National Laboratory Nuclear Theory and Applications Group, T-2.

The problems were used as given in LA-12212,¹¹ except that the time bin structure was divided into 2 nanosecond bins over the entire range to correspond to the experimental data. Sample input decks for some of the problems can be found in the appendix.

TABLE I. Livermore Pulsed Spheres Target Material Outline.

Material	Radius (mfp)	Used for ENDF/B-VI
^6Li	0.5	✓
	1.1	
	1.6	✓
^7Li	0.5	✓
	1.0	
	1.6	✓
Beryllium	0.8	✓
Carbon	0.5	✓
	1.3	
	2.9	✓
Nitrogen	1.1	✓
	3.1	✓
Oxygen	0.7	✓
Magnesium	0.7	✓
	1.2	
	1.9	✓
Aluminum	0.9	✓
	1.6	
	2.6	✓
Titanium	1.2	✓
	2.2	
	3.5	✓
Iron	0.9	✓
	2.9	
	4.8	✓
Lead	1.4	✓
H_2O	1.1	✓
	1.9	✓

TABLE I (cont.) Livermore Pulsed Spheres Target Material Outline.

Material	Radius (mfp)	Used for ENDF/B-VI
D_2O	1.2	✓
	2.1	✓
CH_2	0.7	✓
	1.6	
	3.0	✓
CF_2	0.9	✓
	1.8	
	2.9	✓
Concrete	2.0	✓
	3.8	

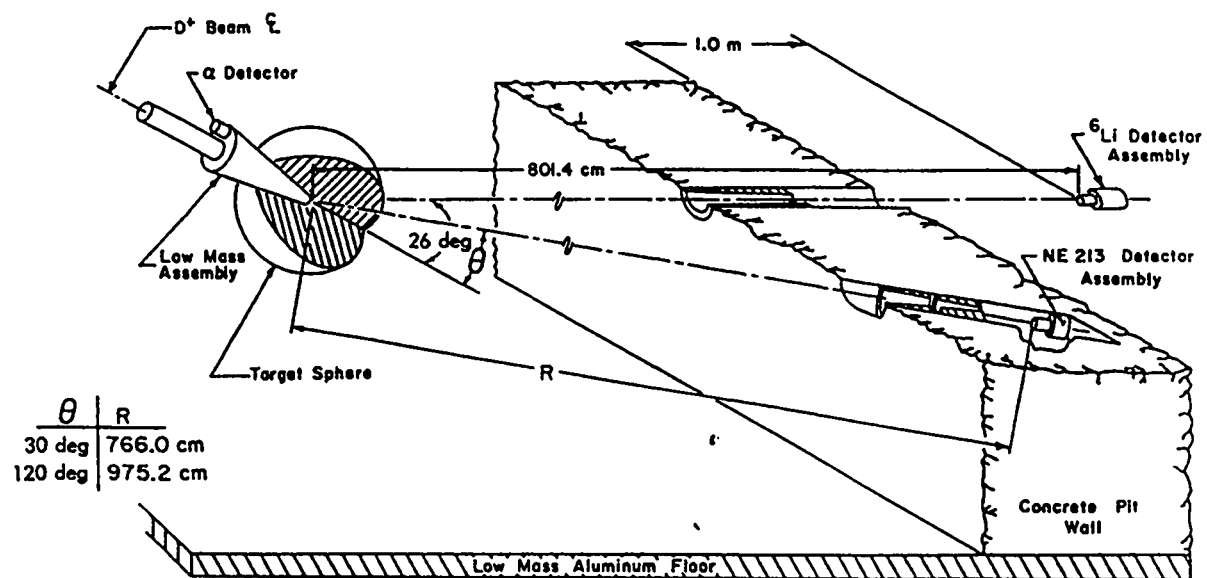


Fig. 1. Lawrence Livermore pulsed spheres experimental layout.

TABLE II. Data Set Comparison.

Material	ENDF/B-V	MCNP Rec.	ENDF/B-VI	At. %
¹ H	1001.50c		1001.60c	100
² D	1002.50c	1002.55c	1002.60c	100
⁶ Li	3006.50c		3006.60c	100
⁷ Li	3007.50c	3007.55c	3007.60c	100
⁹ Be	4009.50c		4009.60c	100
Carbon	6000.50c		6000.60c	100
¹⁴ N	7014.50c		7014.60c	100
¹⁶ O	8016.50c		8016.60c	100
¹⁹ F	9019.50c		9019.60c	100
²³ Na	11023.50c		11023.60c	100
Magnesium	12000.50c		12000.60c	100
²⁷ Al	13027.50c		13027.60c	100
Silicon	14000.50c		14000.60c	100
³¹ P	15031.50c		15031.60c	100
³² S	16032.50c		16032.60c	100
Calcium	20000.50c		20000.60c	100
Titanium	22000.50c		22000.60c	100
Chromium	24000.50c		24050.60c 24052.60c 24053.60c 24054.60c	4.345 83.79 9.5 2.365
⁵⁵ Mn	25055.50c		25055.60c	100
Iron	26000.50c	26000.55c	26054.60c 26056.60c 26057.60c 26058.60c	5.9 91.72 2.1 0.28
Nickel	28000.50c		28058.60c 28060.60c 28061.60c 28062.60c 28064.60c	68.27 26.10 1.13 3.59 0.91
Lead	82000.50c		82206.60c 82207.60c 82208.60c	24.1 22.1 52.4

Integrated values were produced by integrating the binned results of the MCNP calculations as well as the experimental data over the energy ranges 12 to 16 MeV, and 2 to 16 MeV. These energy ranges were chosen based on the relativistic time it would take a neutron of a certain energy to pass through a vacuum to a specified detector location. Specifically, for detector distances on the order of 750 cm, the value corresponding to 12 MeV was taken to be 16 Shakes, and for detector distances on the order of 950 cm, the value corresponding to 12 MeV was taken to be 20.5 Shakes. Thus, the energy range 12 to 16 MeV was approximately modeled by the time bin range of 16 Shakes or less for the 750 cm distance, and by the time bin range of 20.5 Shakes or less for the 950 cm distance. Furthermore, the 2 to 16 MeV energy range was approximately modeled by the time bin range of 35 Shakes or less for the 750 cm distance, and 47.7 Shakes or less for the 950 cm distance. All contributions from times above 35 and 47.7 Shakes were negligible and ignored. The upper energy value is not truly given by the value of 16 MeV. The upper energy range is actually taken out as far as values are available for each problem.

The MCNP calculations have to be normalized in relation to the flux registered at the detector in air only. Thus, in order to compare experimental to calculational results, the calculational results must be divided by the source flux in air.

IV. Results

The results for the ENDF/B-V, MCNP Recommended, and ENDF/B-VI libraries are compared to experimental results in Figures 2 through 100. These plots show that the ENDF/B-VI results generally give better or comparable results to ENDF/B-V except as noted below.

Table III contains the integrated results for the three data libraries. In general, ENDF/B-VI gives as good as or better results than ENDF/B-V. In the case of ^7Li , beryllium, nitrogen, iron, lead, polyethylene, and teflon, these new ENDF/B-VI evaluations give better results than ENDF/B-V. For magnesium, aluminum, titanium, and concrete, the results are much the same in both cases, which is to be expected because magnesium, aluminum, and titanium are merely the same data translated from ENDF/B-V to ENDF/B-VI and reprocessed with NJOY.

Some of the results were mixed, such as ^6Li . The 0.5 and 1.6 mfp 12-16 MeV results were not as good, while the 2-16 MeV range showed as good or better results from ENDF/B-VI. For iron, ENDF/B-VI provided better results, except for the 4.8 mfp 12-16 MeV range, where ENDF/B-VI proved much better than ENDF/B-V, but not as good as the MCNP Recommended Library, which is a special iron evaluation developed by the Los Alamos National Laboratory Nuclear Theory and Applications Group, T-2, for the Fusion Materials Irradiation Test Facility (FMIT).¹² Better results were obtained for ENDF/B-VI beryllium in the 12-16 MeV range, whereas the 2-16 MeV range showed somewhat poorer results.

Of the three T-2 evaluations in the MCNP Recommended Library, iron appears better than ENDF/B-VI, and much better than ENDF/B-V. For ^7Li , ENDF/B-VI and the T-2 evaluation agree, and from Table III, give somewhat better results than ENDF/B-V. In the case of deuterium, T-2 agrees with ENDF/B-V, and ENDF/B-VI gives poorer results.

In the cases of oxygen, water, and heavy water, the results from ENDF/B-VI are not as good as ENDF/B-V, but the difference in most cases was small.

The most significant difference between ENDF/B-VI and experimental results occurs for 0.5 mfp carbon. The time-of-flight distribution for this particular case does not agree well with experimental results, as seen in Figures 21 through 26. However, from Table III it can be seen that the overall difference is not overwhelming, and is not any worse than the ENDF/B-V results for iron, lead, titanium, magnesium, and aluminum.

TABLE III. Ratio of Calculated to Experimental Results.

Material	Radius (mfp)	Energy Range (MeV)	ENDF/B-V	MCNP Rec.	ENDF/B-VI
${}^6\text{Li}$	0.5	12-16	0.980	0.982	0.951
		2-16	0.986	0.987	0.984
	1.6	12-16	1.022	1.028	0.929
		2-16	1.037	1.041	0.997
${}^7\text{Li}$	0.5	12-16	0.961	0.992	0.993
		2-16	0.983	0.990	0.989
	1.6	12-16	0.940	1.036	1.032
		2-16	1.003	1.027	1.018
Beryllium	0.8	12-16	0.936	*	0.962
		2-16	1.000	*	0.988
Carbon	0.5	12-16	0.974	*	0.995
		2-16	0.994	*	1.022
	2.9	12-16	0.942	*	1.017
		2-16	0.971	*	1.066
Nitrogen	1.1	12-16	0.903	0.903	0.952
		2-16	0.965	0.965	0.988
	3.1	12-16	0.849	0.851	0.938
		2-16	0.982	0.983	1.017
Oxygen	0.7	12-16	0.934	0.934	0.927
		2-16	0.996	0.996	0.990
Magnesium	0.7	12-16	1.044	*	1.045
		2-16	1.033	*	1.032
	1.9	12-16	0.997	*	0.998
		2-16	0.965	*	0.965
Aluminum	0.9	12-16	0.939	*	0.939
		2-16	0.947	*	0.947
	2.6	12-16	0.794	*	0.796
		2-16	0.843	*	0.843

^aEnergy range corresponds to 16 Shakes or less for all materials except concrete, which corresponds to 20.5 Shakes or less.

^bEnergy range corresponds to 35 Shakes or less for all materials except concrete, which corresponds to 47.7 Shakes or less.

*No T-2 evaluations were contained in these materials.

TABLE III (cont.) Ratio of Calculated to Experimental Results.

Material	Radius (mfp)	Energy Range (MeV)	ENDF/B-V	MCNP Rec.	ENDF/B-VI
Titanium	1.2	12-16	1.060	*	1.063
		2-16	0.988	*	0.988
	3.5	12-16	1.088	*	1.088
		2-16	0.945	*	0.943
Iron	0.9	12-16	0.989	1.001	0.999
		2-16	0.984	1.007	1.006
	4.8	12-16	0.866	0.934	0.903
		2-16	0.834	0.946	0.952
Lead	1.4	12-16	0.883	0.883	0.885
		2-16	0.861	0.860	0.911
Water H_2O	1.1	12-16	0.897	0.898	0.891
		2-16	0.955	0.995	0.947
	1.9	12-16	1.015	1.014	1.005
		2-16	1.074	1.073	1.062
Heavy Water D_2O	1.2	12-16	0.875	0.875	0.868
		2-16	0.927	0.922	0.912
	2.1	12-16	1.015	0.986	0.975
		2-16	1.029	1.024	1.012
Polyethylene CH_2	0.7	12-16	0.973	*	0.991
		2-16	1.002	*	1.020
	3.0	12-16	0.898	*	0.953
		2-16	0.988	*	1.038
Teflon CF_2	0.9	12-16	0.962	*	1.027
		2-16	0.978	*	1.045
	2.9	12-16	0.754	*	0.920
		2-16	0.778	*	0.942
Concrete	2.0	12-16	1.004	1.004	0.999
		2-16	1.052	1.052	1.042

^aEnergy range corresponds to 16 Shakes or less for all materials except concrete, which corresponds to 20.5 Shakes or less.

^bEnergy range corresponds to 35 Shakes or less for all materials except concrete, which corresponds to 47.7 Shakes or less.

*No T-2 evaluations were contained in these materials.

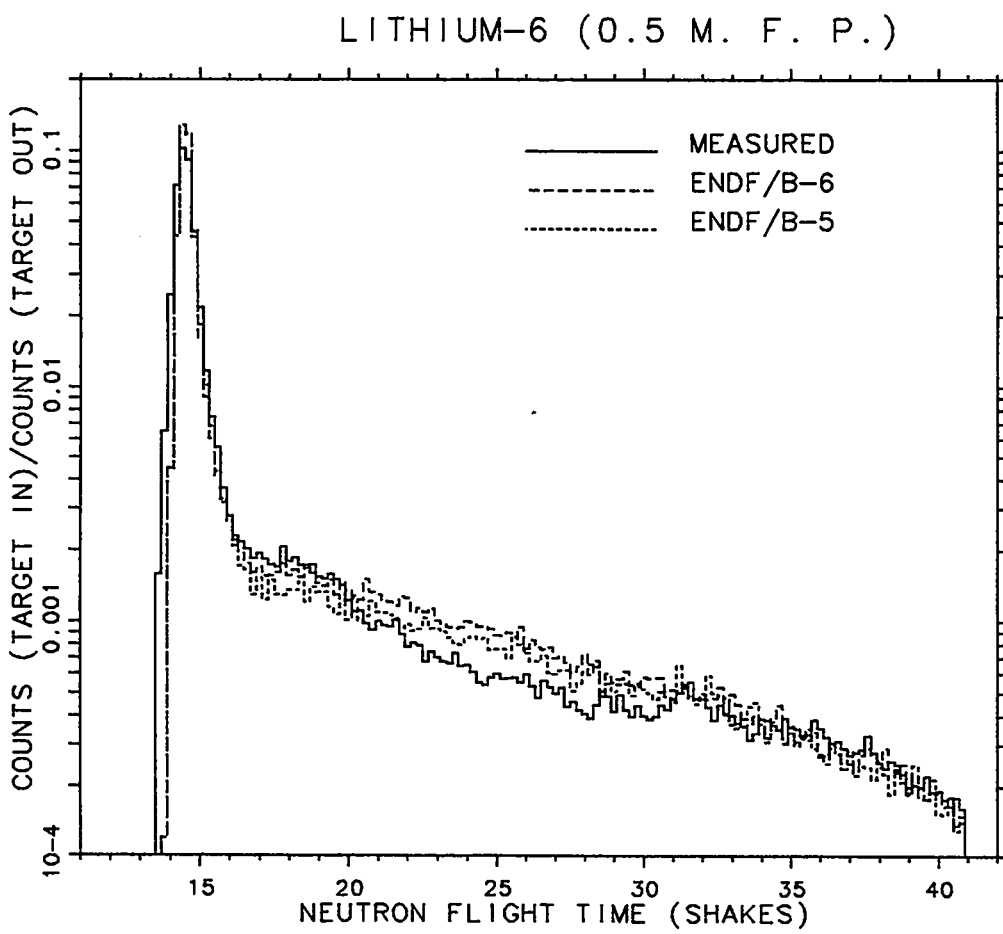


Fig. 2. Plot of experimental and calculated count rates as a function of time for a ${}^6\text{Li}$ sphere with 0.5 mean free path radius. The detector was located 765.2 cm from the center of the sphere at 30 degrees with respect to the deuteron beam. (1 shake = 10 ns)

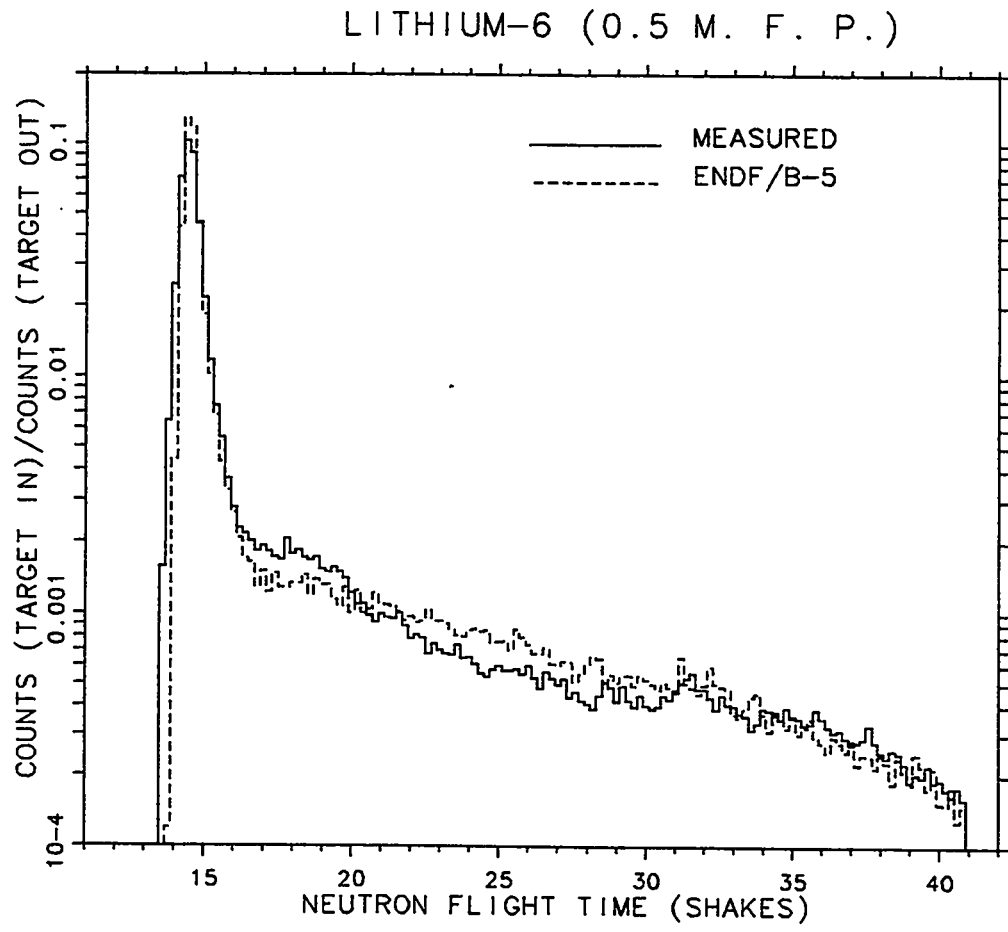


Fig. 3. Plot of experimental and ENDF/B-V calculated count rates for the ${}^6\text{Li}$ sphere of 0.5 mean free path radius.

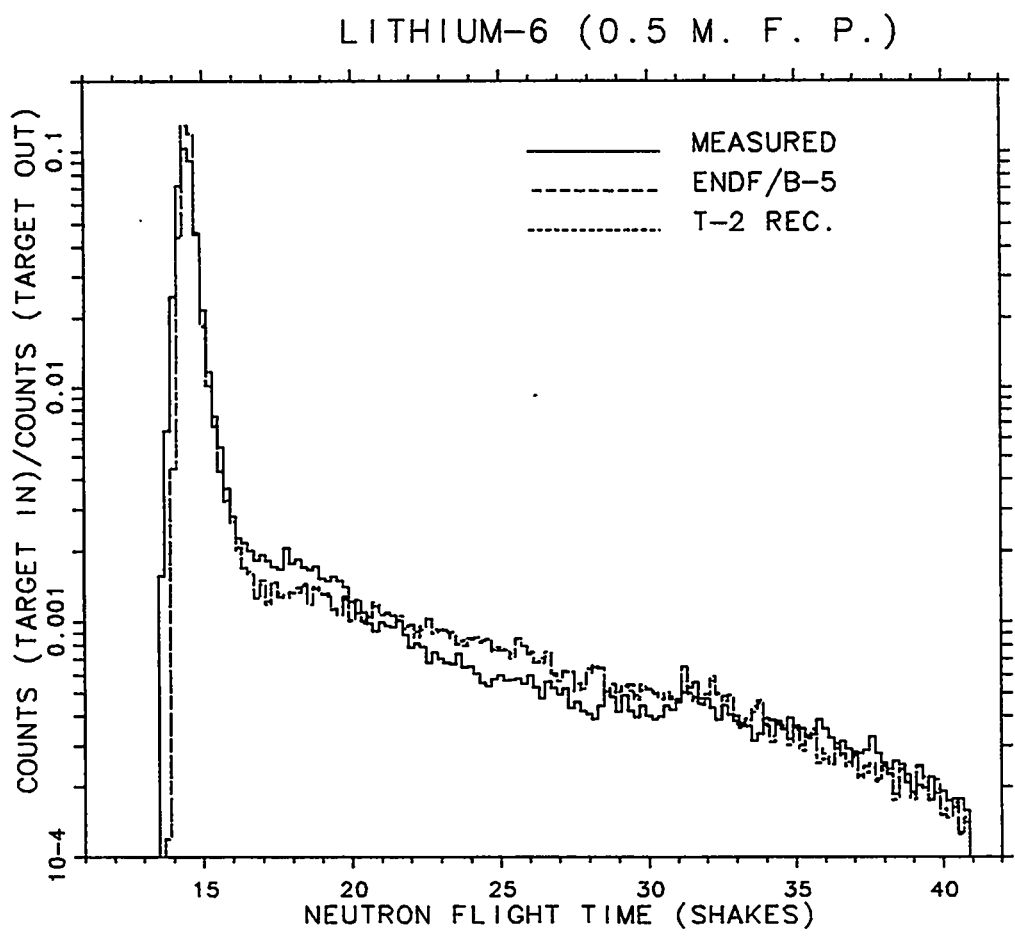


Fig. 4. Plot of experimental, ENDF/B-V calculated, and MCNP recommended calculated rates for the ${}^6\text{Li}$ sphere with 0.5 mean free path radius.

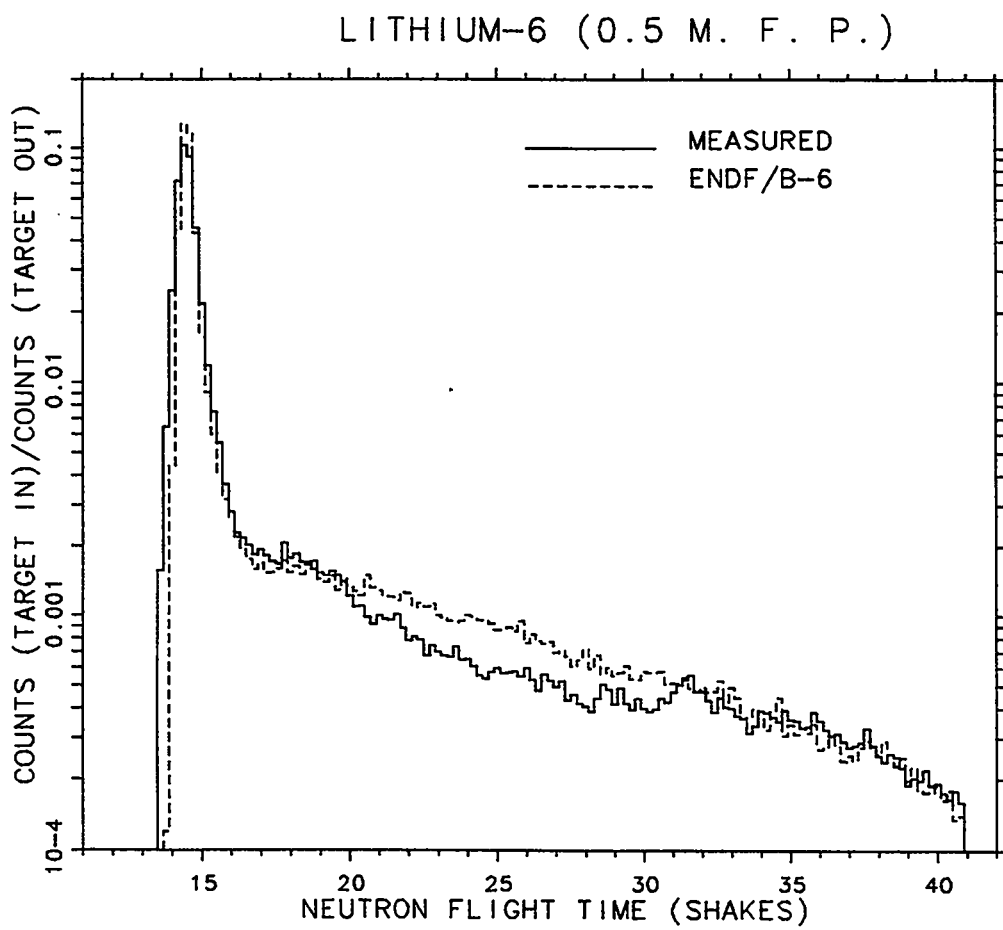


Fig. 5. Plot of experimental and ENDF/B-VI calculated count rates for the ${}^6\text{Li}$ sphere of 0.5 mean free path radius.

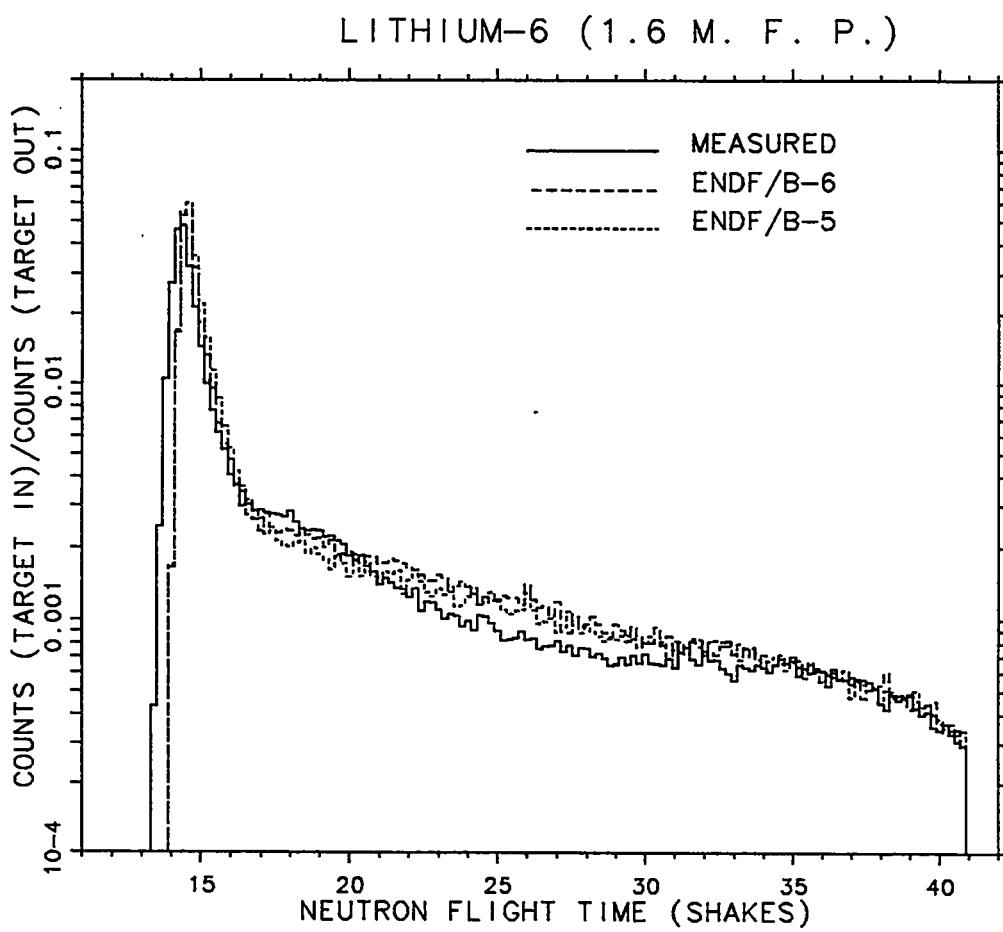


Fig. 6. Plot of experimental and calculated count rates as a function of time for an ${}^6\text{Li}$ sphere with 1.6 mean free path radius. The detector was located 765.2 cm from the center of the sphere at 30 degrees with respect to the deuteron beam. (1 shake = 10 ns)

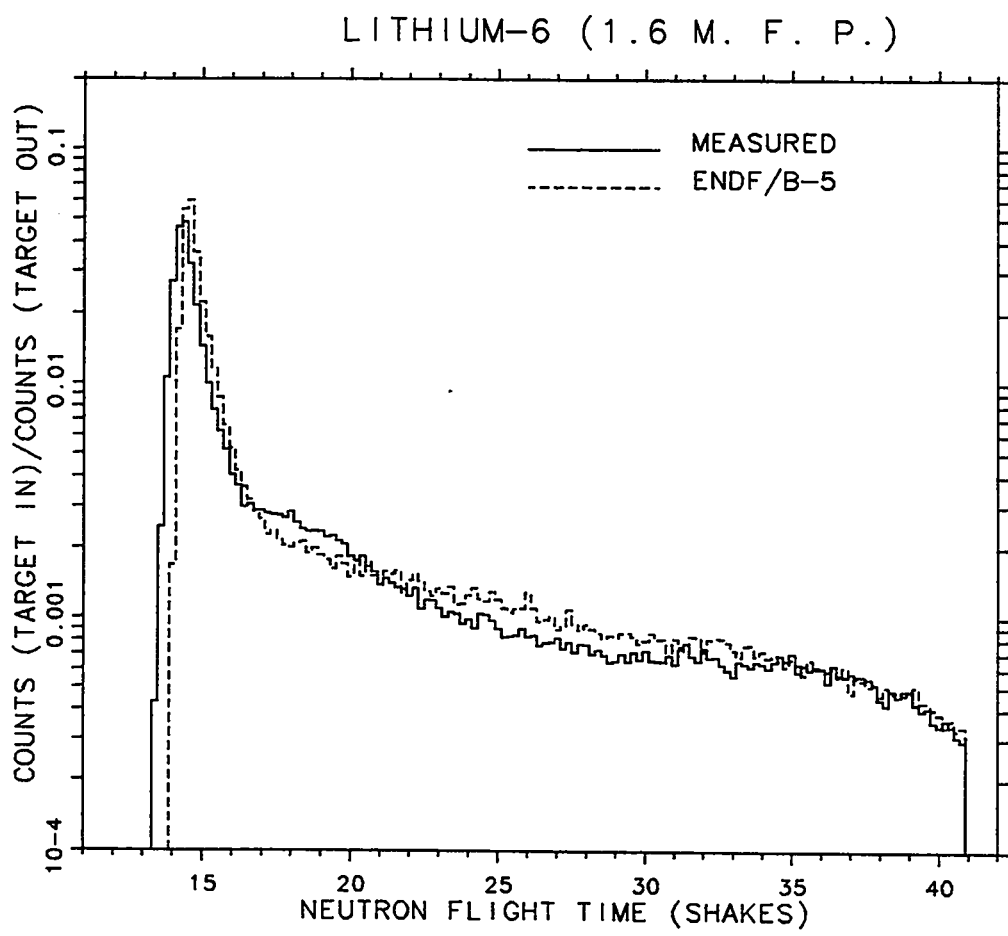


Fig. 7. Plot of experimental and ENDF/B-V calculated count rates for the ${}^6\text{Li}$ sphere of 1.6 mean free path radius.

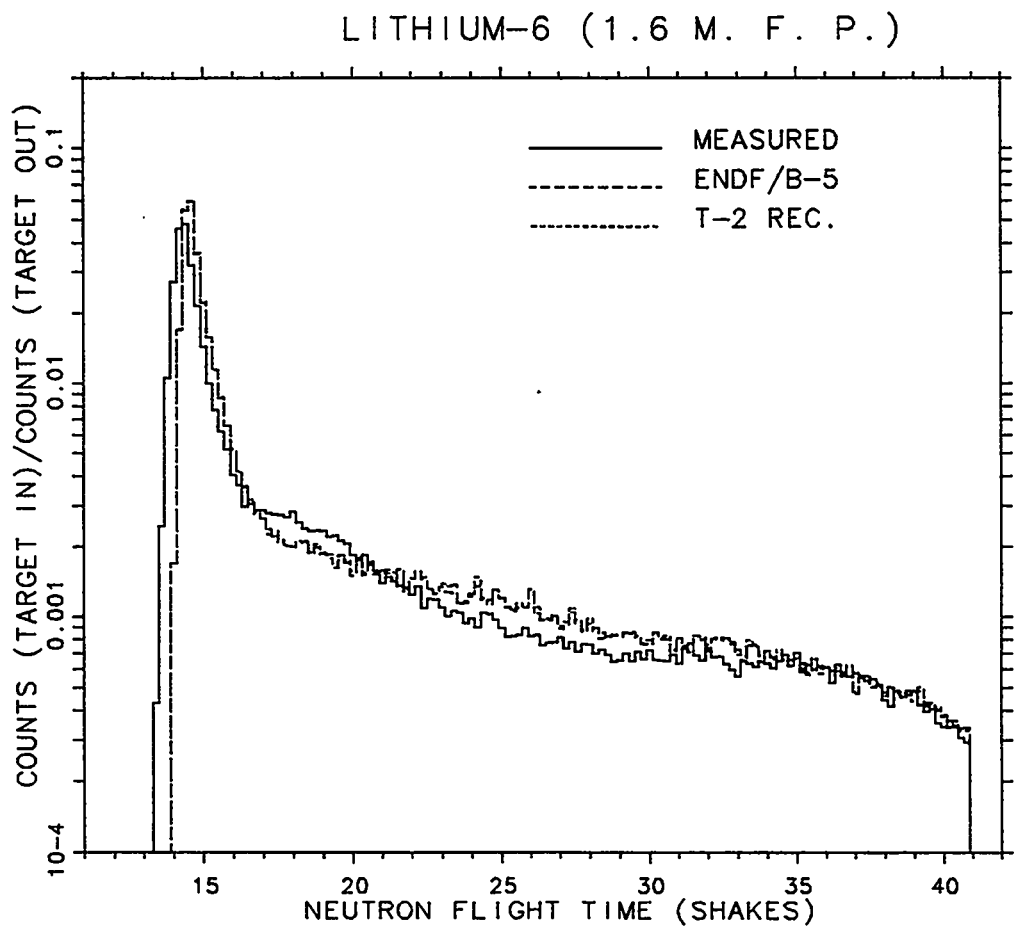


Fig. 8. Plot of experimental, ENDF/B-V calculated, and MCNP recommended calculated rates for the ${}^6\text{Li}$ sphere with 1.6 mean free path radius.

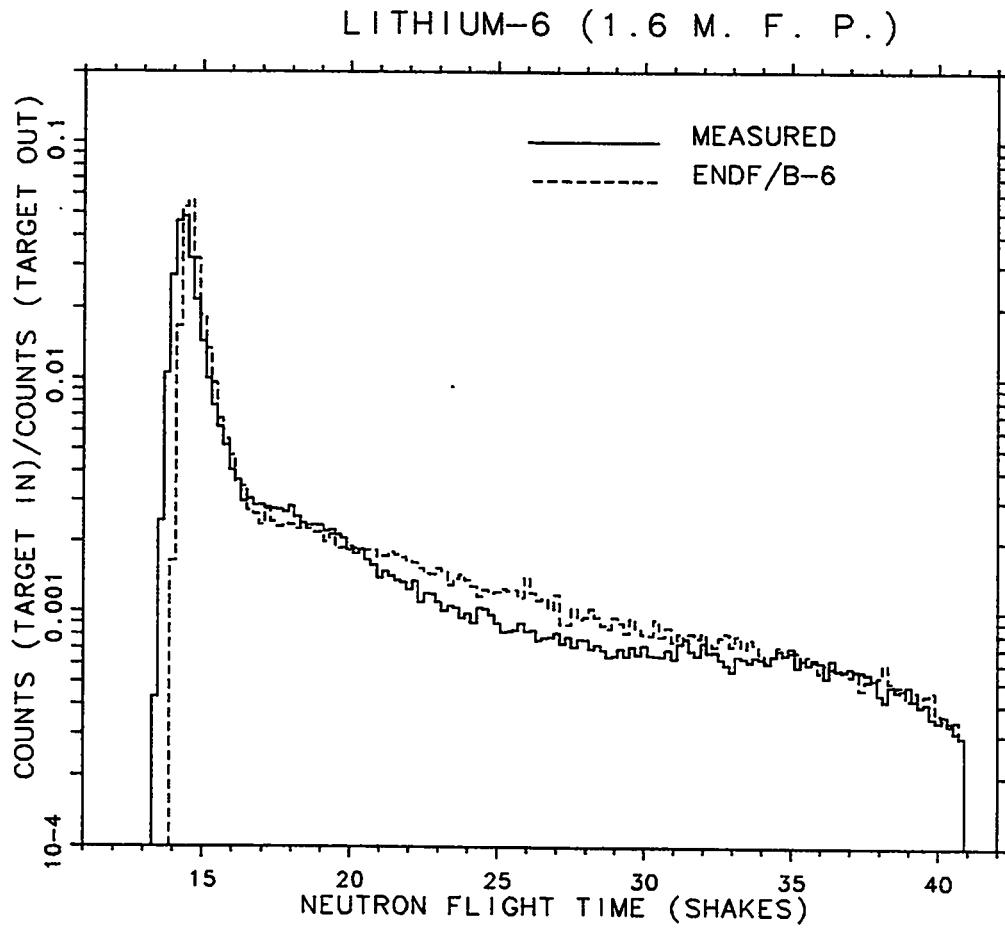


Fig. 9. Plot of experimental and ENDF/B-VI calculated count rates for the ${}^6\text{Li}$ sphere of 1.6 mean free path radius.

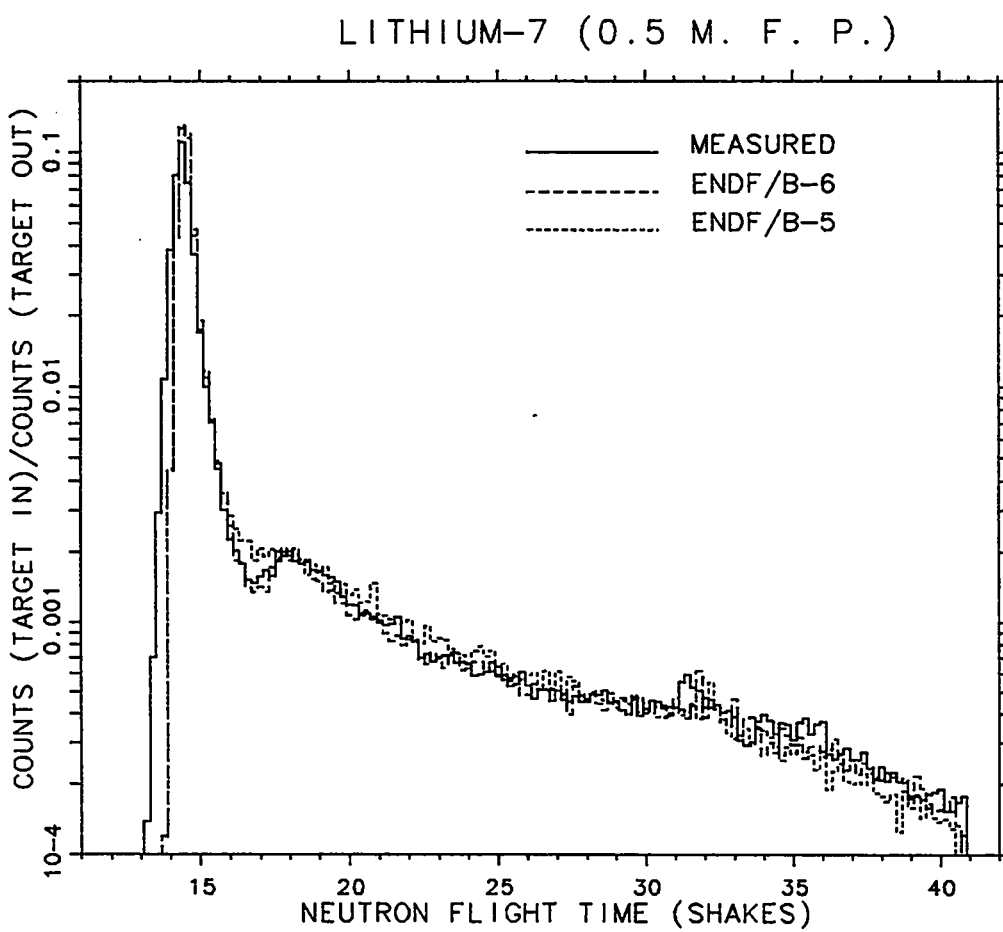


Fig. 10. Plot of experimental and calculated count rates as a function of time for a ${}^7\text{Li}$ sphere with 0.5 mean free path radius. The detector was located 765.2 cm from the center of the sphere at 30 degrees with respect to the deuteron beam. (1 shake = 10 ns)

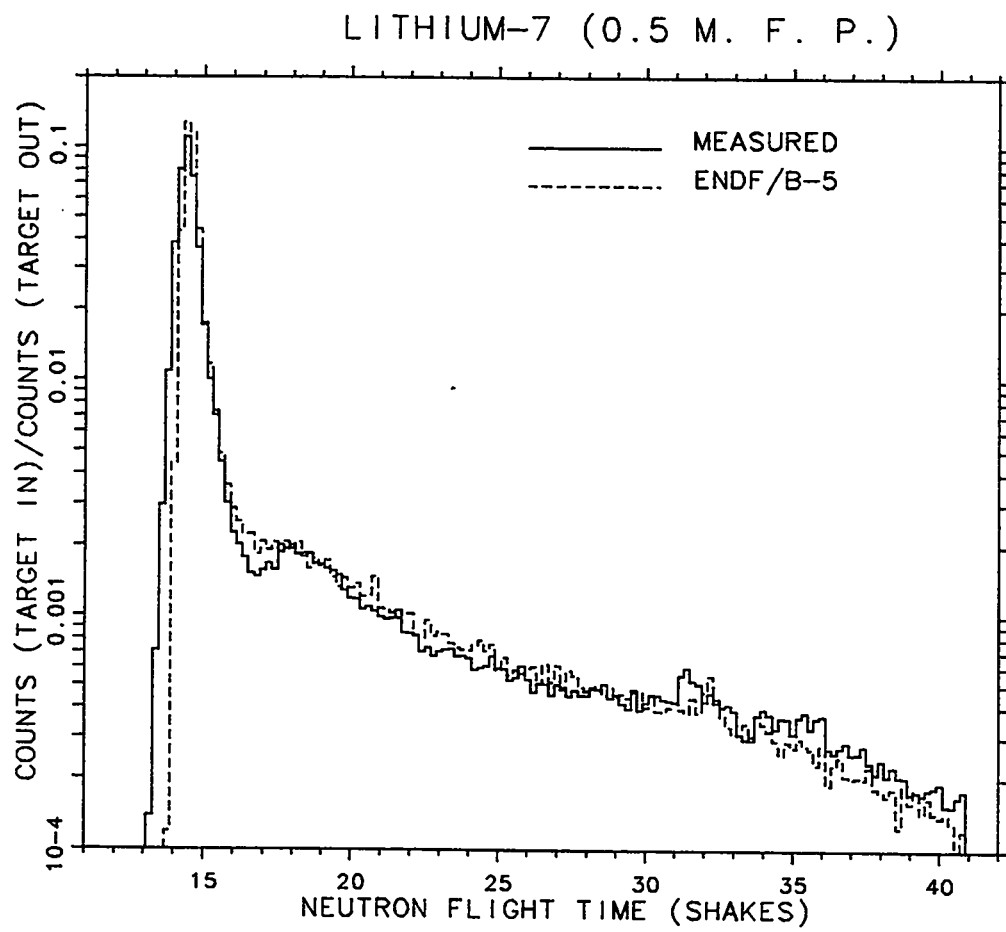


Fig. 11. Plot of experimental and ENDF/B-V calculated count rates for the ${}^7\text{Li}$ sphere of 0.5 mean free path radius.

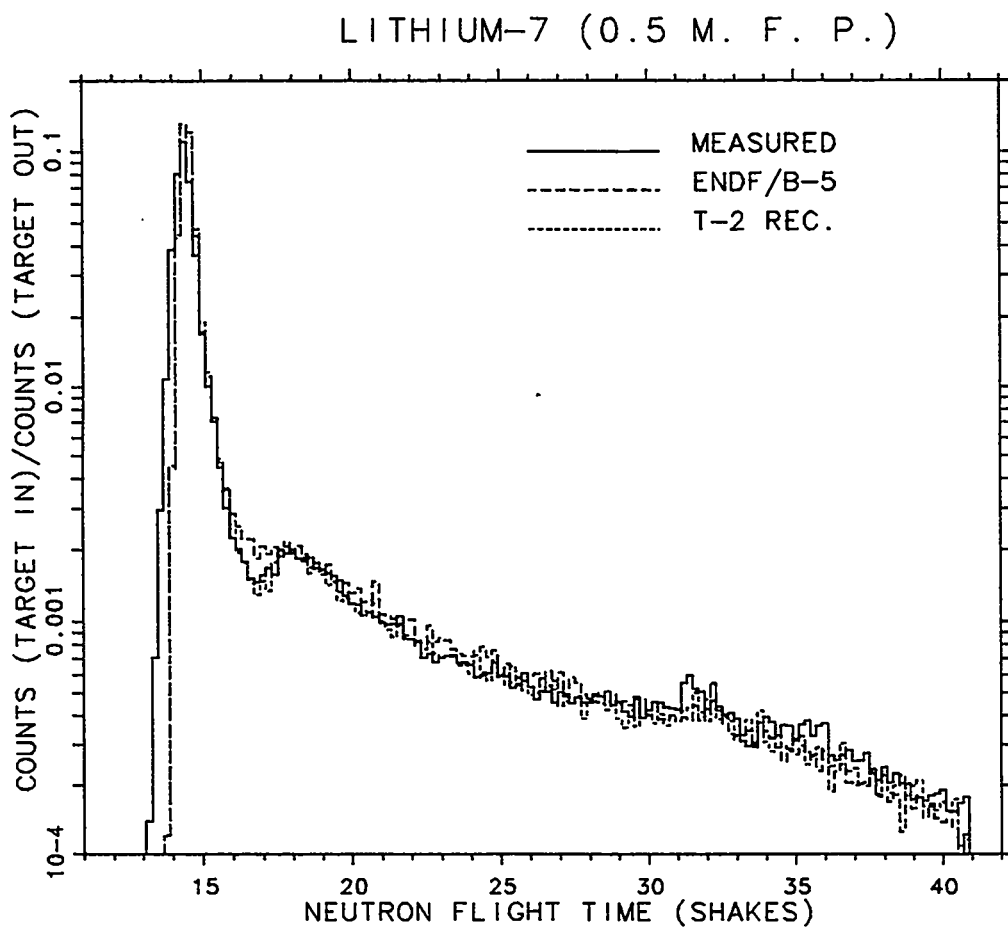


Fig. 12. Plot of experimental, ENDF/B-V calculated, and MCNP recommended calculated rates for the ^7Li sphere with 0.5 mean free path radius.

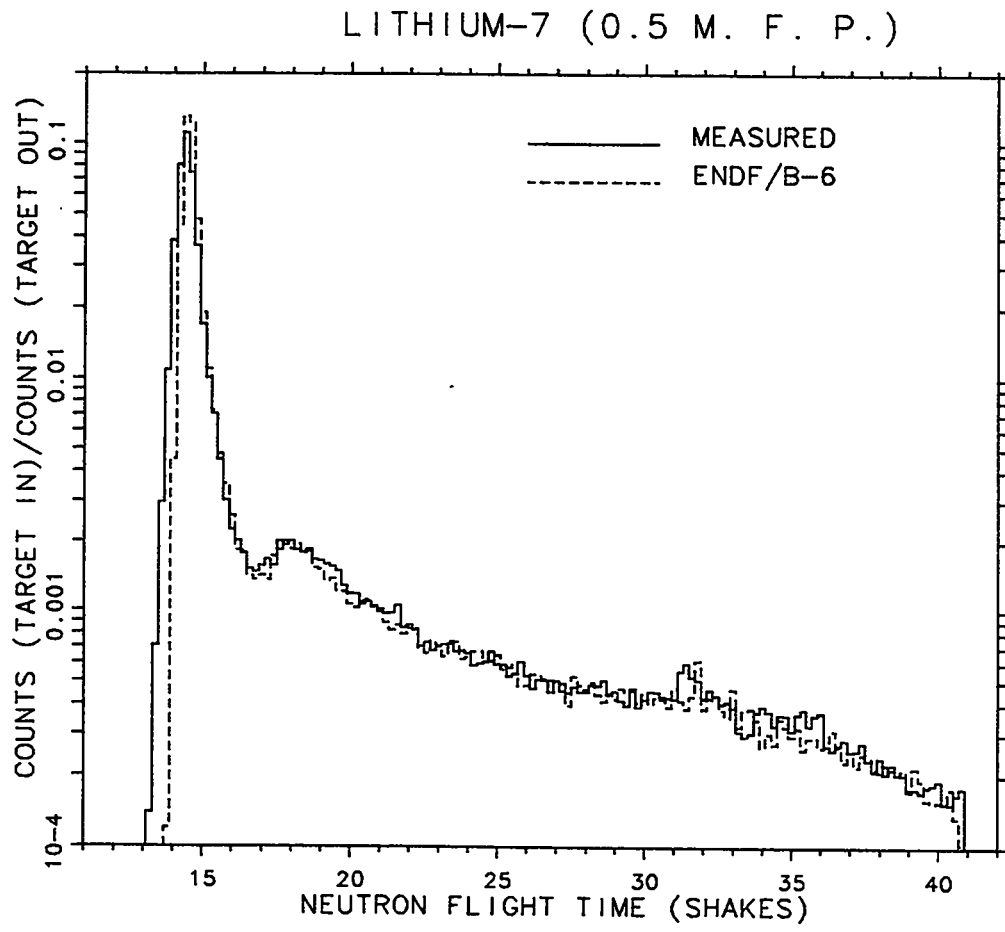


Fig. 13. Plot of experimental and ENDF/B-VI calculated count rates for the ${}^7\text{Li}$ sphere of 0.5 mean free path radius.

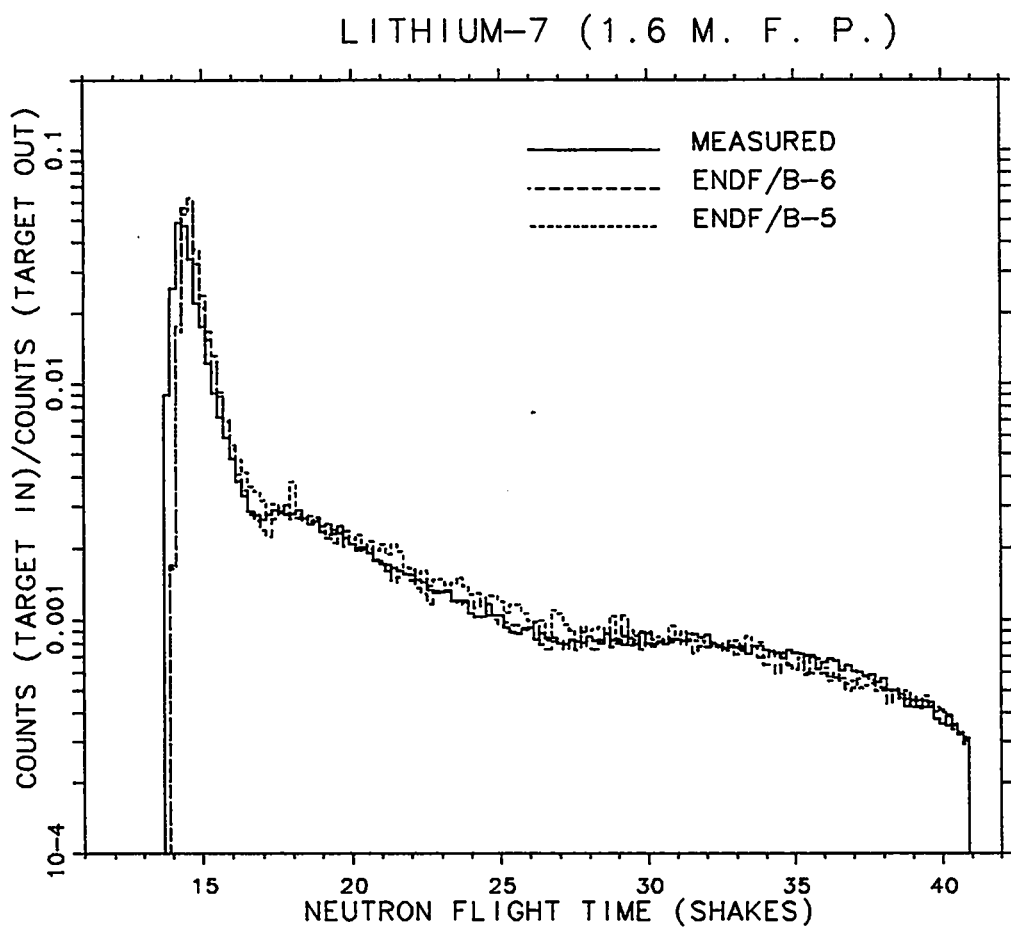


Fig. 14. Plot of experimental and calculated count rates as a function of time for a ^{7}Li sphere with 1.6 mean free path radius. The detector was located 765.2 cm from the center of the sphere at 30 degrees with respect to the deuteron beam. (1 shake = 10 ns)

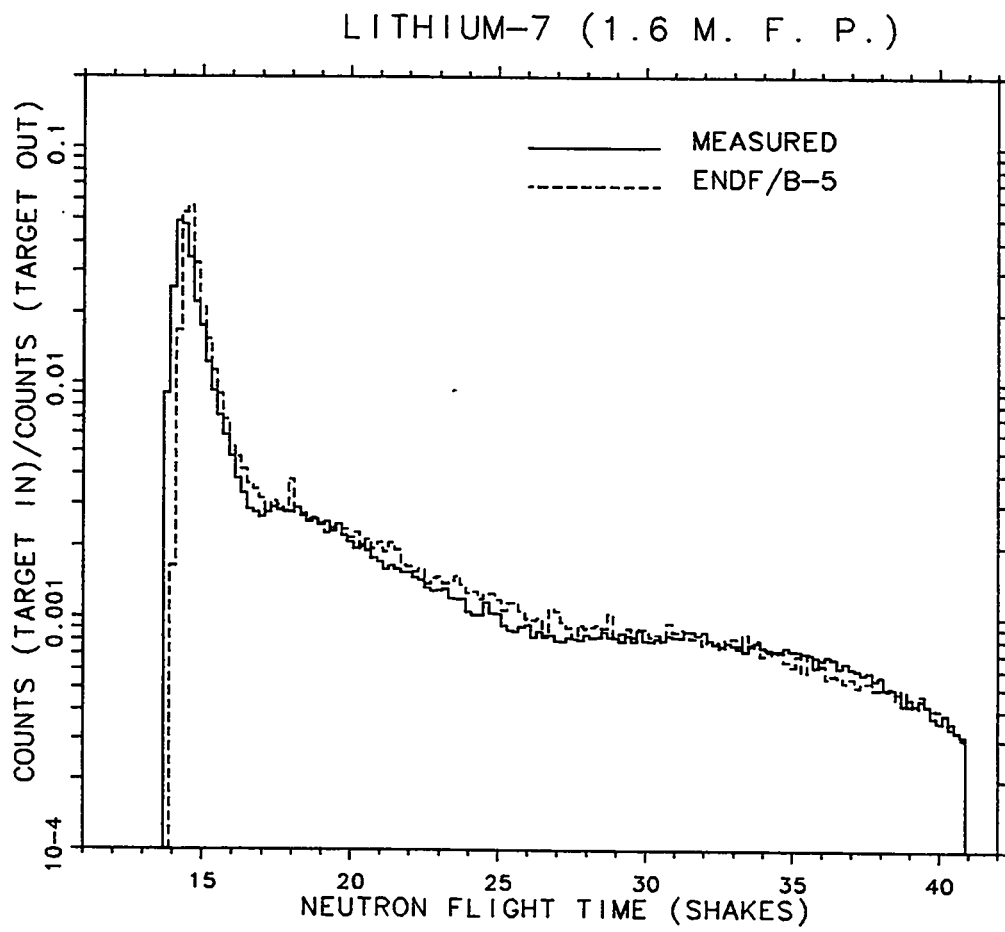


Fig. 15. Plot of experimental and ENDF/B-V calculated count rates for the ^7Li sphere of 1.6 mean free path radius.

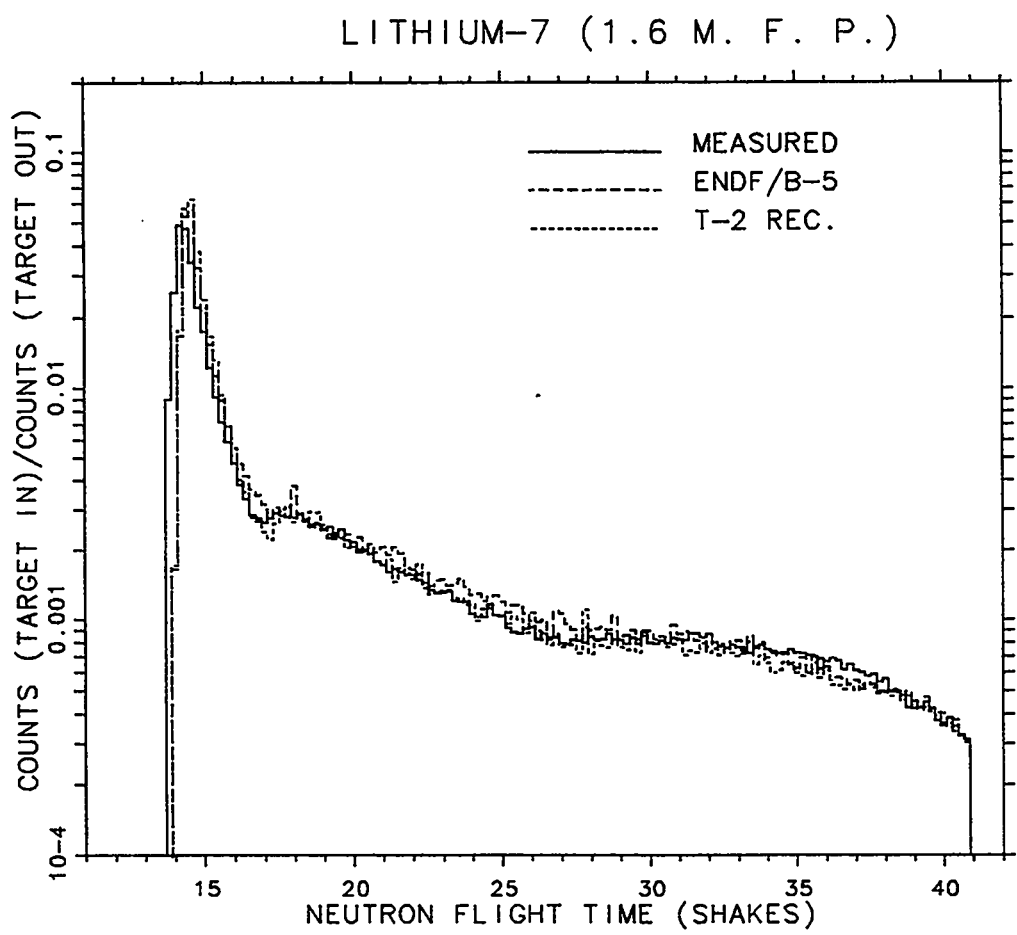


Fig. 16. Plot of experimental, ENDF/B-V calculated, and MCNP recommended calculated rates for the ^7Li sphere with 1.6 mean free path radius.

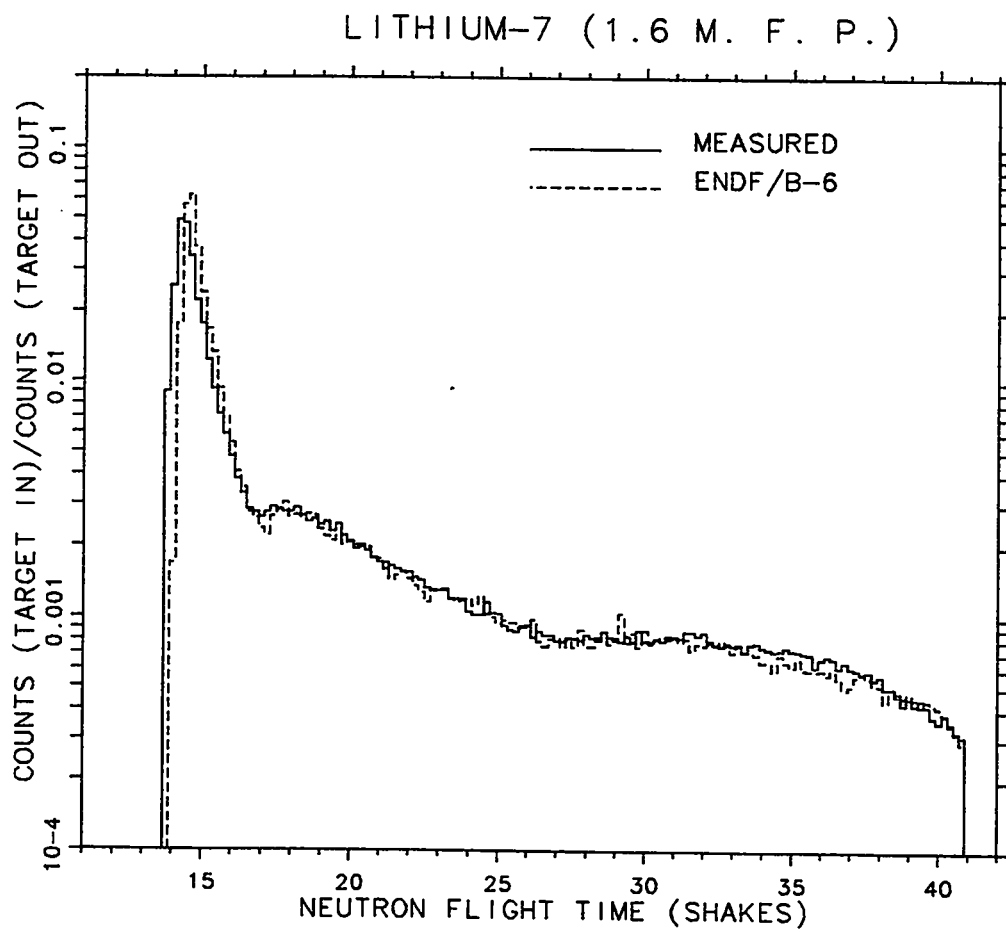


Fig. 17. Plot of experimental and ENDF/B-VI calculated count rates for the ${}^7\text{Li}$ sphere of 1.6 mean free path radius.

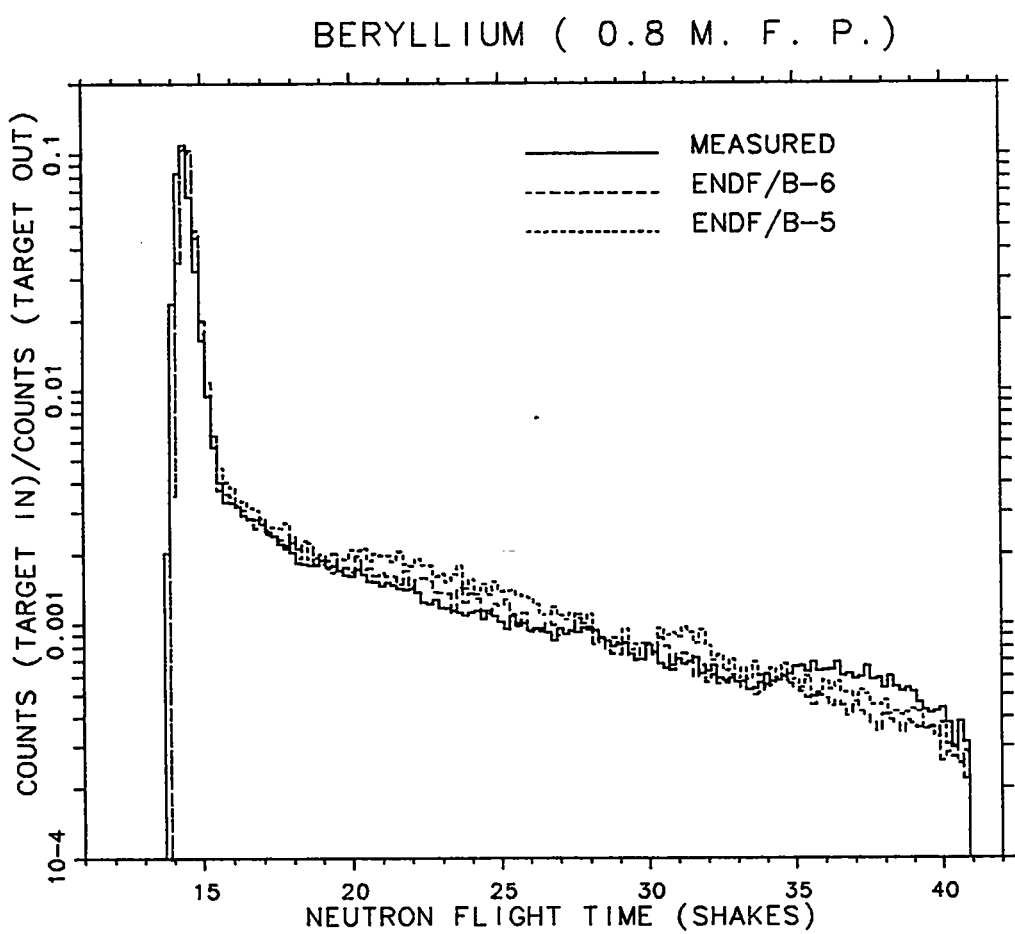


Fig. 18. Plot of experimental and calculated count rates as a function of time for a beryllium sphere with 0.8 mean free path radius. The detector was located 765.2 cm from the center of the sphere at 30 degrees with respect to the deuteron beam. (1 shake = 10 ns)

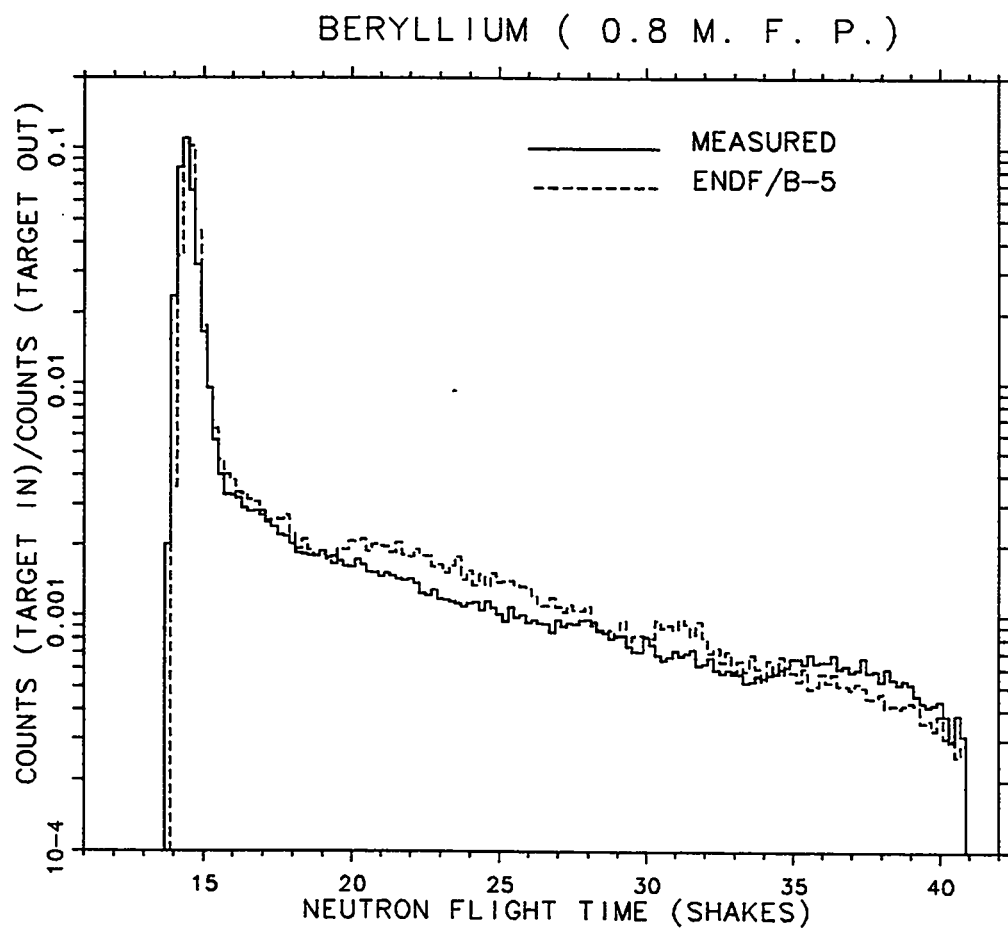


Fig. 19. Plot of experimental and ENDF/B-V calculated count rates for the beryllium sphere of 0.8 mean free path radius.

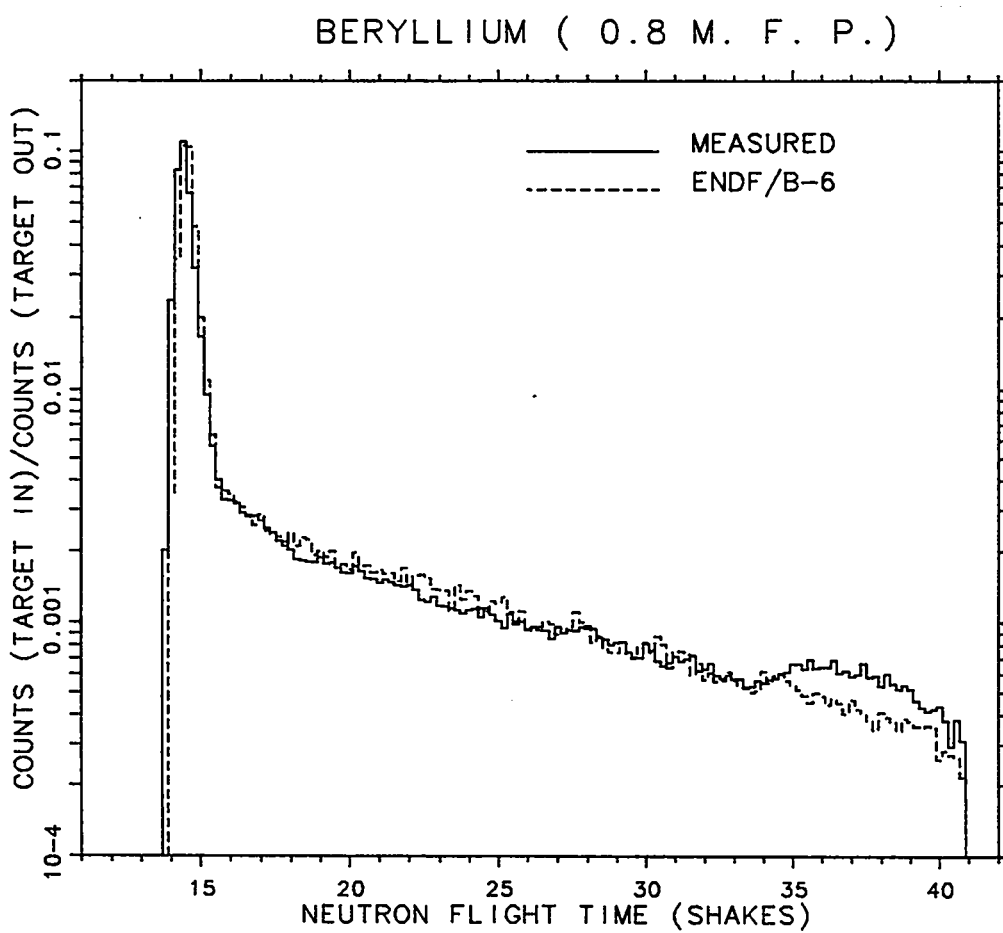


Fig. 20. Plot of experimental and ENDF/B-VI calculated count rates for the beryllium sphere of 0.8 mean free path radius.

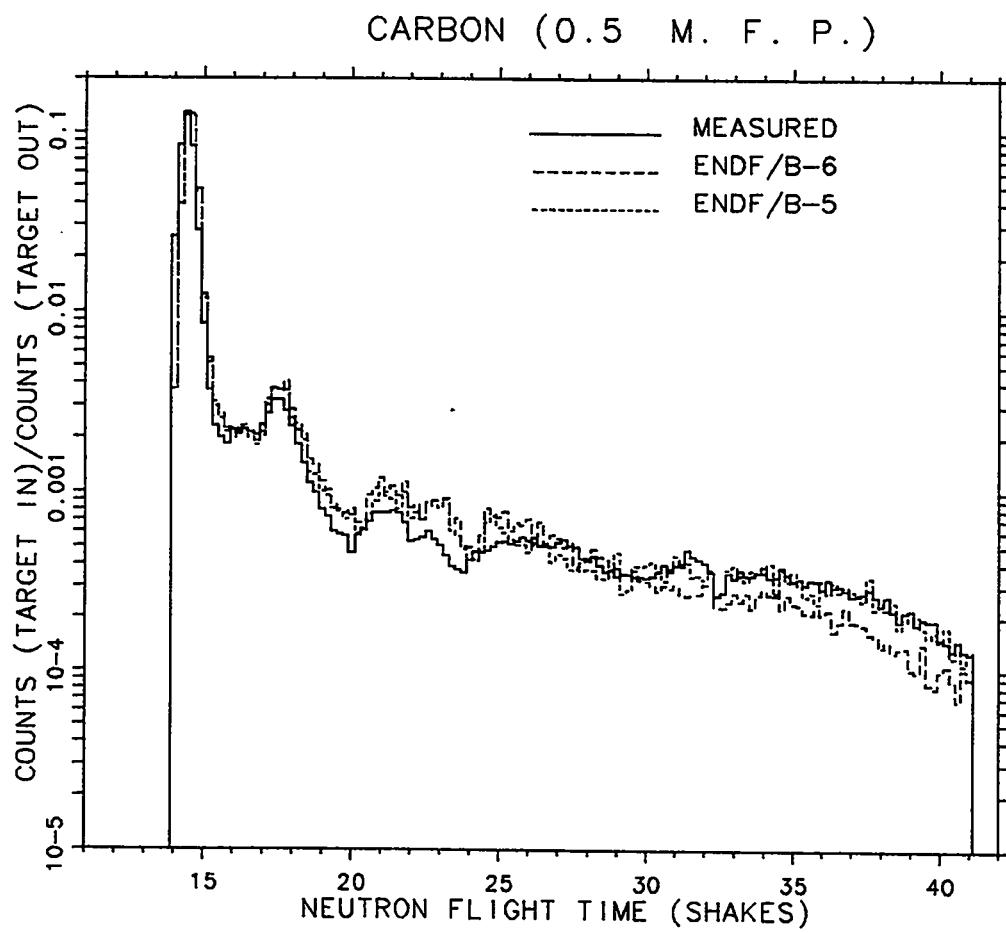


Fig. 21. Plot of experimental and calculated count rates as a function of time for a carbon sphere with 0.5 mean free path radius. The detector was located 766.0 cm from the center of the sphere at 30 degrees with respect to the deuteron beam. (1 shake = 10 ns)

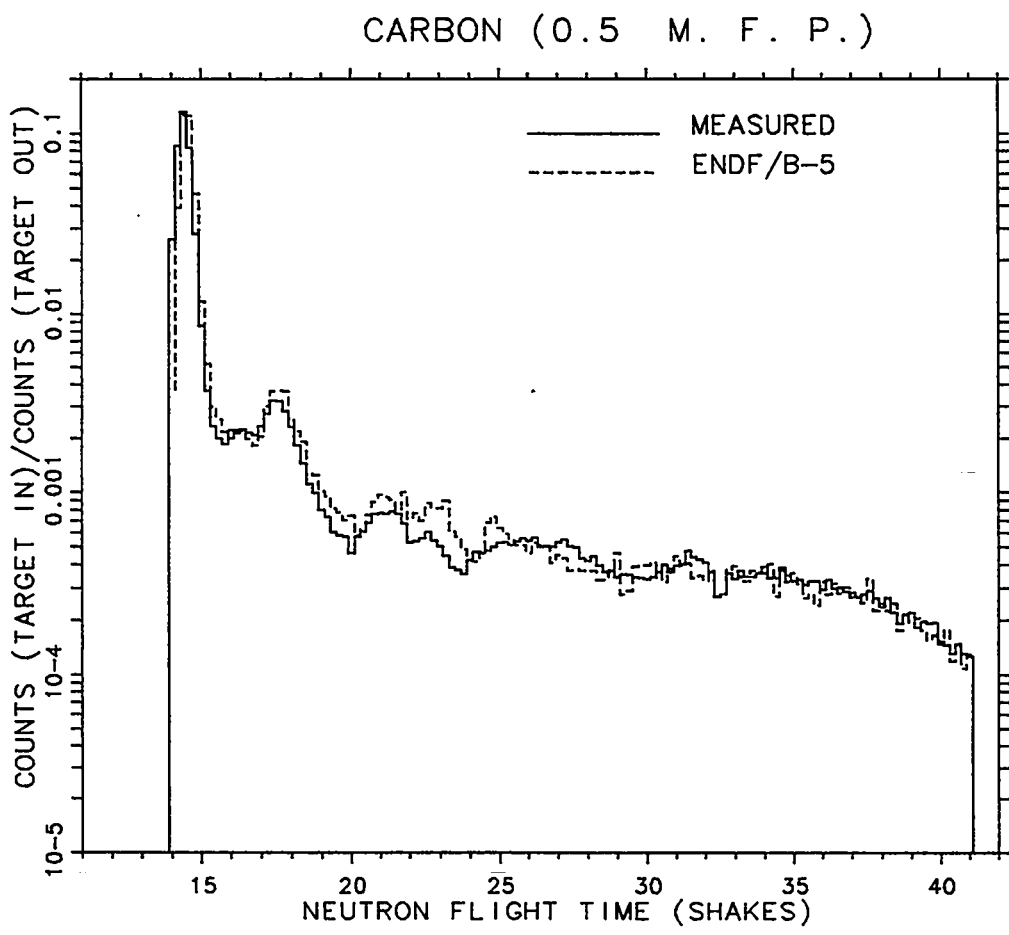


Fig. 22. Plot of experimental and ENDF/B-V calculated count rates for the carbon sphere of 0.5 mean free path radius.

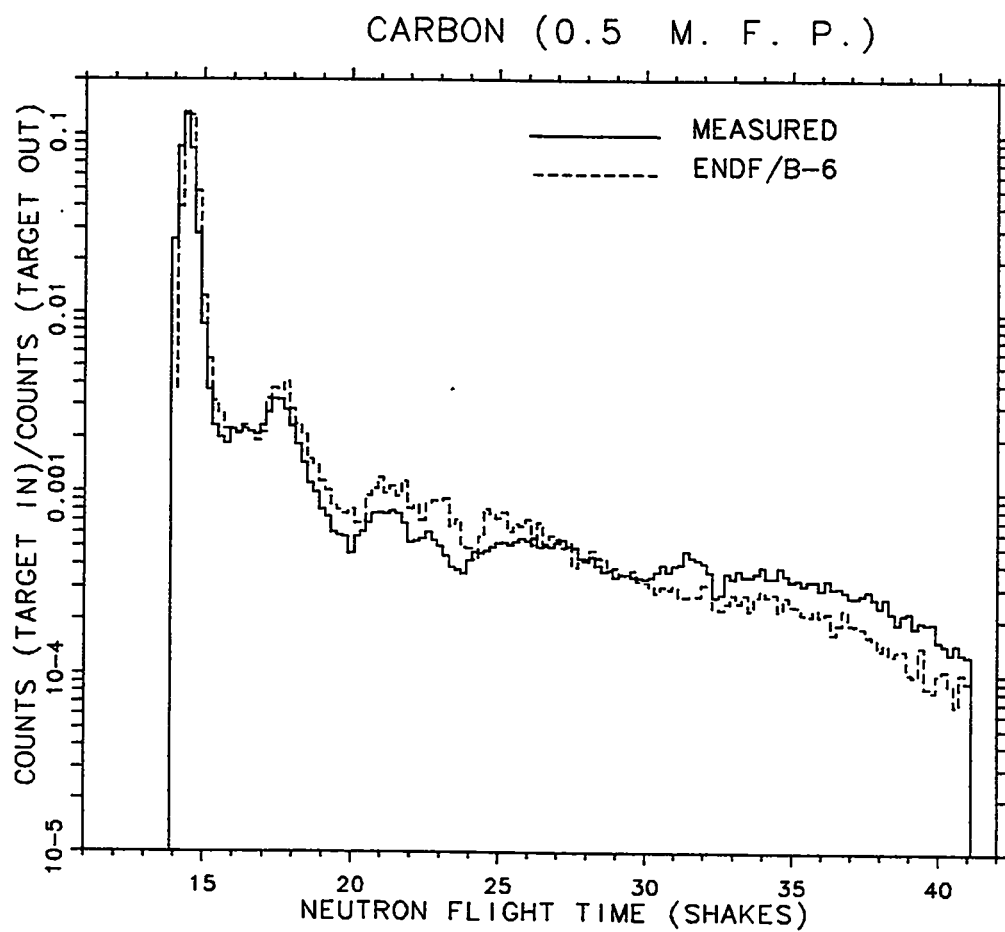


Fig. 23. Plot of experimental and ENDF/B-VI calculated count rates for the carbon sphere of 0.5 mean free path radius.

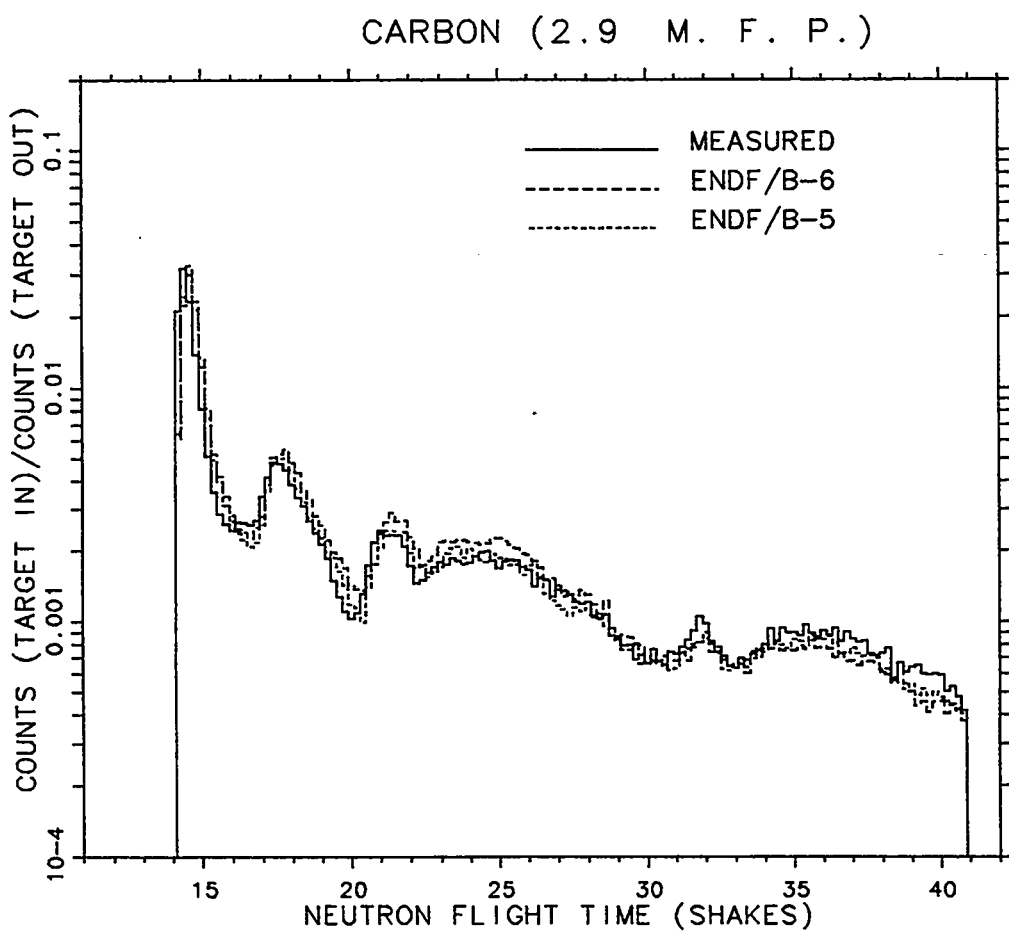


Fig. 24. Plot of experimental and calculated count rates as a function of time for a carbon sphere with 2.9 mean free path radius. The detector was located 766.0 cm from the center of the sphere at 30 degrees with respect to the deuteron beam. (1 shake = 10 ns)

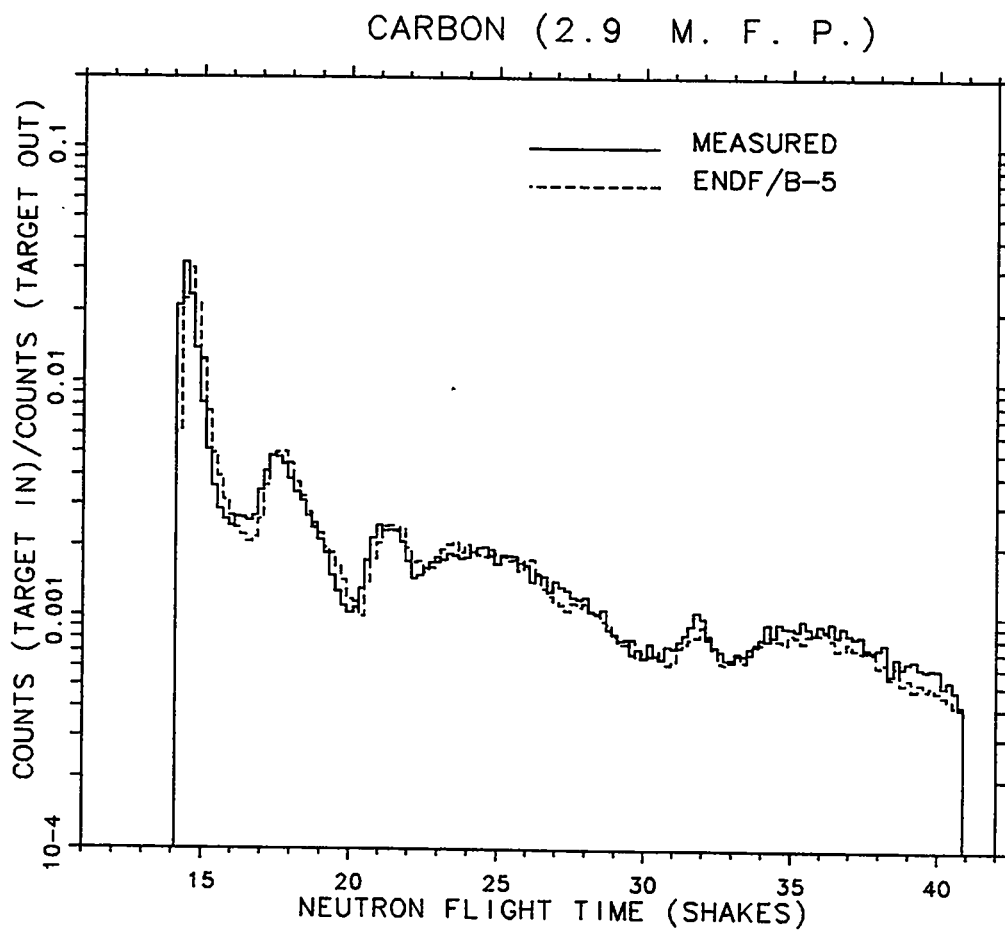


Fig. 25. Plot of experimental and ENDF/B-V calculated count rates for the carbon sphere of 2.9 mean free path radius.

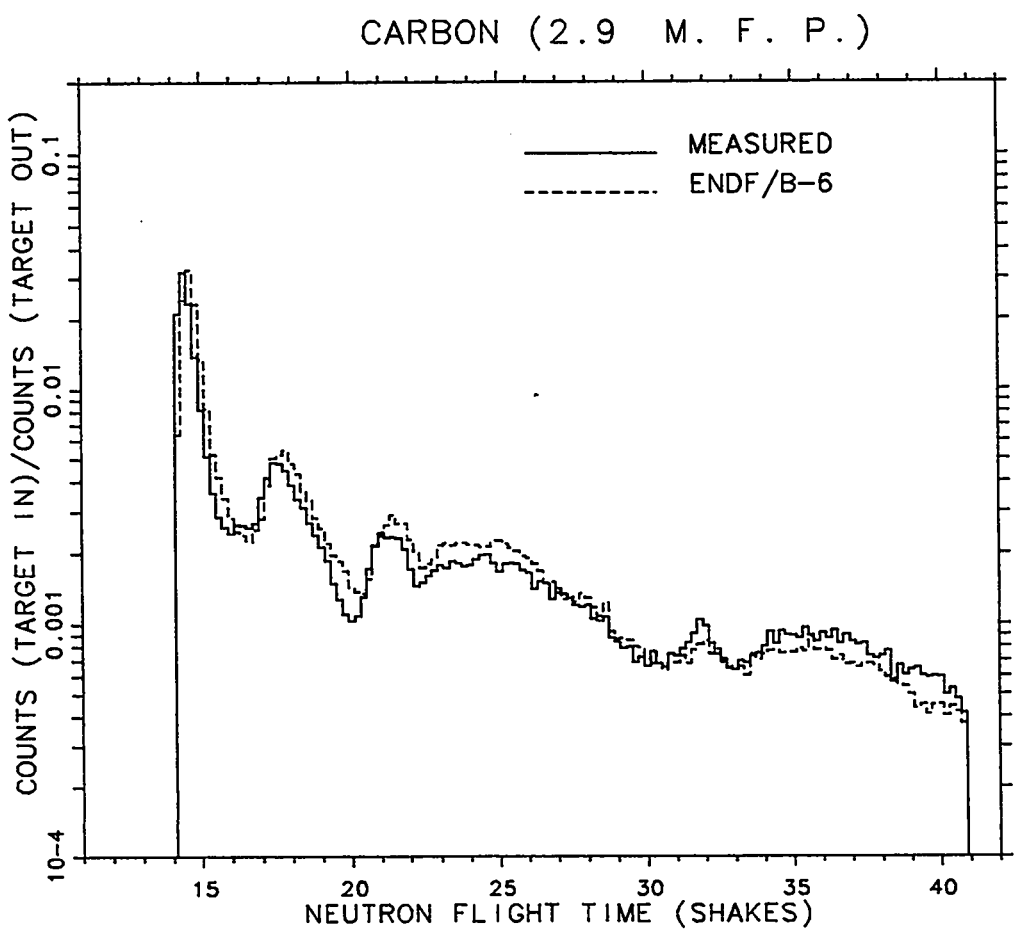


Fig. 26. Plot of experimental and ENDF/B-VI calculated count rates for the carbon sphere of 2.9 mean free path radius.

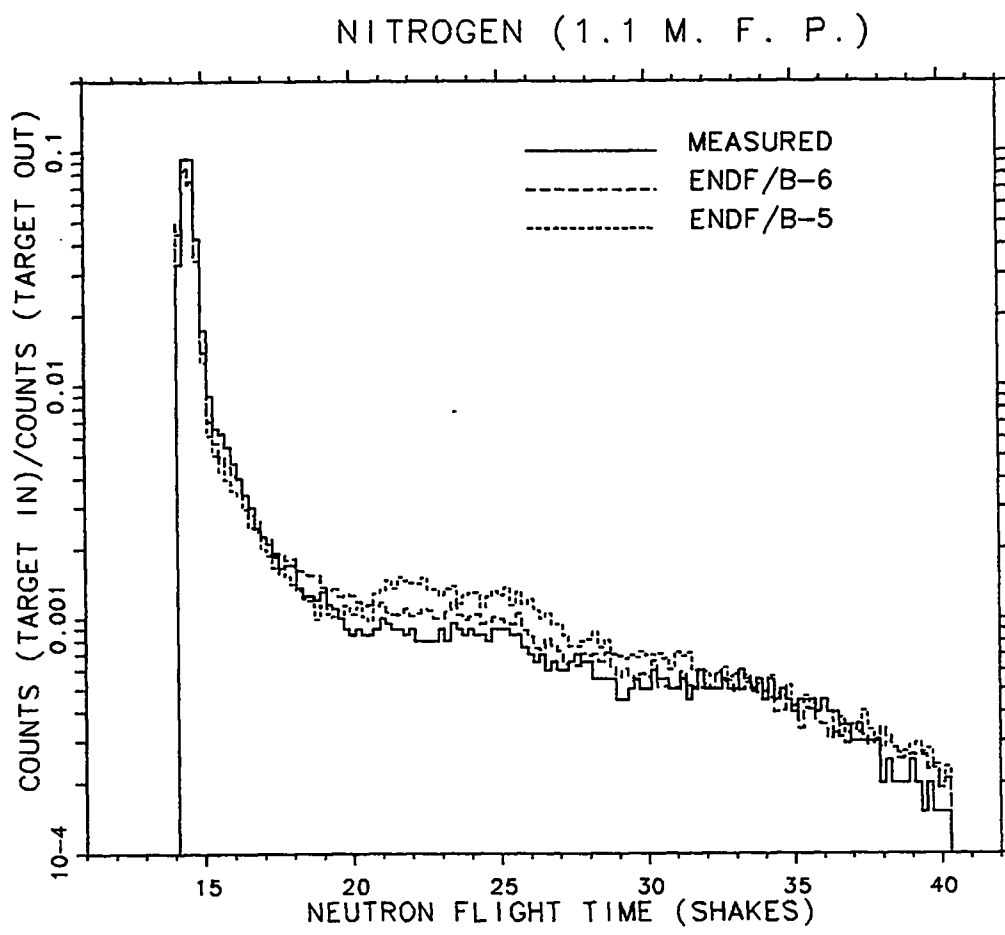


Fig. 27. Plot of experimental and calculated count rates as a function of time for an nitrogen sphere with 1.1 mean free path radius. The detector was located 763.3 cm from the center of the sphere at 30 degrees with respect to the deuteron beam. (1 shake = 10 ns)

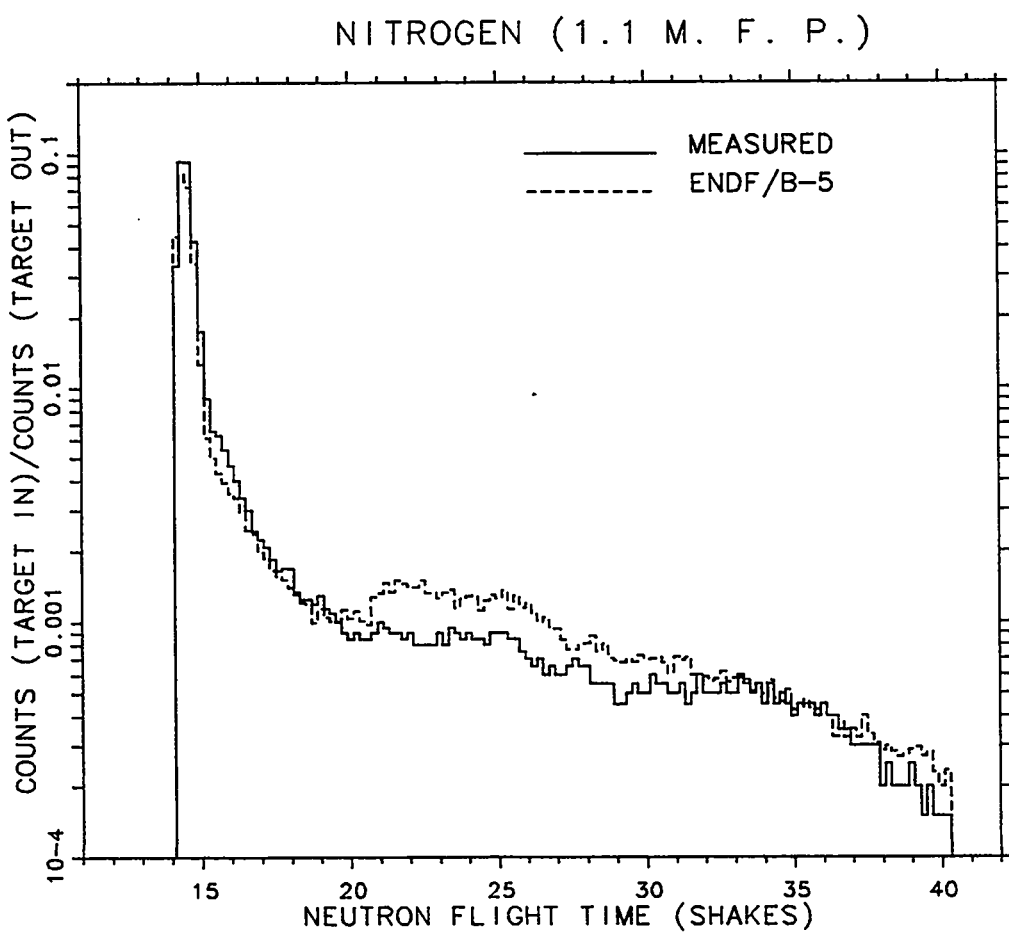


Fig. 28. Plot of experimental and ENDF/B-V calculated count rates for the nitrogen sphere of 1.1 mean free path radius.

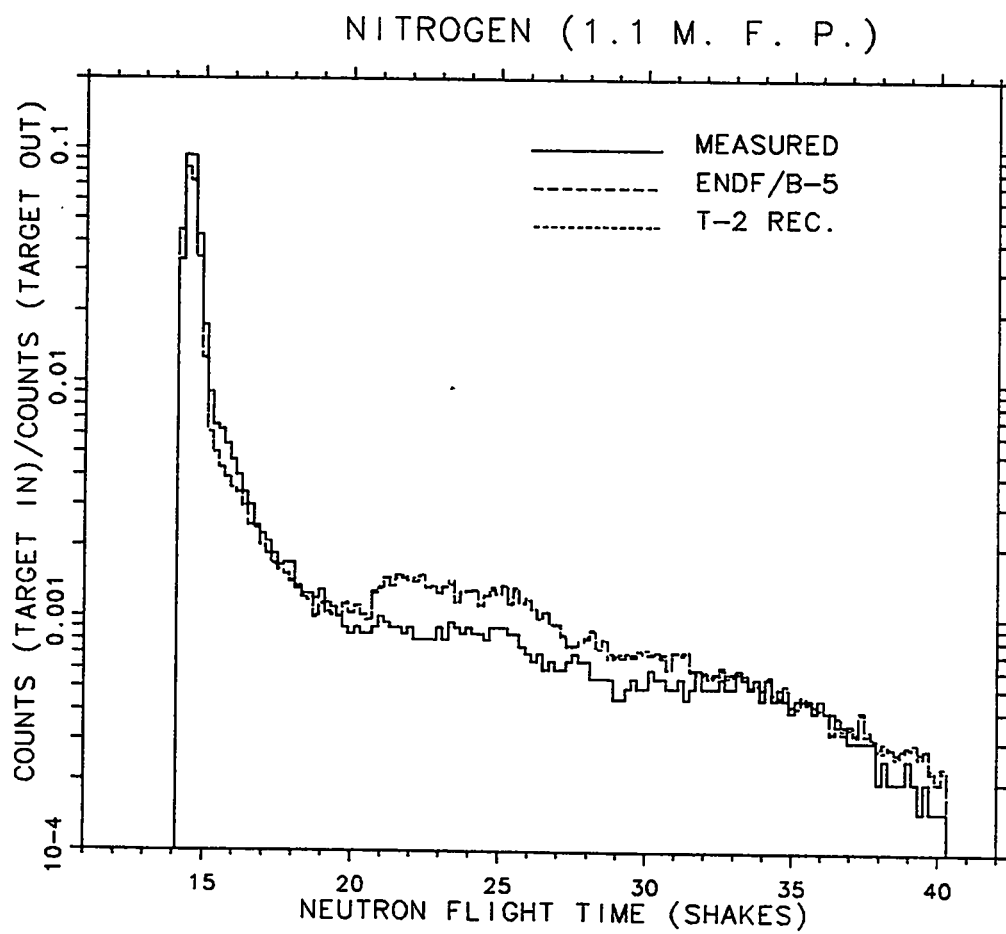


Fig. 29. Plot of experimental, ENDF/B-V calculated, and MCNP recommended calculated rates for the nitrogen sphere with 1.1 mean free path radius.

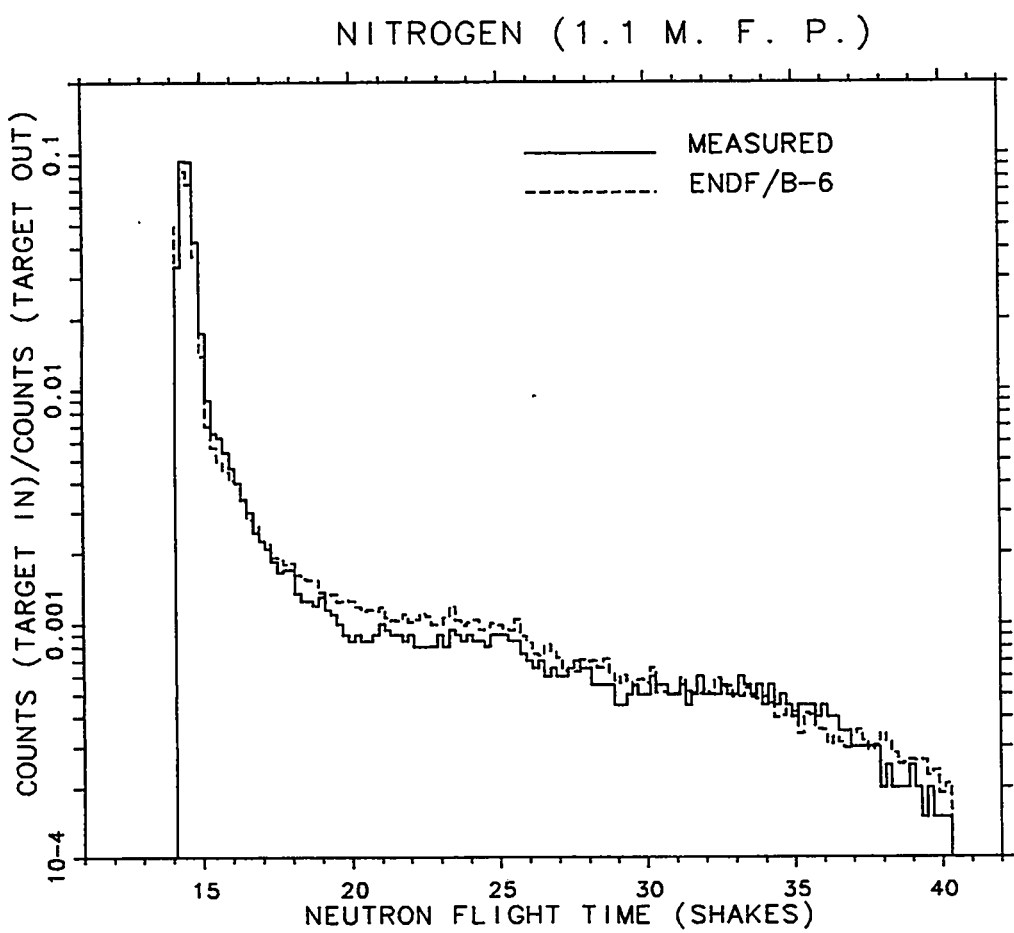


Fig. 30. Plot of experimental and ENDF/B-VI calculated count rates for the nitrogen sphere of 1.1 mean free path radius.

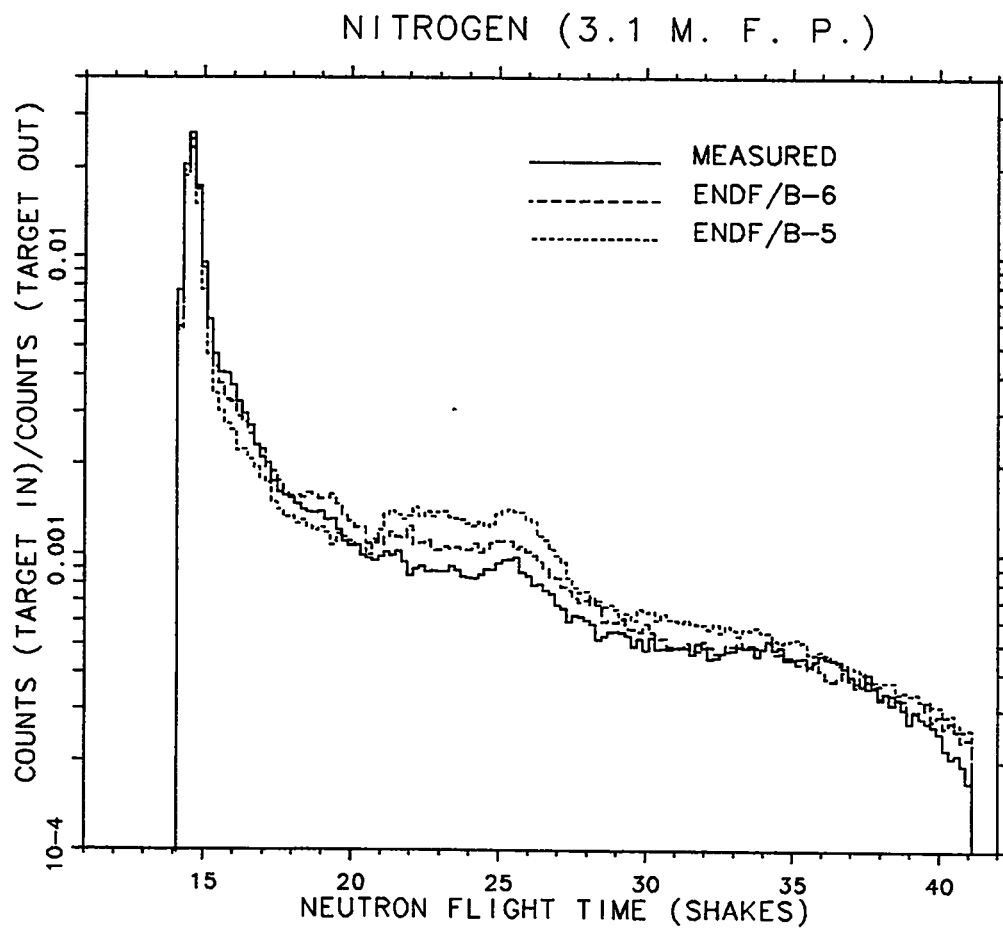


Fig. 31. Plot of experimental and calculated count rates as a function of time for a 3 cm from the center of the sphere at 30 degrees with respect to the deuteron beam. (1 shake = 10 ns)

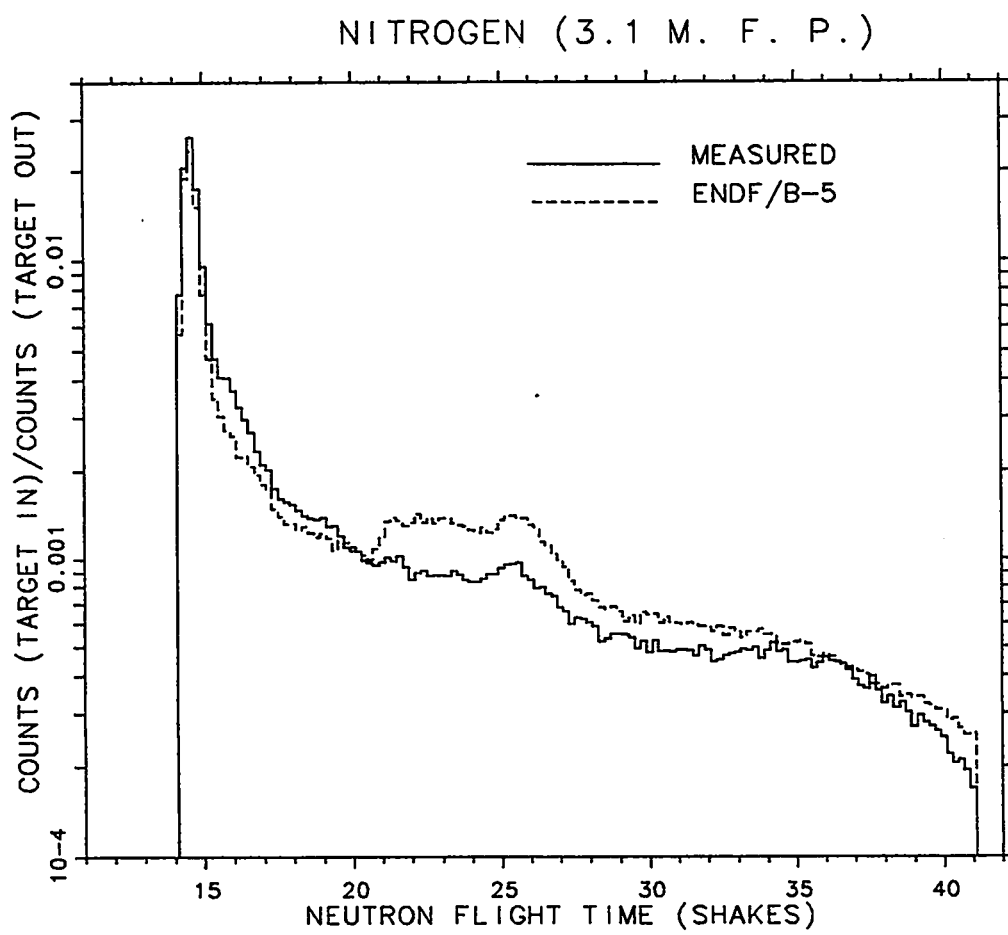


Fig. 32. Plot of experimental and ENDF/B-V calculated count rates for the nitrogen sphere of 3.1 mean free path radius.

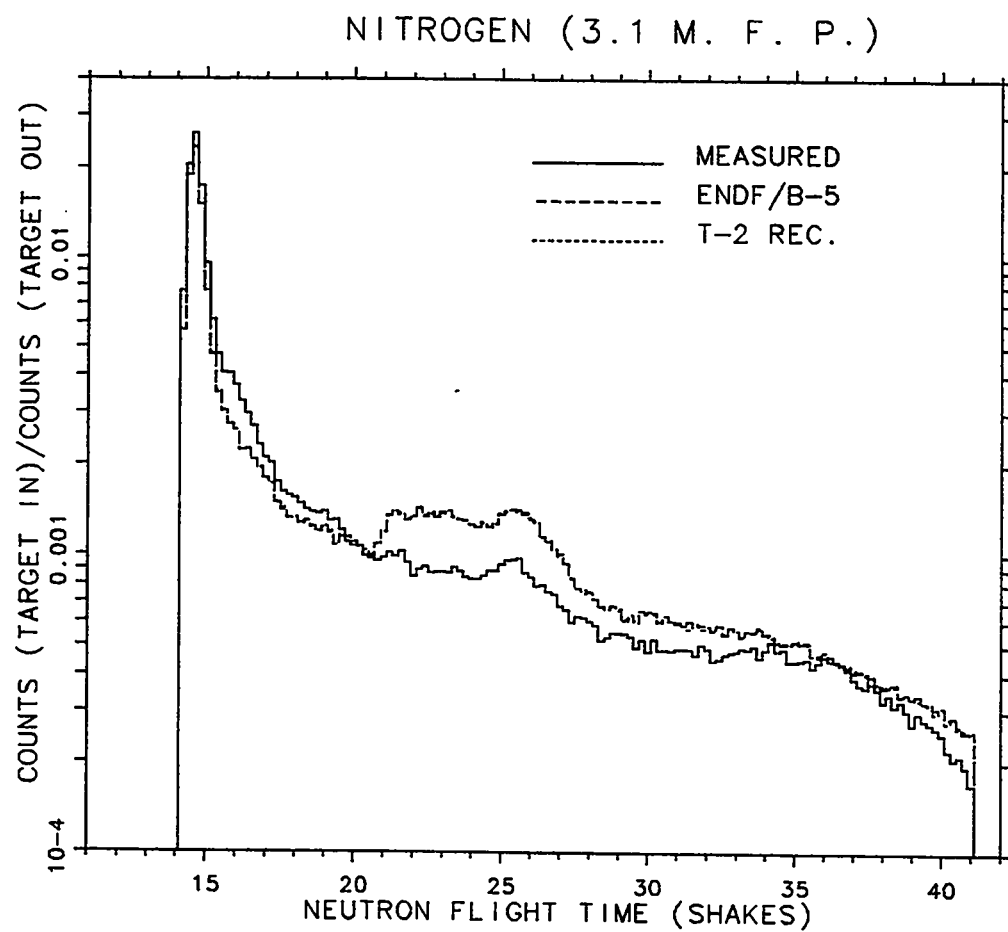


Fig. 33. Plot of experimental, ENDF/B-V calculated, and MCNP recommended calculated rates for the nitrogen sphere with 3.1 mean free path radius.

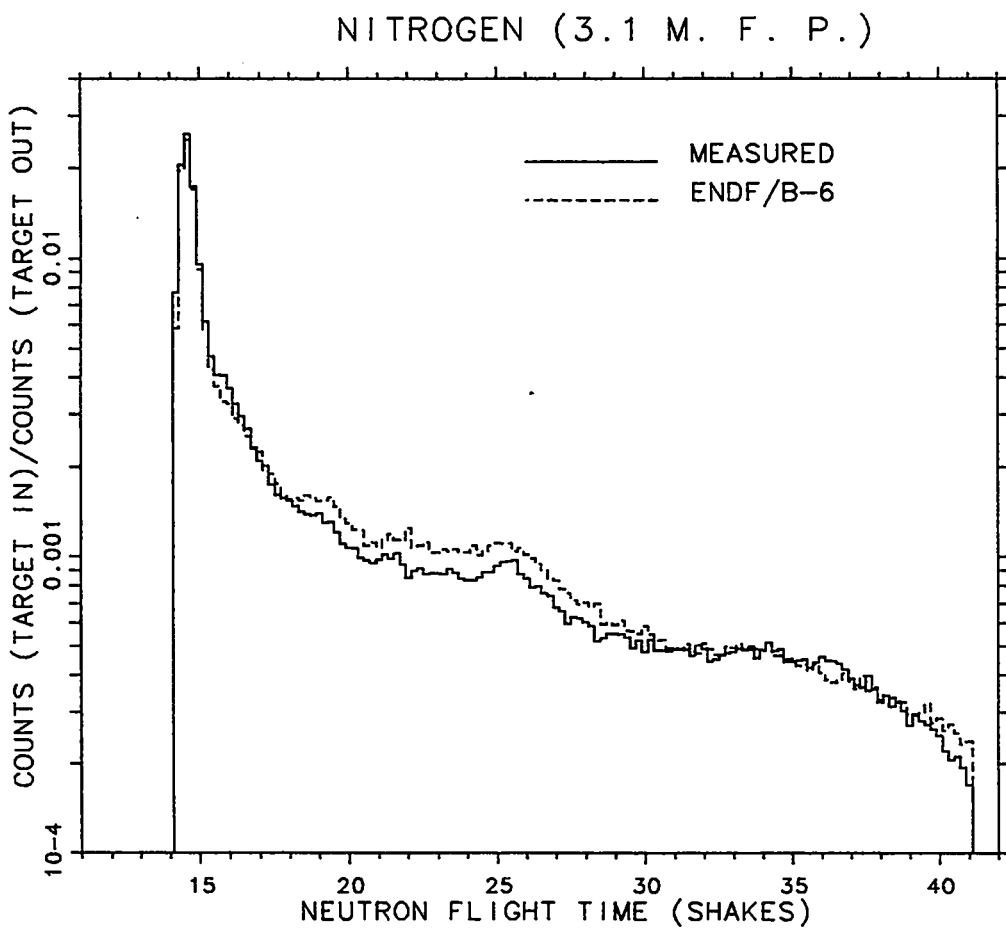


Fig. 34. Plot of experimental and ENDF/B-VI calculated count rates for the nitrogen sphere of 3.1 mean free path radius.

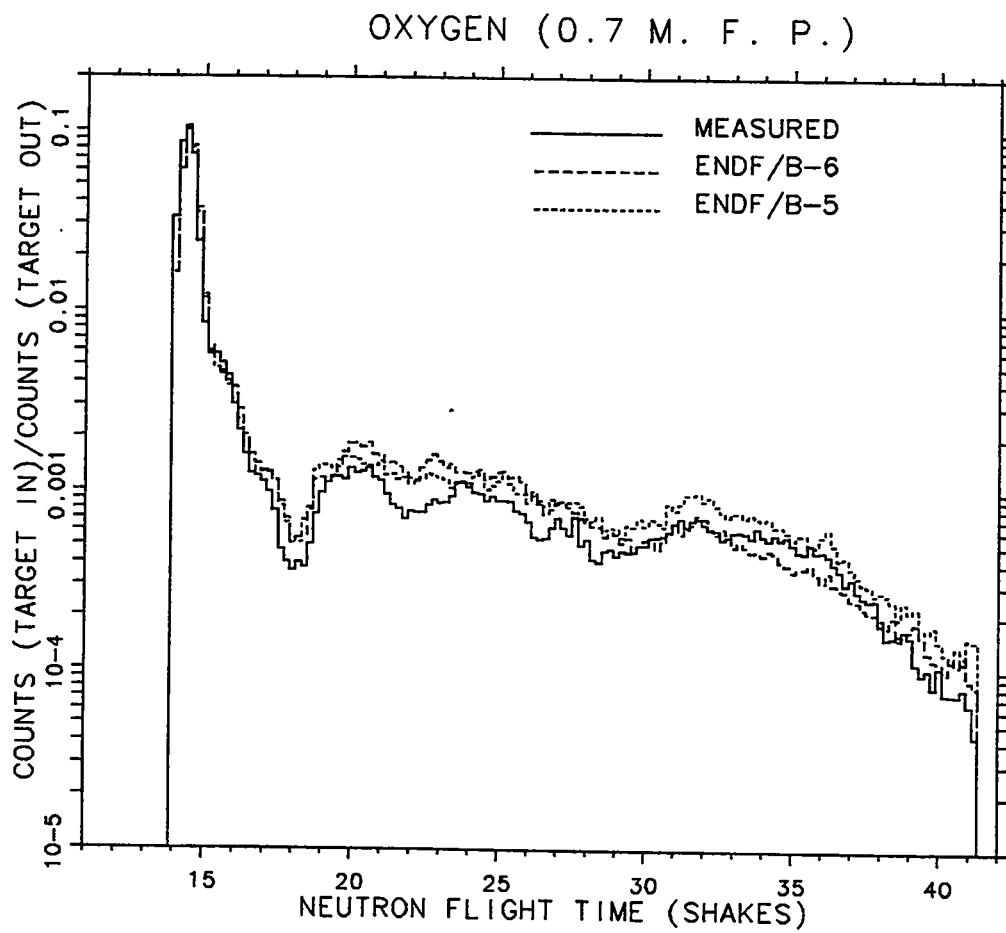


Fig. 35. Plot of experimental and calculated count rates as a function of time for an oxygen sphere with 0.7 mean free path radius. The detector was located 754.0 cm from the center of the sphere at 30 degrees with respect to the deuteron beam. (1 shake = 10 ns)

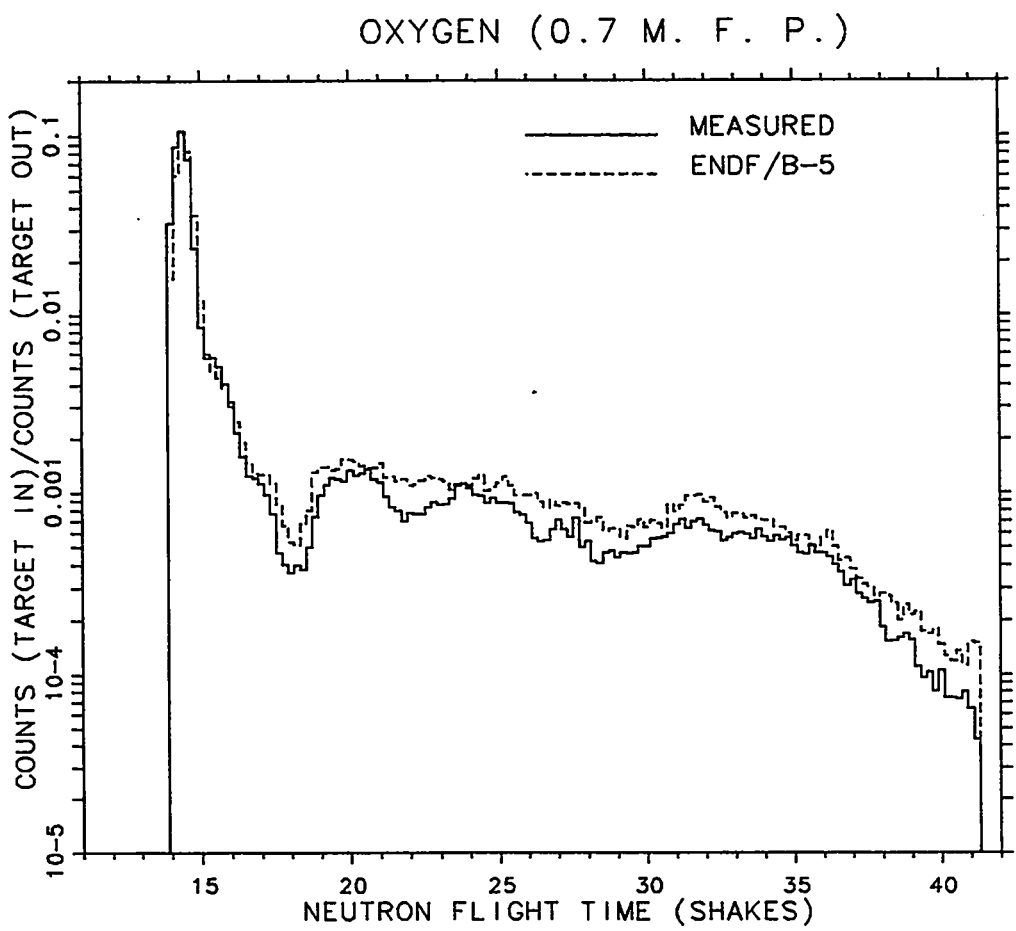


Fig. 36. Plot of experimental and ENDF/B-V calculated count rates for the oxygen sphere of 0.7 mean free path radius.

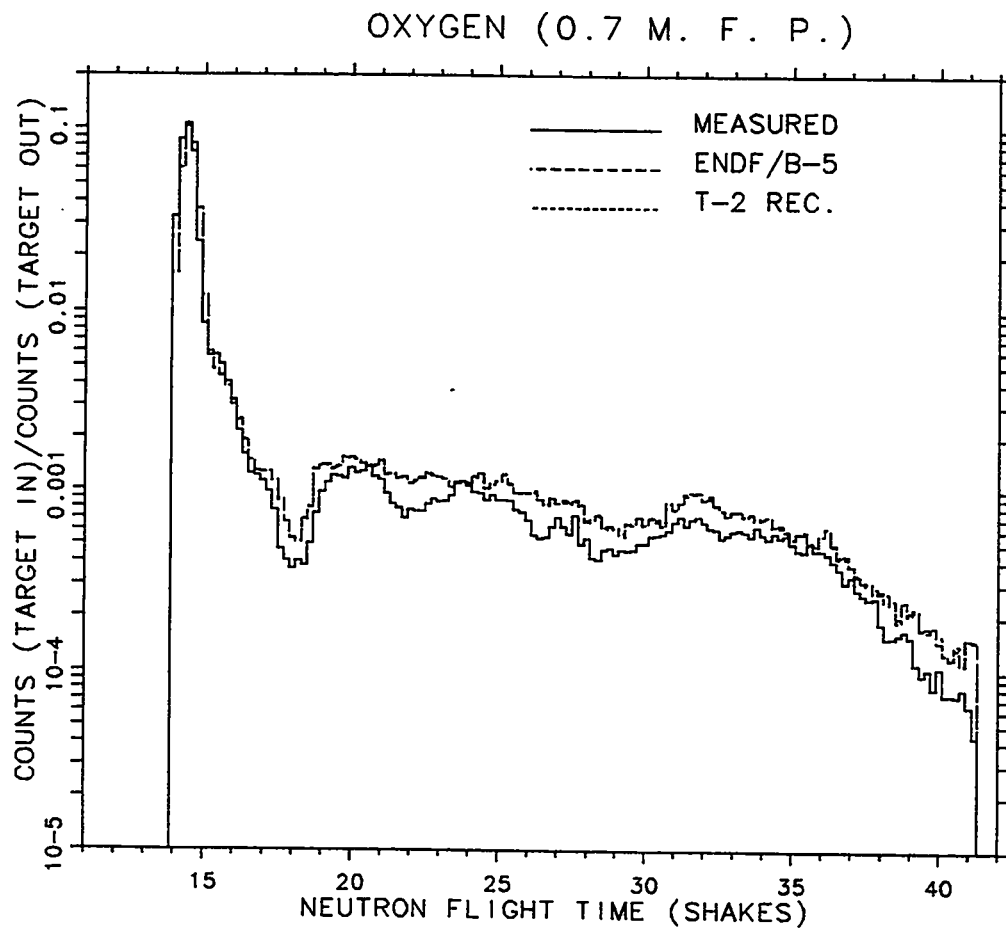


Fig. 37. Plot of experimental, ENDF/B-V calculated, and MCNP recommended calculated rates for the oxygen sphere with 0.7 mean free path radius.

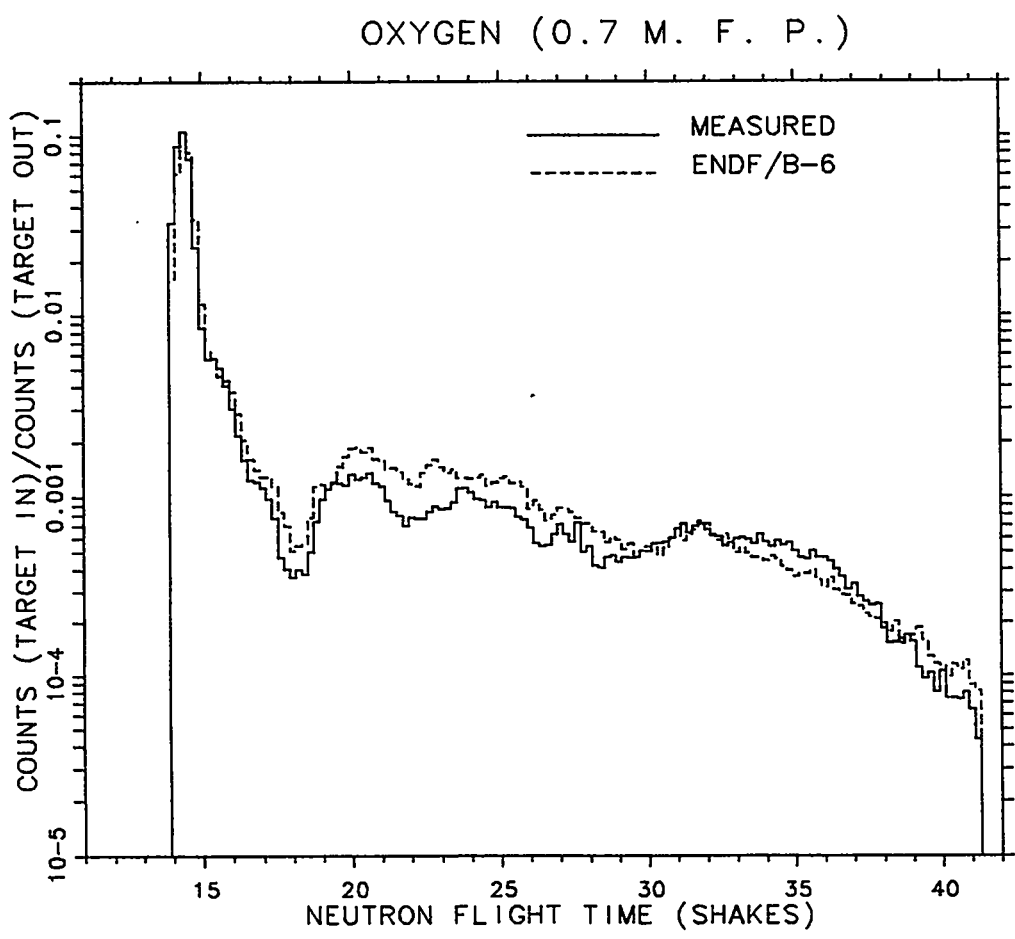


Fig. 38. Plot of experimental and ENDF/B-VI calculated count rates for the oxygen sphere of 0.7 mean free path radius.

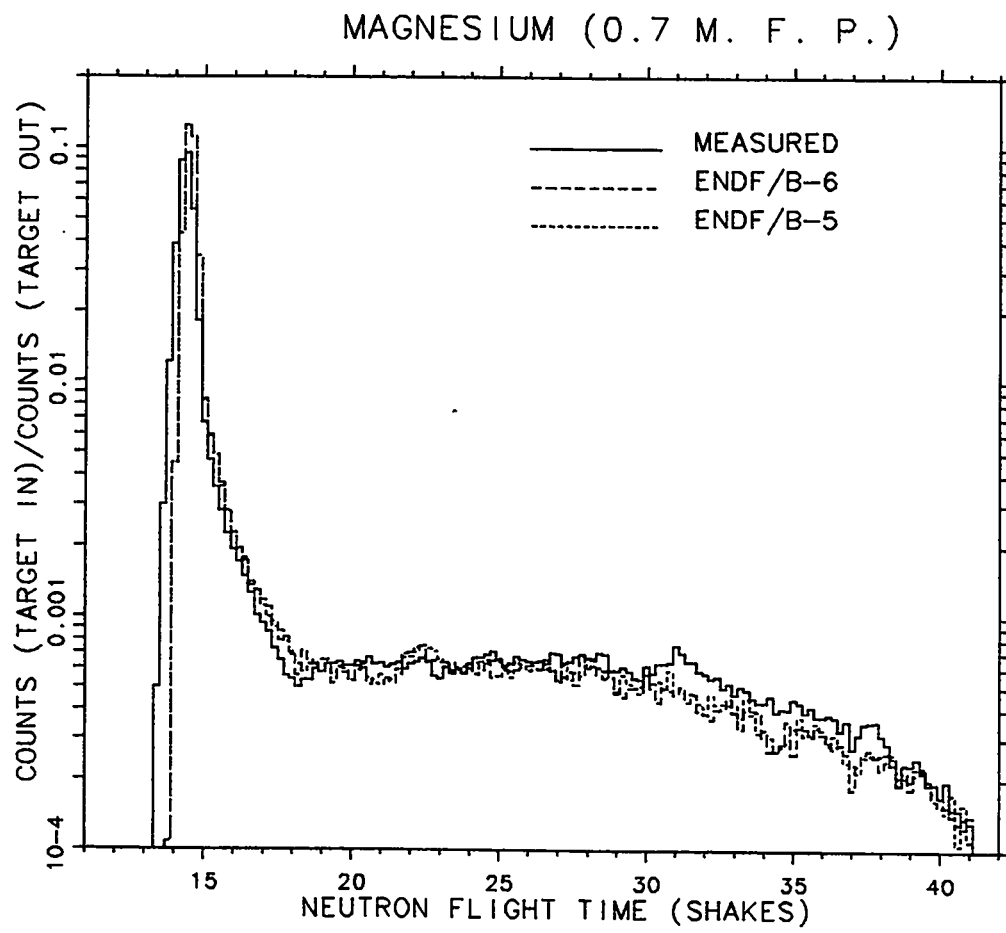


Fig. 39. Plot of experimental and calculated count rates as a function of time for a magnesium sphere with 0.7 mean free path radius. The detector was located 765.2 cm from the center of the sphere at 30 degrees with respect to the deuteron beam. (1 shake = 10 ns)

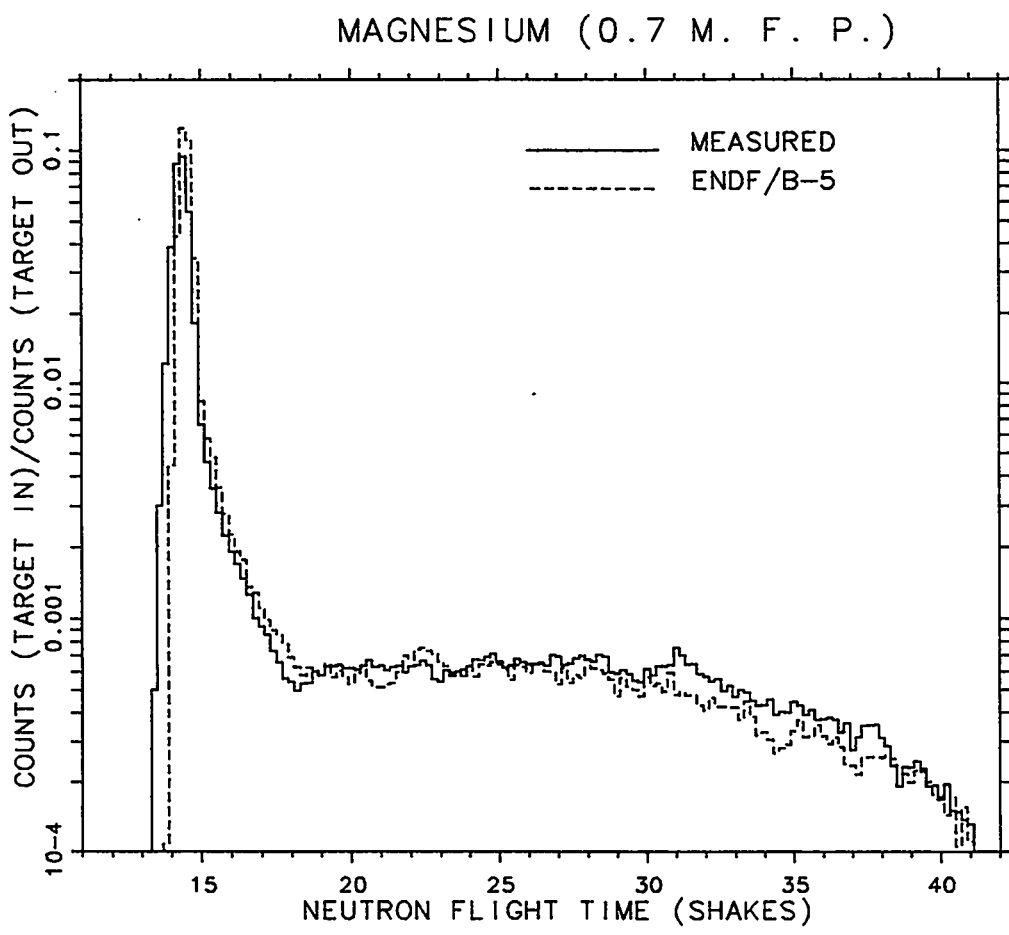


Fig. 40. Plot of experimental and ENDF/B-V calculated count rates for the magnesium sphere of 0.7 mean free path radius.

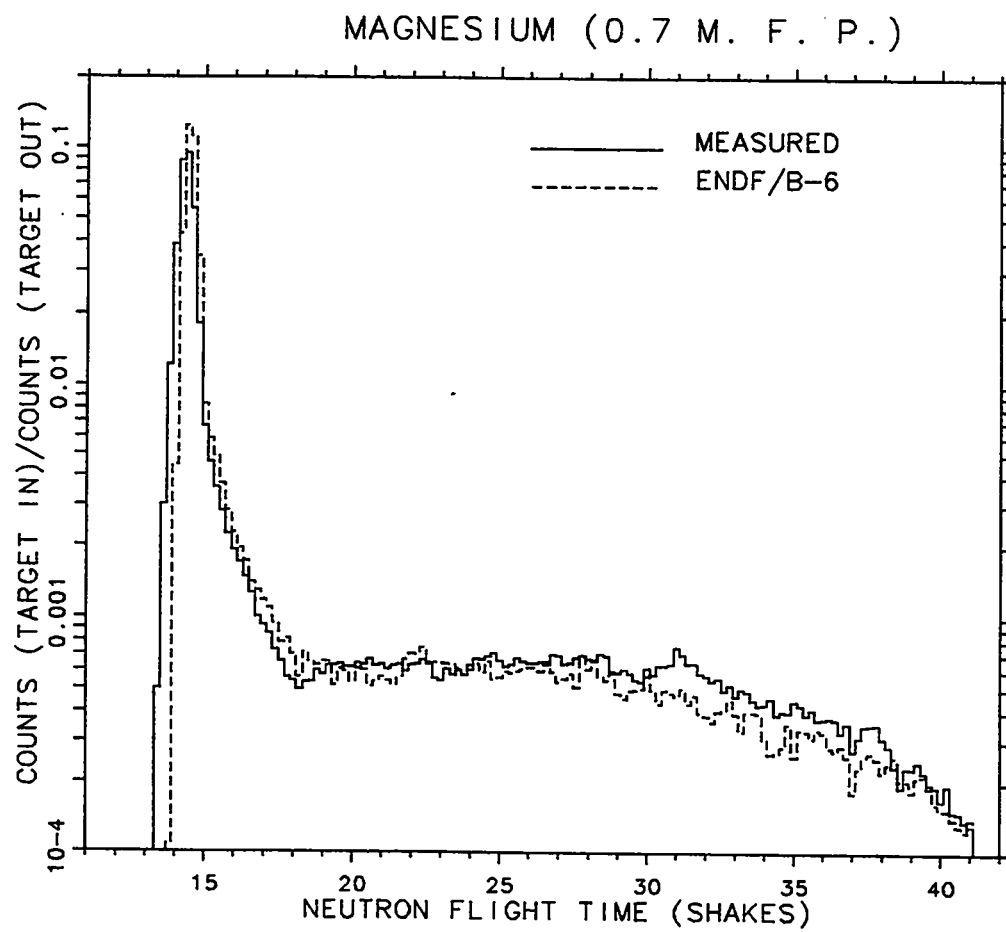


Fig. 41. Plot of experimental and ENDF/B-VI calculated count rates for the magnesium sphere of 0.7 mean free path radius.

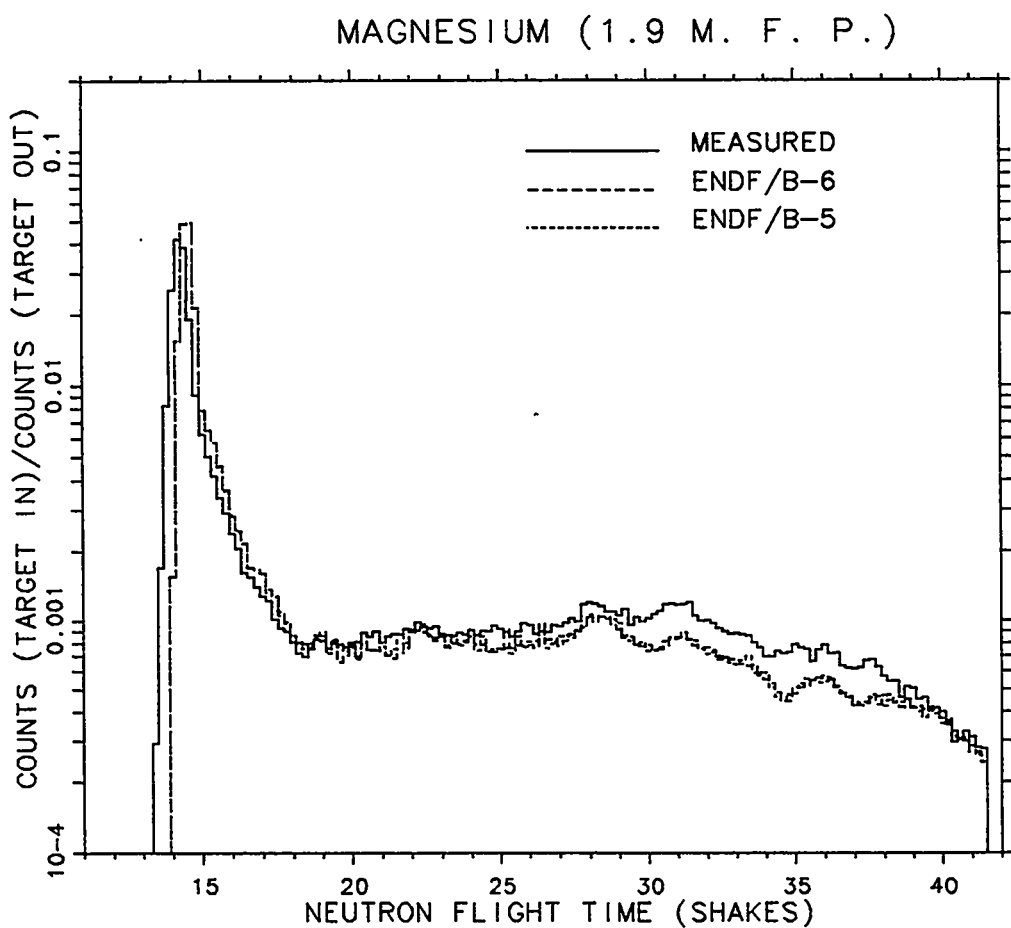


Fig. 42. Plot of experimental and calculated count rates as a function of time for a magnesium sphere with 1.9 mean free path radius. The detector was located 765.2 cm from the center of the sphere at 30 degrees with respect to the deuteron beam. (1 shake = 10 ns)

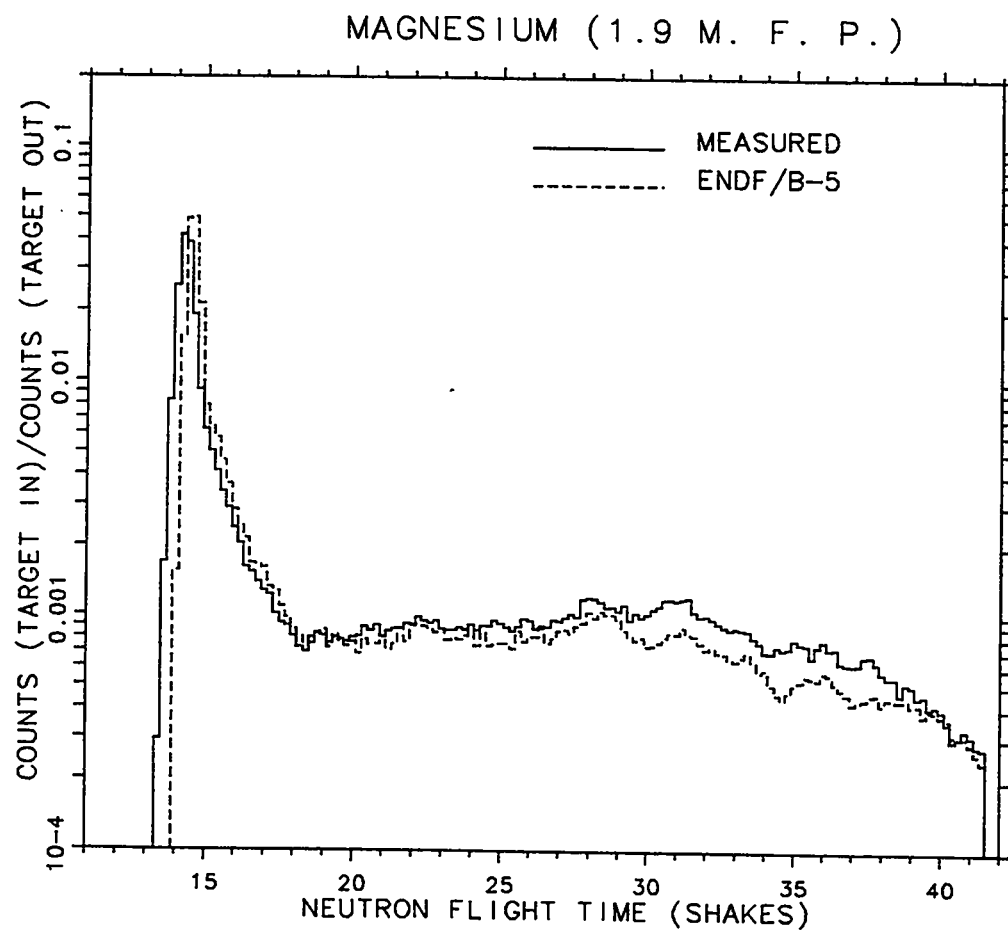


Fig. 43. Plot of experimental and ENDF/B-V calculated count rates for the magnesium sphere of 1.9 mean free path radius.

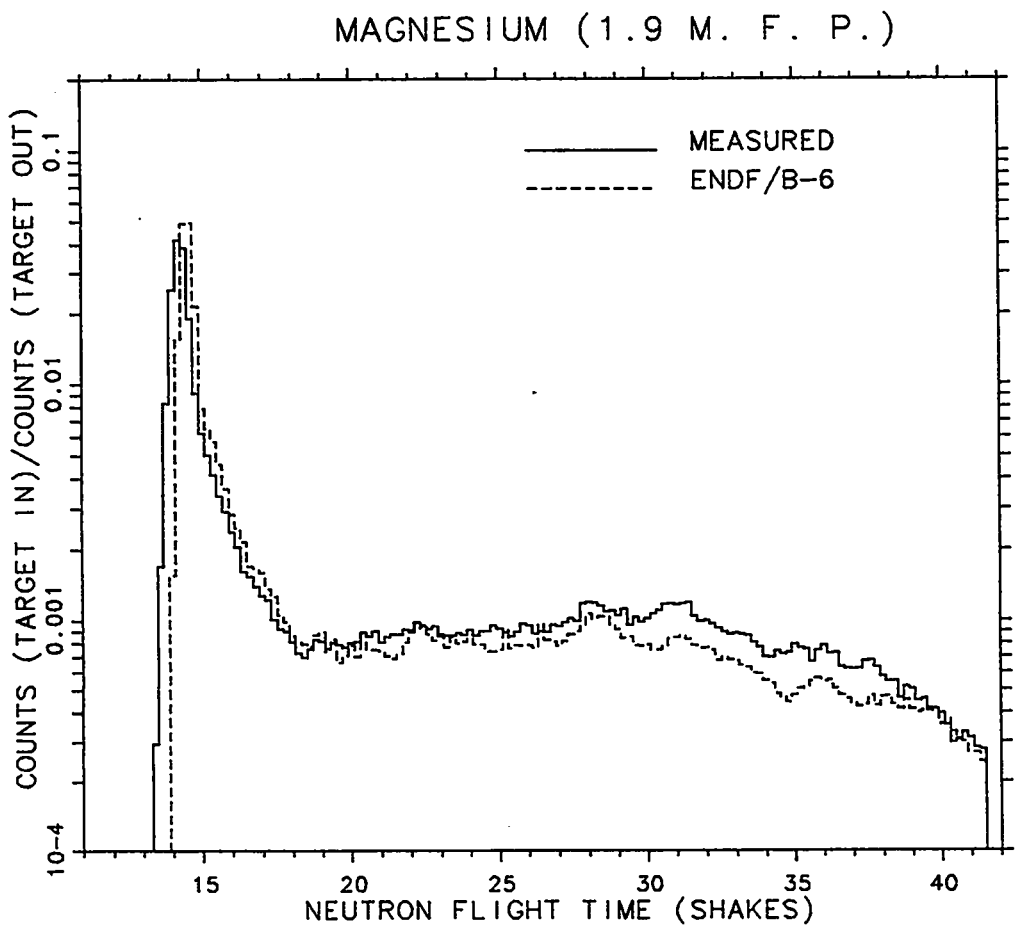


Fig. 44. Plot of experimental and ENDF/B-VI calculated count rates for the magnesium sphere of 1.9 mean free path radius.

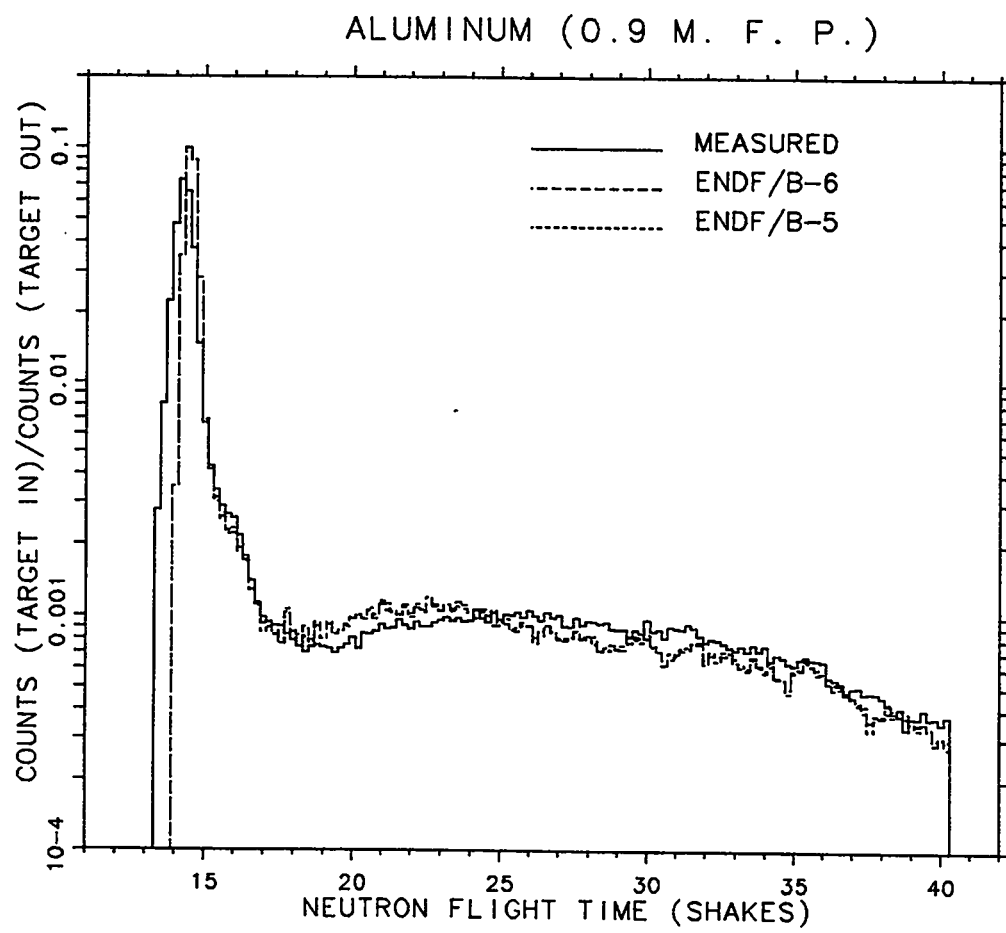


Fig. 45. Plot of experimental and calculated count rates as a function of time for an aluminum sphere with 0.9 mean free path radius. The detector was located 765.2 cm from the center of the sphere at 30 degrees with respect to the deuteron beam. (1 shake = 10 ns)

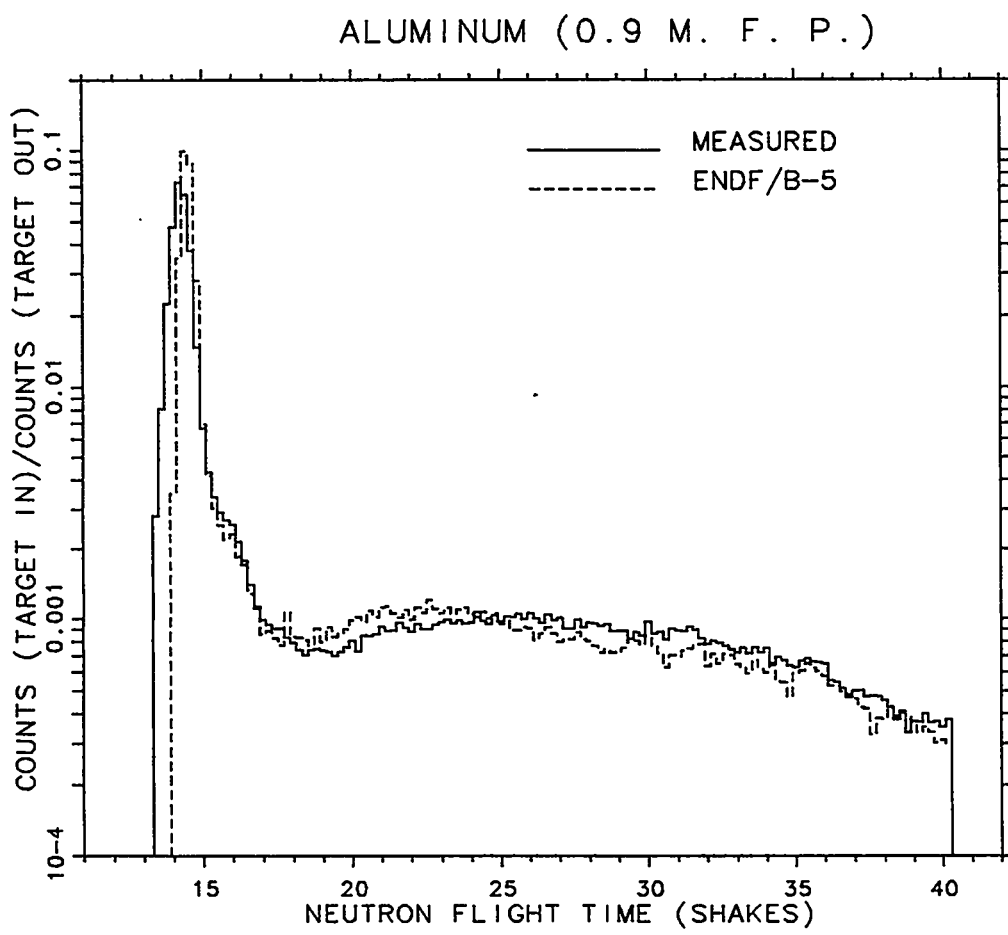


Fig. 46. Plot of experimental and ENDF/B-V calculated count rates for the aluminum sphere of 0.9 mean free path radius.

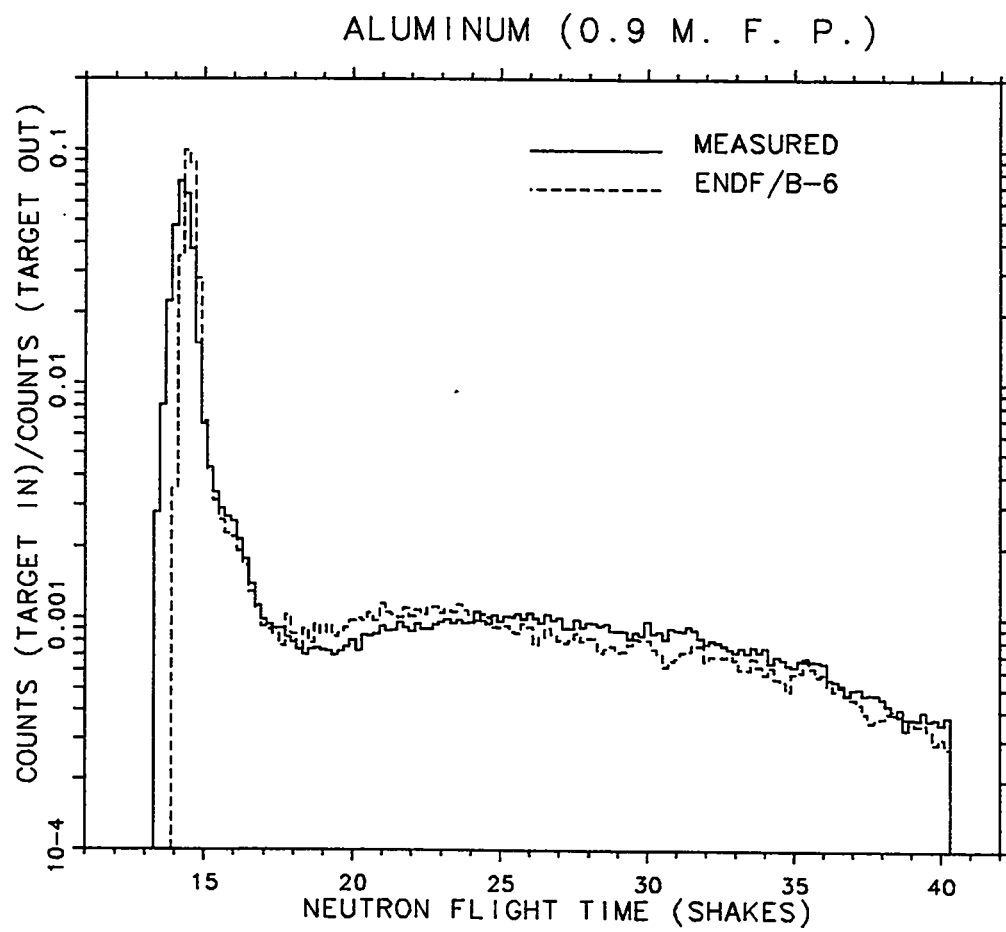


Fig. 47. Plot of experimental and ENDF/B-VI calculated count rates for the aluminum sphere of 0.9 mean free path radius.

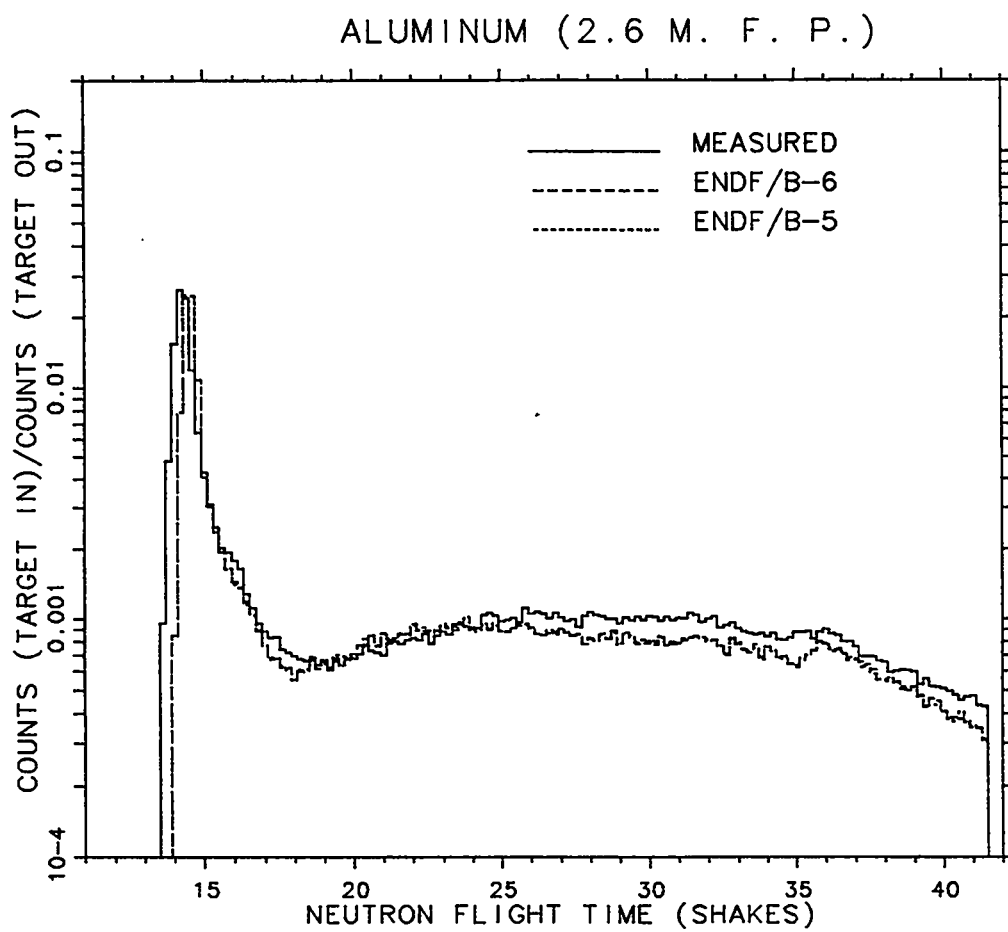


Fig. 48. Plot of experimental and calculated count rates as a function of time for an aluminum sphere with 2.6 mean free path radius. The detector was located 765.2 cm from the center of the sphere at 30 degrees with respect to the deuteron beam. (1 shake = 10 ns)

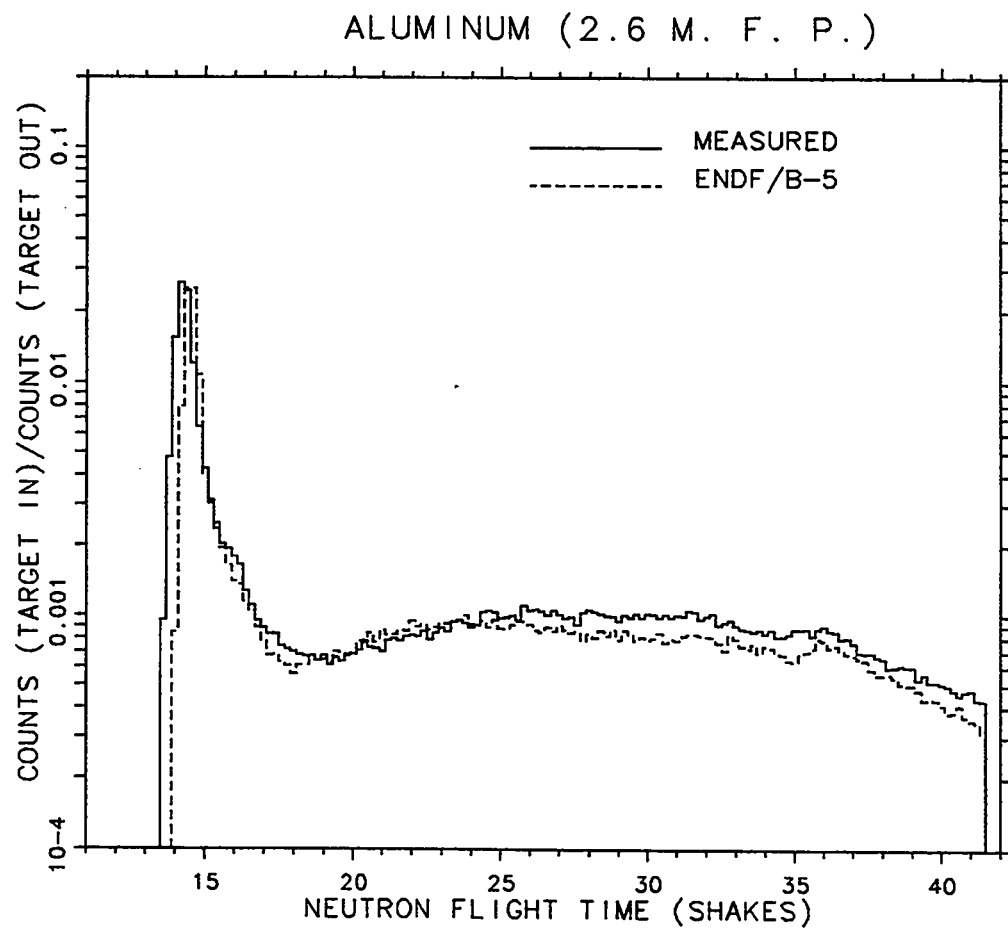


Fig. 49. Plot of experimental and ENDF/B-V calculated count rates for the aluminum sphere of 2.6 mean free path radius.

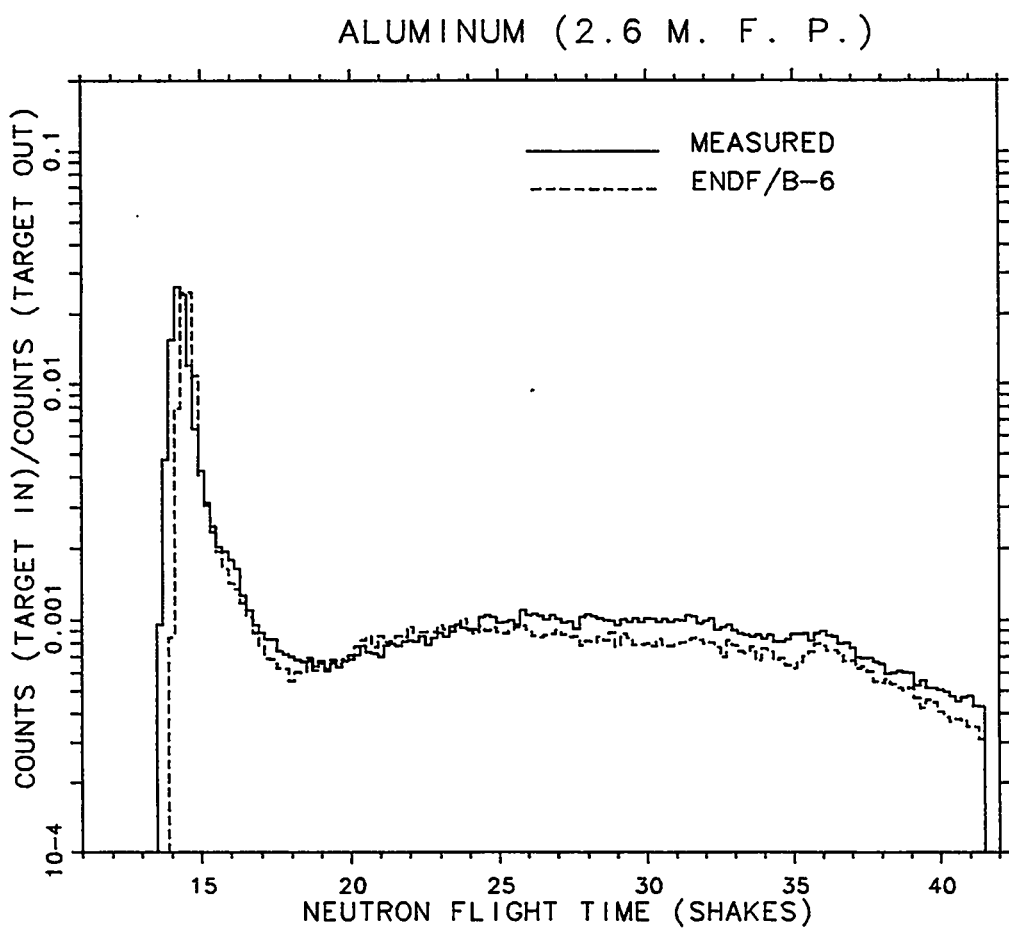


Fig. 50. Plot of experimental and ENDF/B-VI calculated count rates for the aluminum sphere of 2.6 mean free path radius.

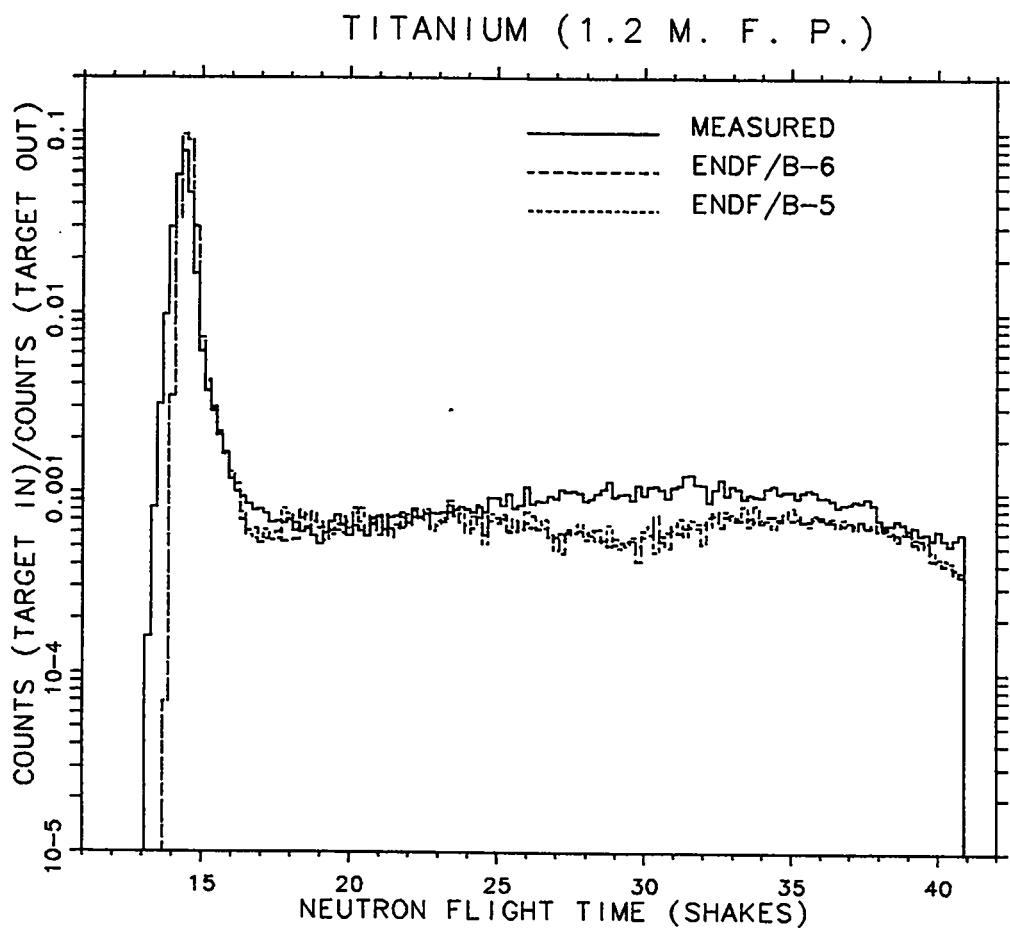


Fig. 51. Plot of experimental and calculated count rates as a function of time for a titanium sphere with 1.2 mean free path radius. The detector was located 765.2 cm from the center of the sphere at 30 degrees with respect to the deuteron beam. (1 shake = 10 ns)

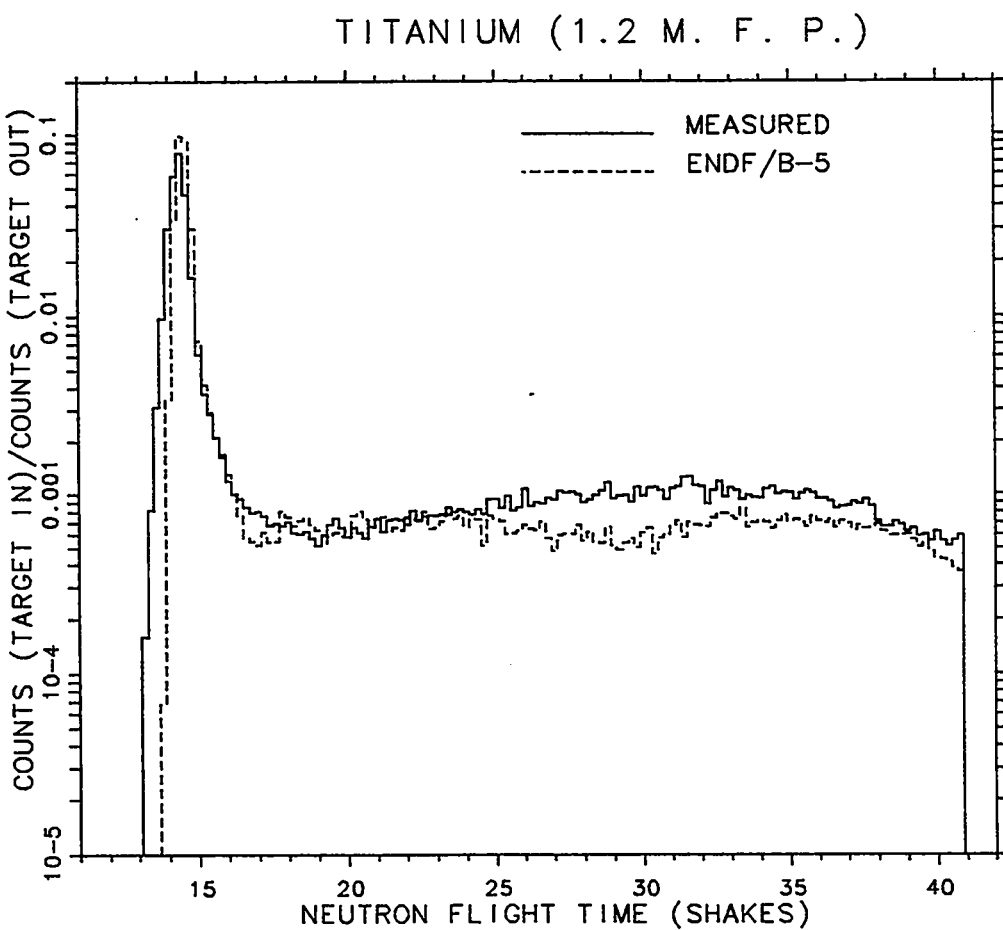


Fig. 52. Plot of experimental and ENDF/B-V calculated count rates for the titanium sphere of 1.2 mean free path radius.

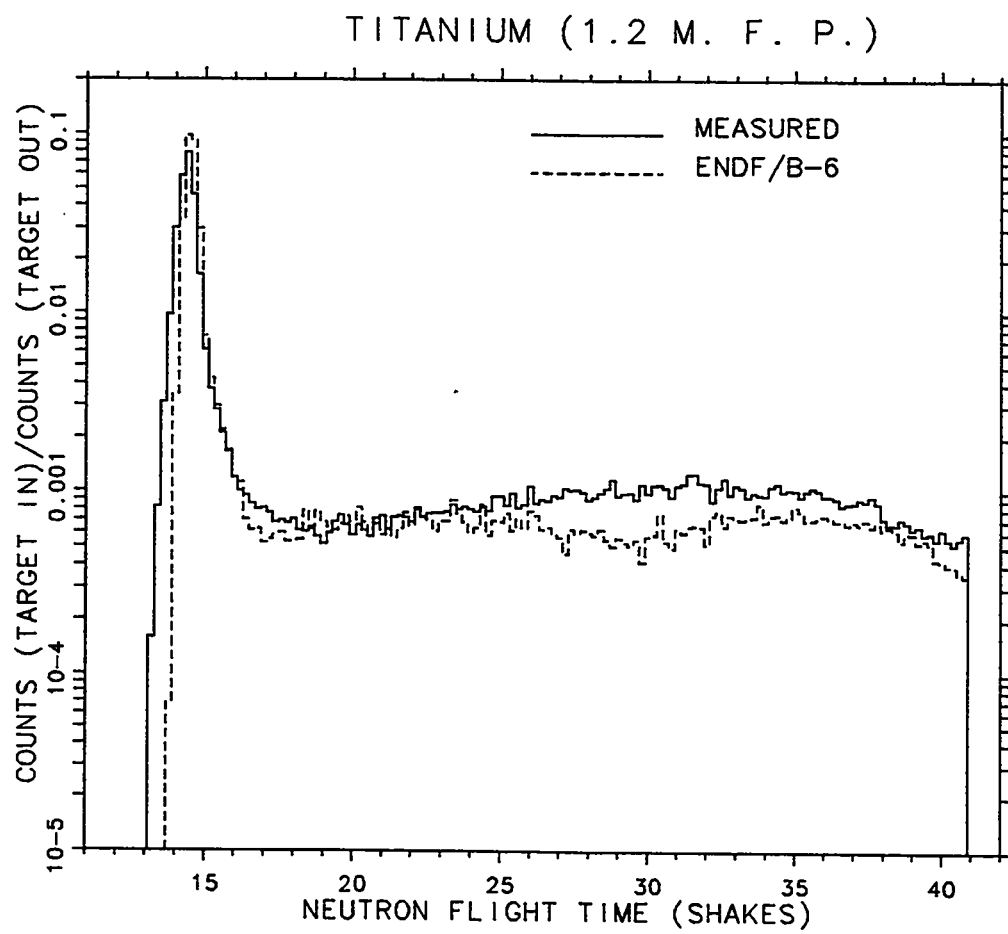


Fig. 53. Plot of experimental and ENDF/B-VI calculated count rates for the titanium sphere of 1.2 mean free path radius.

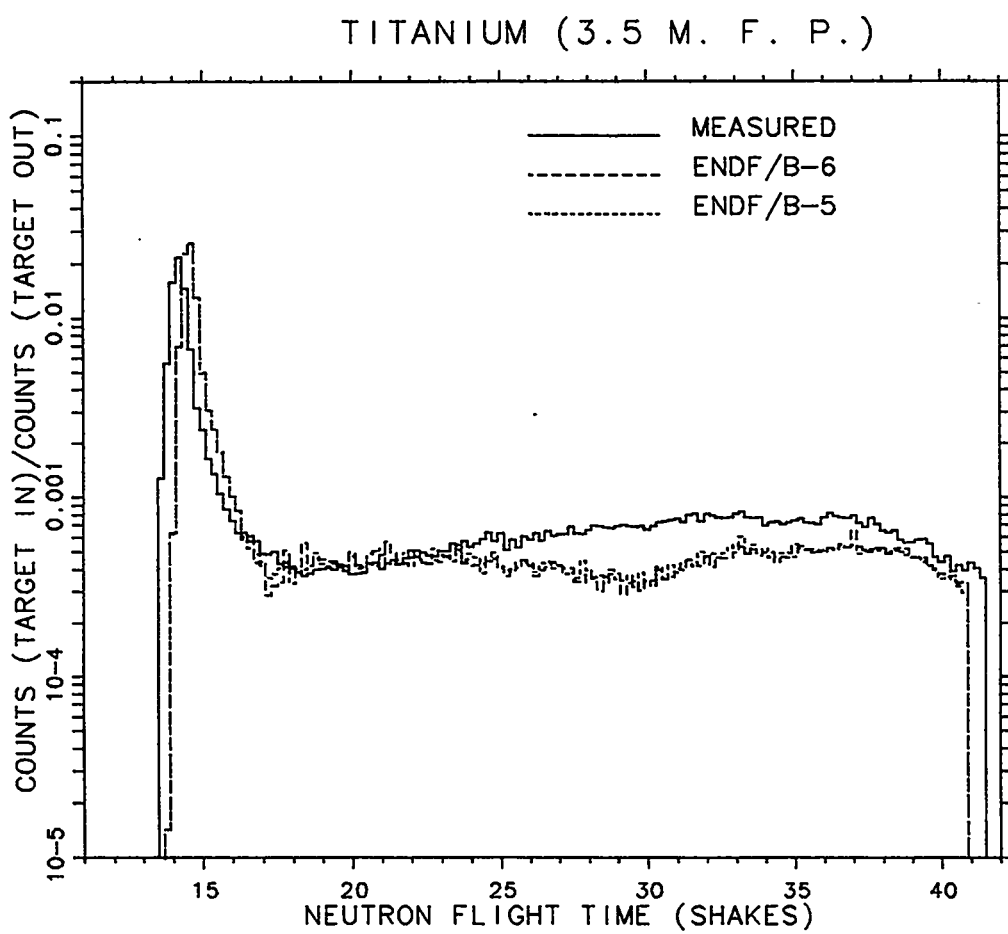


Fig. 54. Plot of experimental and calculated count rates as a function of time for a titanium sphere with 3.5 mean free path radius. The detector was located 765.2 cm from the center of the sphere at 30 degrees with respect to the deuteron beam. (1 shake = 10 ns)

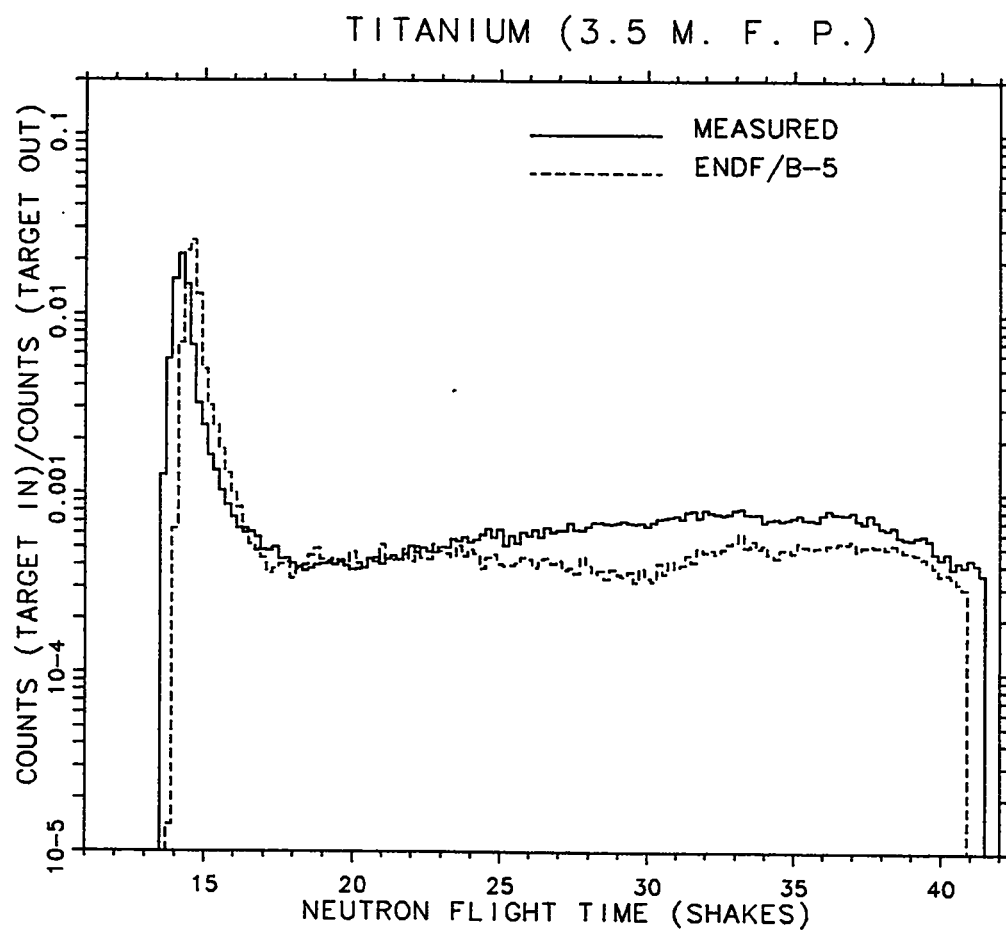


Fig. 55. Plot of experimental and ENDF/B-V calculated count rates for the titanium sphere of 3.5 mean free path radius.

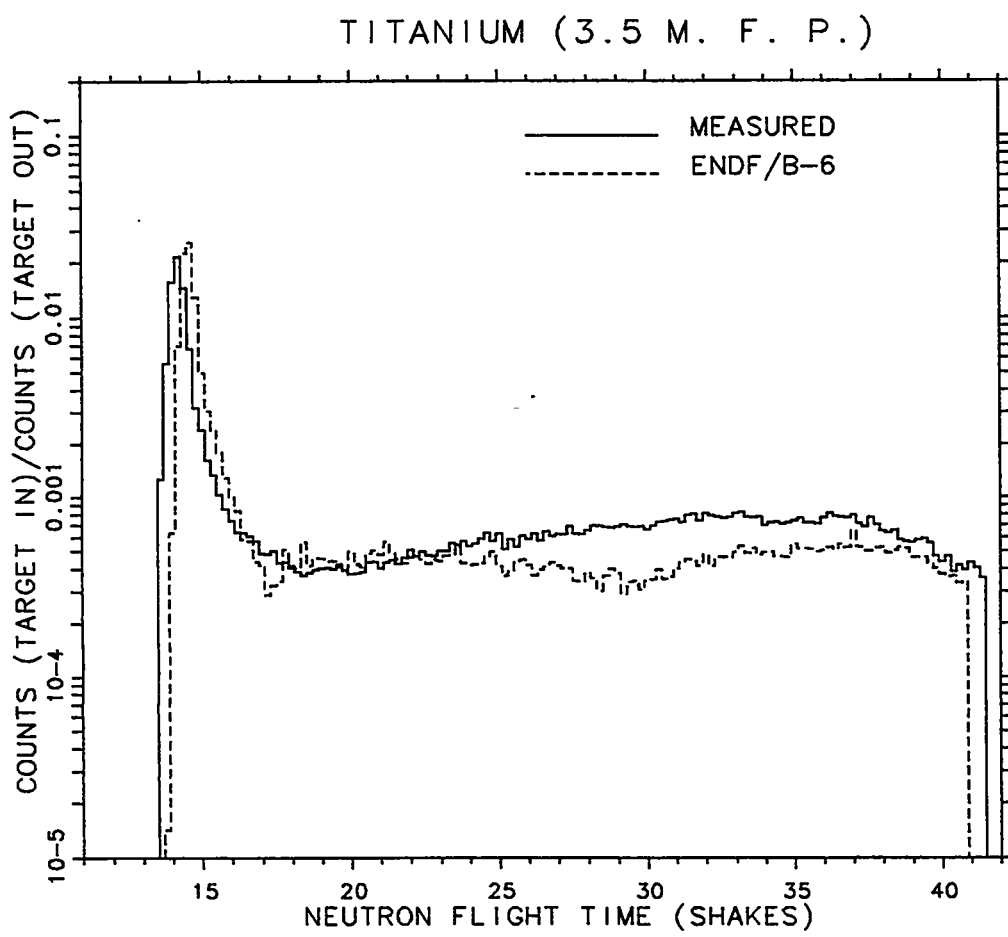


Fig. 56. Plot of experimental and ENDF/B-VI calculated count rates for the titanium sphere of 3.5 mean free path radius.

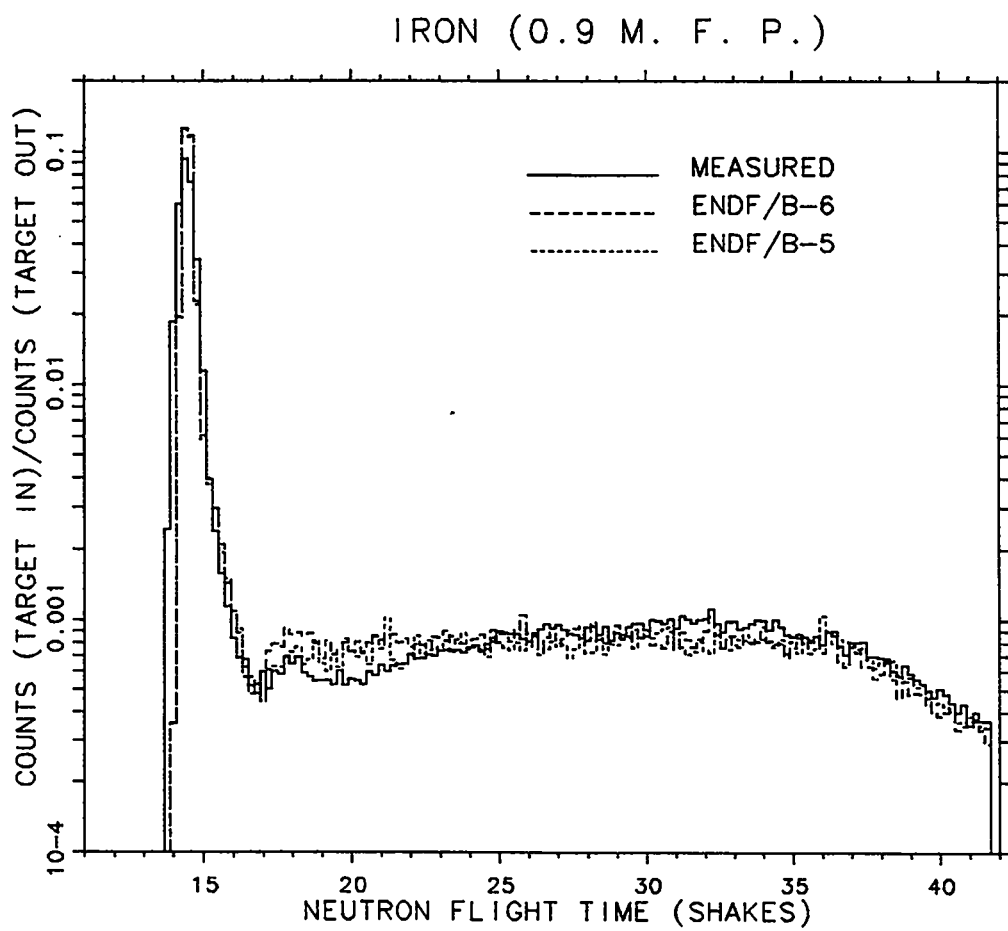


Fig. 57. Plot of experimental and calculated count rates as a function of time for an iron sphere with 0.9 mean free path radius. The detector was located 766.0 cm from the center of the sphere at 30 degrees with respect to the deuteron beam. (1 shake = 10 ns)

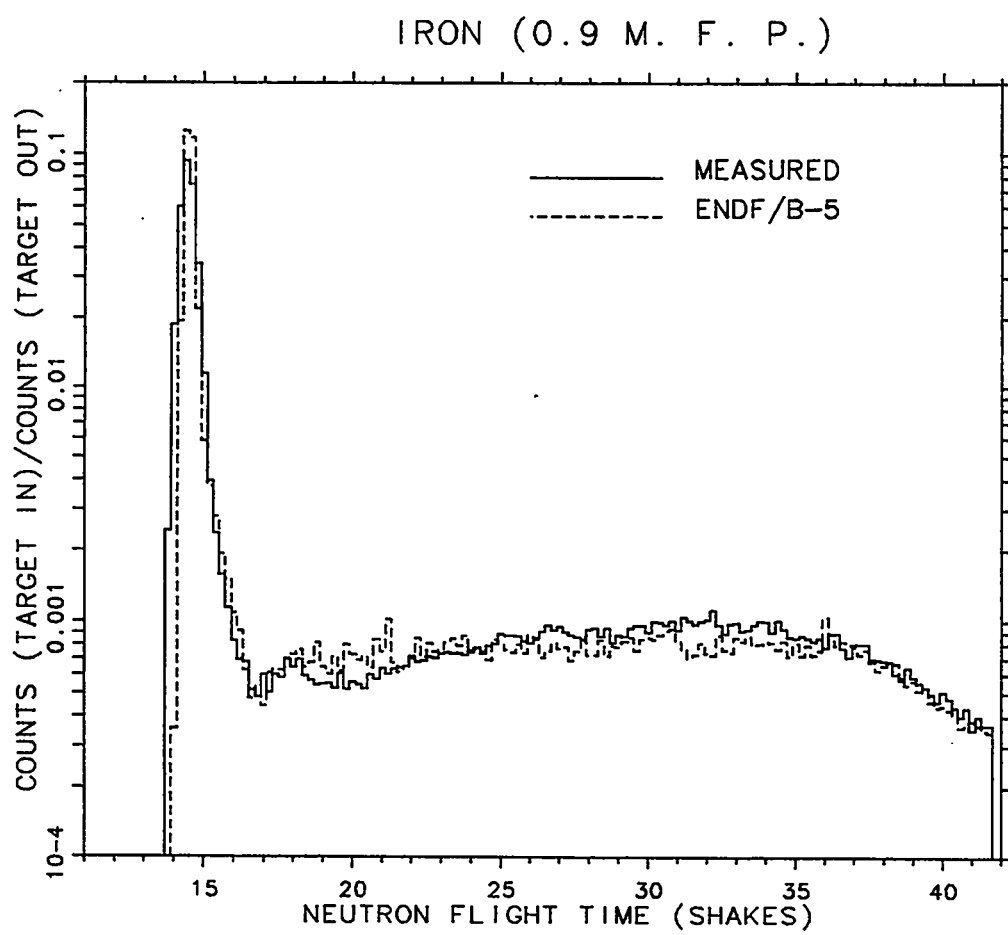


Fig. 58. Plot of experimental and ENDF/B-V calculated count rates for the iron sphere of 0.9 mean free path radius.

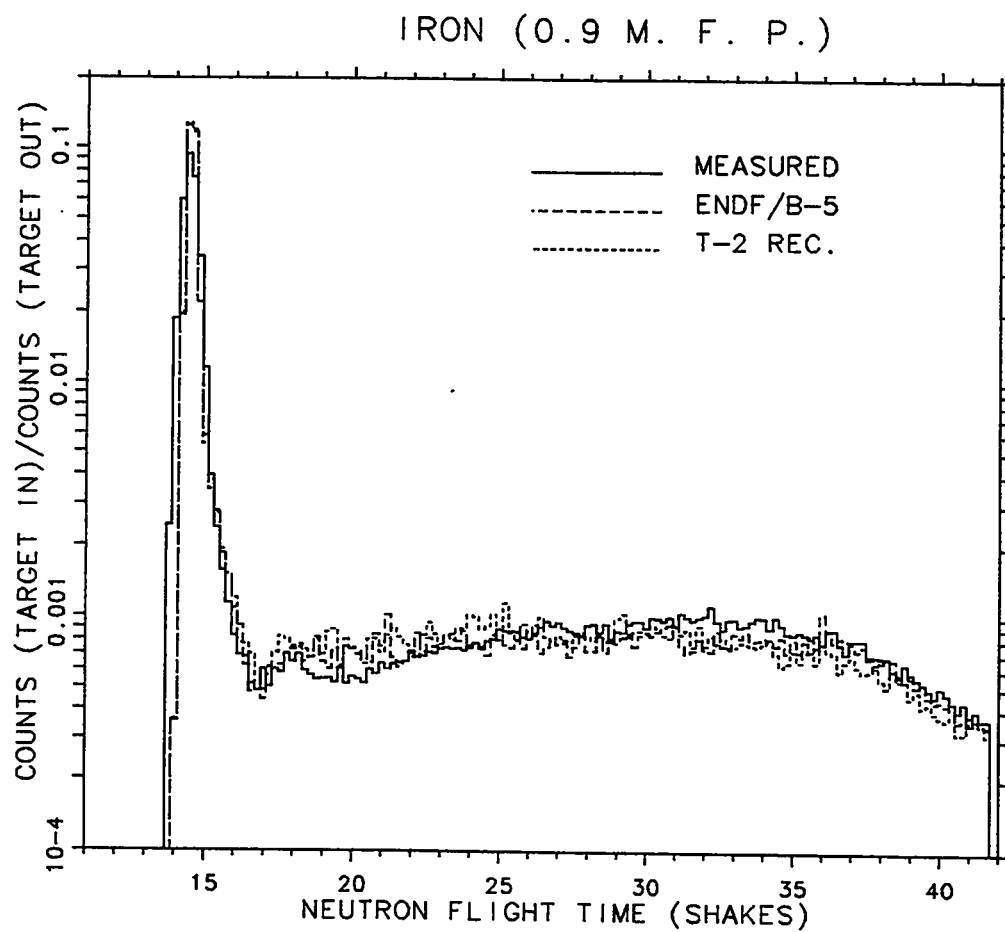


Fig. 59. Plot of experimental, ENDF/B-V calculated, and MCNP recommended calculated rates for the iron sphere with 0.9 mean free path radius.

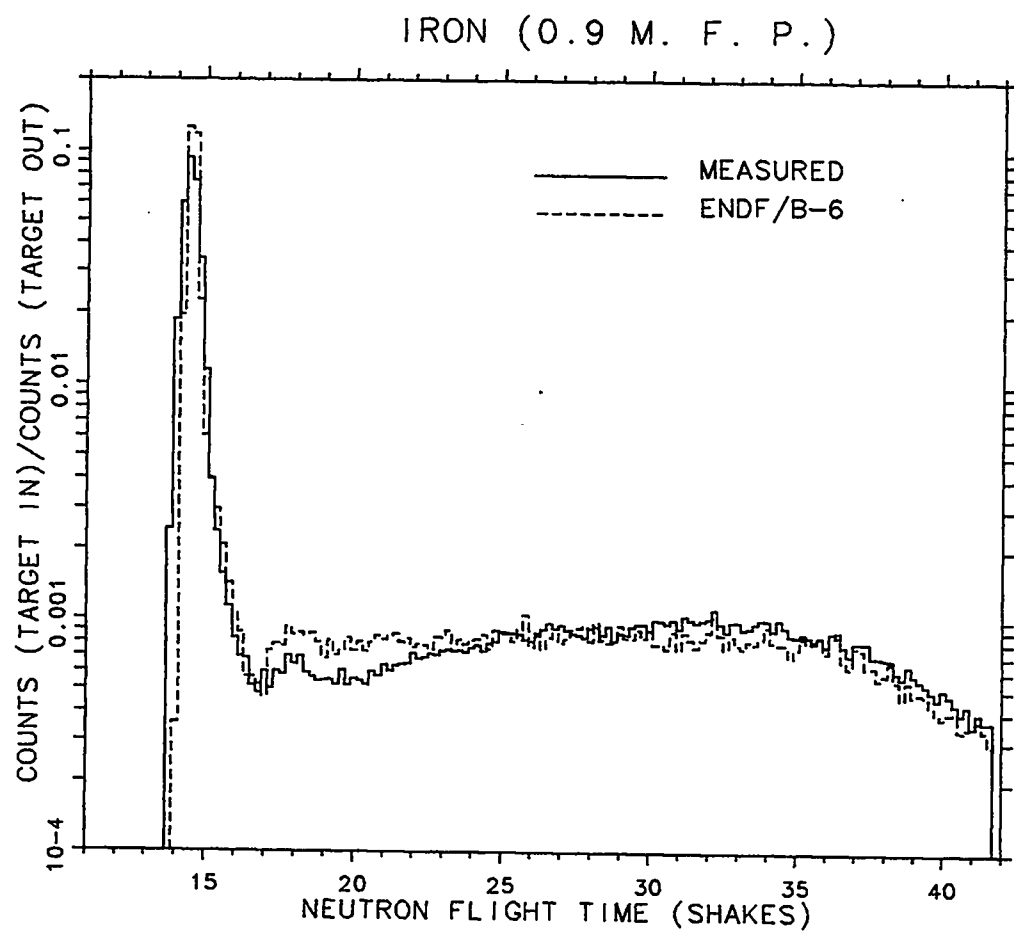


Fig. 60. Plot of experimental and ENDF/B-VI calculated count rates for the iron sphere of 0.9 mean free path radius.

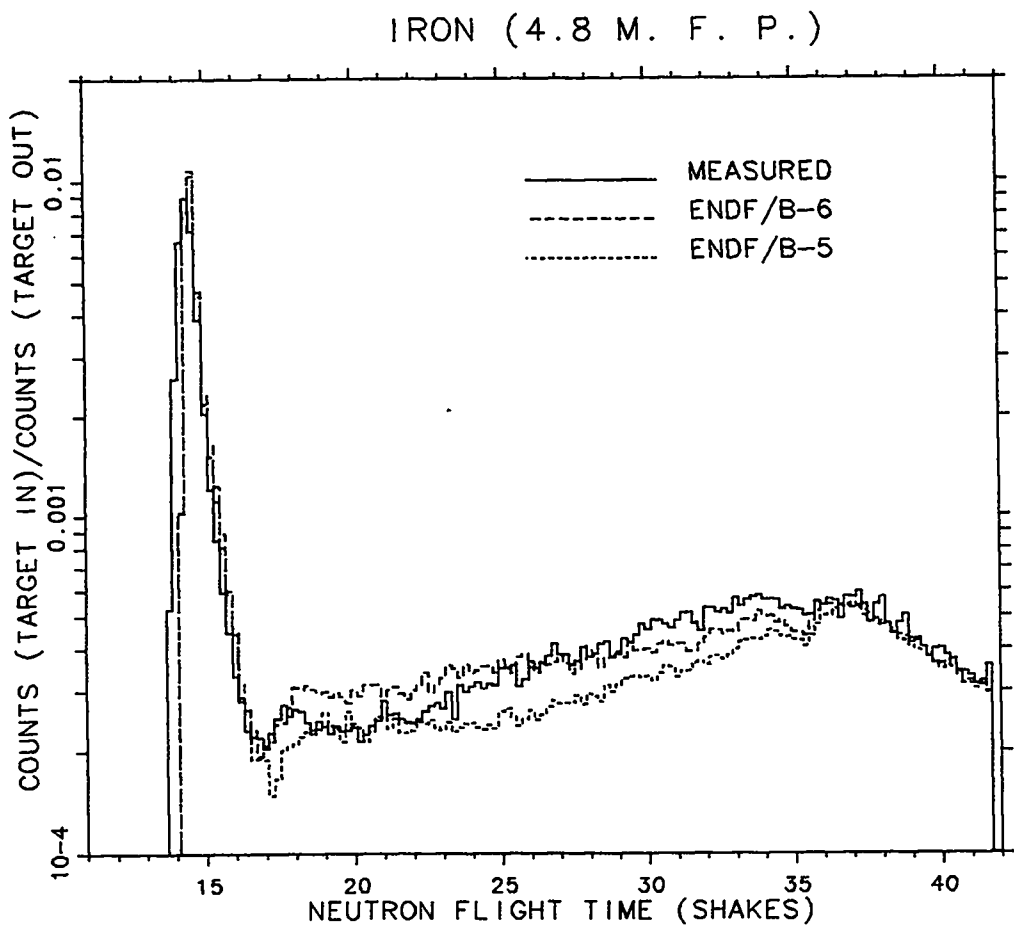


Fig. 61. Plot of experimental and calculated count rates as a function of time for an iron sphere with 4.8 mean free path radius. The detector was located 766.0 cm from the center of the sphere at 30 degrees with respect to the deuteron beam. (1 shake = 10 ns)

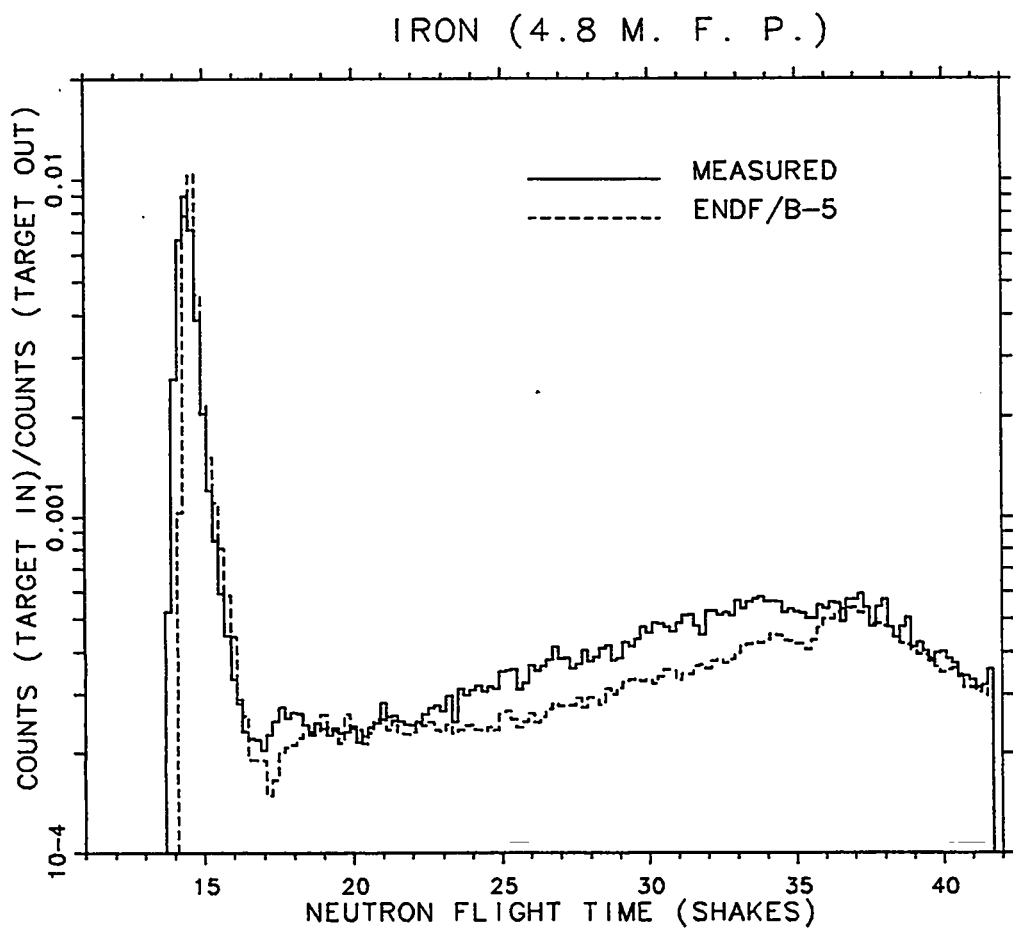


Fig. 62. Plot of experimental and ENDF/B-V calculated count rates for the iron sphere of 4.8 mean free path radius.

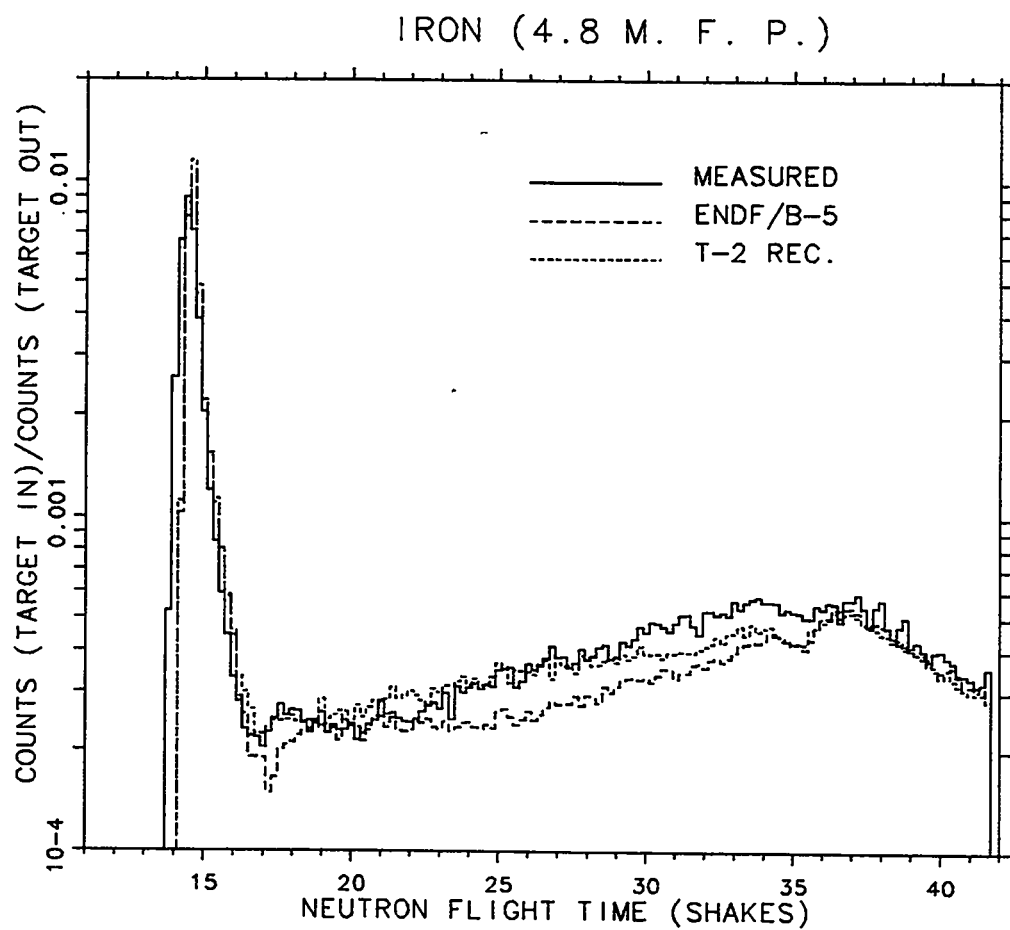


Fig. 63. Plot of experimental, ENDF/B-V calculated, and MCNP recommended calculated rates for the iron sphere with 4.8 mean free path radius.

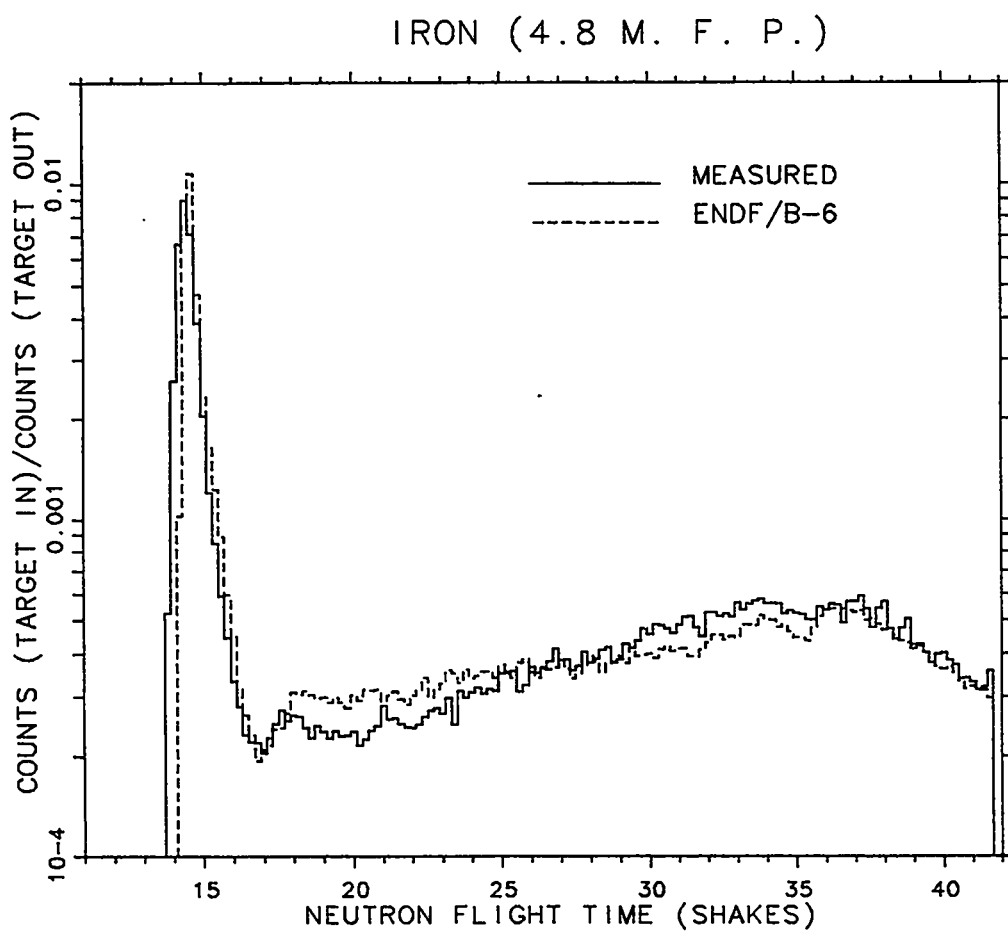


Fig. 64. Plot of experimental and ENDF/B-VI calculated count rates for the iron sphere of 4.8 mean free path radius.

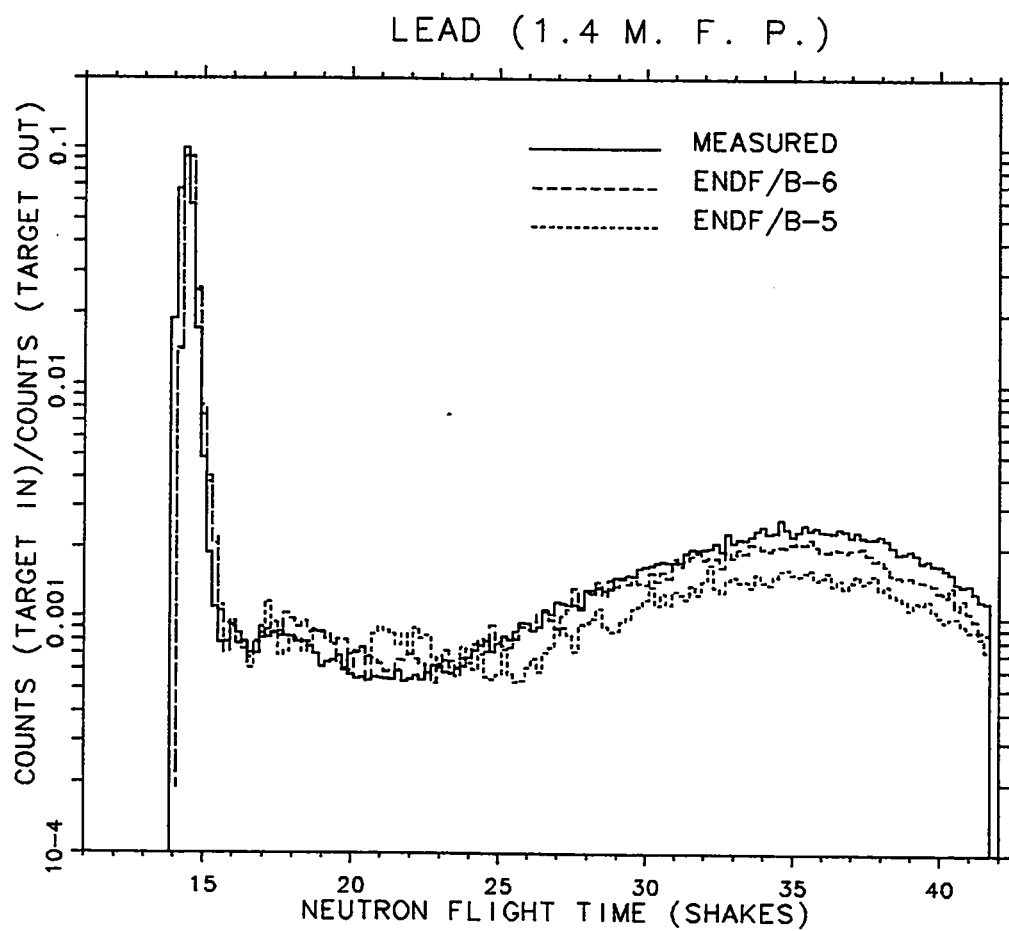


Fig. 65. Plot of experimental and calculated count rates as a function of time for a lead sphere with 1.4 mean free path radius. The detector was located 766.0 cm from the center of the sphere at 30 degrees with respect to the deuteron beam. (1 shake = 10 ns)

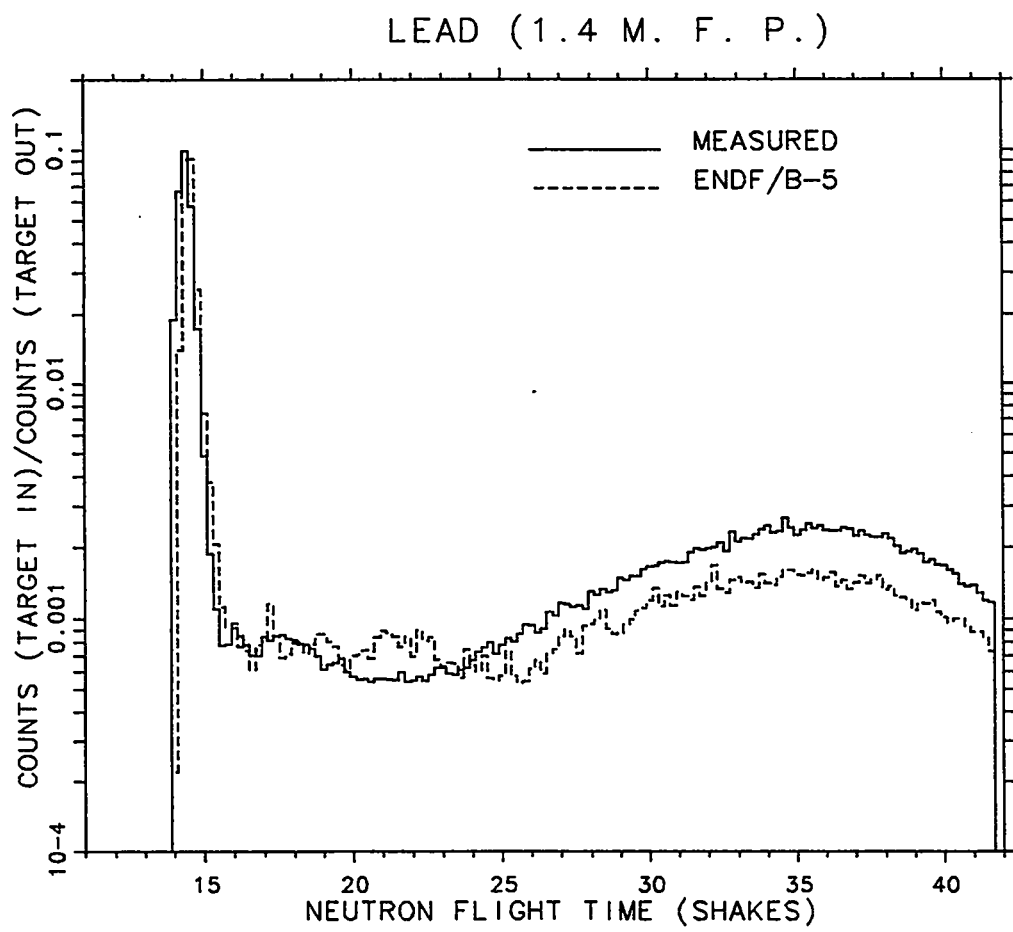


Fig. 66. Plot of experimental and ENDF/B-V calculated count rates for the lead sphere of 1.4 mean free path radius.

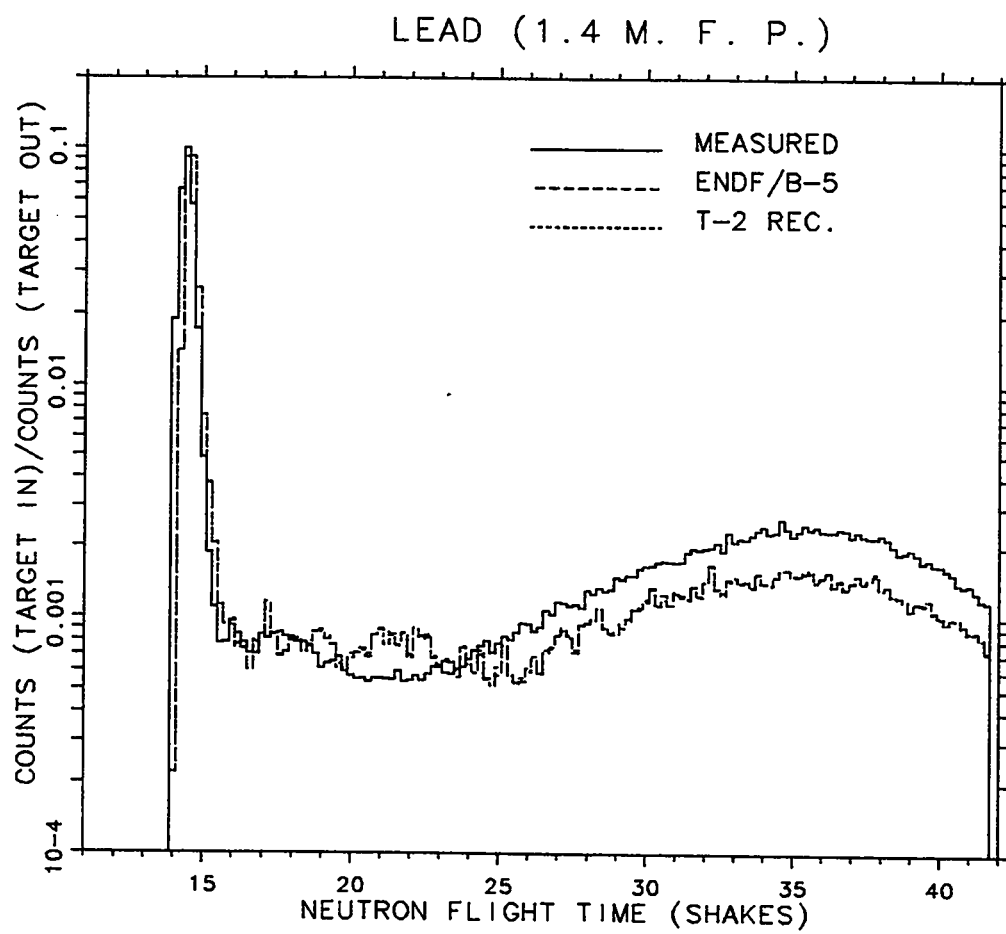


Fig. 67. Plot of experimental, ENDF/B-V calculated, and MCNP recommended calculated rates for the lead sphere with 1.4 mean free path radius.

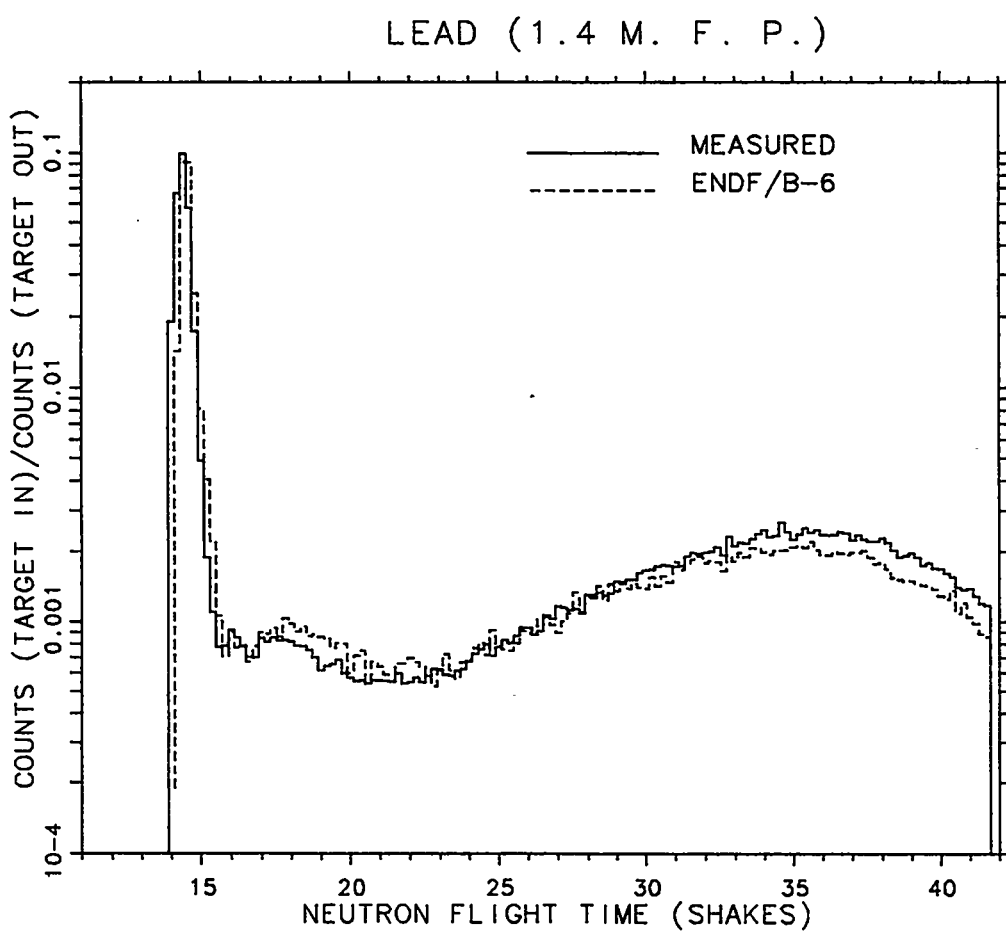


Fig. 68. Plot of experimental and ENDF/B-VI calculated count rates for the lead sphere of 1.4 mean free path radius.

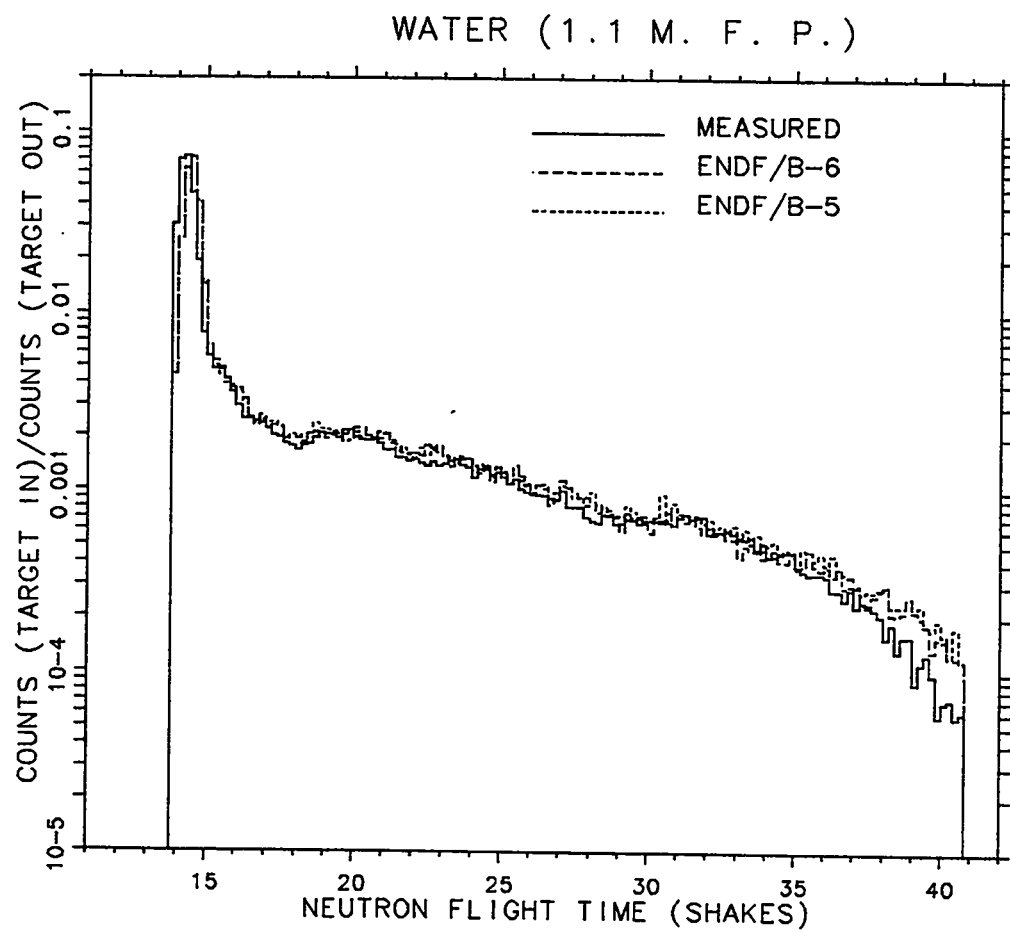


Fig. 69. Plot of experimental and calculated count rates as a function of time for a water sphere with 1.1 mean free path radius. The detector was located 754.0 cm from the center of the sphere at 30 degrees with respect to the deuteron beam. (1 shake = 10 ns)

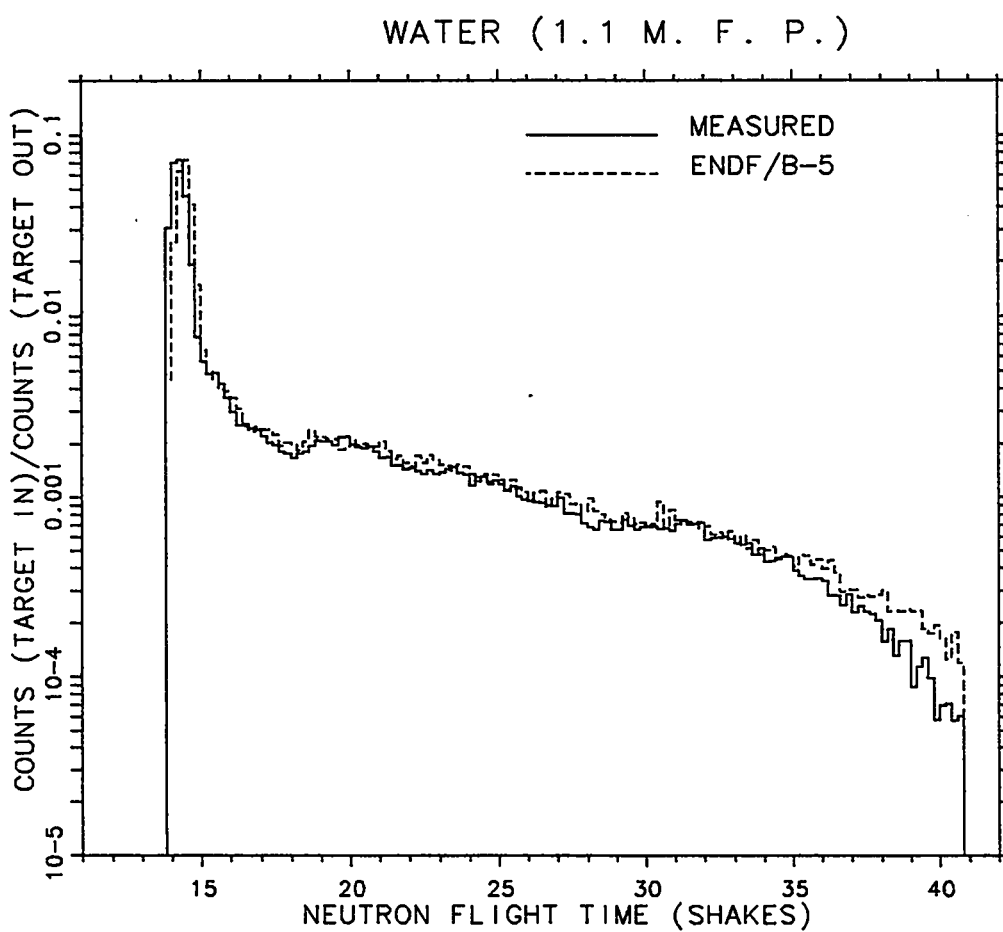


Fig. 70. Plot of experimental and ENDF/B-V calculated count rates for the water sphere of 1.1 mean free path radius.

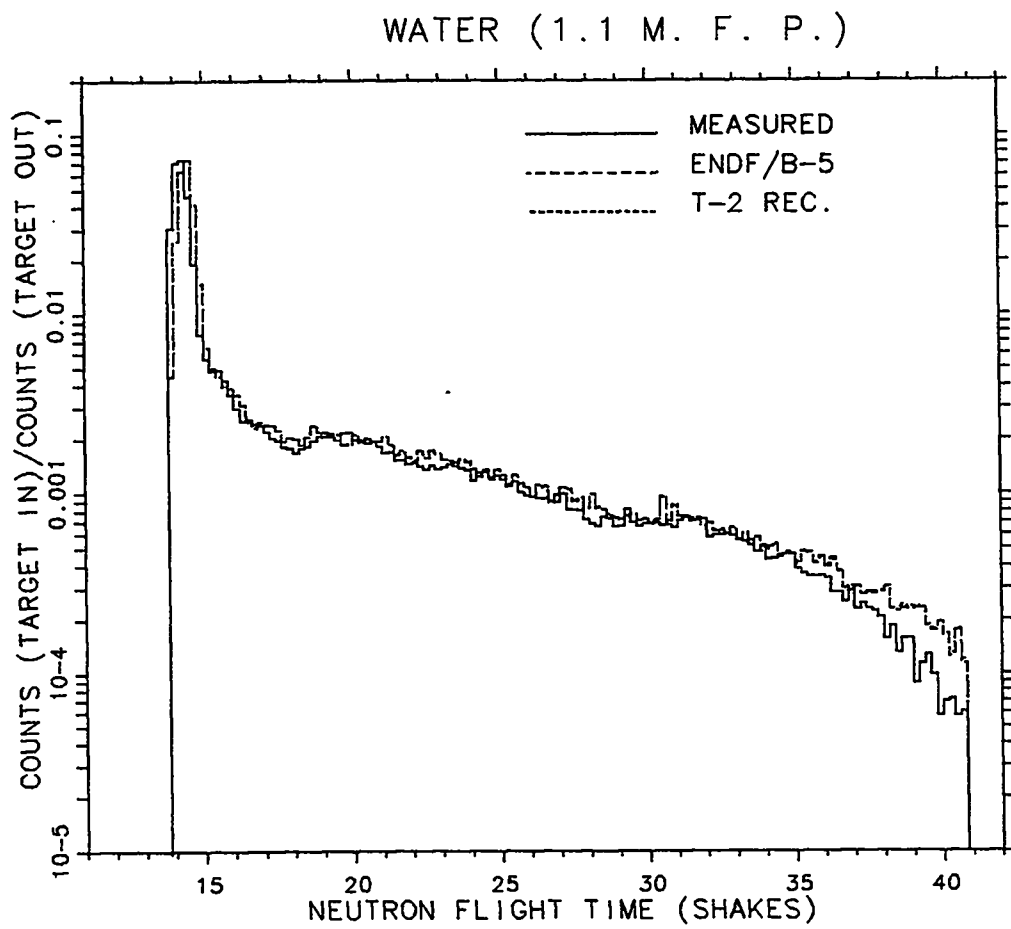


Fig. 71. Plot of experimental, ENDF/B-V calculated, and MCNP recommended calculated rates for the water sphere with 1.1 mean free path radius.

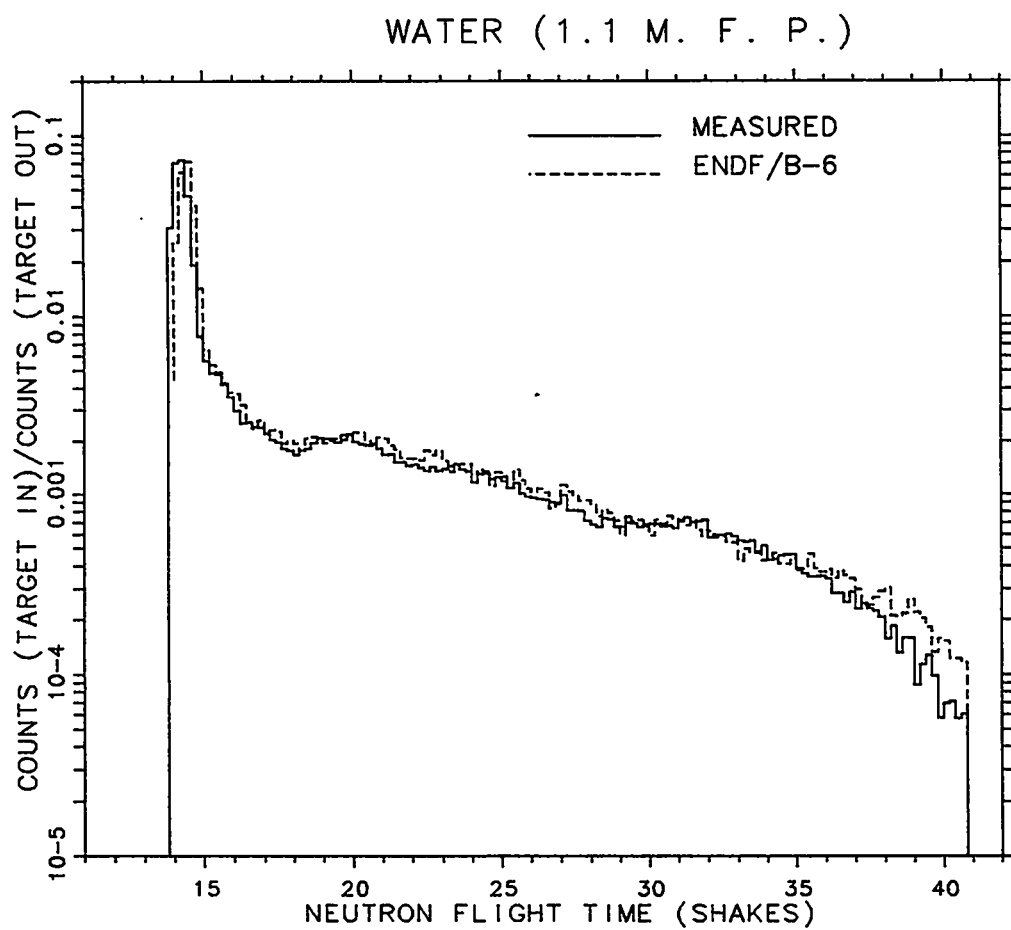


Fig. 72. Plot of experimental and ENDF/B-VI calculated count rates for the water sphere of 1.1 mean free path radius.

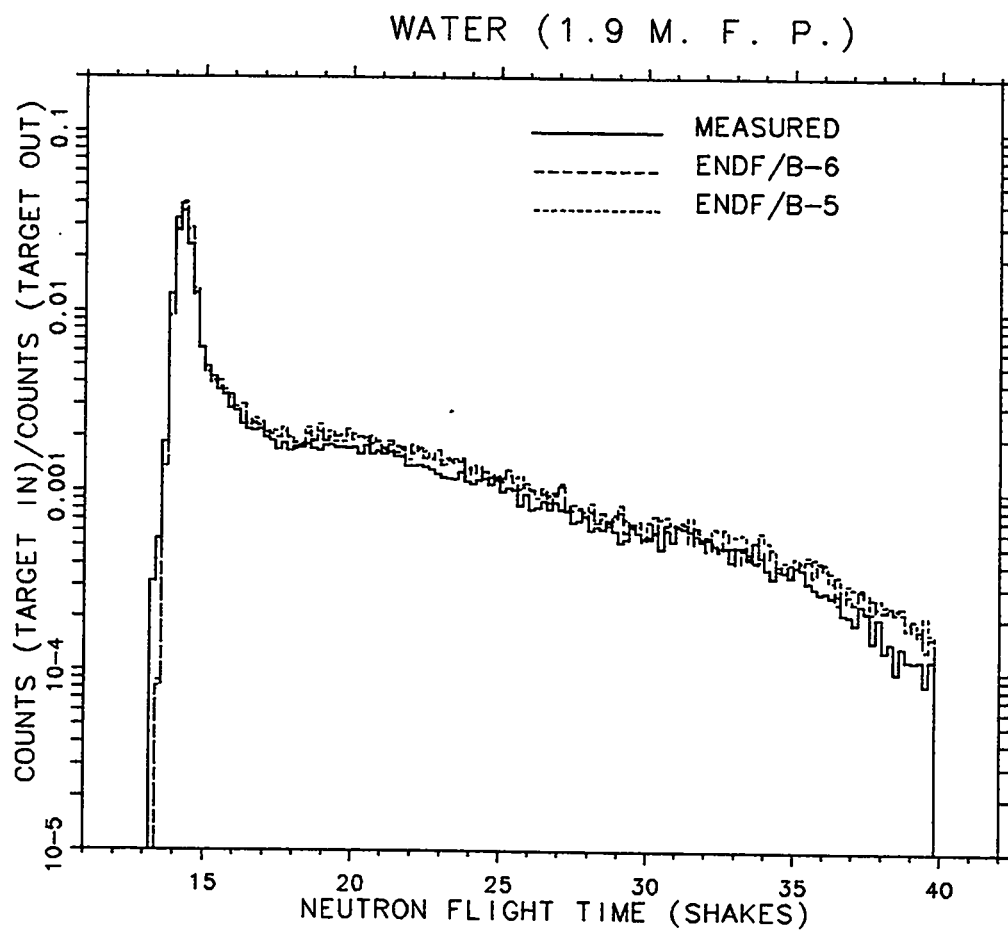


Fig. 73. Plot of experimental and calculated count rates as a function of time for a water sphere with 1.9 mean free path radius. The detector was located 754.0 cm from the center of the sphere at 30 degrees with respect to the deuteron beam. (1 shake = 10 ns)

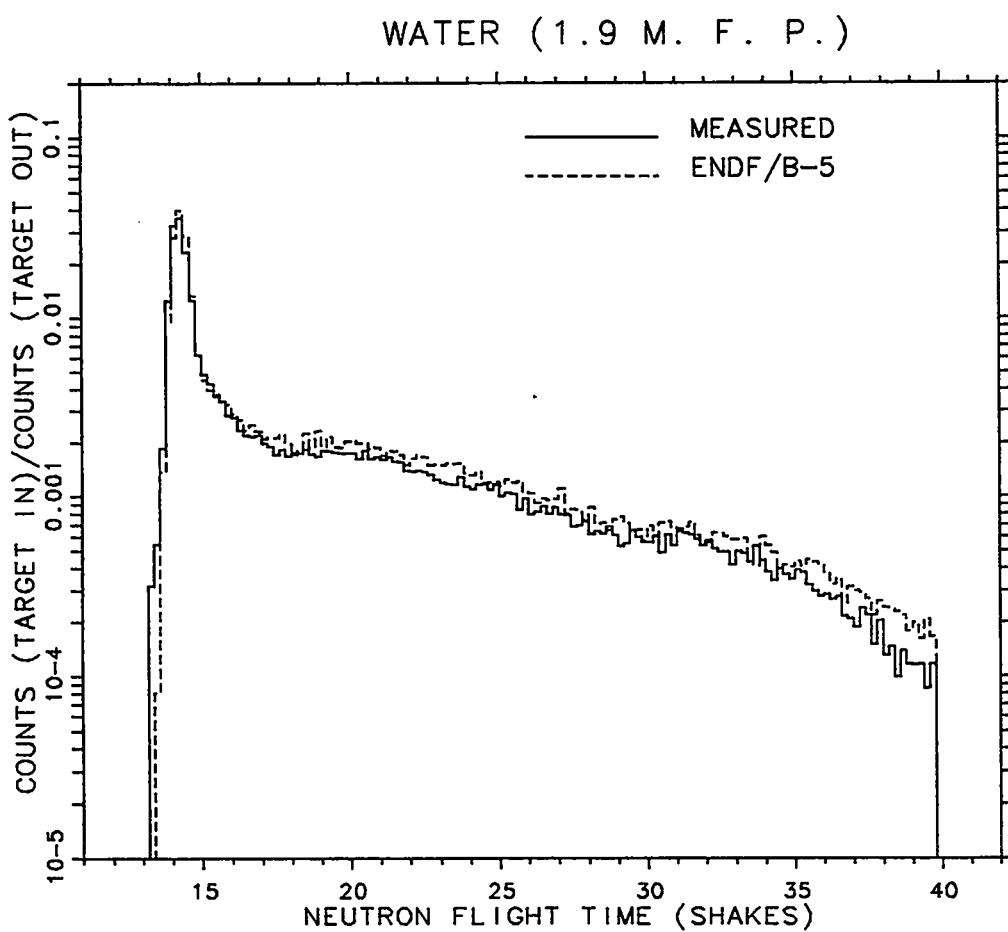


Fig. 74. Plot of experimental and ENDF/B-V calculated count rates for the water sphere of 1.9 mean free path radius.

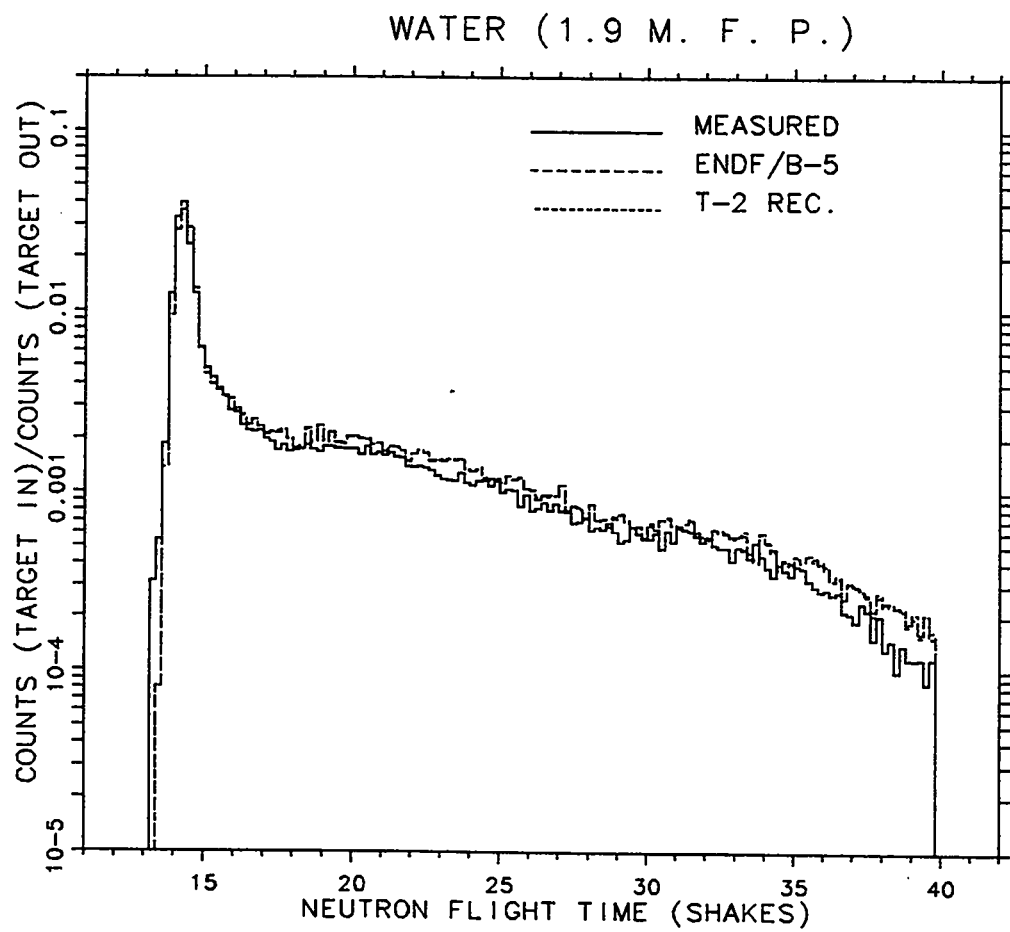


Fig. 75. Plot of experimental, ENDF/B-V calculated, and MCNP recommended calculated rates for the water sphere with 1.9 mean free path radius.

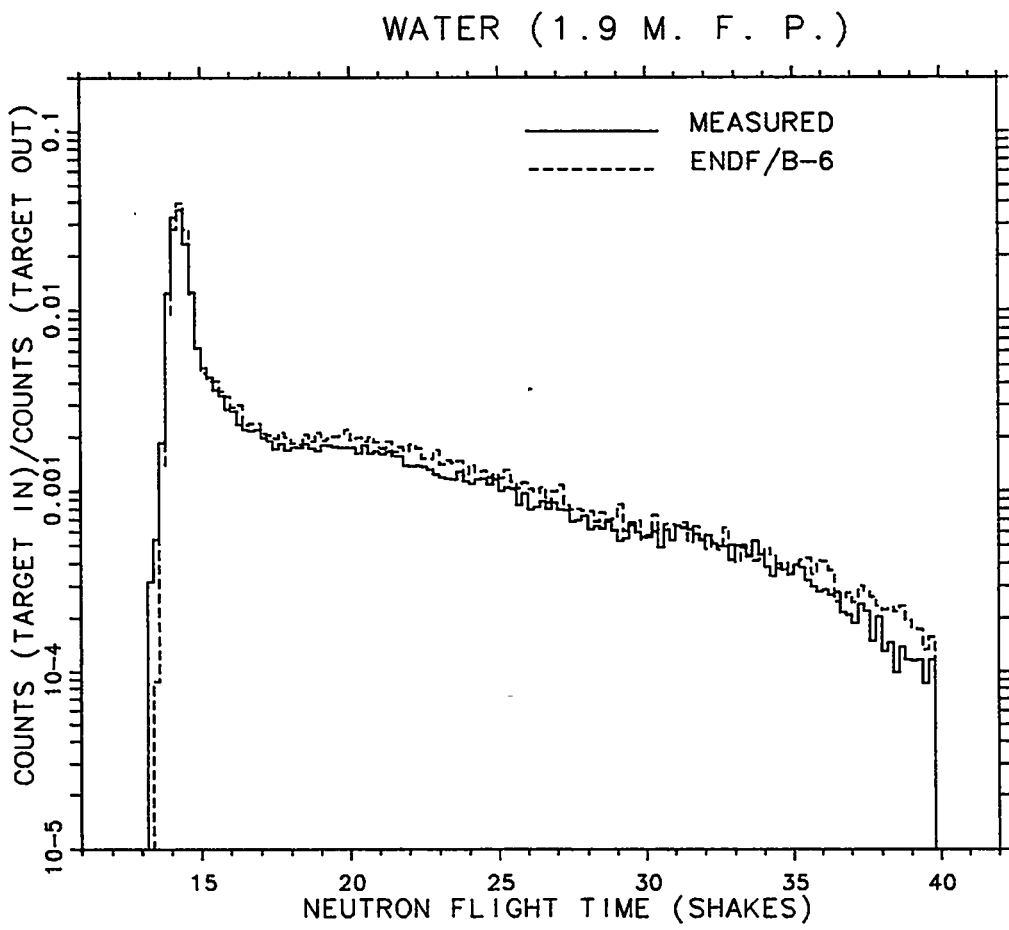


Fig. 76. Plot of experimental and ENDF/B-VI calculated count rates for the water sphere of 1.9 mean free path radius.

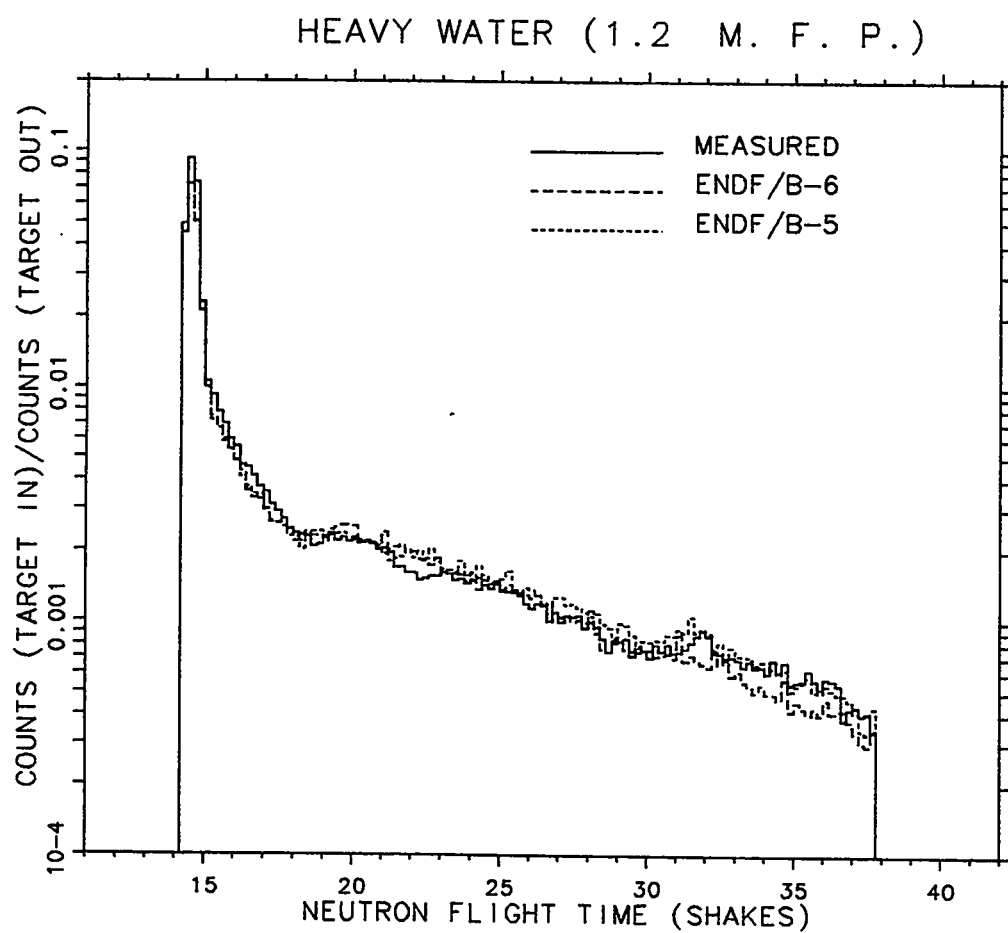


Fig. 77. Plot of experimental and calculated count rates as a function of time for a heavy water sphere with 1.2 mean free path radius. The detector was located 765.2 cm from the center of the sphere at 30 degrees with respect to the deuteron beam. (1 shake = 10 ns)

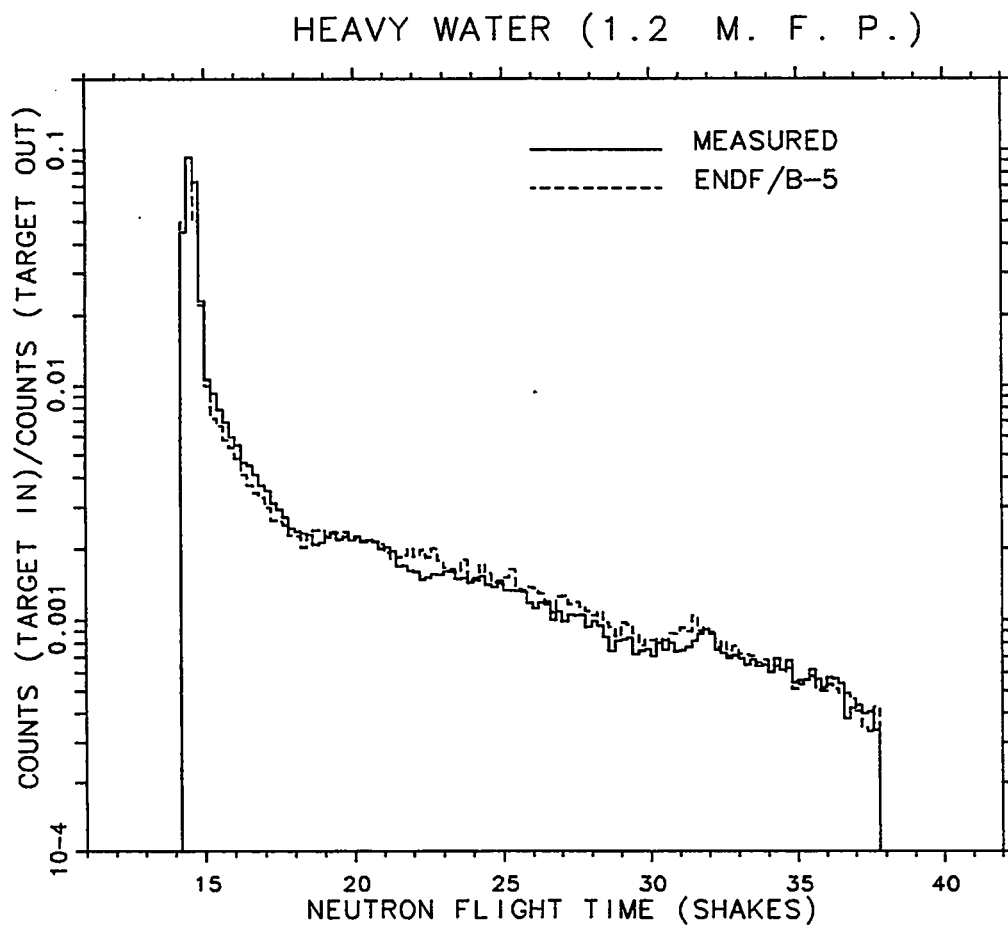


Fig. 78. Plot of experimental and ENDF/B-V calculated count rates for the heavy water sphere of 1.2 mean free path radius.

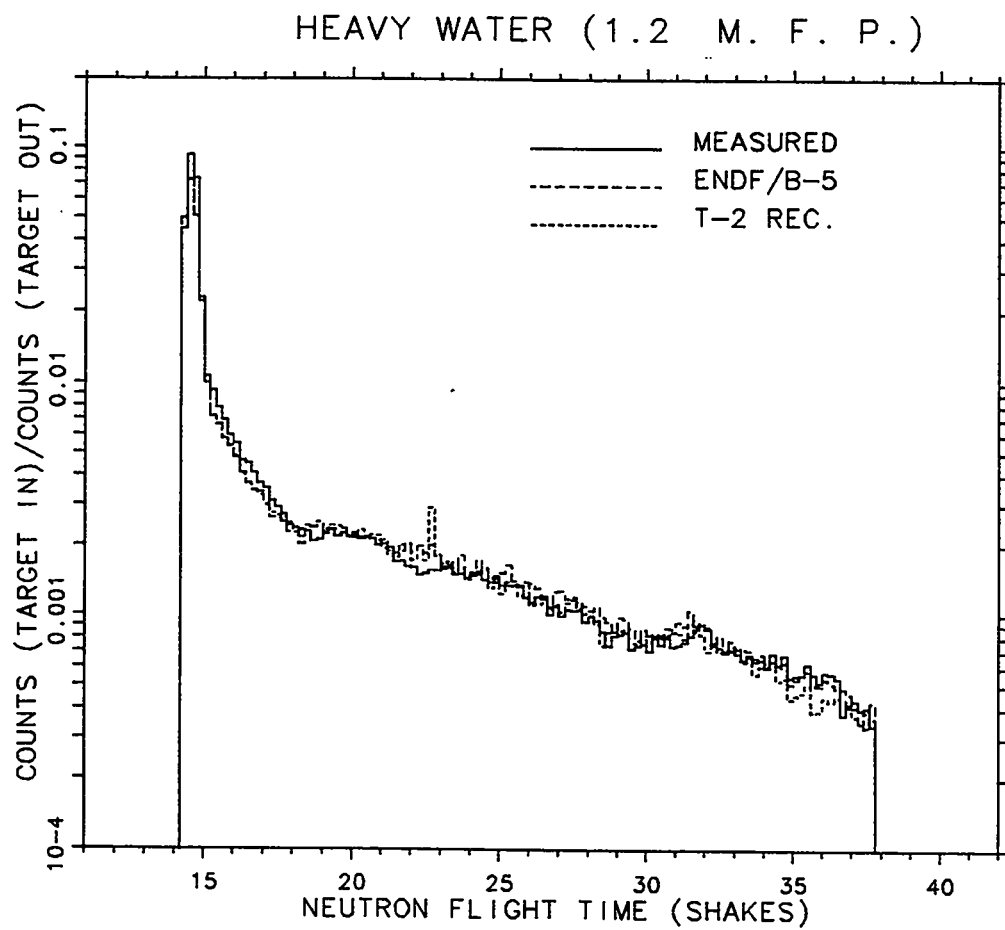


Fig. 79. Plot of experimental, ENDF/B-V calculated, and MCNP recommended calculated rates for the heavy water sphere with 1.2 mean free path radius.

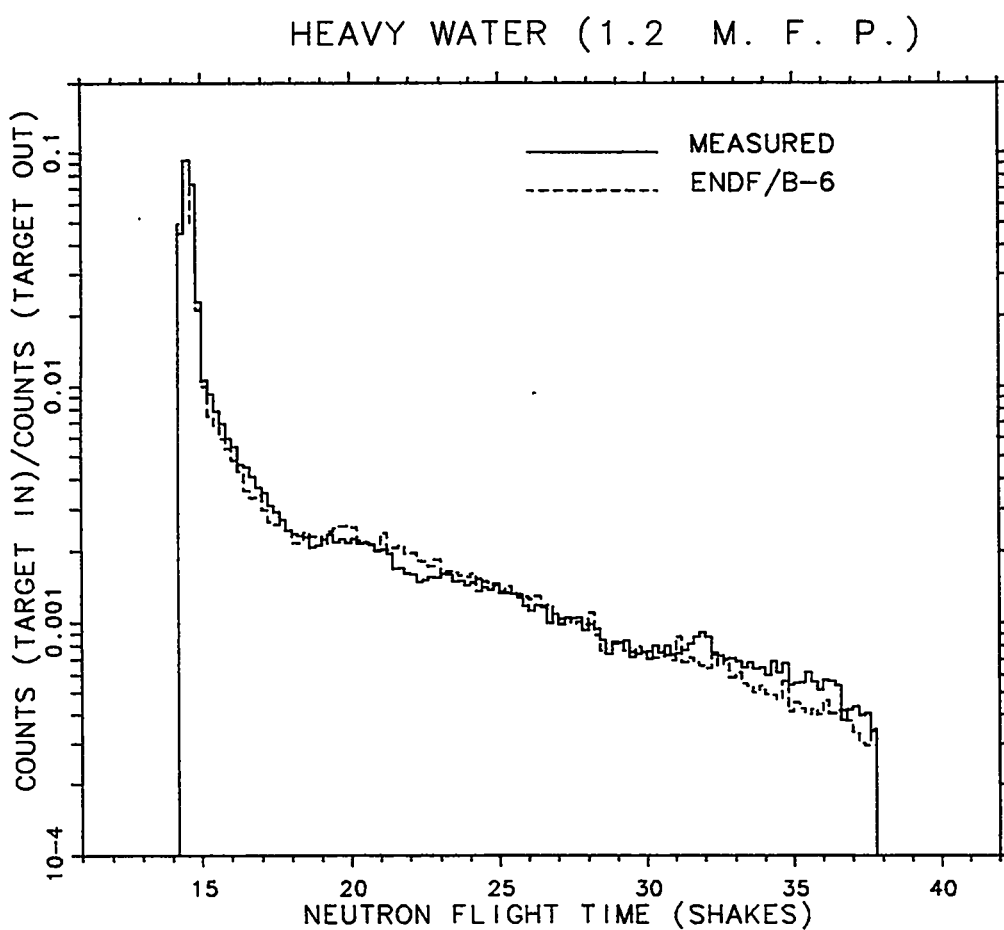


Fig. 80. Plot of experimental and ENDF/B-VI calculated count rates for the heavy water sphere of 1.2 mean free path radius.

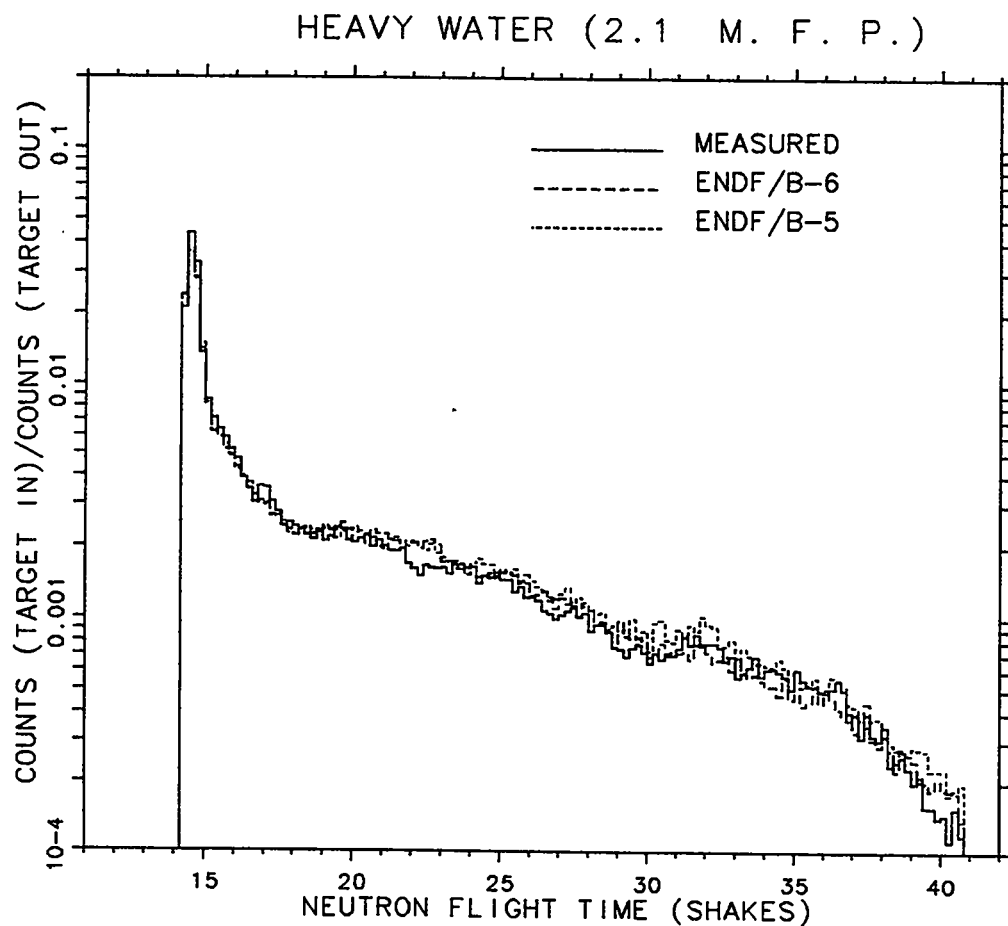


Fig. 81. Plot of experimental and calculated count rates as a function of time for a heavy water sphere with 2.1 mean free path radius. The detector was located 765.2 cm from the center of the sphere at 30 degrees with respect to the deuteron beam. (1 shake = 10 ns)

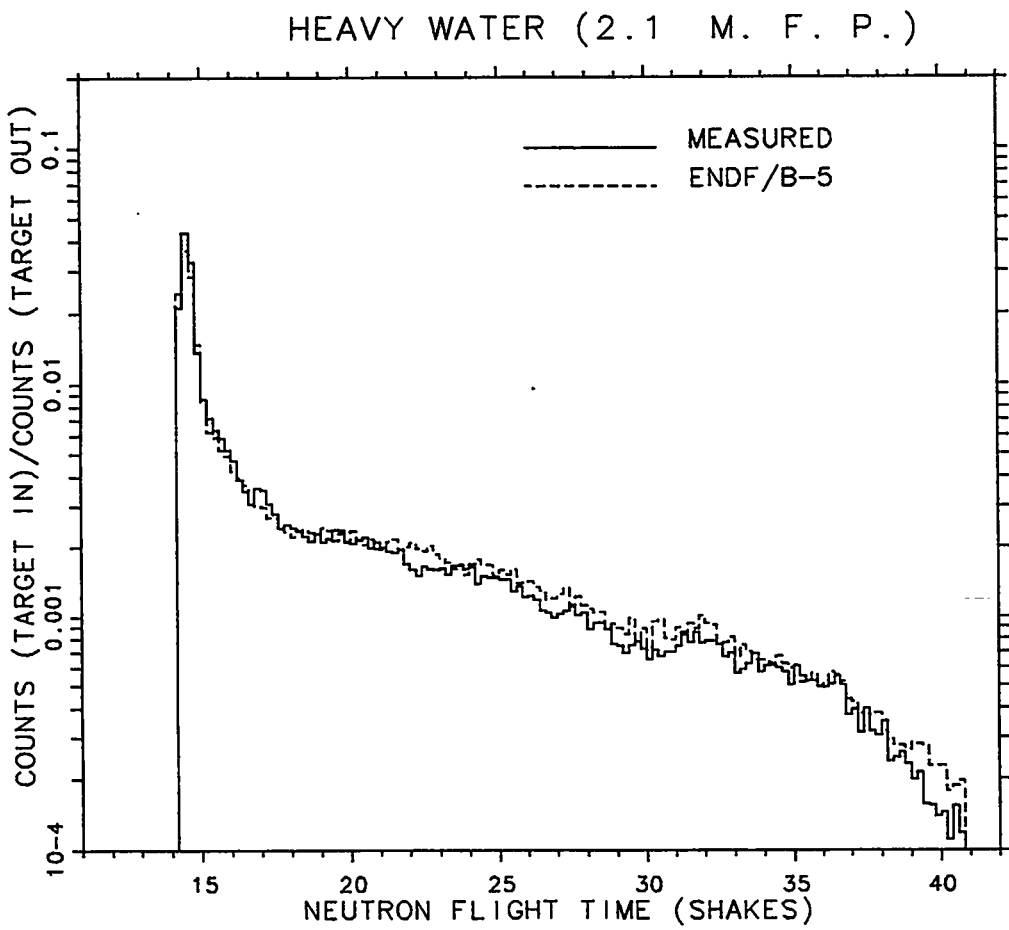


Fig. 82. Plot of experimental and ENDF/B-V calculated count rates for the heavy water sphere of 2.1 mean free path radius.

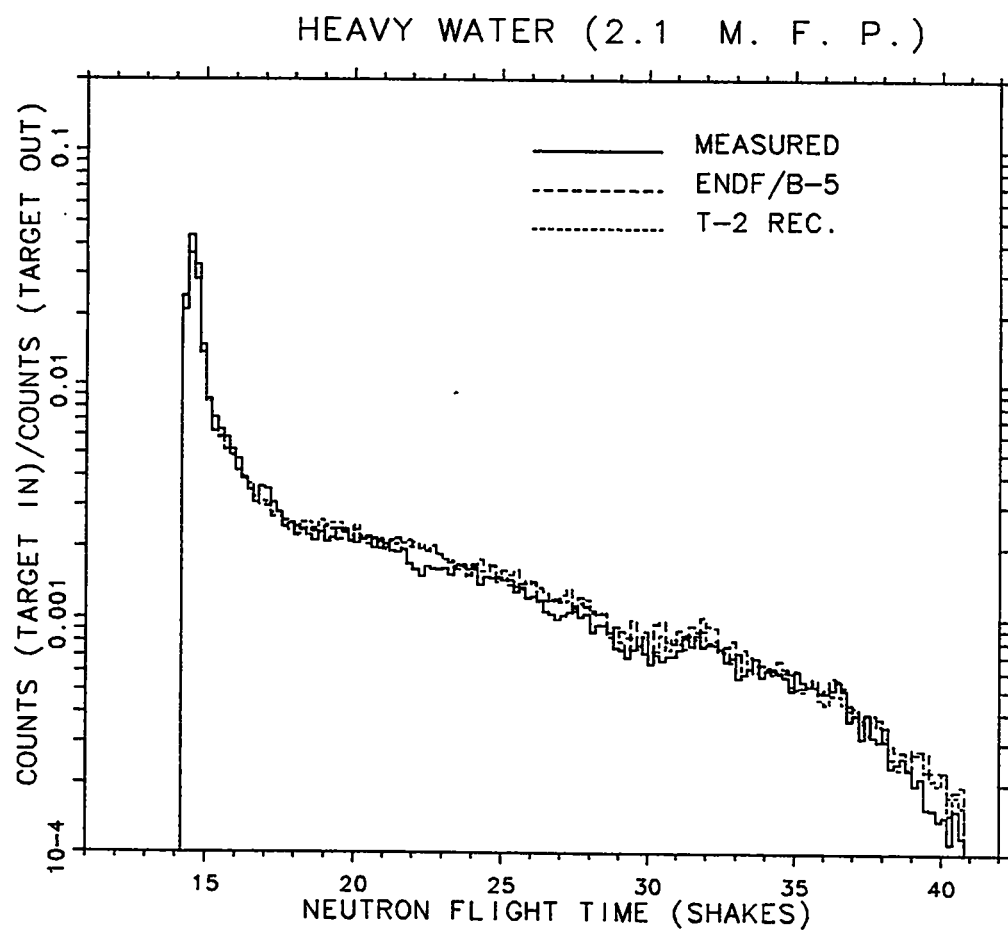


Fig. 83. Plot of experimental, ENDF/B-V calculated, and MCNP recommended calculated rates for the heavy water sphere with 2.1 mean free path radius.

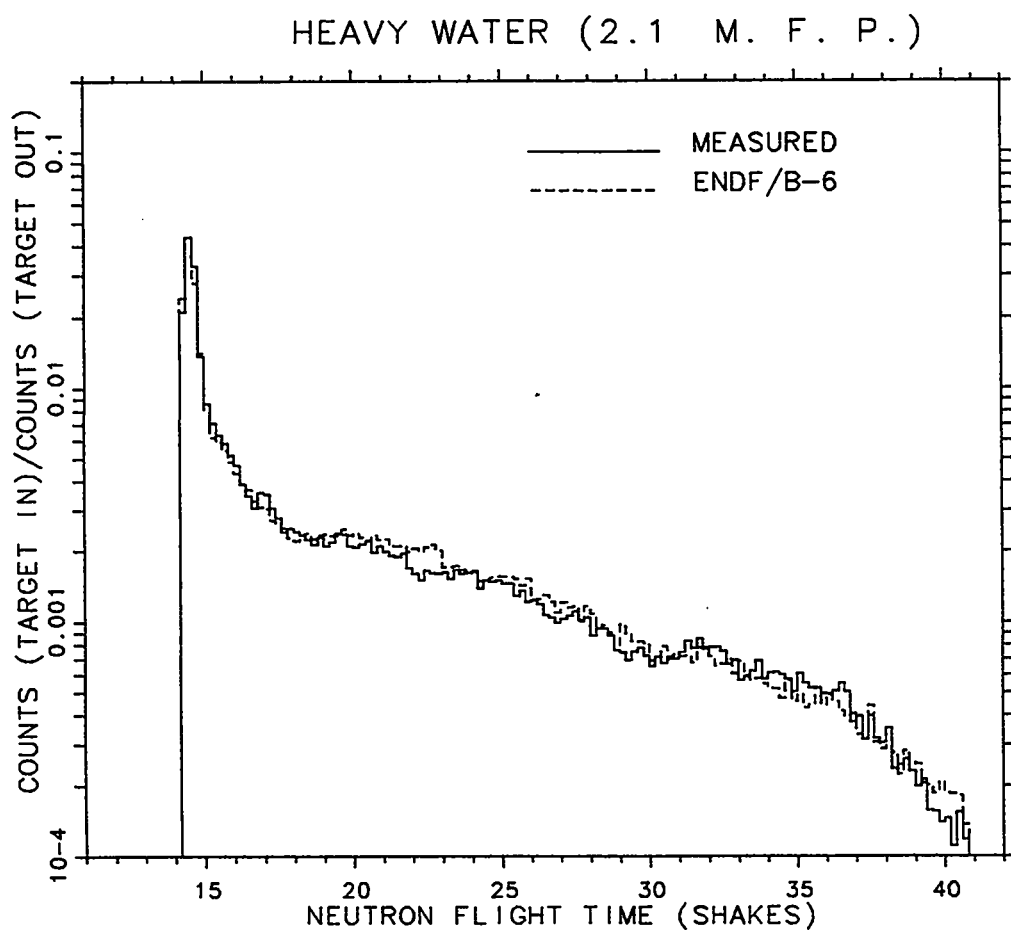


Fig. 84. Plot of experimental and ENDF/B-VI calculated count rates for the heavy water sphere of 2.1 mean free path radius.

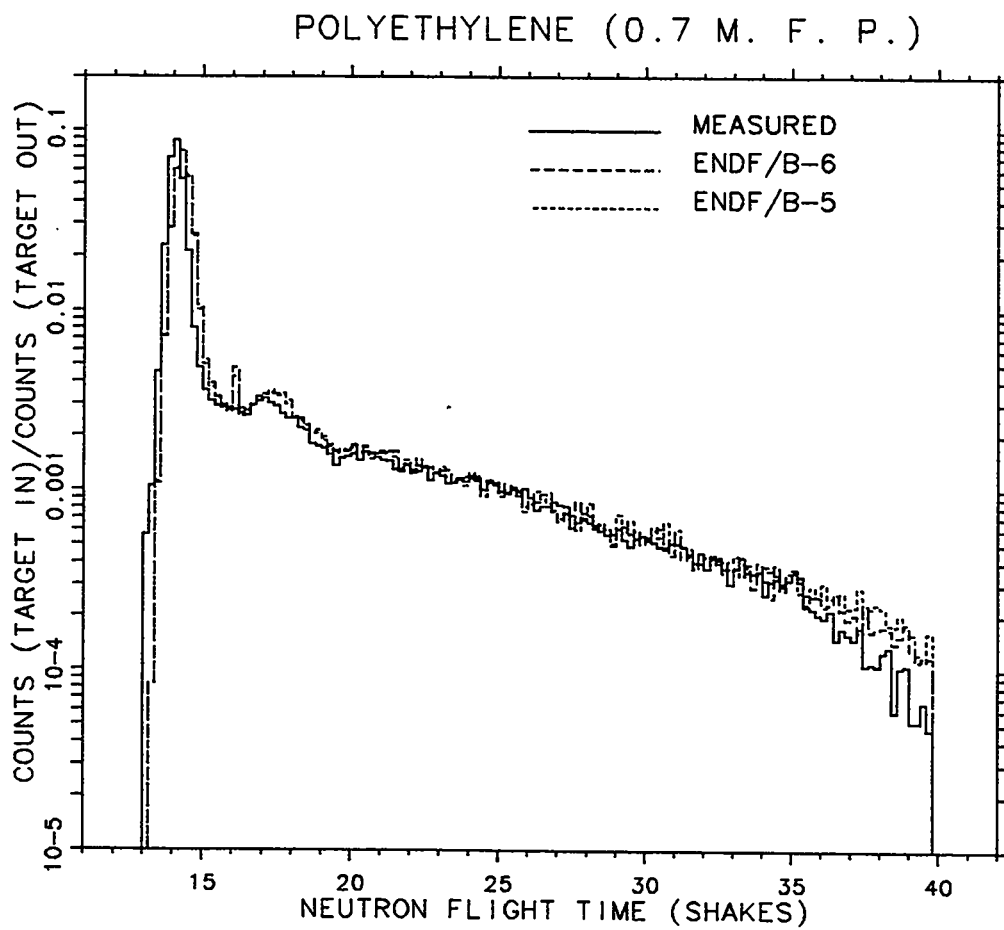


Fig. 85. Plot of experimental and calculated count rates as a function of time for a polyethylene sphere with 0.7 mean free path radius. The detector was located 754.0 cm from the center of the sphere at 30 degrees with respect to the deuteron beam. (1 shake = 10 ns)

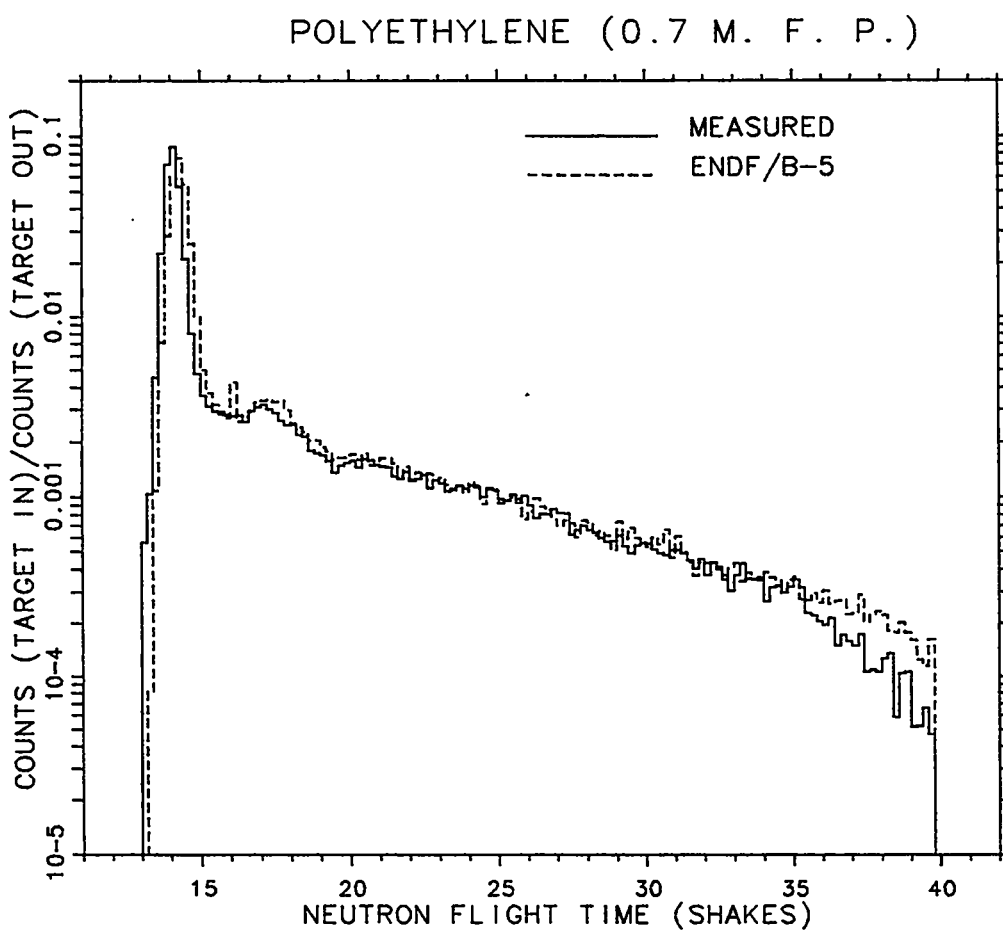


Fig. 86. Plot of experimental and ENDF/B-V calculated count rates for the polyethylene sphere of 0.7 mean free path radius.

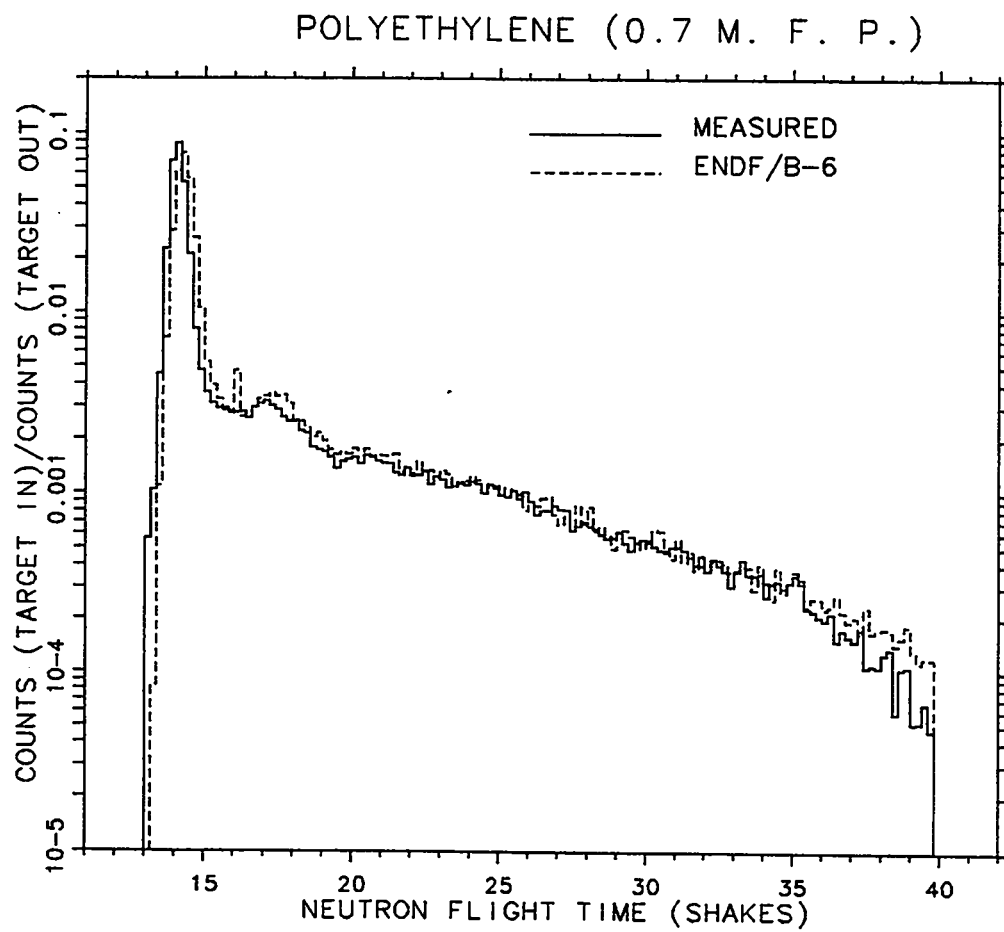


Fig. 87. Plot of experimental and ENDF/B-VI calculated count rates for the polyethylene sphere of 0.7 mean free path radius.

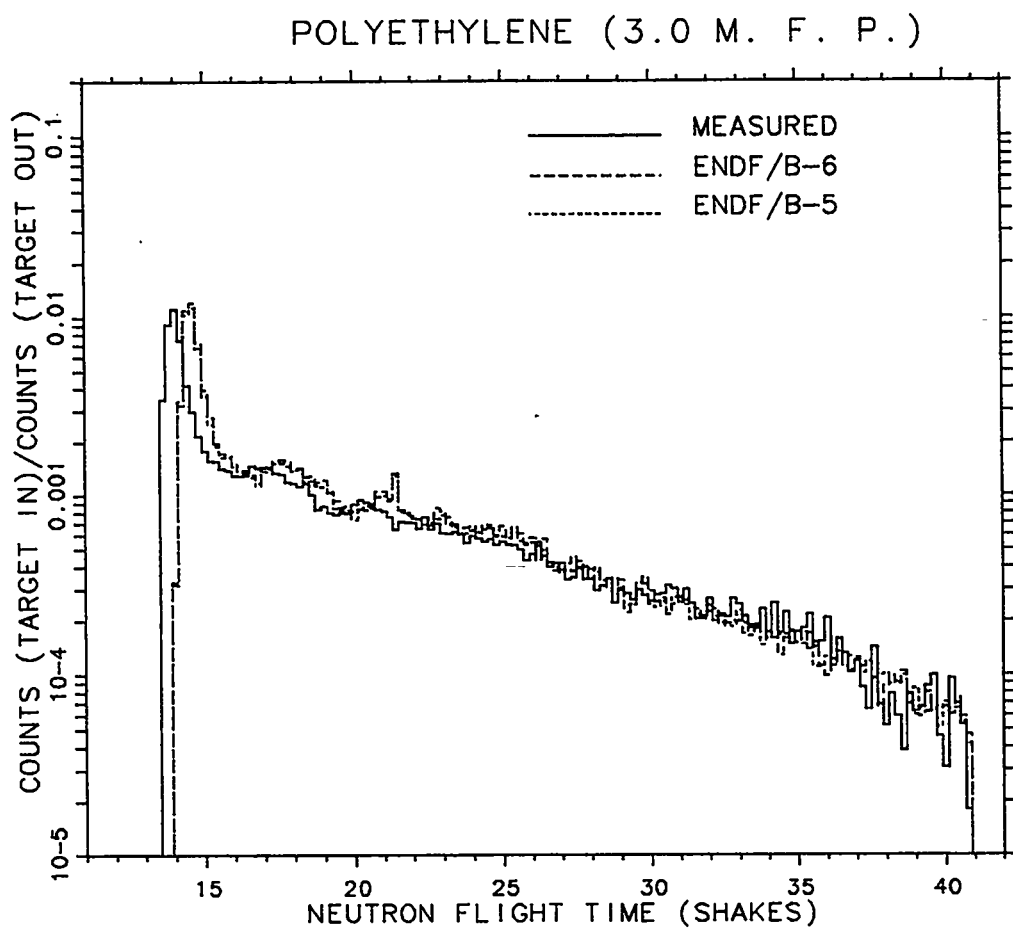


Fig. 88. Plot of experimental and calculated count rates as a function of time for a polyethylene sphere with 3.0 mean free path radius. The detector was located 765.0 cm from the center of the sphere at 30 degrees with respect to the deuteron beam. (1 shake = 10 ns)

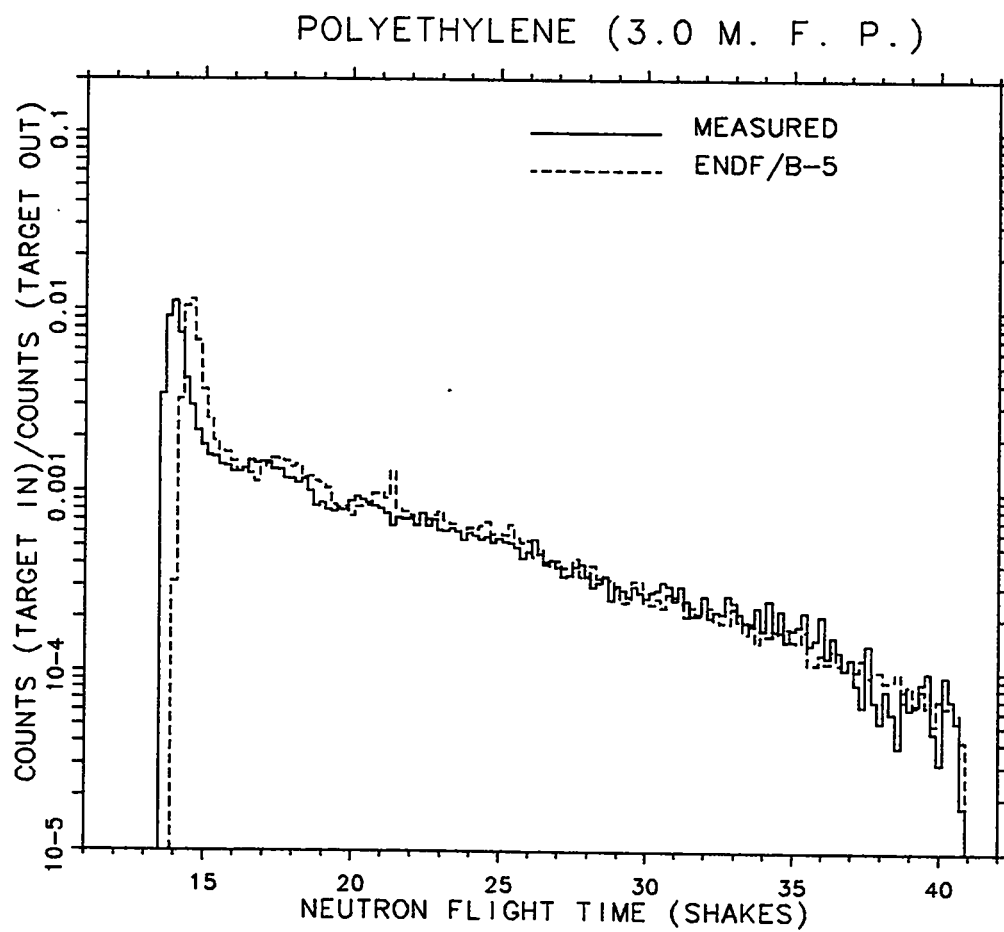


Fig. 89. Plot of experimental and ENDF/B-V calculated count rates for the polyethylene sphere of 3.0 mean free path radius.

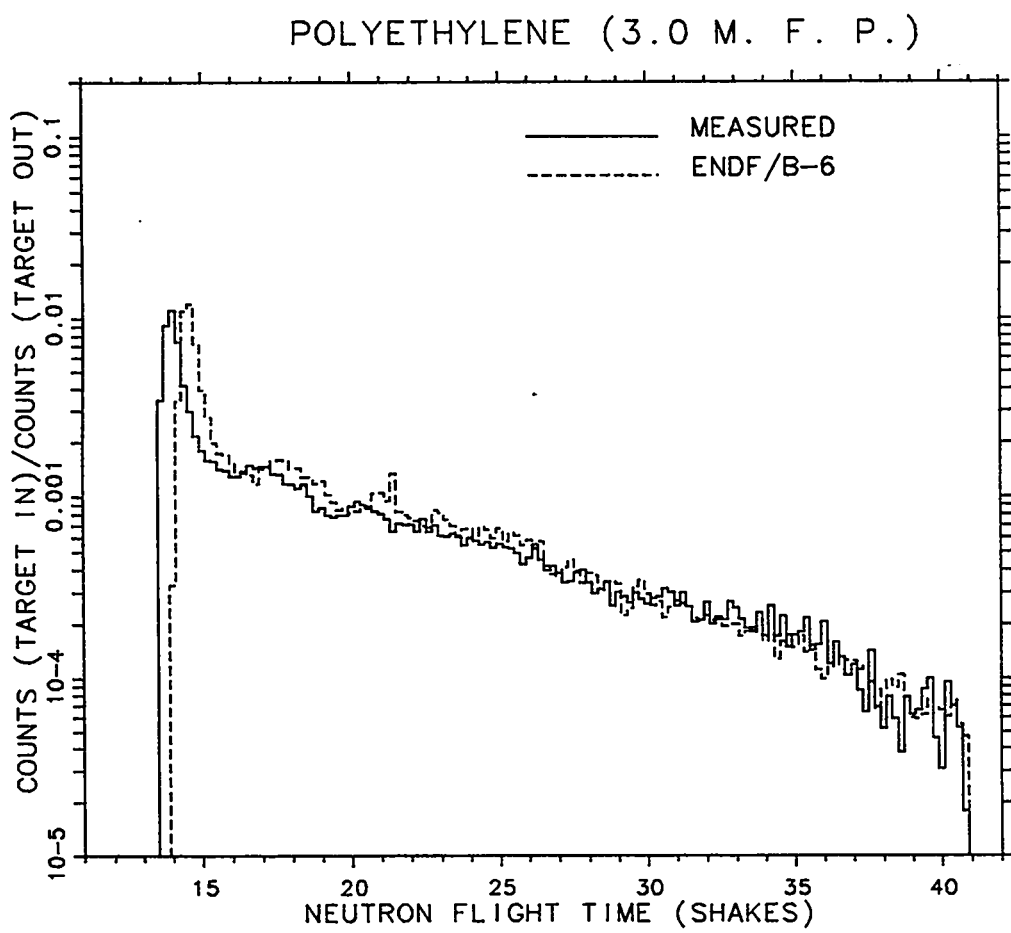


Fig. 90. Plot of experimental and ENDF/B-VI calculated count rates for the polyethylene sphere of 3.0 mean free path radius.

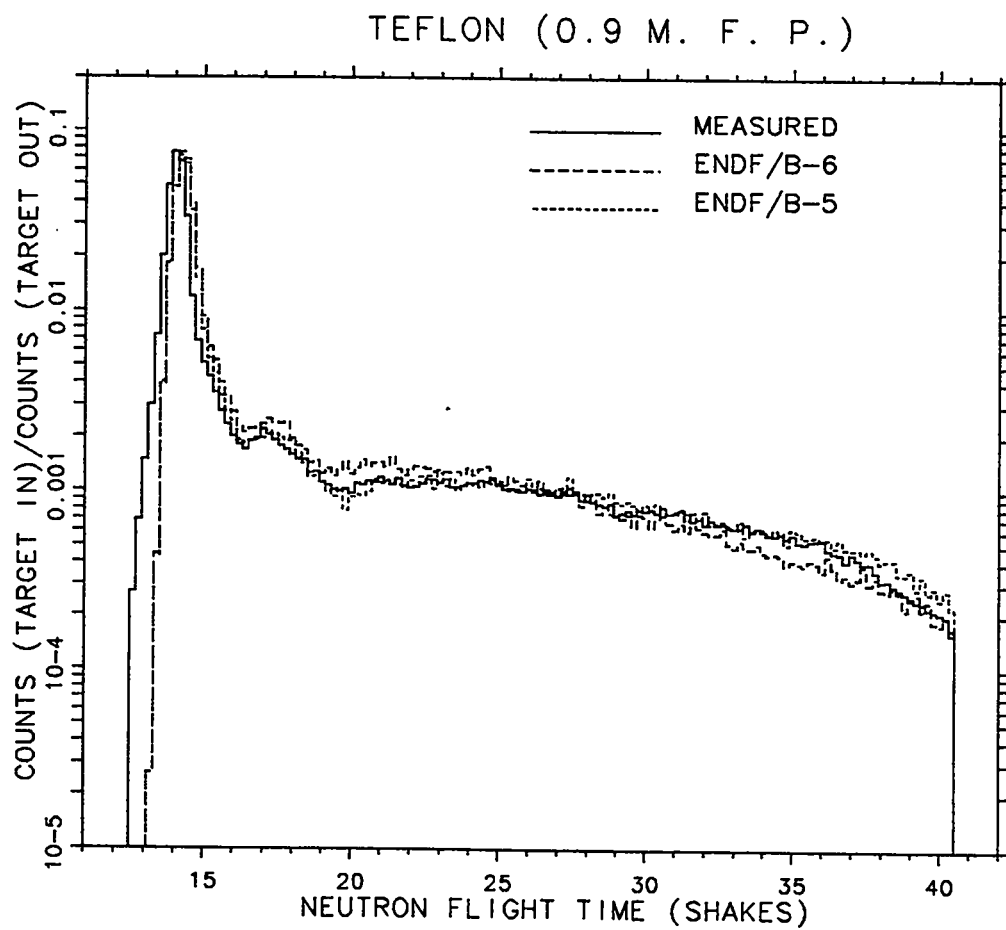


Fig. 91. Plot of experimental and calculated count rates as a function of time for a teflon sphere with 0.9 mean free path radius. The detector was located 752.0 cm from the center of the sphere at 30 degrees with respect to the deuteron beam. (1 shake = 10 ns)

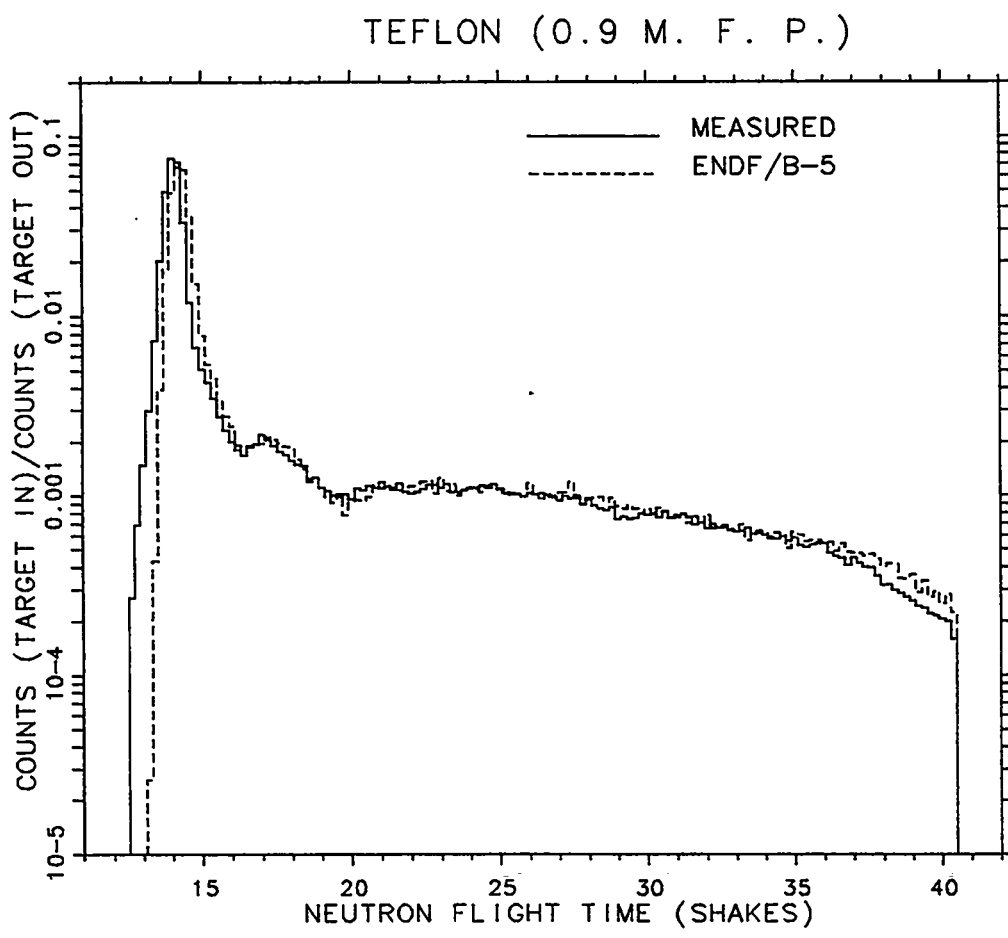


Fig. 92. Plot of experimental and ENDF/B-V calculated count rates for the teflon sphere of 0.9 mean free path radius.

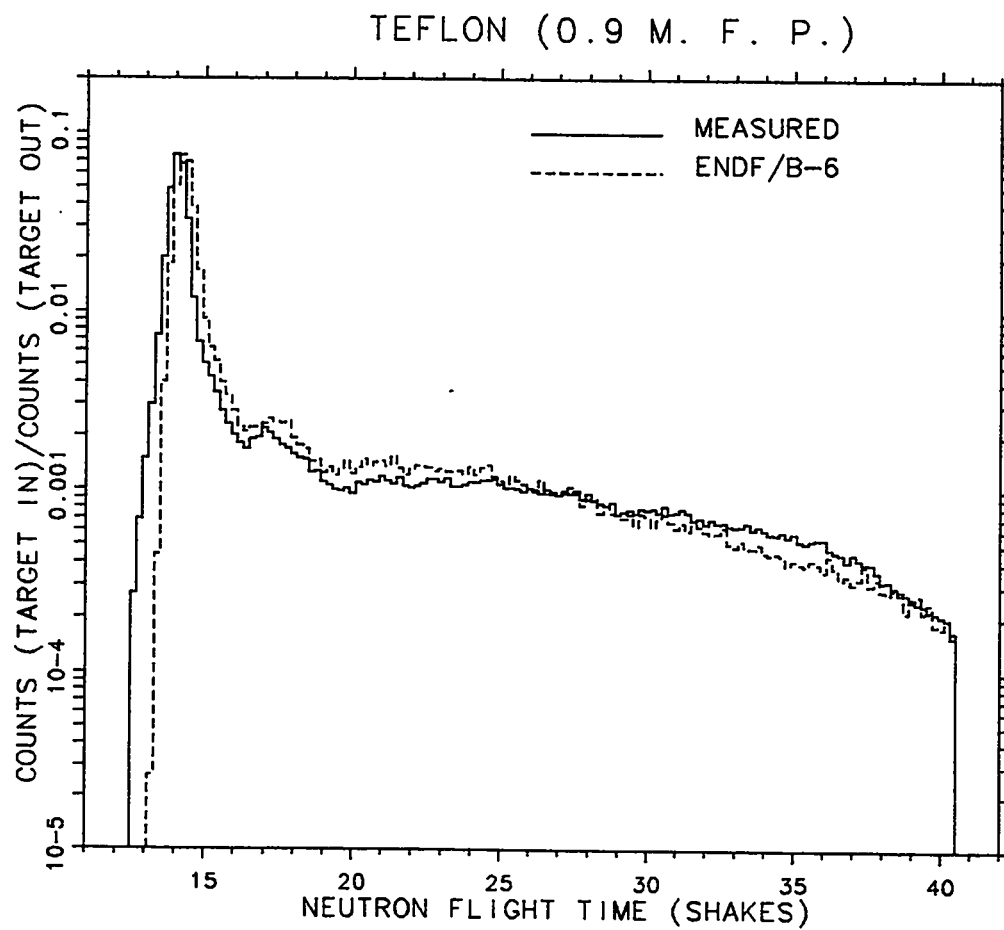


Fig. 93. Plot of experimental and ENDF/B-VI calculated count rates for the teflon sphere of 0.9 mean free path radius.

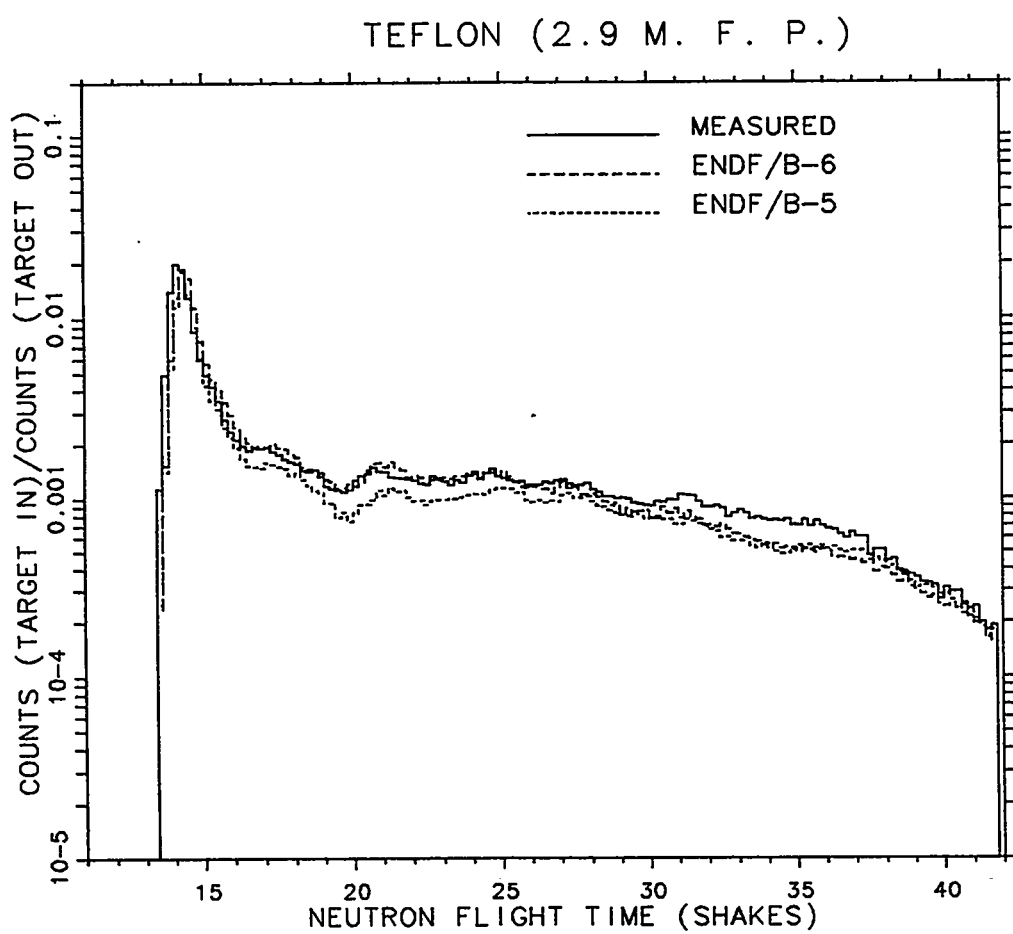


Fig. 94. Plot of experimental and calculated count rates as a function of time for a teflon sphere with 2.9 mean free path radius. The detector was located 752.0 cm from the center of the sphere at 30 degrees with respect to the deuteron beam. (1 shake = 10 ns)

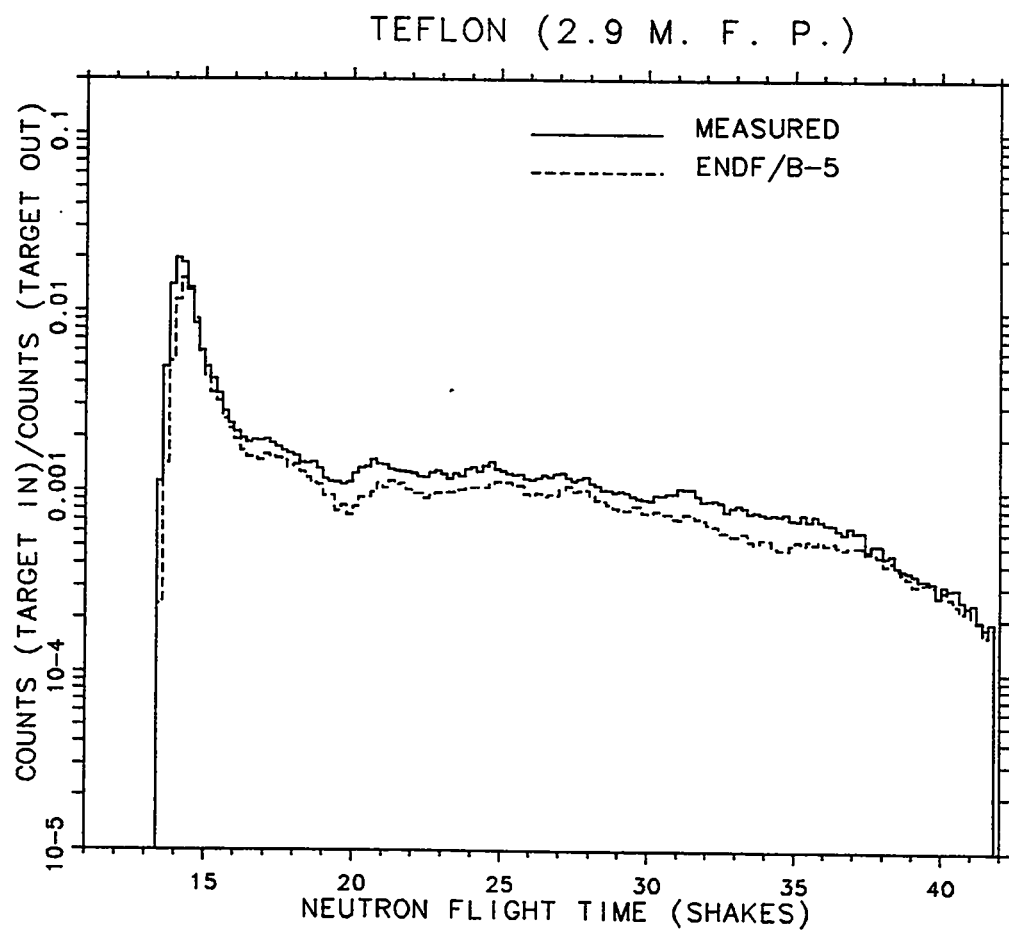


Fig. 95. Plot of experimental and ENDF/B-V calculated count rates for the teflon sphere of 2.9 mean free path radius.

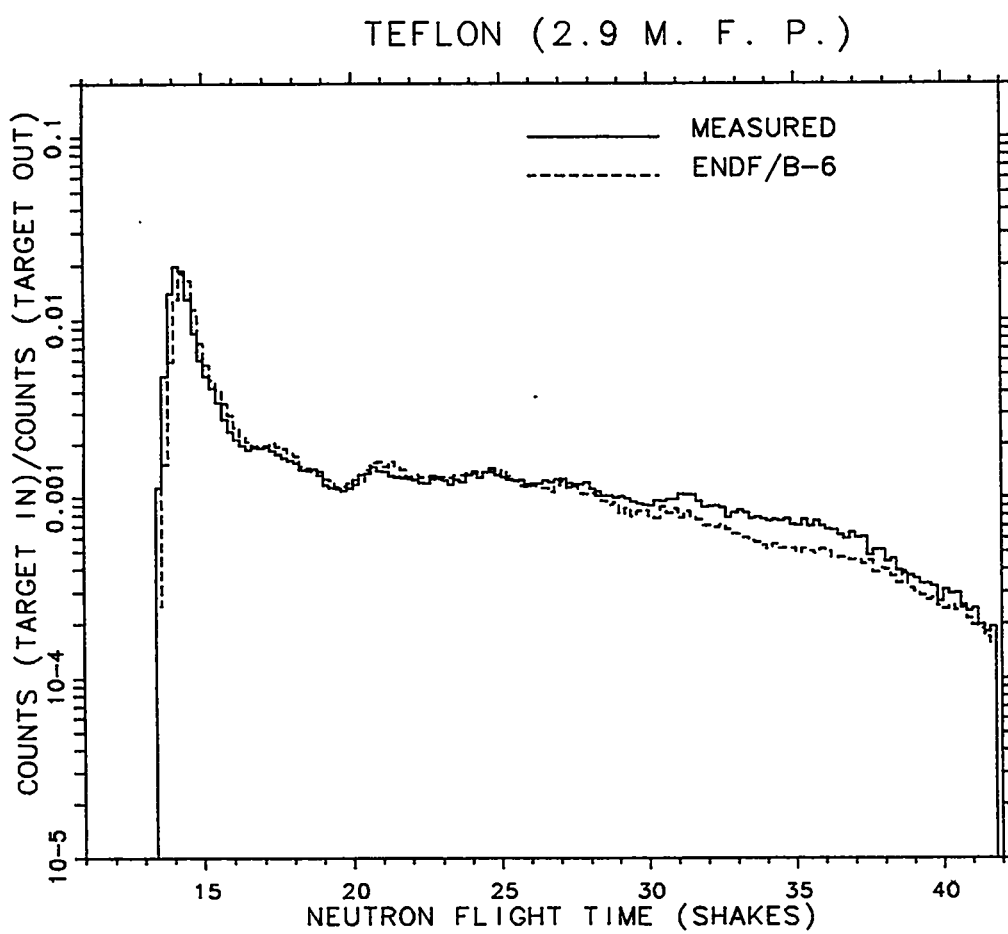


Fig. 96. Plot of experimental and ENDF/B-VI calculated count rates for the teflon sphere of 2.9 mean free path radius.

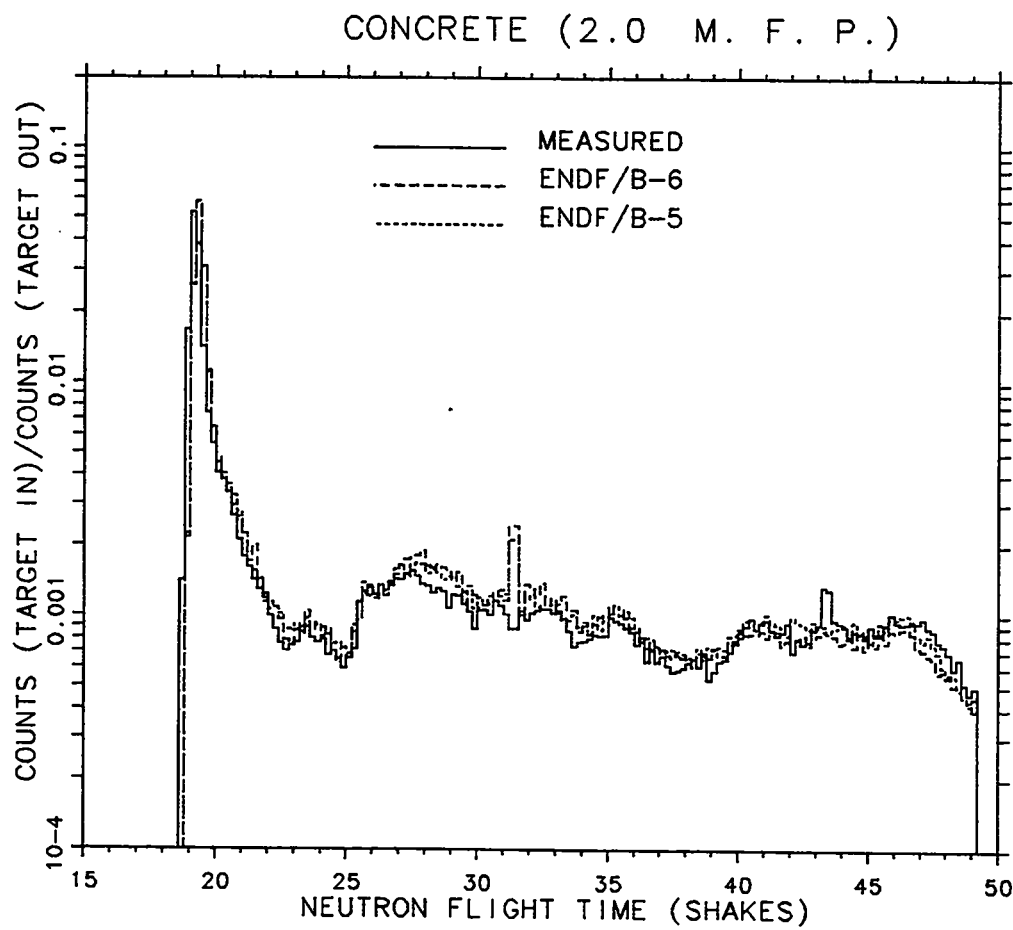


Fig. 97. Plot of experimental and calculated count rates as a function of time for a concrete sphere with 2.0 mean free path radius. The detector was located 975.4 cm from the center of the sphere at 120 degrees with respect to the deuteron beam. (1 shake = 10 ns)

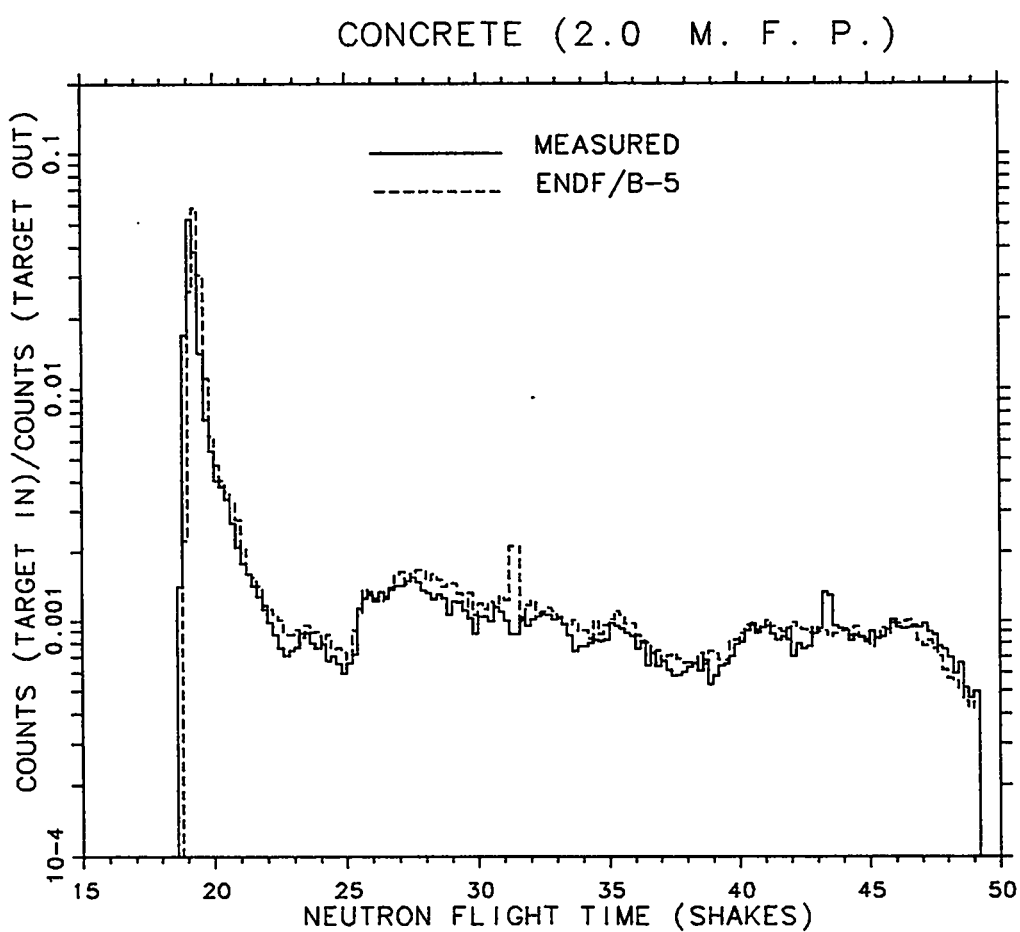


Fig. 98. Plot of experimental and ENDF/B-V calculated count rates for the concrete sphere of 2.0 mean free path radius.

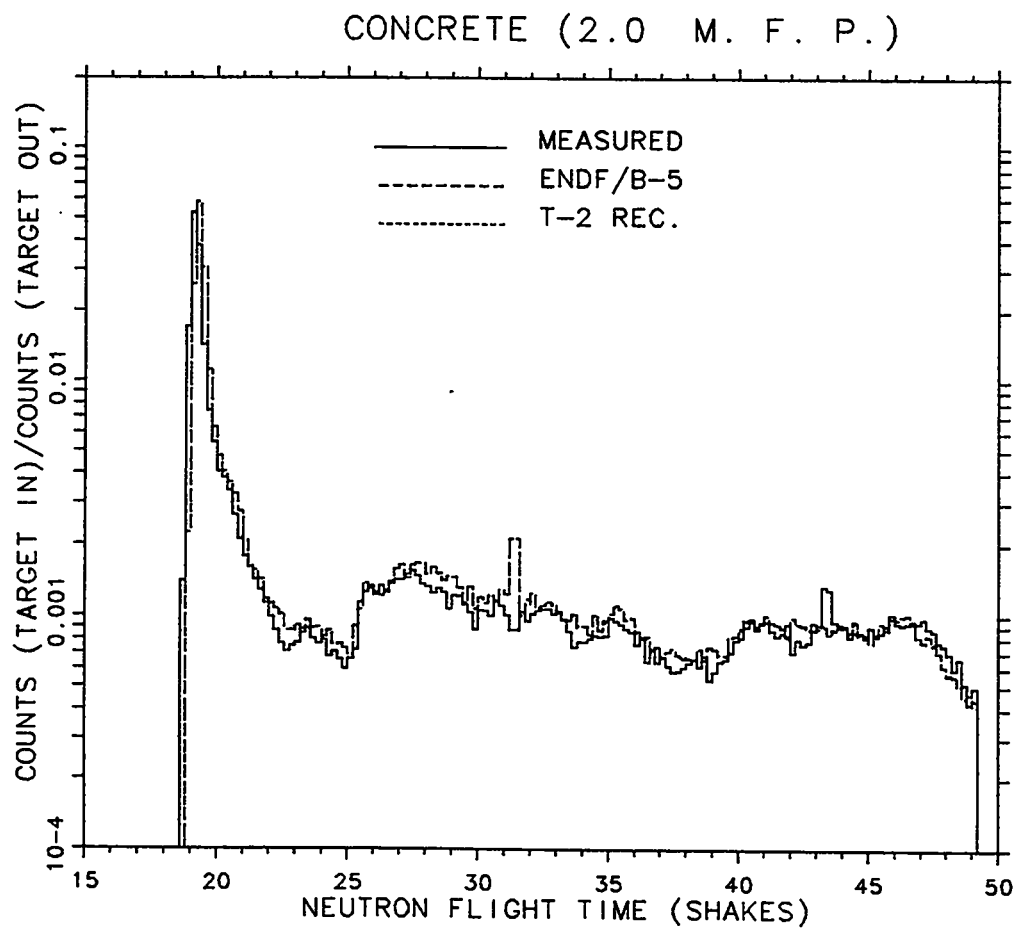


Fig. 99. Plot of experimental, ENDF/B-V calculated, and MCNP recommended calculated rates for the concrete sphere with 2.0 mean free path radius.

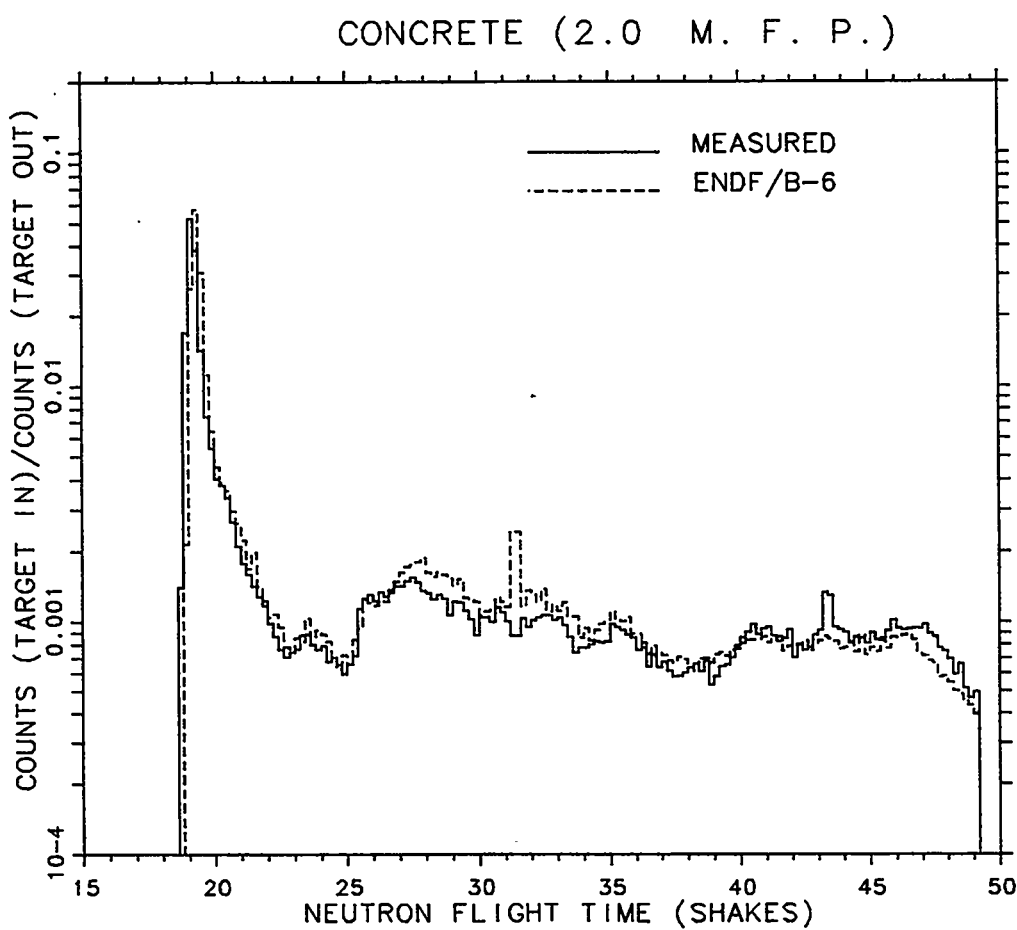


Fig. 100. Plot of experimental and ENDF/B-VI calculated count rates for the concrete sphere of 2.0 mean free path radius.

V. Conclusions

The ENDF/B-VI library seems to give valid answers to a widely accepted benchmark, the Lawrence Livermore Pulsed Sphere experiments, which should provide renewed confidence in the validity of the ENDF/B-VI data as well as MCNP and the NJOY nuclear data processing system.

ENDF/B-VI appears to more closely match the experimental measurements than ENDF/B-V for ^7Li , beryllium, nitrogen, CF_2 (teflon), iron, lead, and CH_2 (polyethylene). The ENDF/B-V and ENDF/B-VI results are about the same for magnesium, aluminum, titanium, and concrete, and close for oxygen, water, and heavy water. Only for carbon does ENDF/B-VI appear significantly worse than ENDF/B-V, and then only in the detailed time-of-flight spectra, not in integral results.

VI. Acknowledgment

We gratefully acknowledge the extensive effort by Robert E. Seamon and Stephanie C. Frankle in support of this work, particularly with respect to the ^{19}F data.

References

1. L. F. Hansen, J. D. Anderson, E. Goldberg, E. F. Plechaty, M. L. Stelts, and C. Wong, *Nuclear Science and Engineering* **35**, 227 (1969).
2. L. F. Hansen, J. D. Anderson, E. Goldberg, E. F. Plechaty, M. L. Stelts, and C. Wong, *Nuclear Science and Engineering* **40**, 262 (1970).
3. M. L. Stelts, J. D. Anderson, L. F. Hansen, E. F. Plechaty, and C. Wong, *Nuclear Science and Engineering* **46**, 53 (1971).
4. C. Wong, J. D. Anderson, P. Brown, L. F. Hansen, J. L. Kammerdiener, C. Logan, and B. Pohl, "Livermore Pulsed Sphere Program: Program Summary Through July 1971," Lawrence Livermore National Laboratory Report UCRL-51144, Rev. 1 (1972).
5. L. F. Hansen, J. D. Anderson, P. S. Brown, R. J. Howerton, J. L. Kammerdiener, C. M. Logan, E. F. Plechaty, and C. Wong, *Nuclear Science and Engineering* **51**, 278 (1973).
6. P. F. Rose and C. L. Dunford, Editors, "ENDF-102 Data Formats and Procedures for the Evaluated Nuclear Data File ENDF-6," Brookhaven National Laboratory Report BNL-NCS-44945 (July 1990).
7. R. E. MacFarlane, D. W. Muir, and R. M. Boicourt, "The NJOY Nuclear Data Processing System, Volume 1: User's Manual," Los Alamos National Laboratory Report LA-9303-M, Vol. I (ENDF-324) (May 1982).
8. J. S. Hendricks, S. C. Frankle, and J. D. Court, "ENDF/B-VI for MCNP," Los Alamos National Laboratory Report LA-12891 (December 1994).
9. J. S. Hendricks, S. C. Frankle, and J. D. Court, "New Data for MCNP," *Trans. Am. Nucl. Soc.* **71**, 399 (1994).
10. J. F. Briesmeister, Ed. "MCNP-A General Monte Carlo N-Particle Transport Code, Version 4A," Los Alamos National Laboratory Report LA-12625-M (November 1993).
11. D. J. Whalen, D. A. Cardon, J. L. Uhle, and J. S. Hendricks, "MCNP: Neutron Benchmark Problems," Los Alamos National Laboratory Report LA-12212 (November 1991).
12. E. D. Arthur and P. G. Young, "Evaluated Neutron-Induced Cross Sections for $^{54,56}\text{Fe}$ to 40 MeV," Los Alamos National Laboratory Report LA-8626-MS (December 1980).

Appendix: MCNP Input Decks

A. Introduction

To conserve space, each of the input decks will not be listed here. When there are two of the same material, an example of one, and the differences from the other will be provided, so that the proper input can be constructed for further study.

B. Source cards

The source cards are common to all of the input decks, so they will only be listed once. The list is to be substituted into the input decks at the appropriate position.

```
sdef pos=0 0 0 dir=d1 erg=fdir=d2 rad=d3 vec=-1 0 0
  sur=100 tme=d4
si1 a -1.0000 -.99619 -.98481 -.96593 -.93969
  -.90631 -.86603 -.81915 -.76604 -.70711
  -.64279 -.57358 -.50000 -.42262 -.34202
  -.25882 -.17365 -.08716 .00000 .08716
  .17365 .25882 .34202 .42262 .50000
  .57358 .64279 .70711 .76604 .81915
  .86603 .90631 .93969 .96593 .98481
  .99619 1.0000
sp1   .874 .874 .875 .876 .877
  .879 .882 .884 .888 .891
  .895 .899 .904 .909 .914
  .919 .924 .930 .935 .941
  .946 .952 .957 .962 .967
  .972 .976 .981 .985 .988
  .991 .994 .996 .998 .999
  1.0 1.0
ds2 q -.99619 180 -.98481 175 -.96593 170 -.93962 165 -.90631 160
  -.86603 155 -.81915 150 -.76604 145 -.70711 140 -.64279 135
  -.57358 130 -.50000 125 -.42262 120 -.34202 115 -.25882 110
  -.17365 105 -.08716 100 0.0000 95 .08716 90 .17365 85
  .25882 80 .34202 75 .42262 70 .50000 65 .57358 60
  .64279 55 .70711 50 .76604 45 .81915 40 .86603 35
  .90631 30 .93969 25 .96593 20 .98481 15 .99619 10
  1.0000 5
si3 h 0 .6
sp3 d -21 1
sp4 -41 .4 0
si5 h 15.106 15.110
sp5 d 0 1
si10 h 15.095 15.106
sp10 d 0 1
si15 h 15.075 15.095
sp15 d 0 1
si20 h 15.049 15.075
sp20 d 0 1
si25 h 15.015 15.049
sp25 d 0 1
si30 h 14.974 15.015
sp30 d 0 1
si35 h 14.927 14.974
sp35 d 0 1
si40 h 14.873 14.927
sp40 d 0 1
si45 h 14.814 14.873
sp45 d 0 1
si50 h 14.750 14.814
sp50 d 0 1
si55 h 14.681 14.750
sp55 d 0 1
si60 h 14.608 14.681
```

```

sp60 d 0 1
si65 h 14.532 14.608
sp65 d 0 1
si70 h 14.453 14.532
sp70 d 0 1
si75 h 14.372 14.453
sp75 d 0 1
si80 h 14.289 14.372
sp80 d 0 1
si85 h 14.206 14.289
sp85 d 0 1
si90 h 14.123 14.206
sp90 d 0 1
si95 h 14.040 14.123
sp95 d 0 1
si100 h 13.958 14.040
sp100 d 0 1
si105 h 13.878 13.958
sp105 d 0 1
si110 h 13.800 13.878
sp110 d 0 1
si115 h 13.725 13.800
sp115 d 0 1
si120 h 13.654 13.725
sp120 d 0 1
si125 h 13.586 13.654
sp125 d 0 1
si130 h 13.522 13.586
sp130 d 0 1
si135 h 13.464 13.522
sp135 d 0 1
si140 h 13.410 13.464
sp140 d 0 1
si145 h 13.362 13.410
sp145 d 0 1
si150 h 13.320 13.362
sp150 d 0 1
si155 h 13.284 13.320
sp155 d 0 1
si160 h 13.254 13.284
sp160 d 0 1
si165 h 13.230 13.254
sp165 d 0 1
si170 h 13.214 13.230
sp170 d 0 1
si175 h 13.203 13.214
sp175 d 0 1
si180 h 13.200 13.203
sp180 d 0 1

```

C. ${}^6\text{Li}$ 0.5 mfp Input Deck

```

Li-6 Sphere: Radius 8.97 with ENDF/B-VI
1   1 -9.0074 1 -2 -3
2   2 -.001288 2 -3 -9
3   1 -9.0074 1 3 -4 -8
4   3 -.4515 (-1:4) (-5:-6:7) -8
5   1 -9.0074 5 6 -7 -8
6   1 -9.0074 8 -9 (-1:3)
21  2 -.001288 9 -10
22  0 10

1   px -.64
2   px -.582
3   x 0.0 1.42 8.5 1.985
4   x 0.0 1.476 8.5 2.043

```

```

5   cx 8.87
6   px -.1
7   px .1
8   so 8.912
9   so 8.97
10  so 1000
100 px 0.0

imp:n 1 6r 0
-----<Source Cards>-----
fc5 Pilot B detector response function, 765.2 flightpath, 30 degrees.
f5x:n -662.7 382.6 0
t5  1.35000E+01  1.37000E+01  1.39000E+01  1.41000E+01  1.43000E+01
    1.45000E+01
    1.47000E+01  1.49000E+01  1.51000E+01  1.53000E+01  1.55000E+01
    1.57000E+01
    1.59000E+01  1.61000E+01  1.63000E+01  1.65000E+01  1.67000E+01
    1.69000E+01
    1.71000E+01  1.73000E+01  1.75000E+01  1.77000E+01  1.79000E+01
    1.81000E+01
    1.83000E+01  1.85000E+01  1.87000E+01  1.89000E+01  1.91000E+01
    1.93000E+01
    1.95000E+01  1.97000E+01  1.99000E+01  2.01000E+01  2.03000E+01
    2.05000E+01
    2.07000E+01  2.09000E+01  2.11000E+01  2.13000E+01  2.15000E+01
    2.17000E+01
    2.19000E+01  2.21000E+01  2.23000E+01  2.25000E+01  2.27000E+01
    2.29000E+01
    2.31000E+01  2.33000E+01  2.35000E+01  2.37000E+01  2.39000E+01
    2.41000E+01
    2.43000E+01  2.45000E+01  2.47000E+01  2.49000E+01  2.51000E+01
    2.53000E+01
    2.55000E+01  2.57000E+01  2.59000E+01  2.61000E+01  2.63000E+01
    2.65000E+01
    2.67000E+01  2.69000E+01  2.71000E+01  2.73000E+01  2.75000E+01
    2.77000E+01
    2.79000E+01  2.81000E+01  2.83000E+01  2.85000E+01  2.87000E+01
    2.89000E+01
    2.91000E+01  2.93000E+01  2.95000E+01  2.97000E+01  2.99000E+01
    3.01000E+01
    3.03000E+01  3.05000E+01  3.07000E+01  3.09000E+01  3.11000E+01
    3.13000E+01
    3.15000E+01  3.17000E+01  3.19000E+01  3.21000E+01  3.23000E+01
    3.25000E+01
    3.27000E+01  3.29000E+01  3.31000E+01  3.33000E+01  3.35000E+01
    3.37000E+01
    3.39000E+01  3.41000E+01  3.43000E+01  3.45000E+01  3.47000E+01
    3.49000E+01
    3.51000E+01  3.53000E+01  3.55000E+01  3.57000E+01  3.59000E+01
    3.61000E+01
    3.63000E+01  3.65000E+01  3.67000E+01  3.69000E+01  3.71000E+01
    3.73000E+01
    3.75000E+01  3.77000E+01  3.79000E+01  3.81000E+01  3.83000E+01
    3.85000E+01
    3.87000E+01  3.89000E+01  3.91000E+01  3.93000E+01  3.95000E+01
    3.97000E+01
    3.99000E+01  4.01000E+01  4.03000E+01  4.05000E+01  4.07000E+01
    4.09000E+01

de5 lin 1.6 2.0 13i 16.0
df5 lin 0.00 2.25 4.10 4.70 4.85 4.85 4.70 4.30
        4.25 4.05 3.85 3.65 3.55 3.60 3.75 3.85
fc15 Pilot B detector response function, 765.2 cm flightpath, 30 degrees.
f15x:n -662.7 382.6 0
t15  15.5 17.5 24.9 39.1
de15 lin 1.6 2.0 13i 16.0
df15 lin 0.00 2.25 4.10 4.70 4.85 4.85 4.70 4.30
        4.25 4.05 3.85 3.65 3.55 3.60 3.75 3.85
c

```

```

c   ENDF/B-VI
m1  26054.60c .039788
    26056.60c .629199
    26057.60 .015092
    26058.60c .001921
    24050.60c .008700
    24052.60c .167580
    24053.60c .019000
    24054.60c .004720
    28058.60c .057346
    28060.60c .021924
    28061.60c .000949
    28062.60c .003016
    28064.60c .000764
    14000.60c .020
    12000.60c .010
m2  7014.60c -.7885
    8016.60c -.2115
m3  3006.60c .95
    3007.60c .05
cut:n 39.1 1.6
print
prdmp 2j 1
nps 200000

```

A. ${}^6\text{Li}$ 1.6 mfp

1. Cell Cards

```

Li-6 Sphere with Radius 25.52 ENDF/B-VI
1   1 -9.0074 1 -2 -3
2   2 -.001288 2 -3 -9
3   1 -9.0074 1 3 -4 -8
4   3 -.4515 (-1:4) (-5:-6:7) -8
5   1 -9.0074 5 6 -7 -8
6   1 -9.0074 8 -9 (-1:3)
7   1 -17.5089 9 -10 (-1:11)
8   3 -.4441 10 -13 -15
9   1 -17.5089 10 13 -14 -15
10  3 -.4411 10 12 14 -15
11  1 -17.5089 10 11 -12 -15 1
12  2 -.001288 9 -11 -16 1
13  1 -17.5089 15 -16 (-1:11)
14  1 -15.4764 16 -17 (-1:18)
15  3 -.4490 -13 17 -20
16  1 -15.4764 13 -14 17 -20
17  3 -.4494 14 17 19 -20
18  1 -15.4764 17 18 -19 -20 1
19  2 -.001288 16 -18 -21 1
20  1 -15.4764 20 -21 (-1:18)
21  2 -.001288 21 -22
22  0 22

```

2. Geometry cards

```

1   px -.64
2   px -.582
3   x 0.0 1.42 8.5 1.985
4   x 0.0 1.478 8.5 2.043
5   cx 8.87
6   px -.1
7   px .1
8   so 8.912
9   so 8.97
10  so 9.028

```

```

11  cx 2.86
12  cx 2.918
13  px -.058
14  px .058
15  so 16.462
16  so 16.52
17  so 16.578
18  cx 3.49
19  cx 3.548
20  so 25.462
21  so 25.52
22  so 1000.0
100 px 0.0

```

3. Tally Cards

```

imp:n 1 20r 0
t5  1.33E+01  1.35000E+01  1.37000E+01  1.39000E+01  1.41000E+01  1.43000E+01
     1.45E+01  1.47000E+01  1.49000E+01  1.51000E+01  1.53000E+01  1.55000E+01
     1.57E+01  1.59000E+01  1.61000E+01  1.63000E+01  1.65000E+01  1.67000E+01
     1.69E+01  1.71000E+01  1.73000E+01  1.75000E+01  1.77000E+01  1.79000E+01
     1.81E+01  1.83000E+01  1.85000E+01  1.87000E+01  1.89000E+01  1.91000E+01
     1.93E+01  1.95000E+01  1.97000E+01  1.99000E+01  2.01000E+01  2.03000E+01
     2.05E+01  2.07000E+01  2.09000E+01  2.11000E+01  2.13000E+01  2.15000E+01
     2.17E+01  2.19000E+01  2.21000E+01  2.23000E+01  2.25000E+01  2.27000E+01
     2.29E+01  2.31000E+01  2.33000E+01  2.35000E+01  2.37000E+01  2.39000E+01
     2.41E+01  2.43000E+01  2.45000E+01  2.47000E+01  2.49000E+01  2.51000E+01
     2.53E+01  2.55000E+01  2.57000E+01  2.59000E+01  2.61000E+01  2.63000E+01
     2.65E+01  2.67000E+01  2.69000E+01  2.71000E+01  2.73000E+01  2.75000E+01
     2.77E+01  2.79000E+01  2.81000E+01  2.83000E+01  2.85000E+01  2.87000E+01
     2.89E+01  2.91000E+01  2.93000E+01  2.95000E+01  2.97000E+01  2.99000E+01
     3.01E+01  3.03000E+01  3.05000E+01  3.07000E+01  3.09000E+01  3.11000E+01
     3.13E+01  3.15000E+01  3.17000E+01  3.19000E+01  3.21000E+01  3.23000E+01
     3.25E+01  3.27000E+01  3.29000E+01  3.31000E+01  3.33000E+01  3.35000E+01
     3.37E+01  3.39000E+01  3.41000E+01  3.43000E+01  3.45000E+01  3.47000E+01
     3.49E+01  3.51000E+01  3.53000E+01  3.55000E+01  3.57000E+01  3.59000E+01
     3.61E+01  3.63000E+01  3.65000E+01  3.67000E+01  3.69000E+01  3.71000E+01
     3.73E+01  3.75000E+01  3.77000E+01  3.79000E+01  3.81000E+01  3.83000E+01
     3.85E+01  3.87000E+01  3.89000E+01  3.91000E+01  3.93000E+01  3.95000E+01
     3.97E+01  3.99000E+01  4.01000E+01  4.03000E+01  4.05000E+01  4.07000E+01
     4.09E+01

```

D. ⁷Li 0.5 mfp Input Deck

```

Li-7 Sphere with Radius 8.97 ENDF/B-VI
1  1 -9.4905 1 -2 -3
2  2 -.001288 2 -3 -9
3  1 -9.4905 1 3 -4 -8
4  3 -.5155 (-1:4) (-5:-6:7) -8
5  1 -9.4905 5 6 -7 -8
6  1 -9.4905 8 -9 (-1:3)
21 2 -.001288 9 -10
22 0 10

1  px -.64
2  px -.582
3  x 0.0 1.42 8.5 1.985
4  x 0.0 1.478 8.5 2.043
5  cx 8.87
6  px -.1
7  px .1
8  so 8.912
9  so 8.97
10 so 1000

```

```

100 px 0.0

imp:n 1 6x 0
-----<Source Cards>-----
fc5 Pilot B detector response function, 765.2 cm flightpath, 30 degrees.
f5x:n -662.7 382.6 0
t5 1.31E+01 1.33000E+01 1.35000E+01 1.37000E+01 1.39000E+01 1.41000E+01
    1.43E+01 1.45000E+01 1.47000E+01 1.49000E+01 1.51000E+01 1.53000E+01
    1.55E+01 1.57000E+01 1.59000E+01 1.61000E+01 1.63000E+01 1.65000E+01
    1.67E+01 1.69000E+01 1.71000E+01 1.73000E+01 1.75000E+01 1.77000E+01
    1.79E+01 1.81000E+01 1.83000E+01 1.85000E+01 1.87000E+01 1.89000E+01
    1.91E+01 1.93000E+01 1.95000E+01 1.97000E+01 1.99000E+01 2.01000E+01
    2.03E+01 2.05000E+01 2.07000E+01 2.09000E+01 2.11000E+01 2.13000E+01
    2.15E+01 2.17000E+01 2.19000E+01 2.21000E+01 2.23000E+01 2.25000E+01
    2.27E+01 2.29000E+01 2.31000E+01 2.33000E+01 2.35000E+01 2.37000E+01
    2.39E+01 2.41000E+01 2.43000E+01 2.45000E+01 2.47000E+01 2.49000E+01
    2.51E+01 2.53000E+01 2.55000E+01 2.57000E+01 2.59000E+01 2.61000E+01
    2.63E+01 2.65000E+01 2.67000E+01 2.69000E+01 2.71000E+01 2.73000E+01
    2.75E+01 2.77000E+01 2.79000E+01 2.81000E+01 2.83000E+01 2.85000E+01
    2.87E+01 2.89000E+01 2.91000E+01 2.93000E+01 2.95000E+01 2.97000E+01
    2.99E+01 3.01000E+01 3.03000E+01 3.05000E+01 3.07000E+01 3.09000E+01
    3.11E+01 3.13000E+01 3.15000E+01 3.17000E+01 3.19000E+01 3.21000E+01
    3.23E+01 3.25000E+01 3.27000E+01 3.29000E+01 3.31000E+01 3.33000E+01
    3.35E+01 3.37000E+01 3.39000E+01 3.41000E+01 3.43000E+01 3.45000E+01
    3.47E+01 3.49000E+01 3.51000E+01 3.53000E+01 3.55000E+01 3.57000E+01
    3.59E+01 3.61000E+01 3.63000E+01 3.65000E+01 3.67000E+01 3.69000E+01
    3.71E+01 3.73000E+01 3.75000E+01 3.77000E+01 3.79000E+01 3.81000E+01
    3.83E+01 3.85000E+01 3.87000E+01 3.89000E+01 3.91000E+01 3.93000E+01
    3.95E+01 3.97000E+01 3.99000E+01 4.01000E+01 4.03000E+01 4.05000E+01
    4.07E+01 4.09000E+01

de5 lin 1.6 2.0 13i 16.0
df5 lin 0.00 2.25 4.10 4.70 4.85 4.85 4.70 4.30
        4.25 4.05 3.85 3.65 3.55 3.60 3.75 3.85
fc15 Pilot B detector response function, 765.2 cm flightpath, 30 degrees.
f15x:n -662.7 382.6 0
t15 15.5 17.5 24.9 39.1
de15 lin 1.6 2.0 13i 16.0
df15 lin 0.00 2.25 4.10 4.70 4.85 4.85 4.70 4.30
        4.25 4.05 3.85 3.65 3.55 3.60 3.75 3.85

c
c   ENDF/B-VI
m1 26054.60c .039788
26056.60c .629199
26057.60c .015092
26058.60c .001921
24050.60c .008700
24052.60c .167580
24053.60c .019000
24054.60c .004720
28058.60c .057346
28060.60c .021924
28061.60c .000949
28062.60c .003016
28064.60c .000764
14000.60c .020
12000.60c .010
m2 7014.60c -.7885
     8016.60c -.2115
m3 3006.60c .0261
     3007.60c .9739
cut:n 39.1 1.6
print
prdmp 2j 1
nps 200000

```

A. ^7Li 1.6 mfp

1. Cell Cards

```
Li-7 Sphere with Radius 25.52  ENDF/B-VI
1  1 -9.4905 1 -2 -3
2  2 -.001288 2 -3 -9
3  1 -9.4905 1 3 -4 -8
4  3 -.5155 (-1:4) (-5:-6:7) -8
5  1 -9.4905 5 6 -7 -8
6  1 -9.4905 8 -9 (-1:3)
7  1 -19.2806 9 -10 (-1:11)
8  3 -.4968 10 -13 -15
9  1 -19.2806 10 13 -14 -15
10 3 -.4960 10 12 14 -15
11 1 -19.2806 10 11 -12 -15 1
12 2 -.001288 9 -11 -16 1
13 1 -19.2806 15 -16 (-1:11)
14 1 -17.2365 16 -17 (-1:18)
15 3 -.5056 -13 17 -20
16 1 -17.2365 13 -14 17 -20
17 3 -.5052 14 17 19 -20
18 1 -17.2365 17 18 -19 -20 1
19 2 -.001288 16 -18 -21 1
20 1 -17.2365 20 -21 (-1:18)
21 2 -.001288 21 -22
22 0 22
```

2. Geometry Cards

```
1 px -.64
2 px -.582
3 x 0.0 1.42 8.5 1.985
4 x 0.0 1.478 8.5 2.043
5 cx 8.87
6 px -.1
7 px .1
8 so 8.912
9 so 8.97
10 so 9.028
11 cx 2.86
12 cx 2.918
13 px -.058
14 px .058
15 so 16.462
16 so 16.52
17 so 16.578
18 cx 3.49
19 cx 3.548
20 so 25.462
21 so 25.52
22 so 1000.0
100 px 0.0
```

3. Tally Cards

```
imp:n 1 20r 0
t5  1.37E+01  1.39000E+01  1.41000E+01  1.43000E+01  1.45000E+01  1.47000E+01
     1.49E+01  1.51000E+01  1.53000E+01  1.55000E+01  1.57000E+01  1.59000E+01
     1.61E+01  1.63000E+01  1.65000E+01  1.67000E+01  1.69000E+01  1.71000E+01
     1.73E+01  1.75000E+01  1.77000E+01  1.79000E+01  1.81000E+01  1.83000E+01
     1.85E+01  1.87000E+01  1.89000E+01  1.91000E+01  1.93000E+01  1.95000E+01
     1.97E+01  1.99000E+01  2.01000E+01  2.03000E+01  2.05000E+01  2.07000E+01
     2.09E+01  2.11000E+01  2.13000E+01  2.15000E+01  2.17000E+01  2.19000E+01
```

	2.21E+01	2.23000E+01	2.25000E+01	2.27000E+01	2.29000E+01	2.31000E+01
2.33E+01	2.35000E+01	2.37000E+01	2.39000E+01	2.41000E+01	2.43000E+01	
2.45E+01	2.47000E+01	2.49000E+01	2.51000E+01	2.53000E+01	2.55000E+01	
2.57E+01	2.59000E+01	2.61000E+01	2.63000E+01	2.65000E+01	2.67000E+01	
2.69E+01	2.71000E+01	2.73000E+01	2.75000E+01	2.77000E+01	2.79000E+01	
2.81E+01	2.83000E+01	2.85000E+01	2.87000E+01	2.89000E+01	2.91000E+01	
2.93E+01	2.95000E+01	2.97000E+01	2.99000E+01	3.01000E+01	3.03000E+01	
3.05E+01	3.07000E+01	3.09000E+01	3.11000E+01	3.13000E+01	3.15000E+01	
3.17E+01	3.19000E+01	3.21000E+01	3.23000E+01	3.25000E+01	3.27000E+01	
3.29E+01	3.31000E+01	3.33000E+01	3.35000E+01	3.37000E+01	3.39000E+01	
3.41E+01	3.43000E+01	3.45000E+01	3.47000E+01	3.49000E+01	3.51000E+01	
3.53E+01	3.55000E+01	3.57000E+01	3.59000E+01	3.61000E+01	3.63000E+01	
3.65E+01	3.67000E+01	3.69000E+01	3.71000E+01	3.73000E+01	3.75000E+01	
3.77E+01	3.79000E+01	3.81000E+01	3.83000E+01	3.85000E+01	3.87000E+01	
3.89E+01	3.91000E+01	3.93000E+01	3.95000E+01	3.97000E+01	3.99000E+01	
4.01E+01	4.03000E+01	4.05000E+01	4.07000E+01	4.09000E+01		

E. Beryllium Input Deck

```

Be Sphere with Outer Radius 12.58  ENDF/B-VI
1   2 -.001288 -1
2   2 -.001288 1 -2 -3 100
3   1 -1.8346 1 -2 (-100:3)
4   2 -.001288 2 -4
5   0 4

1   so 8.00
2   so 12.58
3   cx 2.86
4   so 1000
100  px 0.0

imp:n 1 3r 0
-----<Source Cards>-----
fc5 Pilot B detector response function, 765.2 flightpath, 30 degrees.
f5x:n -662.7 382.6 0
t5  1.37E+01  1.39000E+01  1.41000E+01  1.43000E+01  1.45000E+01  1.47000E+01
    1.49E+01  1.51000E+01  1.53000E+01  1.55000E+01  1.57000E+01  1.59000E+01
    1.61E+01  1.63000E+01  1.65000E+01  1.67000E+01  1.69000E+01  1.71000E+01
    1.73E+01  1.75000E+01  1.77000E+01  1.79000E+01  1.81000E+01  1.83000E+01
    1.85E+01  1.87000E+01  1.89000E+01  1.91000E+01  1.93000E+01  1.95000E+01
    1.97E+01  1.99000E+01  2.01000E+01  2.03000E+01  2.05000E+01  2.07000E+01
    2.09E+01  2.11000E+01  2.13000E+01  2.15000E+01  2.17000E+01  2.19000E+01
    2.21E+01  2.23000E+01  2.25000E+01  2.27000E+01  2.29000E+01  2.31000E+01
    2.33E+01  2.35000E+01  2.37000E+01  2.39000E+01  2.41000E+01  2.43000E+01
    2.45E+01  2.47000E+01  2.49000E+01  2.51000E+01  2.53000E+01  2.55000E+01
    2.57E+01  2.59000E+01  2.61000E+01  2.63000E+01  2.65000E+01  2.67000E+01
    2.69E+01  2.71000E+01  2.73000E+01  2.75000E+01  2.77000E+01  2.79000E+01
    2.81E+01  2.83000E+01  2.85000E+01  2.87000E+01  2.89000E+01  2.91000E+01
    2.93E+01  2.95000E+01  2.97000E+01  2.99000E+01  3.01000E+01  3.03000E+01
    3.05E+01  3.07000E+01  3.09000E+01  3.11000E+01  3.13000E+01  3.15000E+01
    3.17E+01  3.19000E+01  3.21000E+01  3.23000E+01  3.25000E+01  3.27000E+01
    3.29E+01  3.31000E+01  3.33000E+01  3.35000E+01  3.37000E+01  3.39000E+01
    3.41E+01  3.43000E+01  3.45000E+01  3.47000E+01  3.49000E+01  3.51000E+01
    3.53E+01  3.55000E+01  3.57000E+01  3.59000E+01  3.61000E+01  3.63000E+01
    3.65E+01  3.67000E+01  3.69000E+01  3.71000E+01  3.73000E+01  3.75000E+01
    3.77E+01  3.79000E+01  3.81000E+01  3.83000E+01  3.85000E+01  3.87000E+01
    3.89E+01  3.91000E+01  3.93000E+01  3.95000E+01  3.97000E+01  3.99000E+01
    4.01E+01  4.03000E+01  4.05000E+01  4.07000E+01  4.09000E+01

de5  lin 1.6 2.0 13i 16.0
df5  lin 0.00 2.25 4.10 4.70 4.85 4.85 4.70 4.30
      4.25 4.05 3.85 3.65 3.55 3.60 3.75 3.85
fc15 Pilot B detector response function, 765.2 cm flightpath, 30 degrees.
f15x:n -662.7 382.6 0
t15  15.5 17.5 24.9 39.1
de15 lin 1.6 2.0 13i 16.0

```

```

df15 lin 0.00 2.25 4.10 4.70 4.85 4.85 4.70 4.30
      4.25 4.05 3.85 3.65 3.55 3.60 3.75 3.85
c
c     ENDF/B-VI
m1   4009.60c 1.00
m2   7014.60c -.7885
      8016.60c -.2115
cut:n 39.1 1.6
print
prdmp 2j 1
nps  200000

```

F. Carbon 0.5 mfp Input Deck

```

C Sphere with Radius 4.187  ENDF/B-VI
1  2 -.001288 1 -2 -3
2  1 -1.8660 (-1:2) -3
3  2 -.001288 3 -4
4  0 4

1  px -.131
2  cx 1.13
3  so 4.187
4  so 1000
100 px 0.0

imp:n 1 2r 0
-----<Source Cards>-----
fc5  NE213 detector, low bias, 766.0 cm flightpath, 30 degrees.
f5xx:n -663.4 383 0
t5  1.39E+01  1.41000E+01  1.43000E+01  1.45000E+01  1.47000E+01  1.49000E+01
    1.51E+01  1.53000E+01  1.55000E+01  1.57000E+01  1.59000E+01  1.61000E+01
    1.63E+01  1.65000E+01  1.67000E+01  1.69000E+01  1.71000E+01  1.73000E+01
    1.75E+01  1.77000E+01  1.79000E+01  1.81000E+01  1.83000E+01  1.85000E+01
    1.87E+01  1.89000E+01  1.91000E+01  1.93000E+01  1.95000E+01  1.97000E+01
    1.99E+01  2.01000E+01  2.03000E+01  2.05000E+01  2.07000E+01  2.09000E+01
    2.11E+01  2.13000E+01  2.15000E+01  2.17000E+01  2.19000E+01  2.21000E+01
    2.23E+01  2.25000E+01  2.27000E+01  2.29000E+01  2.31000E+01  2.33000E+01
    2.35E+01  2.37000E+01  2.39000E+01  2.41000E+01  2.43000E+01  2.45000E+01
    2.47E+01  2.49000E+01  2.51000E+01  2.53000E+01  2.55000E+01  2.57000E+01
    2.59E+01  2.61000E+01  2.63000E+01  2.65000E+01  2.67000E+01  2.69000E+01
    2.71E+01  2.73000E+01  2.75000E+01  2.77000E+01  2.79000E+01  2.81000E+01
    2.83E+01  2.85000E+01  2.87000E+01  2.89000E+01  2.91000E+01  2.93000E+01
    2.95E+01  2.97000E+01  2.99000E+01  3.01000E+01  3.03000E+01  3.05000E+01
    3.07E+01  3.09000E+01  3.11000E+01  3.13000E+01  3.15000E+01  3.17000E+01
    3.19E+01  3.21000E+01  3.23000E+01  3.25000E+01  3.27000E+01  3.29000E+01
    3.31E+01  3.33000E+01  3.35000E+01  3.37000E+01  3.39000E+01  3.41000E+01
    3.43E+01  3.45000E+01  3.47000E+01  3.49000E+01  3.51000E+01  3.53000E+01
    3.55E+01  3.57000E+01  3.59000E+01  3.61000E+01  3.63000E+01  3.65000E+01
    3.67E+01  3.69000E+01  3.71000E+01  3.73000E+01  3.75000E+01  3.77000E+01
    3.79E+01  3.81000E+01  3.83000E+01  3.85000E+01  3.87000E+01  3.89000E+01
    3.91E+01  3.93000E+01  3.95000E+01  3.97000E+01  3.99000E+01  4.01000E+01
    4.03E+01  4.05000E+01  4.07000E+01  4.09000E+01  4.11000E+01

c     NE213 low bias response function
de5  lin 1.6 1.8 1.9 2.0 2.1 2.2 2.3 2.4 2.5 2.75
      3.0 3.5 4.0 4.5 5.0 5.5 6.0 6.4 6.6 6.8 7.0
      7.5 8.1 8.5 9.0 10.0 11.0 12.0 12.5 13.0
      13.5 14.0 15.0 16.0
df5  lin 0.00 1.46 1.86 2.26 2.58 3.00 3.29 3.42
      3.63 3.95 4.10 4.25 4.33 4.39 4.40 4.37 4.28
      4.15 4.20 4.18 4.12 3.97 3.80 3.77 3.65 3.44
      3.24 3.06 3.01 2.98 2.98 3.01 3.08 3.25
fc15  NE213 detector, low bias, 766.0 cm flightpath, 30 degrees.
f15x:n -663.4 383 0
t15  15.5 17.5 24.9 39.1
c     NE213 low bias response function

```

```

de15 lin 1.6 1.8 1.9 2.0 2.1 2.2 2.3 2.4 2.5 2.75
      3.0 3.5 4.0 4.5 5.0 5.5 6.0 6.4 6.6 6.8 7.0
      7.5 8.1 8.5 9.0 10.0 11.0 12.0 12.5 13.0
      13.5 14.0 15.0 16.0
df15 lin 0.00 1.46 1.86 2.26 2.58 3.00 3.29 3.42
      3.63 3.95 4.10 4.25 4.33 4.39 4.40 4.37 4.28
      4.15 4.20 4.18 4.12 3.97 3.80 3.77 3.65 3.44
      3.24 3.06 3.01 2.98 2.98 3.01 3.08 3.25
c
c     ENDF/B-VI
m1   6000.60c 1.00
m2   7014.60c -.7885
      8016.60c -.2115
cut:n 39.1 1.6
print
prdmfp 2j 1
nps   200000

```

A. Carbon 2.9 mfp

1. Cell Cards

```

C Sphere with Radius 20.96  ENDF/B-VI
1    1 -1.853 -1 -4
2    1 -1.853 1 2 3 -4
3    2 -.001288 1 (-2:-3) -4
4    2 -.001288 4 -5
5    0 5

```

2. Geometry Cards

```

1    px -.131
2    cx 1.13
3    x 3.73 1.13 20.96 2.335
4    so 20.96
5    so 1000
100  px 0.0

```

3. Tally Cards

```

imp:n 1 3r 0
t5   1.41E+01  1.43000E+01  1.45000E+01  1.47000E+01  1.49000E+01  1.51000E+01
      1.53E+01  1.55000E+01  1.57000E+01  1.59000E+01  1.61000E+01  1.63000E+01
      1.65E+01  1.67000E+01  1.69000E+01  1.71000E+01  1.73000E+01  1.75000E+01
      1.77E+01  1.79000E+01  1.81000E+01  1.83000E+01  1.85000E+01  1.87000E+01
      1.89E+01  1.91000E+01  1.93000E+01  1.95000E+01  1.97000E+01  1.99000E+01
      2.01E+01  2.03000E+01  2.05000E+01  2.07000E+01  2.09000E+01  2.11000E+01
      2.13E+01  2.15000E+01  2.17000E+01  2.19000E+01  2.21000E+01  2.23000E+01
      2.25E+01  2.27000E+01  2.29000E+01  2.31000E+01  2.33000E+01  2.35000E+01
      2.37E+01  2.39000E+01  2.41000E+01  2.43000E+01  2.45000E+01  2.47000E+01
      2.49E+01  2.51000E+01  2.53000E+01  2.55000E+01  2.57000E+01  2.59000E+01
      2.61E+01  2.63000E+01  2.65000E+01  2.67000E+01  2.69000E+01  2.71000E+01
      2.73E+01  2.75000E+01  2.77000E+01  2.79000E+01  2.81000E+01  2.83000E+01
      2.85E+01  2.87000E+01  2.89000E+01  2.91000E+01  2.93000E+01  2.95000E+01
      2.97E+01  2.99000E+01  3.01000E+01  3.03000E+01  3.05000E+01  3.07000E+01
      3.09E+01  3.11000E+01  3.13000E+01  3.15000E+01  3.17000E+01  3.19000E+01
      3.21E+01  3.23000E+01  3.25000E+01  3.27000E+01  3.29000E+01  3.31000E+01
      3.33E+01  3.35000E+01  3.37000E+01  3.39000E+01  3.41000E+01  3.43000E+01
      3.45E+01  3.47000E+01  3.49000E+01  3.51000E+01  3.53000E+01  3.55000E+01
      3.57E+01  3.59000E+01  3.61000E+01  3.63000E+01  3.65000E+01  3.67000E+01
      3.69E+01  3.71000E+01  3.73000E+01  3.75000E+01  3.77000E+01  3.79000E+01
      3.81E+01  3.83000E+01  3.85000E+01  3.87000E+01  3.89000E+01  3.91000E+01
      3.93E+01  3.95000E+01  3.97000E+01  3.99000E+01  4.01000E+01  4.03000E+01

```

4.05E+01 4.07000E+01 4.09000E+01

G. Nitrogen 1.1 mfp Input Deck

```
# Sphere with 1.1 M.F.P. ENDf/B-VI
1 2 -.001288 2 -3 -6
2 3 -7.9 2 3 -4 -6
3 3 -7.9 1 -2 -4
4 1 -.808 1 4 -5
5 1 -.808 -1 -5
6 3 -7.9 1 4 5 -6
7 3 -7.9 -1 5 -6
8 2 -.000001 1 6 -7
9 2 -.000001 -1 6 -7
10 3 -7.9 1 7 -8
11 3 -7.9 -1 7 -8
12 2 -.001288 8 -9
13 0 9

1 px -.741
2 px -.7
3 x -.7 1.25 19.0 1.5
4 x -.7 1.291 19.0 1.541
5 so 19.05
6 so 19.11
7 so 22.40
8 so 22.55
9 so 1000
100 px 0.0

imp:n 1 11x 0
-----<Source Cards>-----
fc5 Pilot B detector response function, 763.30 cm flightpath, 30 degrees.
f5x:n -661.0 381.7 0
t5 1.41E+01 1.43000E+01 1.45000E+01 1.47000E+01 1.49000E+01 1.51000E+01
  1.53E+01 1.55000E+01 1.57000E+01 1.59000E+01 1.61000E+01 1.63000E+01
  1.65E+01 1.67000E+01 1.69000E+01 1.71000E+01 1.73000E+01 1.75000E+01
  1.77E+01 1.79000E+01 1.81000E+01 1.83000E+01 1.85000E+01 1.87000E+01
  1.89E+01 1.91000E+01 1.93000E+01 1.95000E+01 1.97000E+01 1.99000E+01
  2.01E+01 2.03000E+01 2.05000E+01 2.07000E+01 2.09000E+01 2.11000E+01
  2.13E+01 2.15000E+01 2.17000E+01 2.19000E+01 2.21000E+01 2.23000E+01
  2.25E+01 2.27000E+01 2.29000E+01 2.31000E+01 2.33000E+01 2.35000E+01
  2.37E+01 2.39000E+01 2.41000E+01 2.43000E+01 2.45000E+01 2.47000E+01
  2.49E+01 2.51000E+01 2.53000E+01 2.55000E+01 2.57000E+01 2.59000E+01
  2.61E+01 2.63000E+01 2.65000E+01 2.67000E+01 2.69000E+01 2.71000E+01
  2.73E+01 2.75000E+01 2.77000E+01 2.79000E+01 2.81000E+01 2.83000E+01
  2.85E+01 2.87000E+01 2.89000E+01 2.91000E+01 2.93000E+01 2.95000E+01
  2.97E+01 2.99000E+01 3.01000E+01 3.03000E+01 3.05000E+01 3.07000E+01
  3.09E+01 3.11000E+01 3.13000E+01 3.15000E+01 3.17000E+01 3.19000E+01
  3.21E+01 3.23000E+01 3.25000E+01 3.27000E+01 3.29000E+01 3.31000E+01
  3.33E+01 3.35000E+01 3.37000E+01 3.39000E+01 3.41000E+01 3.43000E+01
  3.45E+01 3.47000E+01 3.49000E+01 3.51000E+01 3.53000E+01 3.55000E+01
  3.57E+01 3.59000E+01 3.61000E+01 3.63000E+01 3.65000E+01 3.67000E+01
  3.69E+01 3.71000E+01 3.73000E+01 3.75000E+01 3.77000E+01 3.79000E+01
  3.81E+01 3.83000E+01 3.85000E+01 3.87000E+01 3.89000E+01 3.91000E+01
  3.93E+01 3.95000E+01 3.97000E+01 3.99000E+01 4.01000E+01 4.03000E+01

de5 lin 1.6 2.0 13i 16.0
df5 lin 0.00 2.25 4.10 4.70 4.85 4.85 4.70 4.30
        4.25 4.05 3.85 3.65 3.55 3.60 3.75 3.85
fc15 Pilot B detector response function, 763.3 cm flightpath, 30 degrees.
f15x:n -661.0 381.7 0
t15 15.5 17.5 24.9 39.1
de15 lin 1.6 2.0 13i 16.0
df15 lin 0.00 2.25 4.10 4.70 4.85 4.85 4.70 4.30
        4.25 4.05 3.85 3.65 3.55 3.60 3.75 3.85
fc25 NE213, 1.6 MeV bias, Dec.15,1976 data, 782.3 cm flightpath, 26 degrees.
```

```

f25x:n -703.1 342.9 0
t25 15.90 17.98 25.26 40.11
c   NE213 low bias response function
de25 lin 1.6 1.8 1.9 2.0 2.1 2.2 2.3 2.4 2.5 2.75
     3.0 3.5 4.0 4.5 5.0 5.5 6.0 6.4 6.6 6.8 7.0
     7.5 8.1 8.5 9.0 10.0 11.0 12.0 12.5 13.0
     13.5 14.0 15.0 16.0
df25 lin 0.00 1.46 1.86 2.26 2.58 3.00 3.29 3.42
     3.63 3.95 4.10 4.25 4.33 4.39 4.40 4.37 4.28
     4.15 4.20 4.18 4.12 3.97 3.80 3.77 3.65 3.44
     3.24 3.06 3.01 2.98 2.98 3.01 3.08 3.25
c
c   ENDf/B-VI
m1  7014.60c 1.00
m2  7014.60c -.7885
     8016.60c -.2115
m3  26054.60c .039788
     26056.60c .629199
     26057.60c .015092
     26058.60c .001921
     24050.60c .008700
     24052.60c .167580
     24053.60c .019000
     24054.60c .004720
     28058.60c .057346
     28060.60c .021924
     28061.60c .000949
     28062.60c .003016
     28064.60c .000764
     14000.60c .020
     12000.60c .010
cut:n 50 1.6
print
prdmp 2j 1
nps 200000

```

A. Nitrogen 3.1 mfp

1. Geometry Cards

```

1  px -1.6
2  px -1.55
3  x  -1.5 2.86 55.9 6.8
4  x  -1.5 2.91 55.9 6.85
5  so 55.88
6  so 55.93
7  so 60.96
8  so 61.11
9  so 1000
100 px 0.0

```

2. Tally Cards

```

fc5 Pilot B detector response function, 765.20 cm flightpath, 30 degrees.
f5x:n -662.7 382.6 0
t5  1.41E+01  1.43000E+01  1.45000E+01  1.47000E+01  1.49000E+01  1.51000E+01
    1.53E+01  1.55000E+01  1.57000E+01  1.59000E+01  1.61000E+01  1.63000E+01
    1.65E+01  1.67000E+01  1.69000E+01  1.71000E+01  1.73000E+01  1.75000E+01
    1.77E+01  1.79000E+01  1.81000E+01  1.83000E+01  1.85000E+01  1.87000E+01
    1.89E+01  1.91000E+01  1.93000E+01  1.95000E+01  1.97000E+01  1.99000E+01
    2.01E+01  2.03000E+01  2.05000E+01  2.07000E+01  2.09000E+01  2.11000E+01
    2.13E+01  2.15000E+01  2.17000E+01  2.19000E+01  2.21000E+01  2.23000E+01
    2.25E+01  2.27000E+01  2.29000E+01  2.31000E+01  2.33000E+01  2.35000E+01
    2.37E+01  2.39000E+01  2.41000E+01  2.43000E+01  2.45000E+01  2.47000E+01
    2.49E+01  2.51000E+01  2.53000E+01  2.55000E+01  2.57000E+01  2.59000E+01

```

	2.61E+01	2.63000E+01	2.65000E+01	2.67000E+01	2.69000E+01	2.71000E+01
2.73E+01	2.75000E+01	2.77000E+01	2.79000E+01	2.81000E+01	2.83000E+01	
2.85E+01	2.87000E+01	2.89000E+01	2.91000E+01	2.93000E+01	2.95000E+01	
2.97E+01	2.99000E+01	3.01000E+01	3.03000E+01	3.05000E+01	3.07000E+01	
3.09E+01	3.11000E+01	3.13000E+01	3.15000E+01	3.17000E+01	3.19000E+01	
3.21E+01	3.23000E+01	3.25000E+01	3.27000E+01	3.29000E+01	3.31000E+01	
3.33E+01	3.35000E+01	3.37000E+01	3.39000E+01	3.41000E+01	3.43000E+01	
3.45E+01	3.47000E+01	3.49000E+01	3.51000E+01	3.53000E+01	3.55000E+01	
3.57E+01	3.59000E+01	3.61000E+01	3.63000E+01	3.65000E+01	3.67000E+01	
3.69E+01	3.71000E+01	3.73000E+01	3.75000E+01	3.77000E+01	3.79000E+01	
3.81E+01	3.83000E+01	3.85000E+01	3.87000E+01	3.89000E+01	3.91000E+01	
3.93E+01	3.95000E+01	3.97000E+01	3.99000E+01	4.01000E+01	4.03000E+01	
4.05E+01	4.07000E+01	4.09000E+01	4.11000E+01			

fc15 Pilot B detector response function, 765.2 cm flightpath, 30 degrees.

f15x:n -662.7 382.6 0

cut:n 39.1 1.6

nps 400000

H. Oxygen Input Deck

0 Sphere with 0.7 M.F.P. ENDF/B-VI

1	2	- .001288	2	-3	-6	
2	3	-7.9	2	3	-4	-6
3	3	-7.9	1	-2	-4	
4	1	-1.14	1	4	-5	
5	1	-1.14	-1	-5		
6	3	-7.9	1	4	-5	-6
7	3	-7.9	-1	5	-6	
8	2	- .000001	1	6	-7	
9	2	- .000001	-1	6	-7	
10	3	-7.9	1	7	-8	
11	3	-7.9	-1	7	-8	
12	2	- .001288	8	-9		
13	0	9				

1	px	- .05			
2	px	- .025			
3	x	- .05	1.44	10.5	1.7
4	x	- .05	1.481	10.5	1.741
5	so	10.48			
6	so	10.50			
7	so	11.24			
8	so	11.28			
9	so	1000			
100	px	0.0			

imp:n 1 11r 0

-----<Source Cards>-----

fc5 Pilot B detector response function, 754.0 cm flightpath, 30 degrees.

f5x:n -663.0 377.0 0

t5	1.39E+01	1.41000E+01	1.43000E+01	1.45000E+01	1.47000E+01	1.49000E+01
	1.51E+01	1.53000E+01	1.55000E+01	1.57000E+01	1.59000E+01	1.61000E+01
	1.63E+01	1.65000E+01	1.67000E+01	1.69000E+01	1.71000E+01	1.73000E+01
	1.75E+01	1.77000E+01	1.79000E+01	1.81000E+01	1.83000E+01	1.85000E+01
	1.87E+01	1.89000E+01	1.91000E+01	1.93000E+01	1.95000E+01	1.97000E+01
	1.99E+01	2.01000E+01	2.03000E+01	2.05000E+01	2.07000E+01	2.09000E+01
	2.11E+01	2.13000E+01	2.15000E+01	2.17000E+01	2.19000E+01	2.21000E+01
	2.23E+01	2.25000E+01	2.27000E+01	2.29000E+01	2.31000E+01	2.33000E+01
	2.35E+01	2.37000E+01	2.39000E+01	2.41000E+01	2.43000E+01	2.45000E+01
	2.47E+01	2.49000E+01	2.51000E+01	2.53000E+01	2.55000E+01	2.57000E+01
	2.59E+01	2.61000E+01	2.63000E+01	2.65000E+01	2.67000E+01	2.69000E+01
	2.71E+01	2.73000E+01	2.75000E+01	2.77000E+01	2.79000E+01	2.81000E+01
	2.83E+01	2.85000E+01	2.87000E+01	2.89000E+01	2.91000E+01	2.93000E+01
	2.95E+01	2.97000E+01	2.99000E+01	3.01000E+01	3.03000E+01	3.05000E+01
	3.07E+01	3.09000E+01	3.11000E+01	3.13000E+01	3.15000E+01	3.17000E+01
	3.19E+01	3.21000E+01	3.23000E+01	3.25000E+01	3.27000E+01	3.29000E+01

```

3.31E+01 3.33000E+01 3.35000E+01 3.37000E+01 3.39000E+01 3.41000E+01
3.43E+01 3.45000E+01 3.47000E+01 3.49000E+01 3.51000E+01 3.53000E+01
3.55E+01 3.57000E+01 3.59000E+01 3.61000E+01 3.63000E+01 3.65000E+01
3.67E+01 3.69000E+01 3.71000E+01 3.73000E+01 3.75000E+01 3.77000E+01
3.79E+01 3.81000E+01 3.83000E+01 3.85000E+01 3.87000E+01 3.89000E+01
3.91E+01 3.93000E+01 3.95000E+01 3.97000E+01 3.99000E+01 4.01000E+01
4.03E+01 4.05000E+01 4.07000E+01 4.09000E+01 4.11000E+01 4.13000E+01
de5 lin 1.6 2.0 13i 16.0
df5 lin 0.00 2.25 4.10 4.70 4.85 4.85 4.70 4.30
        4.25 4.05 3.85 3.65 3.55 3.60 3.75 3.85
fc15 Pilot B detector response function, 754 cm flightpath, 30 degrees.
f15x:n -653.0 377.0
t15 15.5 17.5 24.9 39.1
de15 lin 1.6 2.0 13i 16.0
df15 lin 0.00 2.25 4.10 4.70 4.85 4.85 4.70 4.30
        4.25 4.05 3.85 3.65 3.55 3.60 3.75 3.85
fc25 NE213, 1.6 MeV bias, Dec.15,1976 data, 782.3 cm flightpath, 26 degrees.
f25x:n -703.1 342.9
t25 15.93 18.05 25.34 40.08
c NE213 low bias response function
de25 lin 1.6 1.8 1.9 2.0 2.1 2.2 2.3 2.4 2.5 2.75
        3.0 3.5 4.0 4.5 5.0 5.5 6.0 6.4 6.6 6.8 7.0
        7.5 8.1 8.5 9.0 10.0 11.0 12.0 12.5 13.0
        13.5 14.0 15.0 16.0
df25 lin 0.00 1.46 1.86 2.26 2.58 3.00 3.29 3.42
        3.63 3.95 4.10 4.25 4.33 4.39 4.40 4.37 4.28
        4.15 4.20 4.18 4.12 3.97 3.80 3.77 3.65 3.44
        3.24 3.06 3.01 2.98 2.98 3.01 3.08 3.25
c
c ENDf/B-VI
m1 8016.60c 1.00
m2 7014.60c -.7885
        8016.60c -.2115
m3 26054.60c .039788
        26056.60c .629199
        26057.60c .015092
        26058.60c .001921
        24050.60c .008700
        24052.60c .167580
        24053.60c .019000
        24054.60c .004720
        28058.60c .057346
        28060.60c .021924
        28061.60c .000949
        28062.60c .003016
        28064.60c .000764
        14000.60c .020
        12000.60c .010
cut:n 50 1.6
print
prdmp 2j 1
nps 200000

```

I. Magnesium 0.7 mfp Input Deck

```

Mg Sphere with 0.7 M.F.P.  ENDf/B-VI
1   1 -1.74 -1 -3
2   1 -1.74 1 2 -3
3   2 -.001288 1 -2 -3
4   2 -.001288 3 -4
5   0 4

1   px -.64
2   x 0.0 1.42 8.94 1.985
3   so 8.94
4   so 1000

```

```

100 px 0.0

imp:n 1 3r 0
-----<Source Cards>-----
fc5 Pilot B detector response function, 765.2 cm flightpath, 30 degrees.
f5x:n -662.7 382.6 0
t5  1.31E+01  1.33E+01  1.35E+01  1.37E+01  1.39E+01  1.41E+01
     1.43E+01  1.45E+01  1.47E+01  1.49E+01  1.51E+01  1.53E+01
     1.55E+01  1.57E+01  1.59E+01  1.61E+01  1.63E+01  1.65E+01
     1.67E+01  1.69E+01  1.71E+01  1.73E+01  1.75E+01  1.77E+01
     1.79E+01  1.81E+01  1.83E+01  1.85E+01  1.87E+01  1.89E+01
     1.91E+01  1.93E+01  1.95E+01  1.97E+01  1.99E+01  2.01E+01
     2.03E+01  2.05E+01  2.07E+01  2.09E+01  2.11E+01  2.13E+01
     2.15E+01  2.17E+01  2.19E+01  2.21E+01  2.23E+01  2.25E+01
     2.27E+01  2.29E+01  2.31E+01  2.33E+01  2.35E+01  2.37E+01
     2.39E+01  2.41E+01  2.43E+01  2.45E+01  2.47E+01  2.49E+01
     2.51E+01  2.53E+01  2.55E+01  2.57E+01  2.59E+01  2.61E+01
     2.63E+01  2.65E+01  2.67E+01  2.69E+01  2.71E+01  2.73E+01
     2.75E+01  2.77E+01  2.79E+01  2.81E+01  2.83E+01  2.85E+01
     2.87E+01  2.89E+01  2.91E+01  2.93E+01  2.95E+01  2.97E+01
     2.99E+01  3.01E+01  3.03E+01  3.05E+01  3.07E+01  3.09E+01
     3.11E+01  3.13E+01  3.15E+01  3.17E+01  3.19E+01  3.21E+01
     3.23E+01  3.25E+01  3.27E+01  3.29E+01  3.31E+01  3.33E+01
     3.35E+01  3.37E+01  3.39E+01  3.41E+01  3.43E+01  3.45E+01
     3.47E+01  3.49E+01  3.51E+01  3.53E+01  3.55E+01  3.57E+01
     3.59E+01  3.61E+01  3.63E+01  3.65E+01  3.67E+01  3.69E+01
     3.71E+01  3.73E+01  3.75E+01  3.77E+01  3.79E+01  3.81E+01
     3.83E+01  3.85E+01  3.87E+01  3.89E+01  3.91E+01  3.93E+01
     3.95E+01  3.97E+01  3.99E+01  4.01E+01  4.03E+01  4.05E+01
     4.07E+01  4.09E+01  4.11E+01

de5 lin 1.6 2.0 13i 16.0
df5 lin 0.00 2.25 4.10 4.70 4.85 4.85 4.70 4.30
        4.25 4.05 3.85 3.65 3.55 3.60 3.75 3.85
fc15 Pilot B detector response function, 765.2 cm flightpath, 30 degrees.
f15x:n -662.7 382.6 0
t15  15.5 17.5 24.9 39.1
de15 lin 1.6 2.0 13i 16.0
df15 lin 0.00 2.25 4.10 4.70 4.85 4.85 4.70 4.30
        4.25 4.05 3.85 3.65 3.55 3.60 3.75 3.85

c
c   EENDF/B-VI
m1  12000.60c 1.0
m2  7014.60c -.7885
      8016.60c -.2115
cut:n 39.1 1.6
print
prdmmp 2j 1
nps  200000

```

A. Magnesium 1.9 mfp

1. Geometry Cards

```

1   px -.64
2   x 0.0 1.42 25.5 3.485
3   so 25.5
4   so 1000
100 px 0.0

```

2. Tally Cards

```

t5  1.33E+01  1.35E+01  1.37E+01  1.39E+01  1.41E+01  1.43E+01
     1.45E+01  1.47E+01  1.49E+01  1.51E+01  1.53E+01  1.55E+01
     1.57E+01  1.59E+01  1.61E+01  1.63E+01  1.65E+01  1.67E+01
     1.69E+01  1.71E+01  1.73E+01  1.75E+01  1.77E+01  1.79E+01

```

	1.81E+01	1.83E+01	1.85E+01	1.87E+01	1.89E+01	1.91E+01
1.93E+01	1.95E+01	1.97E+01	1.99E+01	2.01E+01	2.03E+01	
2.05E+01	2.07E+01	2.09E+01	2.11E+01	2.13E+01	2.15E+01	
2.17E+01	2.19E+01	2.21E+01	2.23E+01	2.25E+01	2.27E+01	
2.29E+01	2.31E+01	2.33E+01	2.35E+01	2.37E+01	2.39E+01	
2.41E+01	2.43E+01	2.45E+01	2.47E+01	2.49E+01	2.51E+01	
2.53E+01	2.55E+01	2.57E+01	2.59E+01	2.61E+01	2.63E+01	
2.65E+01	2.67E+01	2.69E+01	2.71E+01	2.73E+01	2.75E+01	
2.77E+01	2.79E+01	2.81E+01	2.83E+01	2.85E+01	2.87E+01	
2.89E+01	2.91E+01	2.93E+01	2.95E+01	2.97E+01	2.99E+01	
3.01E+01	3.03E+01	3.05E+01	3.07E+01	3.09E+01	3.11E+01	
3.13E+01	3.15E+01	3.17E+01	3.19E+01	3.21E+01	3.23E+01	
3.25E+01	3.27E+01	3.29E+01	3.31E+01	3.33E+01	3.35E+01	
3.37E+01	3.39E+01	3.41E+01	3.43E+01	3.45E+01	3.47E+01	
3.49E+01	3.51E+01	3.53E+01	3.55E+01	3.57E+01	3.59E+01	
3.61E+01	3.63E+01	3.65E+01	3.67E+01	3.69E+01	3.71E+01	
3.73E+01	3.75E+01	3.77E+01	3.79E+01	3.81E+01	3.83E+01	
3.85E+01	3.87E+01	3.89E+01	3.91E+01	3.93E+01	3.95E+01	
3.97E+01	3.99E+01	4.01E+01	4.03E+01	4.05E+01	4.07E+01	
4.09E+01	4.11E+01	4.13E+01	4.15E+01			

nps 400000

J. Aluminum 0.9 mfp Input Deck

```

Al Sphere with 0.9 M.F.P.  EMDF/B-VI
1   1 -2.70 -1 -3
2   1 -2.70 1 2 -3
3   2 -.001288 1 -2 -3
4   2 -.001288 3 -4
5   0 4

1  px -.64
2  x 0.0 1.42 8.94 1.985
3  so 8.94
4  so 1000
100 px 0.0

imp:n 1 3x 0
-----<Source Cards>-----
fc5 Pilot B detector response function, 765.2 cm flightpath, 30 degrees.
f5x:n -662.7 382.6 0
t5  1.33E+01  1.35000E+01  1.37000E+01  1.39000E+01  1.41000E+01  1.43000E+01
    1.45E+01  1.47000E+01  1.49000E+01  1.51000E+01  1.53000E+01  1.55000E+01
    1.57E+01  1.59000E+01  1.61000E+01  1.63000E+01  1.65000E+01  1.67000E+01
    1.69E+01  1.71000E+01  1.73000E+01  1.75000E+01  1.77000E+01  1.79000E+01
    1.81E+01  1.83000E+01  1.85000E+01  1.87000E+01  1.89000E+01  1.91000E+01
    1.93E+01  1.95000E+01  1.97000E+01  1.99000E+01  2.01000E+01  2.03000E+01
    2.05E+01  2.07000E+01  2.09000E+01  2.11000E+01  2.13000E+01  2.15000E+01
    2.17E+01  2.19000E+01  2.21000E+01  2.23000E+01  2.25000E+01  2.27000E+01
    2.29E+01  2.31000E+01  2.33000E+01  2.35000E+01  2.37000E+01  2.39000E+01
    2.41E+01  2.43000E+01  2.45000E+01  2.47000E+01  2.49000E+01  2.51000E+01
    2.53E+01  2.55000E+01  2.57000E+01  2.59000E+01  2.61000E+01  2.63000E+01
    2.65E+01  2.67000E+01  2.69000E+01  2.71000E+01  2.73000E+01  2.75000E+01
    2.77E+01  2.79000E+01  2.81000E+01  2.83000E+01  2.85000E+01  2.87000E+01
    2.89E+01  2.91000E+01  2.93000E+01  2.95000E+01  2.97000E+01  2.99000E+01
    3.01E+01  3.03000E+01  3.05000E+01  3.07000E+01  3.09000E+01  3.11000E+01
    3.13E+01  3.15000E+01  3.17000E+01  3.19000E+01  3.21000E+01  3.23000E+01
    3.25E+01  3.27000E+01  3.29000E+01  3.31000E+01  3.33000E+01  3.35000E+01
    3.37E+01  3.39000E+01  3.41000E+01  3.43000E+01  3.45000E+01  3.47000E+01
    3.49E+01  3.51000E+01  3.53000E+01  3.55000E+01  3.57000E+01  3.59000E+01
    3.61E+01  3.63000E+01  3.65000E+01  3.67000E+01  3.69000E+01  3.71000E+01
    3.73E+01  3.75000E+01  3.77000E+01  3.79000E+01  3.81000E+01  3.83000E+01
    3.85E+01  3.87000E+01  3.89000E+01  3.91000E+01  3.93000E+01  3.95000E+01
    3.97E+01  3.99000E+01  4.01000E+01  4.03000E+01

de5 lin 1.6 2.0 13i 16.0
df5 lin 0.00 2.25 4.10 4.70 4.85 4.85 4.70 4.30

```

```

4.25 4.05 3.85 3.65 3.55 3.60 3.75 3.85
fc15 Pilot B detector response function, 765.2 cm flightpath, 30 degrees.
f15x:n -662.7 382.6 0
t15 15.5 17.5 24.9 39.1
de15 lin 1.6 2.0 13i 16.0
df15 lin 0.00 2.25 4.10 4.70 4.85 4.85 4.70 4.30
        4.25 4.05 3.85 3.65 3.55 3.60 3.75 3.85
c
c      ENDF/B-VI
m1    13027.60c 1.0
m2    7014.60c -.7885
        8016.60c -.2115
cut:n 39.1 1.6
print
prdmp 2j 1
nps 200000

```

A. Aluminum 2.6 mfp

1. Geometry Cards

```

1   px -.64
2   x 0.0 1.42 25.5 3.485
3   so 25.50
4   so 1000
100 px 0.0

```

2. Tally Cards

```

t5  1.35E+01  1.37000E+01  1.39000E+01  1.41000E+01  1.43000E+01  1.45000E+01
    1.47E+01  1.49000E+01  1.51000E+01  1.53000E+01  1.55000E+01  1.57000E+01
    1.59E+01  1.61000E+01  1.63000E+01  1.65000E+01  1.67000E+01  1.69000E+01
    1.71E+01  1.73000E+01  1.75000E+01  1.77000E+01  1.79000E+01  1.81000E+01
    1.83E+01  1.85000E+01  1.87000E+01  1.89000E+01  1.91000E+01  1.93000E+01
    1.95E+01  1.97000E+01  1.99000E+01  2.01000E+01  2.03000E+01  2.05000E+01
    2.07E+01  2.09000E+01  2.11000E+01  2.13000E+01  2.15000E+01  2.17000E+01
    2.19E+01  2.21000E+01  2.23000E+01  2.25000E+01  2.27000E+01  2.29000E+01
    2.31E+01  2.33000E+01  2.35000E+01  2.37000E+01  2.39000E+01  2.41000E+01
    2.43E+01  2.45000E+01  2.47000E+01  2.49000E+01  2.51000E+01  2.53000E+01
    2.55E+01  2.57000E+01  2.59000E+01  2.61000E+01  2.63000E+01  2.65000E+01
    2.67E+01  2.69000E+01  2.71000E+01  2.73000E+01  2.75000E+01  2.77000E+01
    2.79E+01  2.81000E+01  2.83000E+01  2.85000E+01  2.87000E+01  2.89000E+01
    2.91E+01  2.93000E+01  2.95000E+01  2.97000E+01  2.99000E+01  3.01000E+01
    3.03E+01  3.05000E+01  3.07000E+01  3.09000E+01  3.11000E+01  3.13000E+01
    3.15E+01  3.17000E+01  3.19000E+01  3.21000E+01  3.23000E+01  3.25000E+01
    3.27E+01  3.29000E+01  3.31000E+01  3.33000E+01  3.35000E+01  3.37000E+01
    3.39E+01  3.41000E+01  3.43000E+01  3.45000E+01  3.47000E+01  3.49000E+01
    3.51E+01  3.53000E+01  3.55000E+01  3.57000E+01  3.59000E+01  3.61000E+01
    3.63E+01  3.65000E+01  3.67000E+01  3.69000E+01  3.71000E+01  3.73000E+01
    3.75E+01  3.77000E+01  3.79000E+01  3.81000E+01  3.83000E+01  3.85000E+01
    3.87E+01  3.89000E+01  3.91000E+01  3.93000E+01  3.95000E+01  3.97000E+01
    3.99E+01  4.01000E+01  4.03000E+01  4.05000E+01  4.07000E+01  4.09000E+01
    4.11E+01  4.13000E+01  4.15000E+01
nps 400000

```

K. Titanium 1.2 mfp Input Deck

```

Ti Sphere with 1.2 M.F.P. ENDF/B-VI
1   1 -4.54 -1 -3
2   1 -4.54 1 2 -3
3   2 -.001288 1 -2 -3
7   2 -.001288 3 -4
8   0 4

```

```

1   px -.64
2   x 0.0 1.42 8.94 1.985
3   so 8.94
4   so 1000
100  px 0.0

imp:n 1 3r 0
-----<Source Cards>-----
fc5 Pilot B detector response function, 765.2 cm flightpath, 30 degrees.
f5x:n -662.7 382.6 0
t5   1.31E+01  1.33E+01  1.35E+01  1.37E+01  1.39E+01  1.41E+01
     1.43E+01  1.45E+01  1.47E+01  1.49E+01  1.51E+01  1.53E+01
     1.55E+01  1.57E+01  1.59E+01  1.61E+01  1.63E+01  1.65E+01
     1.67E+01  1.69E+01  1.71E+01  1.73E+01  1.75E+01  1.77E+01
     1.79E+01  1.81E+01  1.83E+01  1.85E+01  1.87E+01  1.89E+01
     1.91E+01  1.93E+01  1.95E+01  1.97E+01  1.99E+01  2.01E+01
     2.03E+01  2.05E+01  2.07E+01  2.09E+01  2.11E+01  2.13E+01
     2.15E+01  2.17E+01  2.19E+01  2.21E+01  2.23E+01  2.25E+01
     2.27E+01  2.29E+01  2.31E+01  2.33E+01  2.35E+01  2.37E+01
     2.39E+01  2.41E+01  2.43E+01  2.45E+01  2.47E+01  2.49E+01
     2.51E+01  2.53E+01  2.55E+01  2.57E+01  2.59E+01  2.61E+01
     2.63E+01  2.65E+01  2.67E+01  2.69E+01  2.71E+01  2.73E+01
     2.75E+01  2.77E+01  2.79E+01  2.81E+01  2.83E+01  2.85E+01
     2.87E+01  2.89E+01  2.91E+01  2.93E+01  2.95E+01  2.97E+01
     2.99E+01  3.01E+01  3.03E+01  3.05E+01  3.07E+01  3.09E+01
     3.11E+01  3.13E+01  3.15E+01  3.17E+01  3.19E+01  3.21E+01
     3.23E+01  3.25E+01  3.27E+01  3.29E+01  3.31E+01  3.33E+01
     3.35E+01  3.37E+01  3.39E+01  3.41E+01  3.43E+01  3.45E+01
     3.47E+01  3.49E+01  3.51E+01  3.53E+01  3.55E+01  3.57E+01
     3.59E+01  3.61E+01  3.63E+01  3.65E+01  3.67E+01  3.69E+01
     3.71E+01  3.73E+01  3.75E+01  3.77E+01  3.79E+01  3.81E+01
     3.83E+01  3.85E+01  3.87E+01  3.89E+01  3.91E+01  3.93E+01
     3.95E+01  3.97E+01  3.99E+01  4.01E+01  4.03E+01  4.05E+01
     4.07E+01  4.09E+01

de5  lin 1.6 2.0 13i 16.0
df5  lin 0.00 2.25 4.10 4.70 4.85 4.85 4.70 4.30
      4.25 4.05 3.85 3.65 3.55 3.60 3.75 3.85
fc15 Pilot B detector response function, 765.2 cm flightpath, 30 degrees.
f15x:n -662.7 382.6 0
t15  15.6 17.5 24.9 39.1
de15 lin 1.6 2.0 13i 16.0
df15 lin 0.00 2.25 4.10 4.70 4.85 4.85 4.70 4.30
      4.25 4.05 3.85 3.65 3.55 3.60 3.75 3.85
c
c   ENDF/B-VI
m1  22000.60c 1.0
m2  7014.60c -.7885
     8016.60c -.2115
cut:n 39.1 1.6
print
nps 200000
prdmp 2j 1

```

A. Titanium 3.5 mfp

1. Cell Cards

```

Ti Sphere with 3.5 M.F.P. ENDF/B-VI
1   1 -4.54 -1 -3
2   1 -4.54 1 2 -3
3   2 -.001288 1 -2 -3
4   2 -.001288 3 -4
5   0 4

```

2. Geometry Cards

```
1 px -.64
2 x 0.0 1.42 25.5 3.485
3 so 25.5
4 so 1000
100 px 0.0
```

3. Tally Cards

```
t5 1.35000E+01 1.37000E+01 1.39000E+01 1.41000E+01 1.43000E+01
    1.45000E+01
    1.47000E+01 1.49000E+01 1.51000E+01 1.53000E+01 1.55000E+01
    1.57000E+01
    1.59000E+01 1.61000E+01 1.63000E+01 1.65000E+01 1.67000E+01
    1.69000E+01
    1.71000E+01 1.73000E+01 1.75000E+01 1.77000E+01 1.79000E+01
    1.81000E+01
    1.83000E+01 1.85000E+01 1.87000E+01 1.89000E+01 1.91000E+01
    1.93000E+01
    1.95000E+01 1.97000E+01 1.99000E+01 2.01000E+01 2.03000E+01
    2.05000E+01
    2.07000E+01 2.09000E+01 2.11000E+01 2.13000E+01 2.15000E+01
    2.17000E+01
    2.19000E+01 2.21000E+01 2.23000E+01 2.25000E+01 2.27000E+01
    2.29000E+01
    2.31000E+01 2.33000E+01 2.35000E+01 2.37000E+01 2.39000E+01
    2.41000E+01
    2.43000E+01 2.45000E+01 2.47000E+01 2.49000E+01 2.51000E+01
    2.53000E+01
    2.55000E+01 2.57000E+01 2.59000E+01 2.61000E+01 2.63000E+01
    2.65000E+01
    2.67000E+01 2.69000E+01 2.71000E+01 2.73000E+01 2.75000E+01
    2.77000E+01
    2.79000E+01 2.81000E+01 2.83000E+01 2.85000E+01 2.87000E+01
    2.89000E+01
    2.91000E+01 2.93000E+01 2.95000E+01 2.97000E+01 2.99000E+01
    3.01000E+01
    3.03000E+01 3.05000E+01 3.07000E+01 3.09000E+01 3.11000E+01
    3.13000E+01
    3.15000E+01 3.17000E+01 3.19000E+01 3.21000E+01 3.23000E+01
    3.25000E+01
    3.27000E+01 3.29000E+01 3.31000E+01 3.33000E+01 3.35000E+01
    3.37000E+01
    3.39000E+01 3.41000E+01 3.43000E+01 3.45000E+01 3.47000E+01
    3.49000E+01
    3.51000E+01 3.53000E+01 3.55000E+01 3.57000E+01 3.59000E+01
    3.61000E+01
    3.63000E+01 3.65000E+01 3.67000E+01 3.69000E+01 3.71000E+01
    3.73000E+01
    3.75000E+01 3.77000E+01 3.79000E+01 3.81000E+01 3.83000E+01
    3.85000E+01
    3.87000E+01 3.89000E+01 3.91000E+01 3.93000E+01 3.95000E+01
    3.97000E+01
    3.99000E+01 4.01000E+01 4.03000E+01 4.05000E+01 4.07000E+01
    4.09000E+01
nps 400000
```

L. Iron 0.9 mfp Input Deck

```
Fe Sphere with .9 M.F.P. ENDf/B-VI
1   1 -7.85 -1 -3
2   1 -7.85 1 2 -3
3   2 -.001288 1 -2 -3
```

```

4   2 -.001288 3 -4
5   0 4

1   px -.475
2   x 0.0 1.11 22.3 2.67
3   so 4.46
4   so 1000
100  px 0.0

imp:n 1 3x 0
-----<Source Cards>-----
fc5  NE213 detector response function, 766.0 cm flightpath, 30 degrees.
f5x:n -663.4 383 0
t5   1.37E+01  1.39000E+01  1.41000E+01  1.43000E+01  1.45000E+01  1.47000E+01
     1.49E+01  1.51000E+01  1.53000E+01  1.55000E+01  1.57000E+01  1.59000E+01
     1.61E+01  1.63000E+01  1.65000E+01  1.67000E+01  1.69000E+01  1.71000E+01
     1.73E+01  1.75000E+01  1.77000E+01  1.79000E+01  1.81000E+01  1.83000E+01
     1.85E+01  1.87000E+01  1.89000E+01  1.91000E+01  1.93000E+01  1.95000E+01
     1.97E+01  1.99000E+01  2.01000E+01  2.03000E+01  2.05000E+01  2.07000E+01
     2.09E+01  2.11000E+01  2.13000E+01  2.15000E+01  2.17000E+01  2.19000E+01
     2.21E+01  2.23000E+01  2.25000E+01  2.27000E+01  2.29000E+01  2.31000E+01
     2.33E+01  2.35000E+01  2.37000E+01  2.39000E+01  2.41000E+01  2.43000E+01
     2.45E+01  2.47000E+01  2.49000E+01  2.51000E+01  2.53000E+01  2.55000E+01
     2.57E+01  2.59000E+01  2.61000E+01  2.63000E+01  2.65000E+01  2.67000E+01
     2.69E+01  2.71000E+01  2.73000E+01  2.75000E+01  2.77000E+01  2.79000E+01
     2.81E+01  2.83000E+01  2.85000E+01  2.87000E+01  2.89000E+01  2.91000E+01
     2.93E+01  2.95000E+01  2.97000E+01  2.99000E+01  3.01000E+01  3.03000E+01
     3.05E+01  3.07000E+01  3.09000E+01  3.11000E+01  3.13000E+01  3.15000E+01
     3.17E+01  3.19000E+01  3.21000E+01  3.23000E+01  3.25000E+01  3.27000E+01
     3.29E+01  3.31000E+01  3.33000E+01  3.35000E+01  3.37000E+01  3.39000E+01
     3.41E+01  3.43000E+01  3.45000E+01  3.47000E+01  3.49000E+01  3.51000E+01
     3.53E+01  3.55000E+01  3.57000E+01  3.59000E+01  3.61000E+01  3.63000E+01
     3.65E+01  3.67000E+01  3.69000E+01  3.71000E+01  3.73000E+01  3.75000E+01
     3.77E+01  3.79000E+01  3.81000E+01  3.83000E+01  3.85000E+01  3.87000E+01
     3.89E+01  3.91000E+01  3.93000E+01  3.95000E+01  3.97000E+01  3.99000E+01
     4.01E+01  4.03000E+01  4.05000E+01  4.07000E+01  4.09000E+01  4.11000E+01
     4.13E+01  4.15000E+01  4.17000E+01

c   NE213 low bias response function
de5  lim 1.6 1.8 1.9 2.0 2.1 2.2 2.3 2.4 2.5 2.75
     3.0 3.5 4.0 4.5 5.0 5.5 6.0 6.4 6.6 6.8 7.0
     7.5 8.1 8.5 9.0 10.0 11.0 12.0 12.5 13.0
     13.5 14.0 15.0 16.0
df5  lim 0.00 1.46 1.86 2.26 2.58 3.00 3.29 3.42
     3.63 3.95 4.10 4.25 4.33 4.39 4.40 4.37 4.28
     4.15 4.20 4.18 4.12 3.97 3.80 3.77 3.65 3.44
     3.24 3.06 3.01 2.98 2.98 3.01 3.08 3.25
fc15  NE213 detector, low bias, 766.0 cm flightpath, 30 degrees.
f15x:n -663.4 383 0
t15  15.5 17.5 24.9 39.1
c   NE213 low bias response function
de15 lim 1.6 1.8 1.9 2.0 2.1 2.2 2.3 2.4 2.5 2.75
     3.0 3.5 4.0 4.5 5.0 5.5 6.0 6.4 6.6 6.8 7.0
     7.5 8.1 8.5 9.0 10.0 11.0 12.0 12.5 13.0
     13.5 14.0 15.0 16.0
df15 lim 0.00 1.46 1.86 2.26 2.58 3.00 3.29 3.42
     3.63 3.95 4.10 4.25 4.33 4.39 4.40 4.37 4.28
     4.15 4.20 4.18 4.12 3.97 3.80 3.77 3.65 3.44
     3.24 3.06 3.01 2.98 2.98 3.01 3.08 3.25

c
c   ENDF/B-VI
m1  26054.60c .0562600
    26056.60c .8896840
    26057.60c .0213400
    26058.60c .0027160
    6000.60c .012
    25055.60c .010
    15031.60c .007
    16032.60c .001

```

```
m2    7014.60c -.7885  
      8016.60c -.2115  
cut:n 39.1 1.6  
print  
prdmp 2j 1  
nps  200000
```

A. Iron 4.8 mfp

1. Cell Cards

```
Fe Sphere with 4.8 M.F.P.  ENDF/B-VI  
1   1 -7.85 -1 -3  
2   1 -7.85 1 2 -3  
3   2 -.001288 1 -2 -3  
4   1 -7.85 -1 3 -4  
5   1 -7.85 1 2 3 -4  
6   2 -.001288 1 -2 3 -4  
7   1 -7.85 -1 4 -5  
8   1 -7.85 1 2 4 -5  
9   2 -.001288 1 -2 4 -5  
10  1 -7.85 -1 5 -6  
11  1 -7.85 1 2 5 -6  
12  2 -.001288 1 -2 5 -6  
13  2 -.001288 6 -7  
14  0 7
```

2. Geometry Cards

```
1  px -.475  
2  x 0.0 1.11 22.3 2.67  
3  so 6  
4  so 12  
5  so 18  
6  so 22.3  
7  so 1000  
100 px 0.0
```

3. Tally Cards

```
imp:n 1 1 1 2 2 2 4 4 4 8 8 8 8 0  
nps  400000
```

M. Lead Input Deck

```
Pb Sphere with 1.4 M.F.P.  ENDF/B-VI  
1   1 -7.9 1 -2 -3  
2   2 -.001288 2 -3 -9  
3   1 -7.9 1 3 -4 -8  
4   3 -11.35 (-1:4) (-5:-6:7) -8  
5   1 -7.9 5 6 -7 -8  
6   1 -7.9 8 -9 (-1:3)  
21  2 -.001288 9 -10  
22  0 10
```

```
1  px -.64  
2  px -.582  
3  x 0.0 1.42 8.5 1.985  
4  x 0.0 1.478 8.5 2.043  
5  cx 8.87  
6  px -.1
```

```

7   px .1
8   so 8.912
9   so 8.97
10  so 1000
100 px 0.0

imp:n 1 6r 0
-----<Source Cards>-----
fc5 NE213 detector response function, 766.0 cm flightpath, 30 degrees.
f5x:n -663.4 383 0
t5  1.39E+01  1.41000E+01  1.43000E+01  1.45000E+01  1.47000E+01  1.49000E+01
    1.51E+01  1.53000E+01  1.55000E+01  1.57000E+01  1.59000E+01  1.61000E+01
    1.63E+01  1.65000E+01  1.67000E+01  1.69000E+01  1.71000E+01  1.73000E+01
    1.75E+01  1.77000E+01  1.79000E+01  1.81000E+01  1.83000E+01  1.85000E+01
    1.87E+01  1.89000E+01  1.91000E+01  1.93000E+01  1.95000E+01  1.97000E+01
    1.99E+01  2.01000E+01  2.03000E+01  2.05000E+01  2.07000E+01  2.09000E+01
    2.11E+01  2.13000E+01  2.15000E+01  2.17000E+01  2.19000E+01  2.21000E+01
    2.23E+01  2.25000E+01  2.27000E+01  2.29000E+01  2.31000E+01  2.33000E+01
    2.35E+01  2.37000E+01  2.39000E+01  2.41000E+01  2.43000E+01  2.45000E+01
    2.47E+01  2.49000E+01  2.51000E+01  2.53000E+01  2.55000E+01  2.57000E+01
    2.59E+01  2.61000E+01  2.63000E+01  2.65000E+01  2.67000E+01  2.69000E+01
    2.71E+01  2.73000E+01  2.75000E+01  2.77000E+01  2.79000E+01  2.81000E+01
    2.83E+01  2.85000E+01  2.87000E+01  2.89000E+01  2.91000E+01  2.93000E+01
    2.95E+01  2.97000E+01  2.99000E+01  3.01000E+01  3.03000E+01  3.05000E+01
    3.07E+01  3.09000E+01  3.11000E+01  3.13000E+01  3.15000E+01  3.17000E+01
    3.19E+01  3.21000E+01  3.23000E+01  3.25000E+01  3.27000E+01  3.29000E+01
    3.31E+01  3.33000E+01  3.35000E+01  3.37000E+01  3.39000E+01  3.41000E+01
    3.43E+01  3.45000E+01  3.47000E+01  3.49000E+01  3.51000E+01  3.53000E+01
    3.55E+01  3.57000E+01  3.59000E+01  3.61000E+01  3.63000E+01  3.65000E+01
    3.67E+01  3.69000E+01  3.71000E+01  3.73000E+01  3.75000E+01  3.77000E+01
    3.79E+01  3.81000E+01  3.83000E+01  3.85000E+01  3.87000E+01  3.89000E+01
    3.91E+01  3.93000E+01  3.95000E+01  3.97000E+01  3.99000E+01  4.01000E+01
    4.03E+01  4.05000E+01  4.07000E+01  4.09000E+01  4.11000E+01  4.13000E+01
    4.15E+01  4.17000E+01

c   NE213 low bias response function
de5  lin 1.6 1.8 1.9 2.0 2.1 2.2 2.3 2.4 2.5 2.75
     3.0 3.5 4.0 4.5 5.0 5.5 6.0 6.4 6.6 6.8 7.0
     7.5 8.1 8.5 9.0 10.0 11.0 12.0 12.5 13.0
     13.5 14.0 15.0 16.0
df5  lin 0.00 1.46 1.86 2.26 2.58 3.00 3.29 3.42
     3.63 3.95 4.10 4.25 4.33 4.39 4.40 4.37 4.28
     4.15 4.20 4.18 4.12 3.97 3.80 3.77 3.65 3.44
     3.24 3.06 3.01 2.98 2.98 3.01 3.08 3.25
fc15 NE213 detector, low bias, 766.0 cm flightpath, 30 degrees.
f15x:n -663.4 383 0
t15  15.5 17.5 24.9 39.1
c   NE213 low bias response function
de15  lin 1.6 1.8 1.9 2.0 2.1 2.2 2.3 2.4 2.5 2.75
     3.0 3.5 4.0 4.5 5.0 5.5 6.0 6.4 6.6 6.8 7.0
     7.5 8.1 8.5 9.0 10.0 11.0 12.0 12.5 13.0
     13.5 14.0 15.0 16.0
df15  lin 0.00 1.46 1.86 2.26 2.58 3.00 3.29 3.42
     3.63 3.95 4.10 4.25 4.33 4.39 4.40 4.37 4.28
     4.15 4.20 4.18 4.12 3.97 3.80 3.77 3.65 3.44
     3.24 3.06 3.01 2.98 2.98 3.01 3.08 3.25

c
c   EENDF/B-VI
m1  26054.60c .039788
    26056.60c .629199
    26057.60c .015092
    26058.60c .001921
    24050.60c .008700
    24052.60c .167580
    24053.60c .019000
    24054.60c .004720
    28058.60c .057346
    28060.60c .021924
    28061.60c .000949

```

```

28062.60c .003016
28064.60c .000764
14000.60c .020
12000.60c .010
m2    7014.60c -.7885
      8016.60c -.2115
m3    82206.60c .241
      82207.60c .221
      82208.60c .524
cut:n 39.1 1.6
print
prdm p 2j 1
nps 200000

```

N. Water 1.1 mfp Input Deck

Water Sphere with 1.1 M.F.P. ENDF/B-VI

```

1 2 -.001288 2 -3 -6
2 3 -7.9 2 3 -4 -6
3 3 -7.9 1 -2 -4
4 1 -1.0 1 4 -5
5 1 -1.0 -1 -5
6 3 -7.9 1 4 5 -6
7 3 -7.9 -1 5 -6
8 2 -.000001 1 6 -7
9 2 -.000001 -1 6 -7
10 3 -7.9 1 7 -8
11 3 -7.9 -1 7 -8
12 2 -.001288 8 -9
13 0 9

```

```

1 px -.05
2 px -.025
3 x -.05 1.44 10.5 1.7
4 x -.05 1.481 10.5 1.741
5 so 10.48
6 so 10.50
7 so 11.24
8 so 11.28
9 so 1000
100 px 0.0

```

```
imp:n 1 11r 0
```

-----<Source Cards>-----

fc5 Pilot B detector response function, 754.0 cm flightpath, 30 degrees.

```

f5x:n -663.0 377.0 0
t5  1.38E+01  1.40000E+01  1.42000E+01  1.44000E+01  1.46000E+01  1.48000E+01
     1.50E+01  1.52000E+01  1.54000E+01  1.56000E+01  1.58000E+01  1.60000E+01
     1.62E+01  1.64000E+01  1.66000E+01  1.68000E+01  1.70000E+01  1.72000E+01
     1.74E+01  1.76000E+01  1.78000E+01  1.80000E+01  1.82000E+01  1.84000E+01
     1.86E+01  1.88000E+01  1.90000E+01  1.92000E+01  1.94000E+01  1.96000E+01
     1.98E+01  2.00000E+01  2.02000E+01  2.04000E+01  2.06000E+01  2.08000E+01
     2.10E+01  2.12000E+01  2.14000E+01  2.16000E+01  2.18000E+01  2.20000E+01
     2.22E+01  2.24000E+01  2.26000E+01  2.28000E+01  2.30000E+01  2.32000E+01
     2.34E+01  2.36000E+01  2.38000E+01  2.40000E+01  2.42000E+01  2.44000E+01
     2.46E+01  2.48000E+01  2.50000E+01  2.52000E+01  2.54000E+01  2.56000E+01
     2.58E+01  2.60000E+01  2.62000E+01  2.64000E+01  2.66000E+01  2.68000E+01
     2.70E+01  2.72000E+01  2.74000E+01  2.76000E+01  2.78000E+01  2.80000E+01
     2.82E+01  2.84000E+01  2.86000E+01  2.88000E+01  2.90000E+01  2.92000E+01
     2.94E+01  2.96000E+01  2.98000E+01  3.00000E+01  3.02000E+01  3.04000E+01
     3.06E+01  3.08000E+01  3.10000E+01  3.12000E+01  3.14000E+01  3.16000E+01
     3.18E+01  3.20000E+01  3.22000E+01  3.24000E+01  3.26000E+01  3.28000E+01
     3.30E+01  3.32000E+01  3.34000E+01  3.36000E+01  3.38000E+01  3.40000E+01
     3.42E+01  3.44000E+01  3.46000E+01  3.48000E+01  3.50000E+01  3.52000E+01
     3.54E+01  3.56000E+01  3.58000E+01  3.60000E+01  3.62000E+01  3.64000E+01
     3.66E+01  3.68000E+01  3.70000E+01  3.72000E+01  3.74000E+01  3.76000E+01

```

```

3.78E+01 3.80000E+01 3.82000E+01 3.84000E+01 3.86000E+01 3.88000E+01
3.90E+01 3.92000E+01 3.94000E+01 3.96000E+01 3.98000E+01 4.00000E+01
4.02E+01 4.04000E+01 4.06000E+01 4.08000E+01
de5 lin 1.6 2.0 13i 16.0
df5 lin 0.00 2.25 4.10 4.70 4.85 4.85 4.70 4.30
        4.25 4.05 3.85 3.65 3.55 3.60 3.75 3.85
fc15 Pilot B detector response function, 754 cm flightpath, 30 degrees.
f15x:n -653.0 377.0 0
t15 15.5 17.5 24.9 39.1
de15 lin 1.6 2.0 13i 16.0
df15 lin 0.00 2.25 4.10 4.70 4.85 4.85 4.70 4.30
        4.25 4.05 3.85 3.65 3.55 3.60 3.75 3.85
c
c      ENDF/B-VI
m1 1001.60c .667
     8016.60c .333
m2 7014.60c -.7885
     8016.60c -.2115
m3 26054.60c .039788
     26056.60c .629199
     26057.60c .015092
     26058.60c .001921
     24050.60c .008700
     24052.60c .167580
     24053.60c .019000
     24054.60c .004720
     28058.60c .057346
     28060.60c .021924
     28061.60c .000949
     28062.60c .003016
     28064.60c .000764
     14000.60c .020
     12000.60c .010
cnt:n 50 1.6
print
prdmpr 2j 1
nps 200000

```

A. Water 1.9 mfp

1. Geometry Cards

```

1 px -.741
2 px -.7
3 x -.7 1.25 19.0 1.5
4 x -.7 1.291 19.0 1.541
5 so 19.05
6 so 19.11
7 so 22.40
8 so 22.55
9 so 1000
100 px 0.0

```

2. Tally Cards

```

f5x:n -653.0 377.0 0
t5 1.32E+01 1.34000E+01 1.36000E+01 1.38000E+01 1.40000E+01 1.42000E+01
    1.44E+01 1.46000E+01 1.48000E+01 1.50000E+01 1.52000E+01 1.54000E+01
    1.56E+01 1.58000E+01 1.60000E+01 1.62000E+01 1.64000E+01 1.66000E+01
    1.68E+01 1.70000E+01 1.72000E+01 1.74000E+01 1.76000E+01 1.78000E+01
    1.80E+01 1.82000E+01 1.84000E+01 1.86000E+01 1.88000E+01 1.90000E+01
    1.92E+01 1.94000E+01 1.96000E+01 1.98000E+01 2.00000E+01 2.02000E+01
    2.04E+01 2.06000E+01 2.08000E+01 2.10000E+01 2.12000E+01 2.14000E+01
    2.16E+01 2.18000E+01 2.20000E+01 2.22000E+01 2.24000E+01 2.26000E+01
    2.28E+01 2.30000E+01 2.32000E+01 2.34000E+01 2.36000E+01 2.38000E+01

```

	2.40E+01	2.42000E+01	2.44000E+01	2.46000E+01	2.48000E+01	2.50000E+01
1	2.52E+01	2.54000E+01	2.56000E+01	2.58000E+01	2.60000E+01	2.62000E+01
2	2.64E+01	2.66000E+01	2.68000E+01	2.70000E+01	2.72000E+01	2.74000E+01
3	2.76E+01	2.78000E+01	2.80000E+01	2.82000E+01	2.84000E+01	2.86000E+01
4	2.88E+01	2.90000E+01	2.92000E+01	2.94000E+01	2.96000E+01	2.98000E+01
5	3.00E+01	3.02000E+01	3.04000E+01	3.06000E+01	3.08000E+01	3.10000E+01
6	3.12E+01	3.14000E+01	3.16000E+01	3.18000E+01	3.20000E+01	3.22000E+01
7	3.24E+01	3.26000E+01	3.28000E+01	3.30000E+01	3.32000E+01	3.34000E+01
8	3.36E+01	3.38000E+01	3.40000E+01	3.42000E+01	3.44000E+01	3.46000E+01
9	3.48E+01	3.50000E+01	3.52000E+01	3.54000E+01	3.56000E+01	3.58000E+01
10	3.60E+01	3.62000E+01	3.64000E+01	3.66000E+01	3.68000E+01	3.70000E+01
11	3.72E+01	3.74000E+01	3.76000E+01	3.78000E+01	3.80000E+01	3.82000E+01
12	3.84E+01	3.86000E+01	3.88000E+01	3.90000E+01	3.92000E+01	3.94000E+01
13	3.96E+01	3.98000E+01				

O. Heavy Water 1.2 mfp Input Deck

Heavy Water Sphere with 1.2 M.F.P. ENDF/B-VI

```

1 2 -.001288 2 -3 -6
2 3 -7.9 2 3 -4 -6
3 3 -7.9 1 -2 -4
4 1 -1.105 1 4 -5
5 1 -1.105 -1 -5
6 3 -7.9 1 4 5 -6
7 3 -7.9 -1 5 -6
8 2 -.0000001 1 6 -7
9 2 -.0000001 -1 6 -7
10 3 -7.9 1 7 -8
11 3 -7.9 -1 7 -8
12 2 -.001288 8 -9
13 0 9

```

```

1 px -.05
2 px -.025
3 x -.05 1.44 10.5 1.7
4 x -.05 1.481 10.5 1.741
5 so 10.48
6 so 10.50
7 so 11.24
8 so 11.28
9 so 1000
100 px 0.0

```

```

imp:n 1 11r 0
-----<Source Cards>-----

```

```

fc5 Pilot B detector response function, 765.2 cm flightpath, 30 degrees.
f5x:n -662.7 382.6 0

```

t5	1.42E+01	1.44E+01	1.46E+01	1.48E+01	1.50E+01	1.52E+01
1	1.54E+01	1.56E+01	1.58E+01	1.60E+01	1.62E+01	1.64E+01
2	1.66E+01	1.68E+01	1.70E+01	1.72E+01	1.74E+01	1.76E+01
3	1.78E+01	1.80E+01	1.82E+01	1.84E+01	1.86E+01	1.88E+01
4	1.90E+01	1.92E+01	1.94E+01	1.96E+01	1.98E+01	2.00E+01
5	2.02E+01	2.04E+01	2.06E+01	2.08E+01	2.10E+01	2.12E+01
6	2.14E+01	2.16E+01	2.18E+01	2.20E+01	2.22E+01	2.24E+01
7	2.26E+01	2.28E+01	2.30E+01	2.32E+01	2.34E+01	2.36E+01
8	2.38E+01	2.40E+01	2.42E+01	2.44E+01	2.46E+01	2.48E+01
9	2.50E+01	2.52E+01	2.54E+01	2.56E+01	2.58E+01	2.60E+01
10	2.62E+01	2.64E+01	2.66E+01	2.68E+01	2.70E+01	2.72E+01
11	2.74E+01	2.76E+01	2.78E+01	2.80E+01	2.82E+01	2.84E+01
12	2.86E+01	2.88E+01	2.90E+01	2.92E+01	2.94E+01	2.96E+01
13	2.98E+01	3.00E+01	3.02E+01	3.04E+01	3.06E+01	3.08E+01
14	3.10E+01	3.12E+01	3.14E+01	3.16E+01	3.18E+01	3.20E+01
15	3.22E+01	3.24E+01	3.26E+01	3.28E+01	3.30E+01	3.32E+01
16	3.34E+01	3.36E+01	3.38E+01	3.40E+01	3.42E+01	3.44E+01
17	3.46E+01	3.48E+01	3.50E+01	3.52E+01	3.54E+01	3.56E+01
18	3.58E+01	3.60E+01	3.62E+01	3.64E+01	3.66E+01	3.68E+01

```

3.70E+01 3.72E+01 3.74E+01 3.76E+01 3.78E+01
de5 lin 1.6 2.0 13i 16.0
df5 lin 0.00 2.25 4.10 4.70 4.85 4.85 4.70 4.30
        4.25 4.05 3.85 3.65 3.55 3.60 3.75 3.85
fc15 Pilot B detector response function, 765.2 cm flightpath, 30 degrees.
f15x:n -662.7 382.6 0
t15 15.5 17.5 24.9 39.1
de15 lin 1.6 2.0 13i 16.0
df15 lin 0.00 2.25 4.10 4.70 4.85 4.85 4.70 4.30
        4.25 4.05 3.85 3.65 3.55 3.60 3.75 3.85
c
c ENDF/B-VI
m1 1002.60c .667
    8016.60c .333
m2 7014.60c -.7885
    8016.60c -.2115
m3 26054.60c .039788
    26056.60c .629199
    26057.60c .015092
    26058.60c .001921
    24050.60c .008700
    24052.60c .167580
    24053.60c .019000
    24054.60c .004720
    28058.60c .057346
    28060.60c .021924
    28061.60c .000949
    28062.60c .003016
    28064.60c .000764
    14000.60c .020
    12000.60c .010
cut:n 50 1.6
print
prdmmp 2j 1
nps 200000

```

A. Heavy Water 2.1 mfp

1. Geometry Cards

```

1 px -.741
2 px -.7
3 x -.7 1.25 19.0 1.5
4 x -.7 1.291 19.0 1.541
5 so 19.05
6 so 19.11
7 so 22.40
8 so 22.55
9 so 1000
100 px 0.0

```

2. Tally Cards

```

t5 1.42E+01 1.44E+01 1.46E+01 1.48E+01 1.50E+01 1.52E+01
1.54E+01 1.56E+01 1.58E+01 1.60E+01 1.62E+01 1.64E+01
1.66E+01 1.68E+01 1.70E+01 1.72E+01 1.74E+01 1.76E+01
1.78E+01 1.80E+01 1.82E+01 1.84E+01 1.86E+01 1.88E+01
1.90E+01 1.92E+01 1.94E+01 1.96E+01 1.98E+01 2.00E+01
2.02E+01 2.04E+01 2.06E+01 2.08E+01 2.10E+01 2.12E+01
2.14E+01 2.16E+01 2.18E+01 2.20E+01 2.22E+01 2.24E+01
2.26E+01 2.28E+01 2.30E+01 2.32E+01 2.34E+01 2.36E+01
2.38E+01 2.40E+01 2.42E+01 2.44E+01 2.46E+01 2.48E+01
2.50E+01 2.52E+01 2.54E+01 2.56E+01 2.58E+01 2.60E+01
2.62E+01 2.64E+01 2.66E+01 2.68E+01 2.70E+01 2.72E+01
2.74E+01 2.76E+01 2.78E+01 2.80E+01 2.82E+01 2.84E+01

```

	2.86E+01	2.88E+01	2.90E+01	2.92E+01	2.94E+01	2.96E+01
1	2.98E+01	3.00E+01	3.02E+01	3.04E+01	3.06E+01	3.08E+01
2	3.10E+01	3.12E+01	3.14E+01	3.16E+01	3.18E+01	3.20E+01
3	3.22E+01	3.24E+01	3.26E+01	3.28E+01	3.30E+01	3.32E+01
4	3.34E+01	3.36E+01	3.38E+01	3.40E+01	3.42E+01	3.44E+01
5	3.46E+01	3.48E+01	3.50E+01	3.52E+01	3.54E+01	3.56E+01
6	3.58E+01	3.60E+01	3.62E+01	3.64E+01	3.66E+01	3.68E+01
7	3.70E+01	3.72E+01	3.74E+01	3.76E+01	3.78E+01	3.80E+01
8	3.82E+01	3.84E+01	3.86E+01	3.88E+01	3.90E+01	3.92E+01
9	3.94E+01	3.96E+01	3.98E+01	4.00E+01	4.02E+01	4.04E+01
10	4.06E+01	4.08E+01				

P. Polyethylene 0.7 mfp Input Deck

Polyethylene Sphere with 0.8 M.F.P EWDF/B-VI

```

1 2 -.001288 -1 -2
2 2 -.001288 1 -2
3 2 -.001288 1 2 -3 -4
4 1 -.92 -1 2 -4
5 1 -.92 1 2 3 -4
6 2 -.001288 4 -5
7 0 5

```

```

1 px -.1
2 so 8.94
3 x 8.94 2.345 16.50 3.485
4 so 16.5
5 so 1000
100 px 0.0

```

imp:n 1 5r 0

-----<Source Cards>-----

fc5 Pilot B detector response function, 754.0 cm flightpath, 30 degrees.

f5x:n -653.0 377.0 0

t5	1.30E+01	1.32000E+01	1.34000E+01	1.36000E+01	1.38000E+01	1.40000E+01
1	1.42E+01	1.44000E+01	1.46000E+01	1.48000E+01	1.50000E+01	1.52000E+01
2	1.54E+01	1.56000E+01	1.58000E+01	1.60000E+01	1.62000E+01	1.64000E+01
3	1.66E+01	1.68000E+01	1.70000E+01	1.72000E+01	1.74000E+01	1.76000E+01
4	1.78E+01	1.80000E+01	1.82000E+01	1.84000E+01	1.86000E+01	1.88000E+01
5	1.90E+01	1.92000E+01	1.94000E+01	1.96000E+01	1.98000E+01	2.00000E+01
6	2.02E+01	2.04000E+01	2.06000E+01	2.08000E+01	2.10000E+01	2.12000E+01
7	2.14E+01	2.16000E+01	2.18000E+01	2.20000E+01	2.22000E+01	2.24000E+01
8	2.26E+01	2.28000E+01	2.30000E+01	2.32000E+01	2.34000E+01	2.36000E+01
9	2.38E+01	2.40000E+01	2.42000E+01	2.44000E+01	2.46000E+01	2.48000E+01
10	2.50E+01	2.52000E+01	2.54000E+01	2.56000E+01	2.58000E+01	2.60000E+01
11	2.62E+01	2.64000E+01	2.66000E+01	2.68000E+01	2.70000E+01	2.72000E+01
12	2.74E+01	2.76000E+01	2.78000E+01	2.80000E+01	2.82000E+01	2.84000E+01
13	2.86E+01	2.88000E+01	2.90000E+01	2.92000E+01	2.94000E+01	2.96000E+01
14	2.98E+01	3.00000E+01	3.02000E+01	3.04000E+01	3.06000E+01	3.08000E+01
15	3.10E+01	3.12000E+01	3.14000E+01	3.16000E+01	3.18000E+01	3.20000E+01
16	3.22E+01	3.24000E+01	3.26000E+01	3.28000E+01	3.30000E+01	3.32000E+01
17	3.34E+01	3.36000E+01	3.38000E+01	3.40000E+01	3.42000E+01	3.44000E+01
18	3.46E+01	3.48000E+01	3.50000E+01	3.52000E+01	3.54000E+01	3.56000E+01
19	3.58E+01	3.60000E+01	3.62000E+01	3.64000E+01	3.66000E+01	3.68000E+01
20	3.70E+01	3.72000E+01	3.74000E+01	3.76000E+01	3.78000E+01	3.80000E+01
21	3.82E+01	3.84000E+01	3.86000E+01	3.88000E+01	3.90000E+01	3.92000E+01
22	3.94E+01	3.96000E+01	3.98000E+01			

de5 lin 1.6 2.0 13i 16.0

df5 lin 0.00 2.25 4.10 4.70 4.85 4.85 4.70 4.30
4.25 4.05 3.85 3.65 3.55 3.60 3.75 3.85

fc15 Pilot B detector response function, 754 cm flightpath, 30 degrees.

f15x:n -653.0 377.0 0

t15 15.5 17.5 24.9 39.1

de15 lin 1.6 2.0 13i 16.0

df15 lin 0.00 2.25 4.10 4.70 4.85 4.85 4.70 4.30
4.25 4.05 3.85 3.65 3.55 3.60 3.75 3.85

```

c
c      ENDF/B-VI
m1   1001.60c .667
      6000.60c .333
m2   7014.60c -.7885
      8016.60c -.2115
cut:n 39.1 1.6
print
prdmmp 2j 1
nps 200000

```

A. Polyethylene 3.0 mfp

1. Geometry Cards

```

1 px -.1
2 so 8.94
3 x 8.94 2.345 40.40 4.5
4 so 40.40
5 so 1000
100 px 0.0

```

2. Tally Cards

```

fc5 Pilot B detector response function, 765.0 cm flightpath, 30 degrees.
f5x:n -662.5 382.5 0
t5  1.35E+01  1.37000E+01  1.39000E+01  1.41000E+01  1.43000E+01  1.45000E+01
     1.47E+01  1.49000E+01  1.51000E+01  1.53000E+01  1.55000E+01  1.57000E+01
     1.59E+01  1.61000E+01  1.63000E+01  1.65000E+01  1.67000E+01  1.69000E+01
     1.71E+01  1.73000E+01  1.75000E+01  1.77000E+01  1.79000E+01  1.81000E+01
     1.83E+01  1.85000E+01  1.87000E+01  1.89000E+01  1.91000E+01  1.93000E+01
     1.95E+01  1.97000E+01  1.99000E+01  2.01000E+01  2.03000E+01  2.05000E+01
     2.07E+01  2.09000E+01  2.11000E+01  2.13000E+01  2.15000E+01  2.17000E+01
     2.19E+01  2.21000E+01  2.23000E+01  2.25000E+01  2.27000E+01  2.29000E+01
     2.31E+01  2.33000E+01  2.35000E+01  2.37000E+01  2.39000E+01  2.41000E+01
     2.43E+01  2.45000E+01  2.47000E+01  2.49000E+01  2.51000E+01  2.53000E+01
     2.55E+01  2.57000E+01  2.59000E+01  2.61000E+01  2.63000E+01  2.65000E+01
     2.67E+01  2.69000E+01  2.71000E+01  2.73000E+01  2.75000E+01  2.77000E+01
     2.79E+01  2.81000E+01  2.83000E+01  2.85000E+01  2.87000E+01  2.89000E+01
     2.91E+01  2.93000E+01  2.95000E+01  2.97000E+01  2.99000E+01  3.01000E+01
     3.03E+01  3.05000E+01  3.07000E+01  3.09000E+01  3.11000E+01  3.13000E+01
     3.15E+01  3.17000E+01  3.19000E+01  3.21000E+01  3.23000E+01  3.25000E+01
     3.27E+01  3.29000E+01  3.31000E+01  3.33000E+01  3.35000E+01  3.37000E+01
     3.39E+01  3.41000E+01  3.43000E+01  3.45000E+01  3.47000E+01  3.49000E+01
     3.51E+01  3.53000E+01  3.55000E+01  3.57000E+01  3.59000E+01  3.61000E+01
     3.63E+01  3.65000E+01  3.67000E+01  3.69000E+01  3.71000E+01  3.73000E+01
     3.75E+01  3.77000E+01  3.79000E+01  3.81000E+01  3.83000E+01  3.85000E+01
     3.87E+01  3.89000E+01  3.91000E+01  3.93000E+01  3.95000E+01  3.97000E+01
     3.99E+01  4.01000E+01  4.03000E+01  4.05000E+01  4.07000E+01  4.09000E+01
fc15 Pilot B detector response function, 765.0 cm flightpath, 30 degrees.
f15x:n -662.5 382.5 0
nps 400000

```

Q. Teflon 0.9 mfp Input Deck

```

Teflon Sphere with 0.9 M.F.P. ENDF/B-VI
1  2 -.001288 -1 -2
2  2 -.001288 1 -2
3  2 -.001288 1 2 -3 -4
4  1 -2.22 -1 2 -4
5  1 -2.22 1 2 3 -4
6  2 -.001288 4 -5
7  0 5

```

```

1   px -.1
2   so 8.94
3   x 8.94 2.345 16.50 3.485
4   so 16.5
5   so 1000
100 px 0.0

imp:n 1 5r 0
-----<Source Cards>-----
fc5 Pilot B detector response function, 752.0 cm flightpath, 30 degrees.
f6x:n -651.3 376.0 0
t5   1.25E+01  1.27E+01  1.29E+01  1.31E+01  1.33E+01  1.35E+01
     1.37E+01  1.39E+01  1.41E+01  1.43E+01  1.45E+01  1.47E+01
     1.49E+01  1.51E+01  1.53E+01  1.55E+01  1.57E+01  1.59E+01
     1.61E+01  1.63E+01  1.65E+01  1.67E+01  1.69E+01  1.71E+01
     1.73E+01  1.75E+01  1.77E+01  1.79E+01  1.81E+01  1.83E+01
     1.85E+01  1.87E+01  1.89E+01  1.91E+01  1.93E+01  1.95E+01
     1.97E+01  1.99E+01  2.01E+01  2.03E+01  2.05E+01  2.07E+01
     2.09E+01  2.11E+01  2.13E+01  2.15E+01  2.17E+01  2.19E+01
     2.21E+01  2.23E+01  2.25E+01  2.27E+01  2.29E+01  2.31E+01
     2.33E+01  2.35E+01  2.37E+01  2.39E+01  2.41E+01  2.43E+01
     2.45E+01  2.47E+01  2.49E+01  2.51E+01  2.53E+01  2.55E+01
     2.57E+01  2.59E+01  2.61E+01  2.63E+01  2.65E+01  2.67E+01
     2.69E+01  2.71E+01  2.73E+01  2.75E+01  2.77E+01  2.79E+01
     2.81E+01  2.83E+01  2.85E+01  2.87E+01  2.89E+01  2.91E+01
     2.93E+01  2.95E+01  2.97E+01  2.99E+01  3.01E+01  3.03E+01
     3.05E+01  3.07E+01  3.09E+01  3.11E+01  3.13E+01  3.15E+01
     3.17E+01  3.19E+01  3.21E+01  3.23E+01  3.25E+01  3.27E+01
     3.29E+01  3.31E+01  3.33E+01  3.35E+01  3.37E+01  3.39E+01
     3.41E+01  3.43E+01  3.45E+01  3.47E+01  3.49E+01  3.51E+01
     3.53E+01  3.55E+01  3.57E+01  3.59E+01  3.61E+01  3.63E+01
     3.65E+01  3.67E+01  3.69E+01  3.71E+01  3.73E+01  3.75E+01
     3.77E+01  3.79E+01  3.81E+01  3.83E+01  3.85E+01  3.87E+01
     3.89E+01  3.91E+01  3.93E+01  3.95E+01  3.97E+01  3.99E+01
     4.01E+01  4.03E+01  4.05E+01

de5 lin 1.6 2.0 13i 16.0
df5 lin 0.00 2.25 4.10 4.70 4.85 4.85 4.70 4.30
      4.25 4.05 3.85 3.65 3.55 3.60 3.75 3.85
fc15 Pilot B detector response function, 752 cm flightpath, 30 degrees.
f15x:n -651.3 376.0 0
t15  15.5 17.5 24.9 39.1
de15 lin 1.6 2.0 13i 16.0
df15 lin 0.00 2.25 4.10 4.70 4.85 4.85 4.70 4.30
      4.25 4.05 3.85 3.65 3.55 3.60 3.75 3.85

c
c   ENDF/B-VI
m1  9019.60c .667
     6000.60c .333
m2  7014.60c -.7885
     8016.60c -.2115
cut:n 39.1 1.6
print
prdmp 2j 1
nps  200000

```

A. Teflon 2.9 mfp

1. Cell Cards

```

Teflon Sphere with 2.9 M.F.P. ENDF/B-VI
1   1 -2.22 -1 -3
2   1 -2.22 1 2 -3
3   2 -.001288 1 -2 -3
4   2 -.001288 3 -4
5   0 4

```

2. Geometry Cards

```
1 px -.64
2 x 0.0 1.42 25.5 3.485
3 so 25.5
4 so 1000
100 px 0.0
```

3. Tally Cards

```
imp:n 1 3r 0
t5 1.34E+01 1.36E+01 1.38E+01 1.40E+01 1.42E+01 1.44E+01
    1.46E+01 1.48E+01 1.50E+01 1.52E+01 1.54E+01 1.56E+01
    1.58E+01 1.60E+01 1.62E+01 1.64E+01 1.66E+01 1.68E+01
    1.70E+01 1.72E+01 1.74E+01 1.76E+01 1.78E+01 1.80E+01
    1.82E+01 1.84E+01 1.86E+01 1.88E+01 1.90E+01 1.92E+01
    1.94E+01 1.96E+01 1.98E+01 2.00E+01 2.02E+01 2.04E+01
    2.06E+01 2.08E+01 2.10E+01 2.12E+01 2.14E+01 2.16E+01
    2.18E+01 2.20E+01 2.22E+01 2.24E+01 2.26E+01 2.28E+01
    2.30E+01 2.32E+01 2.34E+01 2.36E+01 2.38E+01 2.40E+01
    2.42E+01 2.44E+01 2.46E+01 2.48E+01 2.50E+01 2.52E+01
    2.54E+01 2.56E+01 2.58E+01 2.60E+01 2.62E+01 2.64E+01
    2.66E+01 2.68E+01 2.70E+01 2.72E+01 2.74E+01 2.76E+01
    2.78E+01 2.80E+01 2.82E+01 2.84E+01 2.86E+01 2.88E+01
    2.90E+01 2.92E+01 2.94E+01 2.96E+01 2.98E+01 3.00E+01
    3.02E+01 3.04E+01 3.06E+01 3.08E+01 3.10E+01 3.12E+01
    3.14E+01 3.16E+01 3.18E+01 3.20E+01 3.22E+01 3.24E+01
    3.26E+01 3.28E+01 3.30E+01 3.32E+01 3.34E+01 3.36E+01
    3.38E+01 3.40E+01 3.42E+01 3.44E+01 3.46E+01 3.48E+01
    3.50E+01 3.52E+01 3.54E+01 3.56E+01 3.58E+01 3.60E+01
    3.62E+01 3.64E+01 3.66E+01 3.68E+01 3.70E+01 3.72E+01
    3.74E+01 3.76E+01 3.78E+01 3.80E+01 3.82E+01 3.84E+01
    3.86E+01 3.88E+01 3.90E+01 3.92E+01 3.94E+01 3.96E+01
    3.98E+01 4.00E+01 4.02E+01 4.04E+01 4.06E+01 4.08E+01
    4.10E+01 4.12E+01 4.14E+01 4.16E+01 4.18E+01
nps 400000
```

R. Concrete Input Deck

```
Concrete Sphere with 2.0 M.F.P.  ENDF/B-VI
1 2 -.001288 -1 -3
2 2 -.001288 1 -3
3 1 -2.35 -1 3 -4
4 1 -2.35 1 2 3 -4
5 2 -.001288 1 -2 3 -4
6 2 -.001288 4 -5
7 0 5

1 px -.1
2 x 5.1 1.9 21.0 3.0
3 so 5.1
4 so 21.0
5 so 1000
100 px 0.0

imp:n 1 5r 0
-----<Source Cards>-----
fc5 HE213 detector response function, 975.4 cm flightpath, 120 degrees.
f5x:n 487.7 844.7 5
t5 1.86E+01 1.88000E+01 1.90000E+01 1.92000E+01 1.94000E+01 1.96000E+01
    1.98E+01 2.00000E+01 2.02000E+01 2.04000E+01 2.06000E+01 2.08000E+01
    2.10E+01 2.12000E+01 2.14000E+01 2.16000E+01 2.18000E+01 2.20000E+01
    2.22E+01 2.24000E+01 2.26000E+01 2.28000E+01 2.30000E+01 2.32000E+01
    2.34E+01 2.36000E+01 2.38000E+01 2.40000E+01 2.42000E+01 2.44000E+01
```

```

2.46E+01 2.48000E+01 2.50000E+01 2.52000E+01 2.54000E+01 2.56000E+01
2.58E+01 2.60000E+01 2.62000E+01 2.64000E+01 2.66000E+01 2.68000E+01
2.70E+01 2.72000E+01 2.74000E+01 2.76000E+01 2.78000E+01 2.80000E+01
2.82E+01 2.84000E+01 2.86000E+01 2.88000E+01 2.90000E+01 2.92000E+01
2.94E+01 2.96000E+01 2.98000E+01 3.00000E+01 3.02000E+01 3.04000E+01
3.06E+01 3.08000E+01 3.10000E+01 3.12000E+01 3.16000E+01 3.18000E+01
3.20E+01 3.22000E+01 3.24000E+01 3.26000E+01 3.28000E+01 3.30000E+01
3.32E+01 3.34000E+01 3.36000E+01 3.38000E+01 3.40000E+01 3.42000E+01
3.44E+01 3.46000E+01 3.48000E+01 3.50000E+01 3.52000E+01 3.54000E+01
3.56E+01 3.58000E+01 3.60000E+01 3.62000E+01 3.64000E+01 3.66000E+01
3.68E+01 3.70000E+01 3.72000E+01 3.74000E+01 3.76000E+01 3.78000E+01
3.80E+01 3.82000E+01 3.84000E+01 3.86000E+01 3.88000E+01 3.90000E+01
3.92E+01 3.94000E+01 3.96000E+01 3.98000E+01 4.00000E+01 4.02000E+01
4.04E+01 4.06000E+01 4.08000E+01 4.10000E+01 4.12000E+01 4.14000E+01
4.16E+01 4.18000E+01 4.20000E+01 4.22000E+01 4.24000E+01 4.26000E+01
4.28E+01 4.30000E+01 4.32000E+01 4.34000E+01 4.36000E+01 4.38000E+01
4.40E+01 4.42000E+01 4.44000E+01 4.46000E+01 4.48000E+01 4.50000E+01
4.52E+01 4.54000E+01 4.56000E+01 4.58000E+01 4.60000E+01 4.62000E+01
4.64E+01 4.66000E+01 4.68000E+01 4.70000E+01 4.72000E+01 4.74000E+01
4.76E+01 4.78000E+01 4.80000E+01 4.82000E+01 4.84000E+01 4.86000E+01
4.88E+01 4.90000E+01 4.92000E+01

c   NE213 low bias response function
de5  lin 1.6 1.8 1.9 2.0 2.1 2.2 2.3 2.4 2.5 2.75
      3.0 3.5 4.0 4.5 5.0 5.5 6.0 6.4 6.6 6.8 7.0
      7.5 8.1 8.5 9.0 10.0 11.0 12.0 12.5 13.0
      13.5 14.0 15.0 16.0
df5  lin 0.00 1.46 1.86 2.26 2.58 3.00 3.29 3.42
      3.63 3.95 4.10 4.25 4.33 4.39 4.40 4.37 4.28
      4.15 4.20 4.18 4.12 3.97 3.80 3.77 3.65 3.44
      3.24 3.06 3.01 2.98 2.98 3.01 3.08 3.25

c
c   ENDF/B-VI
m1   8016.60c .557
      1001.60c .151
      14000.60c .149
      20000.60c .036
      13027.60c .032
      6000.60c .031
      12000.60c .018
      11023.60c .013
      26054.60c .0001914
      26056.60c .0030268
      26057.60c .0000726
      22000.60c .0033
      25055.60c .0031
m2   7014.60c -.7885
      8016.60c -.2115
cut:n 50.0 1.6
print
prdmpr 2j 1
nps 200000

```

This report has been reproduced directly from the best available copy.

It is available to DOE and DOE contractors from the Office of Scientific and Technical Information, P.O. Box 62, Oak Ridge, TN 37831. Prices are available from (615) 576-8401.

It is available to the public from the National Technical Information Service, US Department of Commerce, 5285 Port Royal Rd. Springfield, VA 22161.

LOS ALAMOS NAT'L LAB.
LIB. REPT. COLLECTION
RECEIVED

94 DEC 21 AM 7 25



Los Alamos, New Mexico 87545